

Fall 10-31-1993

## Pyrolysis and oxidation of chloromethanes experiment and modeling

Wenpin Ho  
*New Jersey Institute of Technology*

Follow this and additional works at: <https://digitalcommons.njit.edu/dissertations>

 Part of the [Chemical Engineering Commons](#)

---

### Recommended Citation

Ho, Wenpin, "Pyrolysis and oxidation of chloromethanes experiment and modeling" (1993). *Dissertations*. 1177.

<https://digitalcommons.njit.edu/dissertations/1177>

This Dissertation is brought to you for free and open access by the Electronic Theses and Dissertations at Digital Commons @ NJIT. It has been accepted for inclusion in Dissertations by an authorized administrator of Digital Commons @ NJIT. For more information, please contact [digitalcommons@njit.edu](mailto:digitalcommons@njit.edu).

## **Copyright Warning & Restrictions**

The copyright law of the United States (Title 17, United States Code) governs the making of photocopies or other reproductions of copyrighted material.

Under certain conditions specified in the law, libraries and archives are authorized to furnish a photocopy or other reproduction. One of these specified conditions is that the photocopy or reproduction is not to be “used for any purpose other than private study, scholarship, or research.” If a user makes a request for, or later uses, a photocopy or reproduction for purposes in excess of “fair use” that user may be liable for copyright infringement,

This institution reserves the right to refuse to accept a copying order if, in its judgment, fulfillment of the order would involve violation of copyright law.

**Please Note: The author retains the copyright while the New Jersey Institute of Technology reserves the right to distribute this thesis or dissertation**

Printing note: If you do not wish to print this page, then select “Pages from: first page # to: last page #” on the print dialog screen

The Van Houten library has removed some of the personal information and all signatures from the approval page and biographical sketches of theses and dissertations in order to protect the identity of NJIT graduates and faculty.

## **INFORMATION TO USERS**

**This manuscript has been reproduced from the microfilm master. UMI films the text directly from the original or copy submitted. Thus, some thesis and dissertation copies are in typewriter face, while others may be from any type of computer printer.**

**The quality of this reproduction is dependent upon the quality of the copy submitted. Broken or indistinct print, colored or poor quality illustrations and photographs, print bleedthrough, substandard margins, and improper alignment can adversely affect reproduction.**

**In the unlikely event that the author did not send UMI a complete manuscript and there are missing pages, these will be noted. Also, if unauthorized copyright material had to be removed, a note will indicate the deletion.**

**Oversize materials (e.g., maps, drawings, charts) are reproduced by sectioning the original, beginning at the upper left-hand corner and continuing from left to right in equal sections with small overlaps. Each original is also photographed in one exposure and is included in reduced form at the back of the book.**

**Photographs included in the original manuscript have been reproduced xerographically in this copy. Higher quality 6" x 9" black and white photographic prints are available for any photographs or illustrations appearing in this copy for an additional charge. Contact UMI directly to order.**

# **U·M·I**

University Microfilms International  
A Bell & Howell Information Company  
300 North Zeeb Road, Ann Arbor, MI 48106-1346 USA  
313/761-4700 800/521-0600

**Order Number 9409125**

**Pyrolysis and oxidation of chloromethanes: Experiment and modeling**

**Ho, Wenpin, Ph.D.**

**New Jersey Institute of Technology, 1993**

**Copyright ©1993 by Ho, Wenpin. All rights reserved.**

**U·M·I**

**300 N. Zeeb Rd.  
Ann Arbor, MI 48106**

**PYROLYSIS AND OXIDATION OF CHLOROMETHANES  
EXPERIMENT AND MODELING**

**by  
Wenpin Ho**

**A Dissertation  
Submitted to the Faculty of  
New Jersey Institute of Technology  
in Partial Fulfillment of the Requirements for the Degree of  
Doctor of Philosophy**

**Department of Chemical Engineering,  
Chemistry, and Environmental Science**

**October 1993**

---

**Copyright © 1993 by Wenpin Ho  
ALL RIGHTS RESERVED**

## **APPROVAL PAGE**

### **PYROLYSIS AND OXIDATION OF CHLOROMETHANES EXPERIMENT AND MODELING**

**Wenpin Ho**

---

Dr. Joseph W. Bozzelli, Dissertation Advisor  
Distinguished Professor of Chemistry, NJIT

date

---

Dr. Barbara B. Kebbekus, Committee Member  
Professor of Chemistry and Associate Chairperson of the Department  
of Chemical Engineering, Chemistry and Environmental Science, NJIT

date

---

Dr. Henry Shaw, Committee Member  
Professor of Chemical Engineering, NJIT

date

---

Dr. Robert B. Barat, Committee Member  
Assistant Professor of Chemical Engineering, NJIT

date

---

Dr. Edward R. Ritter, Committee Member  
Assistant Professor of Chemical Engineering, Villanova University

date



## **ABSTRACT**

### **Pyrolysis and Oxidation of Chloromethanes Experiment and Modeling**

**by  
Wenpin Ho**

An experimental study on pyrolysis and oxidation of  $\text{CH}_2\text{Cl}_2$  and  $\text{CH}_3\text{Cl}$  in oxygen/hydrogen or oxygen/methane mixtures and argon bath gas was carried out at 1 atmosphere pressure in tubular flow reactors. Degradation of  $\text{CH}_2\text{Cl}_2$ , or  $\text{CH}_3\text{Cl}$ , along with the formation and destruction of intermediate and final products was analyzed systematically over 873 to 1273°K, with average residence times of 0.2 to 2.0 seconds.

Thermochemical parameters: enthalpy, entropy, and heat capacities for many chloro-oxy-carbon products and intermediates are calculated using the techniques of group additivity and the THERM computer code. Kinetic analysis on the reactions of hydroxy radical with vinyl chloride are performed using thermochemical analysis and a statistical chemical activation formalism based on the Quantum Kassel Theory for the addition reactions. The two abstraction paths have been also analyzed by using Evans-Polanyi relation for activation energy and Transition State Theory for pre-exponentials. Good agreement with the experimental data in the literature was obtained.

A nonlinear group additivity formalism to estimate the normal boiling points has been developed because boiling points are important to calculate critical properties needed for flame modeling. The model is straightforward and applies to compounds with a wide range of molecular weight, varied functional groups, and complex structures. We further utilize the proposed model for normal boiling points and adapt Joback's method into Benson type groups to calculate critical properties ( $T_c$ ,  $P_c$ ,  $V_c$ ). Transport coefficients such as Lennard Jones Parameters (collision diameter and well depth), polarizability, and rotational relaxation collision numbers can also be estimated.

The same group information (input data) needed for thermo properties estimation is then used to estimate transport properties required in flame modeling.

A detailed kinetic reaction mechanism based upon fundamental thermochemical and kinetic principles, Transition State Theory and evaluated literature rate constant data is developed. The mechanism is used to model results obtained from our experiments, in addition to results from other studies, on the thermal reactions of  $\text{CH}_2\text{Cl}_2$  and/or  $\text{CH}_3\text{Cl}$ . Comparison of the model to experimental data of other researchers for a wide range of conditions (tubular flow reactor, flat flame, perfect stirred reactor) showed good agreement in most cases.

Sensitivity analysis determined important reactions in the mechanism to several "target" products including reactions effective in inhibiting CO conversion to  $\text{CO}_2$ . The results indicate that the reaction  $\text{OH} + \text{HCl} \rightarrow \text{H}_2\text{O} + \text{Cl}$  is a major cause of OH loss. This decrease in OH effectively stops CO burnout. In addition, the reaction  $\text{H} + \text{HCl} \rightarrow \text{H}_2 + \text{Cl}$  is also important when  $\text{H}_2$  concentrations are very low. Sensitivity analysis also indicates that the reaction  $\text{OH} + \text{OH} \rightleftharpoons \text{H}_2\text{O} + \text{O}$ , which usually forms  $\text{H}_2\text{O}$  during hydrocarbon incineration, reacts in the reverse direction when HCl is present at concentrations comparable to CO, due to the large extent of OH depletion. The addition of moderate levels of high temperature steam are predicted to help CO conversion by shifting the above equilibria to more OH.

Knowledge and application of the reaction mechanisms to emulation of incineration operation allows calculation of modifications to incinerator design and/or feed to minimize pollutant formation. We predict that adding high temperature steam to the incinerators will improve Cl conversion to HCl by shifting the equilibrium of the  $\text{OH} + \text{OH} = \text{H}_2\text{O} + \text{O}$  reaction to the left. The viability of computer modeling is illustrated as a diagnostic for understanding and for improvement or optimization in combustion processes with assumed ideal mixing.

## **BIOGRAPHICAL SKETCH**

**Author:** Wenpin Ho

**Degree:** Doctor of Philosophy in Chemical Engineering

**Date:** October 1993

### **Undergraduate and Graduate Education:**

- Doctor of Philosophy in Chemical Engineering,  
New Jersey Institute of Technology, NJ, 1993
- Master of Science in Environmental Science,  
New Jersey Institute of Technology, NJ, 1989
- Bachelor of Science in Chemical Engineering,  
Chinese Culture University, Taiwan, R.O.C., 1984

**Major:** Chemical Engineering

### **Presentations and Publications :**

Ho, W. and Bozzelli, J.W. "Reaction of OH Radical with  $C_2H_3Cl$  - Reaction Pathway Analysis", Chemical and Physical Processes in Combustion, p 665-669, 1993.

Ho, W. and Bozzelli, J.W. "Validation of A Mechanism for Use in Modeling  $CH_2Cl_2$  and/or  $CH_3Cl$  Combustion and Pyrolysis", Twenty-Fourth International Symposium on Combustion, The Combustion Institute, Pittsburgh, PA, p743-748, 1992.

Ho, W., Yu, Q.R., and Bozzelli, J.W. "Kinetic Study on Pyrolysis and Oxidation of  $CH_3Cl$  in  $Ar/H_2/O_2$  Mixtures", Combustion Science and Technology, vol.85, p23-63, 1992.

Ho, W., Barat, R.B., and Bozzelli, J.W. "Thermal Reaction of  $\text{CH}_2\text{Cl}_2$  in  $\text{O}_2/\text{H}_2$  Mixtures: Implications for Chlorine Inhibition of CO Conversion to  $\text{CO}_2$ ", *Combustion and Flame*, vol.88, p265-295,1992

Ho, W., Yu, Q.R., and Bozzelli, J.W. "Kinetic Study on Pyrolysis and Oxidation of  $\text{CH}_3\text{Cl}/\text{CH}_4/\text{O}_2$  Mixtures", *Chemical and Physical Processes in Combustion*, 1991.

Ho, W., Barat, R.B., and Bozzelli, J.W. "Mechanism of Acceleration and Inhibition in Hydrocarbon Combustion by Chlorocarbons or  $\text{HCl}$ ", *Organohalogen Compounds*, vol.3, p87-90, 1990

Ho, W. and Bozzelli, J.W. "Thermal Decomposition of Dichloromethane in Hydrogen/Oxygen/Argon Mixtures and in Pure Oxygen", *Chemical and Physical Processes in Combustion*, vol. 27, no.1, p4, 1989

**This thesis is dedicated to  
Shu-hsia and Samantha**

## **ACKNOWLEDGMENT**

The author wishes to express his sincere gratitude to his advisor, Professor Joseph W. Bozzelli, for his precious guidance, expert assistance and patience throughout this research. I acknowledge the helpful corrections and productive comments by Dr. Barbara B. Kebbekus, Dr. Henry Shaw, Dr. Robert B. Barat, and Dr. Edward R. Ritter.

Special thanks to Dr. Edward R. Ritter for providing useful computer programs: THERM, CHEMACT, DISSOC, RADICAL, TRANSCAL, and INCIN. It is my pleasure to thank my colleagues at Kinetics Research Laboratory of the New Jersey Institute of Technology: Dr. Yangsoo Won, Dr. Greg Wu, and Dr. Edward R. Ritter who shared with me their experience. My appreciation for the friendship and assistance that I have received from current and past students in the laboratory can not be overstated, nor can it be fully expressed in this space.

Finally, I would like to thank my parents and my wife for their endless love and support. Without their encouragement, I would not have been able to accomplish my goal.

## TABLE OF CONTENTS

Chapter	Page
1 INTRODUCTION .....	1
2 EXPERIMENTAL METHOD.....	10
2.1 Experimental Apparatus .....	10
2.2 Temperature Control and Measurement .....	11
2.3 Quantitative Analysis of Reaction Products.....	12
2.4 Hydrochloric Acid Analysis .....	14
2.5 Qualitative Identification of Reaction Products .....	15
3 ESTIMATION OF THERMOCHEMICAL DATA .....	16
4 ESTIMATION OF KINETIC PARAMETERS.....	20
4.1 Background.....	21
4.2 Unimolecular Dissociation .....	21
4.2.1 Simple Fission .....	21
4.2.2 Complex Fission.....	24
4.2.3 Beta Scission Reactions.....	26
4.3 Bimolecular Reactions.....	26
4.3.1 Abstraction Reactions.....	26
4.3.2 Addition Reactions .....	28
4.3.3 Combination and Insertion Reactions .....	29
5 REACTION OF OH RADICAL WITH C <sub>2</sub> H <sub>3</sub> CL REACTION PATHWAY ANALYSIS.....	30
5.1 Background.....	30
5.2 Quantum Kassel Calculation for Addition Reaction .....	32
5.3 Thermodynamic Properties.....	33
5.4 Addition Reactions .....	34

<b>Chapter</b>	<b>Page</b>
5.4.1 $\alpha$ - Addition .....	34
5.4.2 $\beta$ - Addition .....	36
5.5 Transition-State-Theory Calculation for Abstraction Reaction .....	37
5.6 Results and Discussion .....	41
5.7 Summary.....	45
<b>6 THERMAL REACTIONS OF CH<sub>2</sub>CL<sub>2</sub> IN O<sub>2</sub>/H<sub>2</sub> MIXTURES: IMPLICATIONS FOR CHLORINE INHIBITION OF CO CONVERSION TO CO<sub>2</sub> .....</b>	<b>46</b>
6.1 Background .....	46
6.2 Experimental Result .....	47
6.3 Kinetic Mechanism and Modeling .....	50
6.4 Summary.....	61
<b>7 KINETIC STUDY ON PYROLYSIS AND OXIDATION OF CH<sub>3</sub>CL IN AR/O<sub>2</sub>/H<sub>2</sub> MIXTURES.....</b>	<b>63</b>
7.1 Background .....	63
7.2 Experimental Result .....	65
7.3 Kinetic Mechanism and Modeling .....	66
7.4 Summary.....	77
<b>8 MOLECULAR PARAMETERS FOR TRANSPORT PROPERTIES IN FLAME CODE .....</b>	<b>78</b>
8.1 Prediction of Normal Boiling Point from Group Additivity Model .....	78
8.1.1 Estimation Techniques .....	79
8.1.2 Hydrocarbons .....	81
8.1.3 Chlorocarbons.....	82
8.1.4 Alcohols, Ethers, and Amines .....	83
8.1.5 Results and Discussion.....	84



<b>Chapter</b>	<b>Page</b>
8.1.6 Summary.....	93
8.2 Lennard-Jones Parameters.....	93
8.3 Dipole Moment.....	94
8.4 Polarizability .....	95
8.5 Rotational Relaxation Collision Number .....	96
<b>9 VALIDATION OF A MECHANISM FOR USE IN MODELING CH<sub>2</sub>CL<sub>2</sub> AND/OR CH<sub>3</sub>CL COMBUSTION AND PYROLYSIS.....</b>	<b>101</b>
9.1 Background .....	101
9.2 Numerical Model and Mechanism .....	102
9.3 Results and Discussion .....	104
<b>10 EFFECT OF STEAM AND OTHER ADDITIVES ON POHC CONVERSION AND PICS .....</b>	<b>108</b>
10.1 Background .....	108
10.2 Mechanism and Numerical Simulation .....	111
10.3 Model Validation.....	112
10.4 Numerical Simulation Code .....	112
10.5 Results and Discussion.....	114
10.5.1 Effect of CH <sub>3</sub> Cl Added with CH <sub>4</sub> Feed- Non-additive Conditions.....	114
10.5.2 Fuel Lean Equivalence Ratio 0.8 in The PSR .....	115
10.5.3 Effects on CO/CO <sub>2</sub> Ratio.....	116
10.5.4 CO/CO <sub>2</sub> Fuel Rich Initial Conditions.....	116
10.5.5 CO/CO <sub>2</sub> Ratio Fuel Lean Initial Conditions.....	117
10.5.6 Discussion .....	118
10.6 Conclusions .....	119

<b>Chapter</b>	<b>Page</b>
APPENDIX A THERMODYNAMIC DATABASE.....	120
APPENDIX B DETAILED REACTION MECHANISM .....	124
APPENDIX C CHEMACT INPUT DATA.....	135
APPENDIX D EXPERIMENT AND MODELING RESULTS FIGURES .....	145
REFERENCES.....	225

## LIST OF TABLES

Table	Page
2.1 Average Retention Time of Products.....	13
2.2 Relative Response Factor in FID and TCD.....	14
3.1 New Groups for C/Cl/H/O .....	18
3.2 Validation of Estimation Method.....	19
3.3 New Groups for S <sup>298</sup> and Cp .....	19
4.1 C-H Repture in Hydrocarbon Molecules .....	23
4.2 C-C Repture in Hydrocarbon Molecules.....	24
4.3 C-H Repture in Hydrocarbon Radicals .....	24
4.4 Kinetic Parameters for Various Types of Reactions .....	27
5.1 Thermodynamic Property Data .....	33
5.2 Input Parameters for The QK calculation, C <sub>2</sub> H <sub>3</sub> Cl + OH $\alpha$ - addition .....	35
5.3 Input Parameters for The QK calculation, C <sub>2</sub> H <sub>3</sub> Cl + OH $\beta$ - addition .....	37
5.4 Calculated Contribution to $\Delta S^\ddagger$ for OH + C <sub>2</sub> H <sub>3</sub> Cl Abstraction Reaction.....	40
5.5 Apparent Rate Constants for OH + C <sub>2</sub> H <sub>3</sub> Cl at 760 torr .....	42
5.6 Input Parameters for The RRKM calculation .....	44
6.1 Reactant Feed Ratios.....	48
6.2 Global Rate Constants ( $K_{\text{exp}}$ ) for CH <sub>2</sub> Cl <sub>2</sub> /O <sub>2</sub> /H <sub>2</sub> in Ar .....	50
6.3 Other Researcher's Experimental Conditions .....	57
6.4 Sensitivity Analysis Relative to CO <sub>2</sub> Formation at 1053 K.....	58
7.1 Sensitivity Analysis Relative to CO <sub>2</sub> Formation at Different Conversion.....	73
8.1 Groups of T <sub>b</sub> for Joback and NJIT Methods .....	83
8.2 List of Constant "a" for Different Homologous Series .....	84
8.3 Alkanes Data Set.....	86
8.4 Alkenes Data Set.....	87

<b>Table</b>	<b>Page</b>
8.5 Alkynes Data Set.....	88
8.6 Alcohols Data Set .....	89
8.7 Chlorinated Hydrocarbons Data Set .....	90
8.8 Aromatics Data Set .....	91
8.9 Bond Moment for Vector Contribution Calculation.....	95
8.10 Polarizability Terms for Atoms and Structure Features.....	97
8.11 Calculation Result for Z <sub>298</sub> Using Chung's Method.....	99
10.1 List of Model Validation.....	113

## LIST OF FIGURES

Figure	Page
2.1 Experimental Apparatus.....	146
2.2 Schematic of Voltage and Thermocouple Input to Temperature Controller.....	147
2.3 Temperature Profile .....	148
2.4 Sample Chromatogram of $\text{CH}_2\text{Cl}_2/\text{O}_2/\text{H}_2$ Decomposition (FID) .....	149
2.5 Sample Chromatogram of $\text{CH}_2\text{Cl}_2/\text{O}_2/\text{H}_2$ Decomposition (TCD).....	150
4.1 Energy Barrier for HCl Elimination.....	151
4.2 Evans-Polanyi Plot, $\text{Cl} + \text{CHC} \rightarrow \text{HCl} + \text{R}$ . .....	152
4.3 Evans-Polanyi Plot, $\text{Cl} + \text{RH} \rightarrow \text{HCl} + \text{R}$ . .....	153
4.4 Evans-Polanyi Plot, $\text{H} + \text{RCl} \rightarrow \text{HCl} + \text{R}$ . .....	154
4.5 Evans-Polanyi Plot, $\text{Cl} + \text{RCl} \rightarrow \text{Cl}_2 + \text{R}$ . .....	155
5.1 Energy Level for $\text{C}_2\text{H}_3\text{Cl} + \text{OH}$ alpha addition .....	156
5.2 Energy Level for $\text{C}_2\text{H}_3\text{Cl} + \text{OH}$ beta addition .....	157
5.3 Modified Evans-Polanyi Plot of OH Abstraction of H atom from CHC .....	158
5.4 Plot of The Rate Constant for alpha Addition Reaction versus $1000/T$ .....	159
5.5 Plot of The Rate Constant for beta Addition Reaction versus $1000/T$ .....	160
5.6 Major Reaction Products from The Reaction of Vinyl Chloride + OH Plotted versus Pressure at 300 K .....	161
5.7 Comparison of Calculated Results for $\text{C}_2\text{H}_3\text{Cl} + \text{OH}$ to Experimental Data at 760 torr Versus $1000/T$ .....	162
5.8 Comparison of Calculated Results for $\text{C}_2\text{H}_3\text{Cl} + \text{OH}$ to Experimental Data at Room Temperature Versus Pressure.....	163
5.9 Comparison of Calculated Results for $\text{CH}_2\text{OHC.HCl} \rightarrow \text{C}_2\text{H}_3\text{Cl} + \text{OH}$ Dissociation Reaction at 760 torr Versus $1/T$ .....	164
5.10 Comparison of Calculated Results for $\text{CH}_2\text{OHC.HCl} \rightarrow \text{C}_2\text{H}_3\text{Cl} + \text{OH}$ Dissociation Reaction at 760 torr Versus Pressure .....	165

Figure	Page
6.1 CH <sub>2</sub> Cl <sub>2</sub> Conversion Versus Residence Time at Different Temperature. Reactant Ratio: O <sub>2</sub> :H <sub>2</sub> :CH <sub>2</sub> Cl <sub>2</sub> :Ar=1:1:1:97.....	166
6.2 CH <sub>2</sub> Cl <sub>2</sub> Conversion Versus Residence Time at Different Temperature. Reactant Ratio: O <sub>2</sub> :H <sub>2</sub> :CH <sub>2</sub> Cl <sub>2</sub> =98:1:1 .....	167
6.3 Major Product Distribution for CH <sub>2</sub> Cl <sub>2</sub> Decomposition 1sec.Residence Time. Reactant Ratio: O <sub>2</sub> :H <sub>2</sub> :CH <sub>2</sub> Cl <sub>2</sub> :Ar=2:2:1:95.....	168
6.4 Major Product Distribution for CH <sub>2</sub> Cl <sub>2</sub> Decomposition 1sec.Residence Time. Reactant Ratio: O <sub>2</sub> :H <sub>2</sub> :CH <sub>2</sub> Cl <sub>2</sub> :Ar=2:2:1:95.....	169
6.5 Comparison of CH <sub>2</sub> Cl <sub>2</sub> Conversion and Products at 1053 K, 1% CH <sub>2</sub> Cl <sub>2</sub> with Different O <sub>2</sub> /H <sub>2</sub> Feed Ratios .....	170
6.6 Comparison of CO and CO <sub>2</sub> Production at 1053 K, 1% CH <sub>2</sub> Cl <sub>2</sub> with Different O <sub>2</sub> /H <sub>2</sub> Feed Ratios .....	171
6.7 Arrhenius Behavior of Global K <sub>exp</sub> for CH <sub>2</sub> Cl <sub>2</sub> /O <sub>2</sub> /H <sub>2</sub> .....	172
6.8 Energy Level for CH <sub>2</sub> Cl + H Reaction.....	173
6.9 Energy Level for CH <sub>2</sub> Cl + CH <sub>2</sub> Cl Reaction .....	174
6.10 Energy Level for CH <sub>2</sub> Cl + O <sub>2</sub> Reaction.....	175
6.11 Comparison of Calculated and Experimental Product Distribution versus Temperature, 1sec.Residence Time. Reactant Ratio: O <sub>2</sub> :H <sub>2</sub> :CH <sub>2</sub> Cl <sub>2</sub> :Ar=2:2:1:95 .....	176
6.12 Comparison of Calculated and Experimental Product Distribution versus Temperature, 1sec.Residence Time. Reactant Ratio: O <sub>2</sub> :H <sub>2</sub> :CH <sub>2</sub> Cl <sub>2</sub> :Ar=2:2:1:95 .....	177
6.13 Comparison of Calculated and Experimental Product Distribution versus Temperature, 1sec.Residence Time. Reactant Ratio: O <sub>2</sub> :H <sub>2</sub> :CH <sub>2</sub> Cl <sub>2</sub> :Ar=2:2:1:95 .....	178
6.14 Comparison of Calculated and Experimental Product Distribution versus Residence Time at 1053 K. Reactant Ratio: O <sub>2</sub> :H <sub>2</sub> :CH <sub>2</sub> Cl <sub>2</sub> :Ar=2:2:1:95 .....	179
6.15 Comparison of Calculated and Experimental Product Distribution versus Residence Time at 1053 K. Reactant Ratio: O <sub>2</sub> :H <sub>2</sub> :CH <sub>2</sub> Cl <sub>2</sub> :Ar=2:2:1:95 .....	180

Figure	Page
6.16 Comparison of Calculated and Experimental Product Distribution versus Residence Time at 1053 K. Reactant Ratio: $O_2:H_2:CH_2Cl_2:Ar=2:2:1:95$ .....	181
6.17 Comparison of Experimental Data and Model Prediction with Other Studies..	182
7.1 $CH_3Cl$ Conversion Versus Residence Time at Different Temperature. Reactant Ratio: $O_2:H_2:CH_3Cl:Ar=1:1:2:96$ .....	183
7.2 Major Product Distribution for $CH_3Cl$ Decomposition Versus Residence Time at 1173 K. Reactant Ratio: $O_2:H_2:CH_3Cl:Ar=1:1:2:96$ .....	184
7.3 Major Product Distribution for $CH_3Cl$ Decomposition Versus Residence Time at 1173K. Reactant Ratio: $O_2:H_2:CH_3Cl:Ar=1:1:2:96$ .....	185
7.4 Energy Level for $CH_2Cl + CH_3$ Reaction.....	186
7.5 Comparison of Calculated and Experimental Product Distribution versus Residence Time at 1173 K. Reactant Ratio: $O_2:H_2:CH_3Cl:Ar=1:1:2:96$ .....	187
7.6 Comparison of Calculated and Experimental Product Distribution versus Residence Time at 1173 K. Reactant Ratio: $O_2:H_2:CH_3Cl:Ar=1:1:2:96$ .....	188
7.7 Comparison of Calculated and Experimental Product Distribution versus Temperature, 1sec. Residence Time. Reactant Ratio: $O_2:H_2:CH_3Cl:Ar=1:1:2:96$ .....	189
7.8 Comparison of Calculated and Experimental Product Distribution versus Temperature, 1sec. Residence Time. Reactant Ratio: $O_2:H_2:CH_3Cl:Ar=1:1:2:96$ .....	190
7.9 Comparison of Our Model with Princeton Experimental Data Using Temperature Profile of Princeton Flow Reactor .....	191
7.10 Comparison of Our Model with Princeton Experimental Data for CO Oxidation with Different HCl Concentration Added.....	192
8.1 Plot of Residuals on Tb of Alkanes .....	193
8.2 Plot of Residuals on Tb of Alkenes .....	194
8.3 Plot of Residuals on Tb of Alkynes .....	195
8.4 Plot of Residuals on Tb of Alcohols .....	196

<b>Figure</b>	<b>Page</b>
8.5 Plot of Residuals on Tb of Chlorocarbons.....	197
8.6 Plot of Residuals on Tb of Aromatics.....	198
9.1 Comparison of Calculated and Chiang et al. Experimental Product Distribution versus Temperature at 1 sec. Residence Time .....	199
9.2 Comparison of Calculated and Experimental Product Distribution versus Residence Time at 1173 K. Reactant Ratio: O <sub>2</sub> :CH <sub>4</sub> :CH <sub>3</sub> Cl:Ar=2:1:2:95 .....	200
9.3 Comparison of Our Model with Roesler et al. Experimental Data .....	201
9.4 Comparison of Calculated and Experimental Product Distribution versus Residence Time at 1253 K. Reactant Ratio: O <sub>2</sub> :CH <sub>3</sub> Cl:Ar=2.05:7.32:90.6 .....	202
9.5 Comparison of Our Model with Karra et al. Flame Data.....	203
9.6 Comparison of Our Model with Karra et al. Flame Data.....	204
9.7 Comparison of Our Model with Qun et al. Flame Data.....	205
9.8 Comparison of Our Model with Qun et al. Flame Data.....	206
9.9 Comparison of Our Model with Miller et al. Flame Data.....	207
9.10 Comparison of Our Model with Miller et al. Flame Data.....	208
10.1 Turbulent Flow Incinerator Simulation.....	209
10.2 Incinerator Simulation Temperature Profile .....	210
10.3 Effect of CH <sub>3</sub> Cl Added in CH <sub>4</sub> /Air under Fuel Lean Condition; Calculated in Burnout Zone .....	211
10.4 Effect of CH <sub>3</sub> Cl Added in CH <sub>4</sub> /Air under Fuel Lean Condition; Calculated in Exit 320 K.....	212
10.5 Cl Atom Mole Fraction Versus Reaction Time in The Burnout Zone.....	213
10.6 Cl Atom Mole Fraction Versus Reaction Time in The Cool Down Zone .....	214
10.7 Cl <sub>2</sub> Mole Fraction Versus Reaction Time in The Cool Down Zone .....	215
10.8 HCl Mole Fraction Versus Reaction Time Throughout The Reactor.....	216
10.9 COCl <sub>2</sub> Mole Fraction Versus Reaction Time in The Burnout Zone .....	217



<b>Figure</b>	<b>Page</b>
10.10 $\text{COCl}_2$ Mole Fraction Versus Reaction Time in The Cool Down Zone.....	218
10.11 $\text{CO}/\text{CO}_2$ Ratio Versus Reaction Time under Fuel Rich Condition .....	219
10.12 $\text{CO}/\text{CO}_2$ Ratio Calculated at Exit 320 K under Fuel Rich Condition.....	220
10.13 $\text{CO}/\text{CO}_2$ Ratio Versus Addition of Steam under Fuel Lean Condition.....	221
10.14 $\text{CO}/\text{CO}_2$ Ratio Versus Reaction Time in The Burnout Zone .....	222
10.15 $\text{CO}/\text{CO}_2$ Ratio Versus Reaction Time in The Cool Down Zone.....	223
10.16 Fraction Change in Products Versus Additives .....	224

## **CHAPTER 1**

### **INTRODUCTION**

Chlorinated Hydrocarbons (CHC) have been used on a large scale by industry either as raw materials for production or as solvents; with both cases often leading to the production of large amounts of chlorinated organic wastes. Since the Toxic Substance Control Act (TSCA) was enacted in 1976, the disposal of chlorocarbons as industrial wastes has become more and more difficult and costly. One popular disposal method that has been used is landfill, but this method is not a permanent solution because of potential contamination of ground waters by leakage from the toxic waste site. In the USA where many storage sites that were deemed to be safe by waste producers now require remediation at great cost, with the originators of the wastes having to pick up the bill. Newer processes including biological degradation, incineration and fixation in cement kilns are gaining market acceptance<sup>1</sup>, because they destroy the toxic species, even though they are expensive.

Incineration seems to be a more effective way of handling the disposal of many wastes, such as combustible solids, semi-solids, sludge and concentrated liquid wastes. It reduces, if not eliminates, potential environmental risks and converts wastes into recoverable energy. When one compares incineration with other disposal options, advantages often become evident, especially as more wastes become regulated and added prohibitions and increasingly burdensome costs are placed on land disposal.

Although the incineration of hazardous wastes presents a viable and effective disposal methodology, the use of this technology has been severely hindered by environmental concerns regarding the effluents from such systems. Two important issues are the capability of incinerators to effect the high level of destruction that is desired and the possibility that other hazardous chemicals may be formed and thus impact the environment.

Hazardous waste incineration involving chlorine compounds deserves attention because the behavior of chlorine is unique among the halogenated compounds. Organic chlorine compounds serve as a source of chlorine atoms, which readily abstract H atoms from other organic hydrocarbons accelerating hydrocarbon production and soot formation. HCl is a desirable product because it removes the Cl and can be easily neutralized, but it can also inhibit combustion through reactions like  $\text{OH} + \text{HCl} \rightarrow \text{H}_2\text{O} + \text{Cl}$ , which depletes OH needed for CO burnout.

The incineration of chlorocarbons is generally performed in an oxygen rich environment that contains excess  $\text{O}_2$  and  $\text{N}_2$ , in addition to the carbon and chlorine from the halocarbon, with relatively small amounts of available hydrogen from the limiting fuel operation<sup>2</sup>. One desired and thermodynamically favorable product from a chlorocarbon conversion process is HCl, providing there exists sufficient  $\text{H}_2$  to achieve stoichiometric formation. The O-H bond in water is, however, stronger than the H-Cl bond and oxygen rich conditions favor  $\text{H}_2\text{O}$  and therefore limit hydrogen availability for HCl. Oxygen and Cl are, therefore, both competing for the available fuel hydrogen and this is one reason that chlorocarbons serve as flame inhibitors. The C-Cl bond is the next strongest compared with other possible chlorinated products such as Cl-Cl, N-Cl, or O-Cl bonds. Consequently, C-Cl may persist in a oxygen rich or hydrogen limited atmosphere<sup>2</sup>. This is one reason why emission of toxic chlorine-containing organic products persists through an oxygen-rich incineration, as carbon species are one of the more stable sinks for the chlorine. One possible method to obtain quantitative formation of HCl, as one of the desired and thermodynamically favorable products, from chlorocarbons, might be a straightforward thermal conversion of these compounds under a more reductive atmosphere of hydrogen. Here the carbon would be converted to a hydrocarbon such as ethane or ethylene.

The presence of chlorocarbons has long been known to slow or inhibit the oxidation rate of hydrocarbons through studies of flame velocity, temperature, and flame

stability. Westbrook<sup>2</sup> has modeled the inhibition of hydrocarbon oxidation in laminar flames by halogenated compounds. He suggested that the halogenated species serve to catalyze the recombination of H atoms into relatively nonreactive H<sub>2</sub> molecules, reducing the available radical pool, specifically H atoms, and thereby lowering the overall rate of chain branching. Senkan et. al.<sup>3,4</sup> have developed mechanisms for CH<sub>3</sub>Cl, C<sub>2</sub>H<sub>3</sub>Cl, and HCl-doped CO oxidation flame systems. These later studies reached similar conclusions, suggesting that the reaction of  $\text{H} + \text{HCl} \rightarrow \text{H}_2 + \text{Cl}$  is responsible for the inhibition of CO conversion to CO<sub>2</sub> in the oxidations.

Alternately, Benson and Weissman<sup>5</sup> and Senkan et. al.<sup>3</sup> have reported that use of CH<sub>3</sub>Cl in CH<sub>4</sub> or in CH<sub>4</sub> plus 2-3% O<sub>2</sub> respectively accelerated CH<sub>4</sub> conversion to higher hydrocarbons. They concluded that this might lead to effective methods for converting CH<sub>4</sub> to useful higher molecular weight hydrocarbons without either soot or excessive oxidation occurring<sup>3</sup>.

Both acceleration and inhibition effects are apparent in hydrocarbon reaction systems with a chlorinated hydrocarbon present. Therefore, there is a significant need to develop quantitative insights into the mechanism of chlorocarbon pyrolysis and oxidation in order to better understand and ultimately to optimize these reaction processes, for use in conversion of chlorocarbons by incineration, or for use in CH<sub>4</sub> upgrading or other industrial processes.

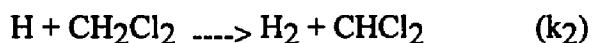
In this study, a global rate constant and a detailed kinetic mechanism for the high temperature pyrolysis in H<sub>2</sub> and of combustion of dichloromethane (CH<sub>2</sub>Cl<sub>2</sub>) and methyl chloride (CH<sub>3</sub>Cl) under fuel rich conditions are presented. I develop and use detailed chemical kinetic mechanisms for the high temperature combustion of chlorocarbons. The mechanisms are developed from fundamental thermochemical principles and used to model results obtained from our tubular flow experimental results. I also compare calculations using our model with data of other researchers, providing a wide range of experimental conditions to validate our mechanism. The data presented will be for 1 atm

reaction systems, but approximately 1/3 of the reactions in the mechanism are analyzed by using Quantum Kassel method of Dean<sup>6,7</sup> so the mechanism can be easily modified for use in other pressure regimes and still incorporate fall-off and pressure dependence.

Reactions of dichloromethane (DCM, CH<sub>2</sub>Cl<sub>2</sub>) with hydrogen but, without the presence of oxygen, have been studied thoroughly and systematically in these laboratories at NJIT.

Tsao<sup>8</sup> studied the thermal decomposition of DCM with hydrogen over the temperature range of 973 - 1173K, in a 1 atm total pressure tubular flow apparatus. Activation energies of the global bulk and wall reactions on hydrogen reaction with DCM were 50.0 Kcal/mol, 57.8 Kcal/mole, with Arrhenius A factors of 2.84E+10 and 2.65E+10 sec.<sup>-1</sup> respectively reported. The major products of reaction of DCM in the temperature range 973 to 1073 K were methane and methyl chloride. The minor products were ethylene, acetylene and HCl. Trace amounts of ethane, chloroethylene, 1,2-dichloroethylene, trichloroethylene, benzene were also observed. No chlorocarbons were found over 1223K and one second residence time where the only products were methane, hydrogen chloride, acetylene, ethane and benzene.

Huang<sup>9</sup> studied the kinetics of the reaction of atomic hydrogen with DCM in a flow system at a pressure of 2.1 to 2.7 mm Hg and room temperature. The major products observed were hydrogen chloride and methane. The extent of conversion of DCM increases first to a maximum and then decreases with increasing concentration of DCM. Through the modeling of the reaction scheme and comparison with experimental data, the rate constant of the initial steps were determined as follows :



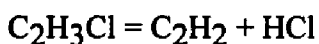
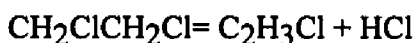
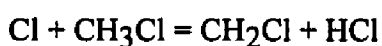
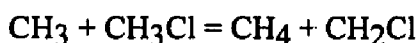
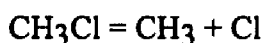
where

$$k_1 = 3.63 \text{ E}+9 \text{ cm}^3/\text{mole}/\text{sec} , 298 \text{ K}$$

$$k_2 = 2.08 \times 10^7 \text{ cm}^3/\text{mole}/\text{sec} \text{ , } 298 \text{ K}$$

Won<sup>10</sup> investigated the decomposition of dichloromethane/1,1,1--trichloroethane mixtures in a hydrogen bath gas. These experiments were carried out at one atmosphere total pressure in a tubular flow reactor. In his study, he demonstrated that selective formation of HCl can result from thermal reaction of chlorocarbon mixture and showed that synergistic effects of 1,1,1--trichloroethane decomposition accelerate the rate of DCM decomposition. There is significant interaction of the decay products from 1,1,1--trichloromethane with the parent dichloromethane.

Earlier kinetic studies on methyl chloride pyrolysis were reported in 1959 by Shilov and Sabirova<sup>11</sup>. Measurements were made at initial CH<sub>3</sub>Cl pressures of 10.1-34.3 torr, temperatures of 1062K-1147K, and at contact times of 0.4- 5.0 seconds. They found HCl, CH<sub>4</sub>, and C<sub>2</sub>H<sub>2</sub> in the ratios of 3:1:0.6. These yields were reported to be consistent with the following proposed mechanism:

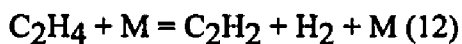
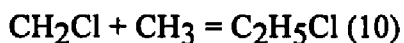
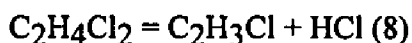
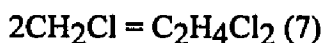
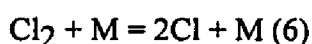
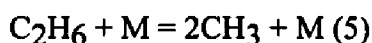
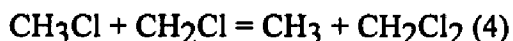
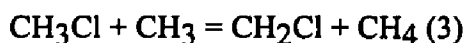


They also reported that the measured apparent first-order rate constants increased with increasing pressure.

Slater's theory was used by Holbrook<sup>12</sup> to calculate the rate constant for the decomposition of CH<sub>3</sub>Cl in the fall-off region. The value obtained was 5-6 orders of magnitude lower than the reported experimental values above. Frost and Laurent<sup>13</sup> obtained a better fit to this value using RRKM theory, where rotations were considered inactive, and activation energy was taken from the experimental data. With harmonic energy levels the calculated rate constant was 32 times smaller than experimental value,

and with a correction for anharmonicity the calculated rate constant was only 20 times smaller. These modeling calculation may have indicated that the rate constants was not correctly fit experimental data.

In 1980, Kondo, Saito, Murakami<sup>14</sup> pyrolyzed  $\text{CH}_3\text{Cl}$  in a shock tube at temperatures between 1680K and 2430K, at total pressures of 1-5 atm, using reactant mixtures of 0.2%-0.5% methyl chloride in argon.  $\text{CH}_3$  concentrations were measured via the  $\text{CH}_3$  absorption band at 216 nm. From the initial rate of  $\text{CH}_3$  formation the elementary rate constant for breaking the C-Cl bond was obtained. The reaction was in the fall-off region even at the highest pressures. For these high temperature shock tube data, the mechanism was considered to include the following likely reactions:



Computer simulation of the  $\text{CH}_3$  profiles without reaction (4), and with  $k_7$  and  $k_{10}$  equal to  $k_5$  fitted the experimental data at high temperatures exactly and were higher by a factor of 2 at low temperatures. Low- and high-pressure rate constants ( $k_0$  [Ar] and  $k_\infty$ ) were obtained from the experimental data by applying a refined RRKM theory which involved a weak collision effect:  $\log k_0/[\text{Ar}] = 12.56 - 59/\theta$  L/mole/sec  $\log k_\infty = 13.86 - 91.0/\theta$  sec<sup>-1</sup>.

The low-pressure rate constant is in agreement with the value derived by Holbrook<sup>12</sup> from the data reported in reference 11.

Data on the pyrolysis of  $\text{CH}_3\text{Cl}$  at a high degree of conversion were reported by LeMoan<sup>15</sup>. The reaction was run at 993K for 30 hours in a batch reactor yielded conversions larger than 95%. The gas phase contained  $\text{HCl}$ ,  $\text{CH}_4$ , and small quantities of  $\text{H}_2$ , benzene, and toluene. Low transient concentrations of  $\text{CH}_2\text{Cl}_2$ ,  $\text{C}_2\text{H}_6$ , and  $\text{C}_2\text{H}_5\text{Cl}$  were detected at the beginning of the pyrolysis. In the liquid phase, benzene (72%), toluene (11%), xylene (1%), and monochlorobenzene (12%) were identified. There were two distinct solid phases: carbon in the reactor and naphthalene and soot at the exit from the reactor. The reaction mechanism, despite the large number of products identified, was considered to be schematically simple. It was proposed that, initially,  $\text{CH}_3\text{Cl}$  would decompose into  $\text{HCl}$  and  $^1\text{CH}_2$ , which would dimerize into  $\text{C}_2\text{H}_4$  or decompose into  $\text{CH} + \text{H}$  or  $\text{C} + \text{H}_2$ . The combination of two  $\text{CH}$  radicals would form acetylene. Acetylene would combine, then cyclize to form benzene, from which the identified higher molecular weight compounds would be formed. The hydrogenation of  $\text{CH}_2$  radicals would lead to methane. As we shall see later, this mechanism is not plausible.

$\text{CH}_3\text{Cl}$  decomposition was also studied by Weissman and Benson<sup>5</sup> using a flow system to generate product distributions at temperatures of 1260 and 1310K and over the pressure range of 180 - 370 torr. They measured  $\text{CH}_4$ ,  $\text{C}_2\text{H}_2$ ,  $\text{C}_2\text{H}_4$ , and  $\text{HCl}$  as the major products with lower quantities of aromatic hydrocarbons and soot using Gas Chromatography and Mass Spectrometry techniques.

In 1988, Senkan et al.<sup>16</sup> constructed a  $\text{CH}_3\text{Cl}$  combustion mechanism by combining a mechanism describing  $\text{CH}_4$  combustion together with a sub-mechanism describing the chlorine inhibition of  $\text{CO}$  oxidation. This mechanism was used to calculate the stable species concentration profiles in atmospheric pressure sooting (fuel rich)  $\text{CH}_3\text{Cl}/\text{CH}_4/\text{O}_2/\text{Ar}$  premixed flat flames. Their studies concluded that  $\text{CH}_3\text{Cl}$  promotes not only the decay of  $\text{CH}_4$  to  $\text{CO}_2$  and  $\text{H}_2\text{O}$  but also soot formation by



simultaneously increasing the rates of  $C_2H_3$  and  $C_2H_2$  formation. However a number of their rate constants were from estimation techniques and their mechanism extended only up to  $C_2$ -species. The  $C_1$  reaction mechanism involving unimolecular decomposition, abstraction, and oxidation is reasonably well understood in describing  $CH_4$  combustion at present. The  $C_2$  chemistry, however, is in need of improvement, specifically the reactions of chlorinated  $C_2$  radicals. Thermal decomposition, oxidation by O and  $O_2$ , recombination and addition of  $CH_3$  and  $C_2$  radicals are five competitive reactions. These are all important because Cl abstracts H rapidly (high Arrhenius A factor and low energy of activation), which produces the active hydrocarbons and a H radical pool early in the reaction. These hydrocarbon radicals combine to form more  $C_2$  radicals due to the presence of Cl atoms. The  $C_2$  chemistry is therefore more important here even though the species at molecular weights above 2 carbons account for under 15% of the carbon in the  $CH_3Cl/CH_4/O_2$  system.

Miller et al.<sup>17</sup> studied the high temperature product distributions from reaction of  $CH_4$  and  $CH_3Cl$  under pyrolysis, preignition oxidation and flame conditions. For pyrolysis and preignition studies, 3% fuel/zero  $O_2$  or stoichiometric  $O_2/10\% N_2/Ar$  were heated behind reflected shocks to temperatures between 1200 - 2600K at a density of  $2.5 \pm 0.25 \times 10^{-5}$  mole/cm<sup>3</sup>. Flame studies were conducted at atmospheric pressure for  $CH_4/air$  and  $CH_3Cl/CH_4/air$  mixtures with equivalence ratios of 1.15 and 1.35 respectively. They reported that  $CH_3Cl$  is more easily decomposed than  $CH_4$  in either pyrolysis or preignition oxidation. In the flame environment, the  $CH_4$  and  $CH_3Cl$  disappear at approximately the same rate. They also reported that the presence of chlorine decreases the measured ethane concentration and promotes the formation of acetylene which may explain the propensity for soot formation from chlorinated hydrocarbons.

Roesler et al.<sup>18</sup> studied moist CO oxidation chemistry inhibited by HCl experimentally and numerically with dilute mixtures of CO (~1%),  $H_2O$  (~0.5%),  $O_2$  and HCl reacting in  $N_2$  at a temperature near 1000K. The effect of increasing the Cl/H ratio

was investigated by increasing HCl concentrations from 0 to 200 ppm while the effect of excess O<sub>2</sub> was studied by varying the fuel oxidizer equivalence ratio from 1.0 to 0.33. The results showed that small quantities of HCl inhibit CO oxidation and that increasing O<sub>2</sub> concentrations to stoichiometric mixtures further decreases the oxidation rate, a counter intuitive result. They used sensitivity and reaction flux analysis to determine the rate-controlling inhibition steps/pathways created by HCl. They found the principal chain terminating step at 1000K to be the reaction  $\text{Cl} + \text{HO}_2 \rightarrow \text{HCl} + \text{O}_2$ .

Experimental and numerical studies of the thermal destruction of CH<sub>3</sub>Cl in the post-flame zone of a turbulent combustor under fuel lean conditions (equivalence ratio 0.3 - 0.6) were conducted by Koshland et al.<sup>19</sup> Their results showed that there is an optimal concentration level (ca. 100 ppm) where CH<sub>3</sub>Cl is most effectively destroyed in the post-flame region, with higher or lower levels more difficult to destroy. They proposed that the injection of fuels into the post-flame region (under fuel lean conditions) can increase the destruction efficiency or reduce the peak temperature needed for adequate destruction of CH<sub>3</sub>Cl and its by-products by increasing the radical concentrations and the rate of subsequent destruction reactions.

A recent study on the pyrolysis and oxidation of CH<sub>3</sub>Cl was also conducted by Huang and Pfefferle<sup>20</sup> using a tubular flow reactor at 863.4 torr and a temperature range from 1100 to 1350K. They modified two models published by Senkan and by Miller primarily increasing the rate for the initial CH<sub>3</sub>Cl pyrolysis and by adding two routes for reaction of oxygen with CH<sub>2</sub>Cl to formaldehyde and chloroformaldehyde. They concluded that the CH<sub>3</sub>Cl decomposition was faster than previously reported.

Although some investigations of the reaction of H<sub>2</sub>/O<sub>2</sub> with chloromethanes have been implemented, detailed kinetic models of these reactions are necessary to explain the experimentally observed behavior. It is hoped that, taken together, these steps will adequately describe the experimental observations.

## **CHAPTER 2**

### **EXPERIMENTAL METHOD**

#### **2.1 Experimental Apparatus**

A diagram of the experimental apparatus is shown in Figure 2.1. The high temperature tubular flow reactors, operated isothermally and at atmospheric pressure in this study. The tubular flow reactor was made of quartz and maintained at a constant temperature by a three-zone oven, with each zone controlled separately.

Argon, carrier gas, was passed through one set of series saturation bubblers in parallel to pick up the Dichloromethane which was kept at 0°C using an ice bath. A second line of argon (after the bubblers) was brought in as make-up to meet the exact ratio of flow needed. Oxygen and hydrogen were then brought into the flow stream as required. Before entering the reactor, the mixtures were preheated to limit cooling at the reactor entrance and help ease the reactor heating requirement. Each quartz reactor tube was housed within a three--zone Lindberg electric tube furnace.

The reactor effluent was monitored by an on-line Gas Chromatograph (GC) equipped with a Flame Ionization Detector (FID) and either a Thermal Conductivity Detector (TCD) or a methanation catalyst converter (for CO and CO<sub>2</sub>) & FID. The lines between the reactor exit and the GC were heated to 80°C to limit condensation. When the reactor inlet switch valves were properly selected, the vapor mixture would be transferred directly from the bubbler to the GC sampling inlet via a reactor by-pass line. This was necessary to determine the GC peak area which corresponded to the initial input concentration (and ratio) of the mixtures. The reactor effluent gas passed through a heated 85°C transfer line to the GC gas sample valve and exhaust.

In this experiment, three different diameter reactors were studied. They were 4.0, 10.5, and 16 mm ID and allowed us to vary reactor surface to volume (S/V) ratio. Use of these S/V ratios allowed us to decouple apparent wall and bulk phase decomposition rates

using a plug flow assumption and pseudo first order reaction system. The pseudo first order reaction was first validated for each reactor via straight line graphs on a  $\ln C/C_0$  versus time plot where  $C$  is concentration of parent chlorocarbon.

Outlet gases from the reactor were passed to the GC through Pyrex tubing, packed with glass wool to trap carbon particles and prevent contamination of the GC sampling valve. The bulk of the effluent was passed through a sodium bicarbonate ( $\text{NaHCO}_3$ ) flask for neutralization before release to the atmosphere via a fume hood.

## 2.2 Temperature Control and Measurement

This study was carried out with nearly isothermal reaction conditions ( $\pm 5^\circ\text{C}$ ) at the desired temperature using a three zone furnace. Each zone was equipped with independent solid state temperature controllers (Omega Engineering, Inc.). These controllers operated a solenoid for switching of a controlled voltage (time proportional switching) to the respective heater.

The circuitry for the temperature controller operated solenoids and Variac control of the switched voltage (via relays) was designed at NJIT. It is described here for completeness.

1. Both the relays and Omega temperature controllers were operated via 110 volt AC; i.e. the coil in the relays was run at 110 VAC.
2. The voltage applied to the relay contacts; i.e. voltage that is applied to the heater coils, was controlled with a Variac of proper current rating.
3. The resistance heater voltage was typically 50% of the rated capacity of the heater and thus insured long life of the heater elements.
4. A schematic of voltage and thermocouple inputs to temperature controller is shown in Fig 2.2.

The actual temperature profile of the tubular reactor was obtained using a K type thermocouple which could be moved coaxially within reactor from one end to the other. The temperature measurement was performed with a steady flow rate of argon gas through the reactor to emulate actual reaction conditions. Temperature profiles obtained as shown in Figure 2.3 were isothermal to within  $\pm 5^{\circ}\text{C}$  for 41.9 cm of reactor length.

### 2.3 Quantitative Analysis of Reaction Products

A Perkin Elmer 900 gas chromatograph with FID/TCD or FID/catalyst converter FID was used on-line to quantitatively determine the concentration of the reaction products. The lines between the reactor exit and the GC were heated to  $85^{\circ}\text{C}$  to limit condensation. The GC column for the FID is a 1.5 m long by 1/8" O.D. stainless steel tube packed with 1 % Alltech AT-1000 on Graphpac GB and the column for the TCD is a 1.8 m long by 1/8" O.D. stainless steel tube packed with GCA-013 SPHEROCARB 100/120 mesh.

The GC inlet sampling used a ten port sample valve (Valco Instrument Co.) with two 1.0 ml volume loops maintained at  $175^{\circ}\text{C}$  and 1 atm pressure (allowed dual sample injections onto each GC column). When the sample valve was in the load position, Helium, carrier gas, passed directly to GC column and reactor effluent gas filled these two sample loops. Turning the valve to the inject position, Helium would go into the sample loops and then flush the sample into the two different columns and detectors.

Integration of the peaks on each chromatogram was performed with a dual channel Spectraphysics 4270 integrator using an attenuation of 1 and chart speed of 0.25 cm/min. Representative chromatograms are shown in Figure 2.4, 2.5 and Table 2.1 with retention times and peak identification.

**Table 2.1 Average Retention Time of Products**

Compounds	Average Retention Time (min.)
CH <sub>4</sub>	1.55
C <sub>2</sub> H <sub>2</sub>	1.95
C <sub>2</sub> H <sub>4</sub>	2.20
CH <sub>3</sub> Cl	3.65
C <sub>3</sub> H <sub>6</sub> + C <sub>3</sub> H <sub>8</sub>	5.45
C <sub>2</sub> H <sub>3</sub> Cl	6.40
CH <sub>2</sub> Cl <sub>2</sub>	8.80
C <sub>4</sub> H <sub>10</sub>	10.40
CH <sub>2</sub> CCl <sub>2</sub>	11.15
CHClCHCl	12.45
CHCl <sub>3</sub>	15.10
CHClCCl <sub>2</sub>	16.70
CH <sub>2</sub> ClCHCl <sub>2</sub>	17.60
H <sub>2</sub>	0.9 (TCD)
O <sub>2</sub>	1.9 (TCD)
CO	3.1 (TCD)
CH <sub>4</sub>	6.3 (TCD)
CO <sub>2</sub>	9.8 (TCD)

Calibration of the flame ionization detector to obtain appropriate molar response factors was done by injecting a known quantity of the relevant compound such as CH<sub>4</sub>, C<sub>2</sub>H<sub>6</sub>, CH<sub>2</sub>Cl<sub>2</sub>, C<sub>2</sub>H<sub>3</sub>Cl etc., into the injection port then measuring the corresponding response area. The relative response factor has been determined for compounds shown in Table 2.2. The response factors for C<sub>1</sub> compounds are all similar which is consistent with the converter that FID's are carbon counters and that we had sufficient H<sub>2</sub> flow to convert the Cl's to HCl as well as hydrogen to H<sub>2</sub>O, and the response factor of C<sub>2</sub> compounds are nearly twice the response of C<sub>1</sub> compounds. These results agree with the general principle of flame ionization detector which is well known as a carbon counter<sup>21</sup>. Thus, the effect of chlorine on the relative response factor can be neglected for this flame ionization detector and the relative response factors can be considered to correspond the number of carbon in the molecule. Based on the experimentally verified relative response

factors, the specific component peak area from each set of samples was converted to the equivalent number of moles of each compound.

A series of eight residence times at each reaction temperature were run for a given inlet concentration set by systematic variation in the total flow rate, while maintaining a constant reactant ratio. Every third run was repeated to ensure reproducibility of results.

**Table 2.2 Relative Response Factor in FID and TCD**

Compounds	Relative Response Factor (RRF)
Methane $\text{CH}_4$	1.07
Acetylene $\text{C}_2\text{H}_2$	1.60
Ethylene $\text{C}_2\text{H}_4$	2.00
Ethane $\text{C}_2\text{H}_6$	1.96
Propene $\text{C}_3\text{H}_6$	3.47
Propane $\text{C}_3\text{H}_8$	3.42
Dichloromethane $\text{CH}_2\text{Cl}_2$	1.00
Butane $\text{C}_4\text{H}_{10}$	4.31
1,1 Dichloroethylene $\text{CH}_2\text{CCl}_2$	2.10
1,1,1 Trichloroethane $\text{CH}_3\text{CCl}_3$	1.85
Chloroform $\text{CHCl}_3$	0.98
Tetrachloromethane $\text{CCl}_4$	1.18
1,1,2 Trichloroethane $\text{CH}_2\text{ClCHCl}_2$	2.10
Hydrogen $\text{H}_2$	0.02 (TCD)
Oxygen $\text{O}_2$	1.71 (TCD)
Carbon monoxide $\text{CO}$	2.25 (TCD)
Carbon dioxide $\text{CO}_2$	1.82 (TCD)

## 2.4 Hydrochloric Acid Analysis

Quantitative analysis of HCl product was performed for reactions in each reactor and residence time. The samples for HCl analysis were collected independently from the GC sampling as illustrated as Figure 4.1. In this analysis, the effluent was bubbled through a two stage bubbler before being exhausted to the fume hood. Each stage contained 20 ml of 0.01 M NaOH and two drops of phenolphthalein indicator. The gas passed through

these two stage bubblers until the first stage solution reached its end point. The time required for this to occur was recorded. At this point, the bubbling was stopped and the two solutions were combined. The effluent HCl concentration was calculated based upon titration of the combined solution with standardized 0.01 M HCl to the phenolphthalein end point. Several titrations were performed using buffered solution (pH 4.7) to discern if CO<sub>2</sub> was affecting the quantitative measurement of HCl. No significant effect was observed due to the relatively low levels of CO<sub>2</sub>.

### **2.5 Qualitative Identification of Reaction Products**

Positive identifications of all reactor effluent species were made by GC/Mass Spectrometry applied to batch samples drawn from the reactor exit into previously evacuated 25 ml stainless steel or Pyrex glass sample cylinders. A Finnigan 4000 series GC/MS, with a 50m×0.22mm I.D. methyl silicone stationary phase column was used. Gas samples were inlet by cryofocussing (at 78 K) on a 12 cm length of the capillary column.



## CHAPTER 3

### ESTIMATION OF THERMOCHEMICAL DATA

Thermochemical data are required to determine the energy balance in chemical reactions and in determining the Gibbs free energy of a reaction as a function of temperature. It also provides a convenient way to determine reverse reaction rate constants from the calculated equilibrium constant of the reaction and the known forward rate. In this study, a detailed elementary reaction mechanism has been developed based upon literature data, general trends, fundamental thermodynamic principles and Transition-State-Theory<sup>22</sup>. An accurate thermodynamic database for all radical and molecular species in the mechanism is extremely important. In addition, the thermochemical parameters including enthalpy of formation, entropy and heat capacities for many chloro-oxy-carbon products and intermediates have not been previously measured or calculated and they are required for input to detailed modeling codes.

The thermochemical database including enthalpy of formation ( $H_f$ ), entropy ( $S_f$ ), and heat capacities ( $C_p$ ) is based upon our evaluation of the best currently available thermochemical data. Appendix A shows a summary of the species involved and thermochemical quantities employed. When experimental thermochemical data were not available, the values were estimated using the techniques of group additivity and the THERM<sup>23,24</sup> computer code.

The use of group additivity methods and THERM is described in detail in references 23, 24, and THERM user manual. Thermodynamic data can often be calculated easier and faster using THERM than if one searched through the literature.

When required properties for various Benson type groups<sup>22</sup> were not available, estimates were made based on reasonable modifications of the properties of groups from similar compounds or from properties of a series of species with the concerned chemical functional group. Items considered were structure, number of chlorines, effect of Cl atom

on intramolecular bond strength and Cl - Cl repulsion. After estimating the data, the estimated data were compared to recently published experimental data where available. If the experimental measured data were not available, the estimated data were judged reasonable if similar results were obtained by two different estimation methods such as shown in the following example.

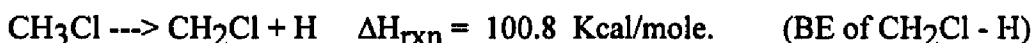
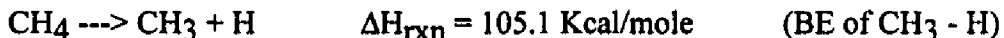
Two different methods are used and their results compared to estimate the  $H_f^{298}$  for  $CH_2ClOH$ . Group additivity was then used to back calculate the C/Cl/H<sub>2</sub>/O group.

Method 1.  $CH_2ClOH \rightarrow CH_2Cl + OH$

$$\begin{aligned}\Delta H_{rxn} &= -H_f(CH_2ClOH) + H_f(CH_2Cl) + H_f(OH) = BE \\ &= -H_f(CH_2ClOH) + 29.1 + 9.45 = -H_f(CH_2ClOH) + 38.6\end{aligned}$$

$H_f^{298}$  of 29.1 Kcal/mole for  $CH_2Cl$ , 9.45 Kcal/mole for OH. The existence of Cl affects a Resonant Stabilization Energy (RSE) as illustrated below:

BE of  $CH_3 - H$  and BE of  $CH_2Cl - H$ , that is,  $105.1 - 100.8 = 4.3$  Kcal/mole



The RSE due to Cl is  $105.1 - 100.8 = 4.3$  Kcal/mole. Hence BE of  $CH_2Cl - OH$  is  $92.7 - 4.3 = 88.4$  Kcal/mole, where 92.7 is the  $CH_3 - OH$  bond.

Therefore

$$H_f(CH_2ClOH) = 38.6 - 88.4 = -49.8 \text{ Kcal/mole}$$

Method 2.  $CH_2ClOH \rightarrow CH_2OH + Cl$

$$\begin{aligned}\Delta H_{rxn} &= -H_f(CH_2ClOH) + H_f(CH_2OH) + H_f(Cl) = BE \\ &= -H_f(CH_2ClOH) - 2.16 + 28.9 = -H_f(CH_2ClOH) + 26.74\end{aligned}$$

Start with the bond energy of  $CH_3 - Cl$ , which is 83.61 Kcal/mole. Here the presence of OH effects a Resonant Stabilization Energy (RSE) as shown:

BE of  $CH_3 - H$  and BE of  $CH_2OH - H$ , that is,  $105.1 - 98 = 7.1$  Kcal/mole for the RSE due to OH.



Hence  $83.61 - 7.1 = 76.51$  Kcal/mole is the BE for  $\text{CH}_2\text{Cl} - \text{OH}$ . Therefore

$$H_f(\text{CH}_2\text{ClOH}) = 26.74 - 76.51 = -49.77 \text{ Kcal/mole}$$

The enthalpy of formation for  $\text{CH}_2\text{ClOH}$  is  $-49.8$  Kcal/mole. We can now use this  $H_f^{298}$  for calculation of the C/Cl/H<sub>2</sub>/O group

Species	$H_f$
C/Cl/H <sub>2</sub> /O	?
O/C/H	-37.9
$\text{CH}_2\text{ClOH}$	-49.8

$$\text{C/Cl/H}_2\text{/O} = -49.8 - (-37.9) = -11.9$$

We can further calculate corresponding groups using the same estimation method. The calculated results are listed in Table 3.1

**Table 3.1 New groups for C/Cl/H/O**

Groups	$H_f$
C/Cl/H <sub>2</sub> /O	-11.9
C/C/Cl/H/O	-14.6
C/Cl <sub>2</sub> /H/O	-15.1
C/C/Cl <sub>2</sub> /O	-18.37

The above groups were input into the THERM computer code to calculate  $H_f$  for  $\text{CH}_2\text{ClOOH}$  and  $\text{CHCl}_2\text{OOH}$ . Results were compared with the estimation method results. As shown in Table 3.2, the estimation results are in good agreement with the THERM<sup>20</sup> group additivity.

Estimations of entropy and heat capacity are made based on reasonable modifications of the values of similar groups. In this example, the contribution of S of (C/C/Cl/H/O) can be estimated from the S of (C/C<sub>2</sub>/Cl/H) because the carbon atom is similar to oxygen atom in mass. This assumption must be verified and compensate the

difference between C and O. We can look at the difference between  $S(C/C_2/H_2)$  group versus  $S(C/C/H_2/O)$  group and  $S(C/C/H_3)$  group versus  $S(C/H_3/O)$  group.

**Table 3.2 Validation of estimation method**

Reaction	BE	H <sub>f</sub>	THERM
$CH_2ClOOH \rightarrow C.H_2OOH + Cl$	72.51	-32.59	-32.7
$CH_2ClOOH \rightarrow CH_2Cl. + OOH$	64.90	-32.30	
$CH_2ClOOH \rightarrow CH_2ClO. + OH$	104.0	-32.68	
$CHCl_2OOH \rightarrow C.HClOOH + Cl$	69.70	-36.30	-35.90
$CHCl_2OOH \rightarrow CHCl_2. + OOH$	62.90	-35.90	
$CHCl_2OOH \rightarrow CHCl_2O. + OH$	44.28	-35.88	

From THERM group database,

$$S(C/C_2/H_2) - S(C/C/H_2/O) = 9.42 - 9.8 = -0.38$$

$$S(C/C/H_3) - S(C/H_3/O) = 30.41 - 30.41 = 0.0$$

Set the adjustment in  $S^{298}$  as -0.38 for substitution of O for C. Then:

$$S(C/C_2/Cl/H) - S(C/C/Cl/H/O) = S(C/C_2/H_2) - S(C/C/H_2/O) = -0.38$$

$$S(C/C/Cl/H/O) = S(C/C_2/Cl/H) + 0.38 = 17.6 + 0.38 = 17.98$$

Based upon the above calculation, we can further estimate  $S(C/Cl/H_2/O)$  group.

$$S(C/C_2/Cl/H) - S(C/C/Cl/H_2) = S(C/C/Cl/H/O) - S(C/Cl/H_2/O)$$

$$S(C/C/Cl/H_2/O) = S(C/C/Cl/H/O) - S(C/C_2/Cl/H) + S(C/C/Cl/H_2)$$

$$= 0.38 + 37.8 = 38.18$$

The estimation technique for heat capacity is similar to the above calculations for S. The final calculation results are listed in Table 3.3.

**Table 3.3 New groups for  $S^{298}$  and  $C_p$**

Groups	$S^{298}$	Cp300	Cp400	Cp500	Cp600	Cp800	Cp1000
C/Cl/H <sub>2</sub> /O	38.18	8.39	10.60	12.35	13.48	15.35	16.69
C/C/Cl/H/O	17.98	8.49	9.80	9.95	11.28	13.94	14.59
C/Cl <sub>2</sub> /H/O	44.08	11.59	13.90	15.45	16.58	17.94	18.69
C/C/Cl <sub>2</sub> /O	22.78	11.69	14.78	16.00	16.56	17.00	17.01

## **CHAPTER 4**

### **ESTIMATION OF KINETIC PARAMETERS**

#### **4.1 Background**

Benson postulated that in a dilute gas there are only two type of elementary kinetic processes. The first is unimolecular process wherein an energetically activated chemical species reacts, when it is isolated from other gas phase species by internal rearrangement of atoms, breaking a bond, or molecular elimination. The second process is bimolecular and requires the collision of two chemical species to form a collision complex. The resulting collision complex is an energized adduct which follows a subsequent unimolecular chemical process.

There are extensive rate constant data for hydrocarbon (HC) oxidation processes and methods have been developed for making estimations. Allara and Shaw<sup>25</sup> carried out a systematic kinetic study on the thermal degradation of n-alkane molecules. Unfortunately, most of those measurements are at low temperature; therefore, the results must be extrapolated and a certain degree of error is introduced here.

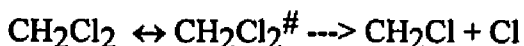
Baulch et al.<sup>26</sup> have published an extensive review of the kinetic data for the reaction of inorganic chlorinated species with themselves and with other atoms and diatoms likely to be found in a combustion system. There exists a considerable base of older data on the reactions of chlorine with organic systems due to the industrial importance of the chlorination of hydrocarbons.

Atkinson et al.<sup>27</sup> update and extend the previous critical evaluations of the kinetics and photochemistry of air pollutant chemical reactions on a routine basis. The NIST Chemical Kinetics Database<sup>28</sup> provides a tool for rapidly examining the literature for the chemical kinetics community. The program will find data on a particular reaction, all of the reactions of a species, or subsets of all of the reactions.

## 4.2 Unimolecular Dissociation

### 4.2.1 Simple fission

Based on Transition-State-Theory (TST), the rate constant for simple fission can be expressed in thermodynamic terms, since it is more useful to work with the rate constant in this form than with partition functions. Consider the unimolecular reaction



The first order rate constant for decomposition of  $\text{CH}_2\text{Cl}_2$  is given by

$$k = (k_B T/h) K_{eq}^\#$$

where  $K_{eq}^\#$  is the equilibrium constant for formation of the  $[\text{CH}_2\text{Cl}_2]^\#$  complex.

( $^\#$  denotes a Transition-State-Theory complex)

If the equilibrium constant is expressed in terms of the molar Gibbs free energy using the

van't Hoff relation  $\Delta G^\# = -RT \ln K_{eq}^\#$

the rate constant can be written as

$$k = (k_B T/h) \exp(-\Delta G^\#/RT)$$

where  $k_B$ ,  $h$ ,  $R$  are the Boltzman, Planck's and gas constant respectively.

$\Delta G^\#$  may be expressed in terms of enthalpy ( $\Delta H$ ) and entropy ( $\Delta S$ ) changes by

$$\Delta G^\# = \Delta H^\# - T\Delta S^\#$$

In thermodynamic language

$$k = (k_B T/h) \exp(\Delta S^\#/R) \exp(-\Delta H^\#/RT)$$

This equation is similar to the Arrhenius equation

$$k = A \exp(-E_a/RT)$$

and the thermodynamic parameters can be related to the Arrhenius parameters. We can use thermodynamics and equilibrium theory to estimate the Arrhenius activation energy in terms of the thermodynamic properties of the transition state:

$$d(\ln k) / dT = E_a/RT^2$$

From  $k = (k_B T/h) K_{eq}^\#$  and differentiating with respect to  $T$  gives

$$d(\ln k)/dT = 1/T + d(\ln K_{eq}^\#)/dT$$

Since  $K_{eq}^\#$  is an equilibrium constant, its variation with temperature is given by the Gibbs-Helmholtz equation

$$d(\ln K_{eq}^\#)/dT = \Delta E/RT^2$$

Comparing with Arrhenius activation energy, we can obtain

$$E_a = RT + \Delta E$$

Since  $H = E + PV$ , for a constant-pressure process and there is no change in the number of molecules in going from the reactants to the transition state ( $\Delta V$  is zero); therefore, in this case

$$E_a = \Delta H^\# + RT$$

Insertion of this equation into

$$k = (k_B T/h) \exp(\Delta S^\#/R) \exp(-\Delta H^\#/RT)$$

leads to

$$k = (ek_B T/h) \exp(\Delta S^\#/R) \exp(-E_a/RT)$$

Hence

$$A = (ek_B T/h) \exp(\Delta S^\#/R)$$

where  $T$  is the temperature at which the experiments have been carried out.

Usually,  $\Delta S^\#$  is unknown, therefore  $A$  factors are estimated from literature values or by using generic reaction series. In this case, a comparison of the reaction to a similar reaction system, where the rate parameters are known is made. As listed in Table 4.1, 4.2, and 4.3, the generic reaction series shows a consistent trend based on heat of reaction. We can also estimate  $\Delta S^\#$  from statistical mechanics and an assumed Transition-State structure geometry. In practice we do not use the Transition-State thermodynamic  $E_a^\#$  or  $H^\#$  but often use conventional thermodynamic properties which are known.

**Table 4.1 C-H Rupture in Hydrocarbon Molecules**

Reactions	log A	E <sub>a</sub>	ΔH
CH <sub>4</sub> ---> CH <sub>3</sub> + H	15.4	105.0	104.8
C <sub>2</sub> H <sub>6</sub> ---> C <sub>2</sub> H <sub>5</sub> + H	15.3	100.7	100.7
C <sub>3</sub> H <sub>8</sub> ---> C <sub>3</sub> H <sub>7</sub> + H	15.4	100.7	100.7
C <sub>4</sub> H <sub>10</sub> ---> C <sub>4</sub> H <sub>9</sub> + H	15.4	100.7	100.7

(Ref: Dean, A.M., J. Phys. Chem., 89, 4600, 1985)

Simple unimolecular (elimination) rate constants are determined by two methods similar to beta scission reactions. The unimolecular Quantum Kassel formalism was used. Here, the reverse reaction (combination) parameters for the high pressure case are determined. Then the corresponding high pressure unimolecular beta scission rate constants using microscopic reversibility <MR> are calculated.

$$\Delta G = -RT \ln K_{eq} = \Delta H - T\Delta S \quad \text{for the reaction}$$

$$\Delta H/RT - \Delta S/R = (E_f - E_r)/RT - \ln(A_f / A_r)$$

where f and r denote forward and reverse reaction.

Transforming the above equation to a standard state expressed in concentration units:

$$(\Delta H_c + \Delta nRT)/RT - (\Delta S_c + \Delta nR \ln(R'T))/R = (E_f - E_r)/RT - \ln(A_f / A_r)$$

where Δn is the mole change in the reaction.

$$(E_f - E_r) = \Delta H_c$$

$$\ln(A_f / A_r) = \Delta S_c/R + \Delta n \ln(eR'T)$$

The high pressure unimolecular elimination parameters are then input to the Quantum Kassel formalism to calculate the apparent rate constants at the appropriate pressure. The second method is simple use of the reverse rate constants from the Quantum Kassel combination reaction calculations.



**Table 4.2 C-C Rupture in Hydrocarbon Molecules**

Reactions	log A	E <sub>a</sub>	ΔH
C <sub>2</sub> H <sub>6</sub> ---> CH <sub>3</sub> + CH <sub>3</sub>	16.9	89.4	89.8
C <sub>3</sub> H <sub>8</sub> ---> C <sub>2</sub> H <sub>5</sub> + CH <sub>3</sub>	16.9	84.4	85.5
C <sub>4</sub> H <sub>10</sub> ---> C <sub>3</sub> H <sub>7</sub> + CH <sub>3</sub>	17.0	84.7	85.9
C <sub>4</sub> H <sub>10</sub> ---> C <sub>2</sub> H <sub>5</sub> + C <sub>2</sub> H <sub>5</sub>	16.9	80.2	81.9
C=CC ---> C=C. + CH <sub>3</sub>	16.9	99.5	100.3

(Ref: Dean, A.M., J. Phys. Chem., 89, 4600, 1985)

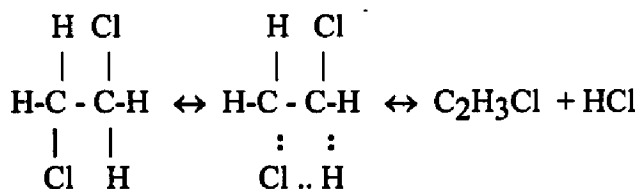
**Table 4.3 C-H Rupture in Hydrocarbon Radicals**

Reactions	log A	E <sub>a</sub>	ΔH
C <sub>2</sub> H <sub>5</sub> ---> C=C + H	13.2	40.9	38.7
CCC. ---> CC=C + H	12.8	38.5	36.0
CCCC. ---> CCC=C + H	12.7	38.3	36.1
C=CC. ---> CC=C=C + H	13.1	61.3	58.9
CC.C ---> CC=C + H	12.8	39.6	38.8
CCC.C ---> CCC=C + H	12.7	39.6	39.1
CCC.C ---> CC=CC + H	12.2	39.6	36.4

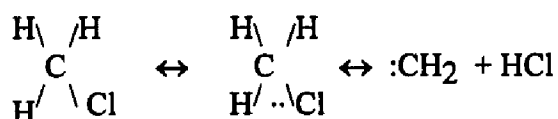
(Ref: Dean, A.M., J. Phys. Chem., 89, 4600, 1985)

**4.2.2 Complex fission (molecular elimination)**

The second kind of unimolecular reaction is the formation of a cyclic transition state and the elimination of a molecule. For example, we may consider the elimination of HCl from chlorinated hydrocarbons (CHCs); for example,



These seem to involve four atoms in a ring transition state and are referred to as four-center reaction. Cases are also found of three-center reactions:



Benson<sup>22</sup> declared that the overall rate constants for these kinds of reactions are dependent on the relative rate of ring closure and biradical fission and are not completely understood. We may estimate Arrhenius A factor from Transition-State-Theory <sup>22</sup>(TST)

$$A = (ek_B T/h) \exp(\Delta S^\ddagger/R) * g$$

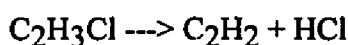
where g is degeneracy; for example,  $\text{CH}_2\text{ClCH}_2\text{Cl} \rightarrow \text{C}_2\text{H}_3\text{Cl} + \text{HCl}$

each of 2 Cl's can react with 2 H's, so  $g = 2 * 2 = 4$ .  $\Delta S^\ddagger$  is about -4.3 cal/mole/K for loss each rotor (C-C bond).

Activation energy  $E_a$  can be estimated as

$$E_a = \Delta H + \text{Energy Barrier}$$

Bozzelli<sup>29</sup> proposed that the energy barrier is about 35 - 45 Kcal/mole. Zabel<sup>30</sup> indicated that for



The energy barrier is 45 Kcal/mole. Here, we break two single bonds add to double bond to form a triple bond, with no rotor loss because of the double bond.

In this study, we calculated a barrier for  $\text{CH}_3\text{Cl}$  three-center reaction to  $^1\text{:CH}_2 + \text{HCl}$  of 3.75 Kcal/mole. The  $E_a$  is from analysis of reaction of  $^1\text{:CH}_2$  which is widely shown to insert into hydrocarbons with an  $E_a$  of 0.0 and on insertion of  $^1\text{:CCl}_2$  into HCl, which we have experimentally measured to be 15 Kcal/mole. One possible reason for this apparent activation energy is that the electrons from the Cl atom may reduce the ability of the un-occupied orbital on the singlet methylene to combine with bonding electrons in the molecule.

An Evans-Polanyi<sup>22</sup> relationship between  $E_a$  and  $\Delta H$  for HCl elimination reaction can be made. A plot of  $E_a$  versus  $\Delta H$  for HCl elimination reaction is shown in Fig. 4.1. A best fit relationship of  $E_a = 1/2 (\Delta H + 100)$  is obtained for the  $\Delta H = 0 - 100$  Kcal/mole range.

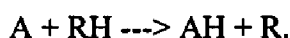
### 4.2.3 Beta Scission Reactions

These reactions utilize the Quantum Kassel formalism and are treated in one of two ways. In the first method, a Quantum Kassel formalism is used. The reverse reaction (addition) parameters for the high pressure case are determined. The corresponding high pressure unimolecular beta scission rate constants using microscopic reversibility <MR> are then calculated. The high pressure unimolecular elimination parameters are then input to the Quantum Kassel formalism to determine the high pressure limit and to calculate the apparent rate constants at the appropriate pressure. The second method is simple use of the reverse rate constants from the QRRK calculations.

## 4.3 Bimolecular reactions

### 4.3.1 Abstraction reaction

There are two types of abstraction reactions: first is atom + stable molecule



second is radical + stable molecule



Abstraction reaction rate constants are not pressure dependent and therefore do not incorporate any Quantum Kassel Analysis. The rate constants are taken from evaluated literature<sup>28,31</sup> wherever possible. When estimation is required for an abstraction rate constant, a generic reaction is used as a model and adjusted for steric effects as best we can. An example of the generic type of Arrhenius A factor analysis is Cl atom abstracting an H from 1,1, dichloroethylene, where experiments can not determine whether the measured values are for the abstraction or the addition reaction. Use the abstraction by Cl of H from 1,1,1 Trichlorethane where both the mass and the reaction degeneracy are similar. The Ea is calculated separately.

Typical A factors range for abstraction reactions range from 1.0E11 to 1.0E14. Bozzelli<sup>29</sup> summarized A factors for different atoms and radicals as listed in Table 4.4.

**Table 4.4 Kinetic Parameters for Various Types of Reactions**

Type of Reaction	A	E <sub>a</sub>
simple fission	1.0E15 - 5.0E17	$\Delta H - RT$
disproportionation	3.0E11 - 2.0E12	0.0
beta scission	3.0E12 - 3.0E13	$\Delta H + 2 - 6$
intermolecular rearrangement	1.0E13 - 1.0E14	$\Delta H + RS + E_{abs}$
abstraction for H atom		
H + RH	1.0E14	literature
OH + RH	3.0E13	or
O + RH	3.0E13	Evans-Polanyi
Cl + RH	1.0E13	
CH <sub>3</sub> + RH	1.0E12	
C <sub>2</sub> H <sub>5</sub> + RH	1.0E11	
addition to olefin		
H	1.0E13	2.0
CH <sub>3</sub>	2.0E11	7.5
C <sub>2</sub> H <sub>5</sub>	5.0E10	7.5
recombination	1.0E12 - 1.0E14	0.0

Evans-Polanyi analysis is used on the reaction in the exothermic direction to estimate the energy of activation for the rate constant. An Evans-Polanyi plot, E<sub>a</sub> versus  $\Delta H$  of reaction, is shown in figure 4.2 for Cl atom abstraction reactions of H atoms from chlorinated hydrocarbons. One may easily see from the shallow slope that there is only a very small E<sub>a</sub> for these reactions and it does not change much for changes in  $\Delta H$  of the reaction. Clearly, the abstraction reaction in an endo-thermic reaction must incorporate the  $\Delta H$  of the reaction or it, the reaction rate constant, will violate thermodynamics and unfortunately there are a number of examples of rate constants in the literature where the estimated E<sub>a</sub> is less than the endothermicity.

Bozzelli<sup>29</sup> summarized a general rule for the activation energy for H atom abstraction by organic radicals and/or H atom from organic molecules. In exothermic reactions, Bozzelli proposed that E<sub>a</sub> can be approximated as

$$E_a = 12.5 \pm 1 - 0.35 \Delta H_{rxn} \text{ (Kcal/mole)}$$

with the stipulation that  $E_a$  can not be less than zero.

Bozzelli further predicts that Cl atom abstractions proceed with low  $E_a$ 's for exothermic reactions (1.5 Kcal/mole or lower) and  $E_a \approx \Delta H_{rxn}$  for endothermic reactions. For organic radicals abstracting F or Br atoms, Benson<sup>22</sup> estimates  $E_a$ 's are 16 and 6 Kcal/mole respectively. Evans-Polanyi plot is a set of a plot of  $E_a$  versus  $\Delta H$  from similar reactions. After completing the plot, the best slope is determined and put into form of general equation for determination of  $E_a$  knowing only  $\Delta H$ . Figs 4.2-4.5 show some Evans-Polanyi plots developed in this study. A good relationship between  $E_a$  and  $\Delta H$  is obtained and serves as useful tool to estimate kinetic parameters of abstraction reaction when literature values are not available.

#### 4.3.2 Addition Reactions

Addition reactions are treated with the Quantum Kassel formalism described above. The reactions involve addition of an atom or radical to an unsaturated species and typically form an energized adduct with ca 20 to 50 Kcal/mole of energy above the ground state. This is sometimes sufficient to allow the adduct to react with other reaction products (lower energy) before stabilization occurs. An example would be H atom addition to vinyl chloride, an olefin, forming one of two chloro-ethyl radicals with ca 40 Kcal/mole energy above the ground state. In the case of H atom addition to the carbon containing the Cl atom, the chloro-ethyl adduct formed  $C_2H_2CH_2Cl$  could rapidly eliminate (beta scission) to form the lower energy products Cl atom plus ethylene. An example of the Quantum Kassel analysis for this reaction is fully described in Bozzelli and Barat<sup>32</sup>.

It is important to note that reactions to other channels as well as isomerization, in addition to stabilization and reverse reaction are included in this calculation.

### 4.3.3 Combination and Insertion Reactions

These reactions involve the combination of two radical species, or an atom and a radical. The energy of the adduct formed before stabilization is equal to the bond energy of the new bond(s) formed and typically on the order of 80 to 120 Kcal/mole. This is usually sufficient for an adduct, with this initial energy above its ground state energy, to react to lower energy products before stabilization occurs. The high pressure limit rate constant for combination is obtained from the literature or estimated from known generic combinations. The Quantum Kassel chemical activation formalism<sup>6,7</sup> is then used to determine the high pressure limit and to calculate the apparent rate constants at the appropriate pressure to all the recognized available channels.

Again, reaction to other channels as well as isomerization, in addition to stabilization and reverse reaction are included in this calculation. This is an important aspect of reaction analysis for both these combination as well as insertion and addition reactions that other modelers do not incorporate.

This leads to a more correct treatment of fall-off and pressure dependence for these non-elementary reaction systems. Rate constants for the model are obtained which incorporate these pressure effects and dependency therefore make the model more fundamentally correct.

## CHAPTER 5

### REACTION OF OH RADICAL WITH C<sub>2</sub>H<sub>3</sub>Cl REACTION PATHWAY ANALYSIS

#### 5.1 Background

The gas phase reactions of OH radical are important in combustion and incineration of chlorinated hydrocarbons (CHCs) as well as atmospheric chemistry. In combustion environments, OH is often the active radical present in the highest concentrations, where it serves to initiate breakdown of hydrocarbons (HCs). It is also very important in CO burnout producing CO<sub>2</sub>, plus energy, and H atoms. Here if temperature is high, the H atoms may react with O<sub>2</sub> in the critically important chain branching step  $H + O_2 \rightarrow OH + O$ . In atmospheric chemistry, OH is probably the most important active species. It abstracts hydrogen atom from saturated hydrocarbons forming HC radicals, which then react with O<sub>2</sub> and NO, sequentially forming intermediates that contribute to photochemical smog. OH radical also adds to unsaturated hydrocarbons and oxy hydrocarbons forming radicals which then further react with O<sub>2</sub> and NO. Previous studies on OH radical reactions with unsaturated hydrocarbons such as vinyl chloride as well as this analysis show that the addition reaction is predominate at low temperature, while abstraction of H atom becomes important at high temperatures.

Howard<sup>33</sup> has determined the rate constant for reaction of OH with vinyl chloride and other halogenated ethylenes at 296 K at low pressure, 0.7 - 7.0 torr, using a discharge flow reactor with Laser Magnetic Resonance (LMR) detection of OH. The rate constant for reaction with vinyl chloride was observed to be pressure dependent (in the fall-off regime), increasing from ca.  $1.2E12 \text{ cm}^3 \text{ mole}^{-1} \text{ s}^{-1}$  at 0.7 torr to ca.  $3.01E12 \text{ cm}^3 \text{ mole}^{-1} \text{ s}^{-1}$  at 7.0 torr, where it still was not at the high pressure limit.

Perry et al.<sup>34</sup> measured absolute rate constants for reactions of OH radical with vinyl chloride, vinyl fluoride, and vinyl bromide by using a flash photolysis-resonance fluorescence technique between 299 - 426 K at a total pressure of 50 torr ( $C_2H_3Cl$  and  $C_2H_3Br$ ) or 100 torr ( $C_2H_3F$ ). They combined their kinetic data on these halogenated ethylenes with the room temperature high pressure rate constant for the reaction of OH with ethylene to obtain the following relative OH radical rate constants:  $C_2H_3F$ , 0.71;  $C_2H_3Cl$ , 0.84;  $C_2H_3Br$ , 0.87;  $C_2H_4$ , 1.00. The above rate constants appear to show a trend with electronegativity of the halogen substituent - the more electronegative the substituent, the lower the rate constant.

Recently Liu et al.<sup>35</sup> studied the gas phase reaction of OH radical with vinyl chloride at atmosphere pressure (760 torr argon) over the temperature range 313 - 1173 K by pulse radiolysis. The temperature dependence of the rate constants showed behavior similar to that of ethylene in that the predominant reaction changed from an addition reaction below 588 K to hydrogen atom abstraction reaction above 723 K. They also observed a negative temperature dependence and proposed the Arrhenius expression rate constant (high pressure limit) for the addition reaction as:  $1.29E12 \exp(700/RT) \text{ cm}^3 \text{ mole}^{-1} \text{ s}^{-1}$ . The nonlinear form Arrhenius rate constant for the H atom abstraction reaction was  $8.43E6 \cdot T^2 \exp(-2400/RT)$  or in linear Arrhenius form  $1.79E13 \exp(-4020/RT) \text{ cm}^3 \text{ mole}^{-1} \text{ s}^{-1}$ .

The low temperature (addition) reactions are, however, complex and non elementary. An adduct is being formed, which can undergo stabilization via collisions, or before stabilization it may undergo unimolecular reaction to products, or reverse reaction - dissociation back to reactants. OH Addition to this unsaturated chloro-olefin can, in addition, occur at the two different carbon atoms. The addition Arrhenius A factors or activation energies may also change with either the increasing size or electronegativity of the halogen atoms. The total addition rate constants for OH radical with  $C_2H_3Cl$  and 1,2 dichloro ethylenes are, in an added complexity, shown to decrease with increasing



temperature<sup>34</sup>.

There are two distinct carbon atom sites where addition of OH may occur and two different types of H atoms where abstraction can occur. It would be helpful in both combustion and atmospheric chemical analysis and kinetic modeling, to know the rate constants and specific reaction pathways for reaction of OH in each of the above four cases. In this work, the addition and abstraction reactions to the two carbon atom sites in vinyl chloride. The addition reactions are analyzed by multi-frequency Quantum Kassel (QK) analysis, with the QK results compared to predictions from RRKM analysis for the specific case of unimolecular dissociation of the  $\text{CH}_2\text{OHC.HCl}$  adduct. The abstraction reactions are analyzed using the Transition-State-Theory (TST) of Benson<sup>22</sup>. Rate constants for the two different abstraction paths and for addition reactions to specific products versus pressure are given. Thermodynamic parameters of the intermediate radicals and products are also listed.

## 5.2 Quantum Kassel Calculations for Addition Reaction

Energized Complex/QK Theory as described by Dean<sup>6,7</sup> and Bozzelli et al.<sup>36</sup> was used to model OH radical addition reactions to  $\text{C}_2\text{H}_3\text{Cl}$ . Further details on specifics of the chemical activation calculation are presented in reference 36. Pre-exponential A factors and activation energies (Ea) for the bimolecular addition reaction at the high pressure limit are obtained from evaluation of experimental data in the literature, combined with thermochemical analysis. Isomerization reactions are analyzed via Transition-State-Theory (TST) and the thermochemical kinetic methods of Benson<sup>22</sup>.

A and Ea for the dissociation reactions come from analysis of thermodynamic heats of formation and entropies for the species involved and by analogy to similar (generic) reactions. Specific kinetic parameters for dissociation to reactants and products are obtained from application of microscopic reversibility, where the reverse-addition or combination reaction rate constant is obtained from experimental data in the

literature.

### 5.3 Thermodynamic Properties

The thermodynamic properties including enthalpy of formation, entropy, and heat capacities were obtained from the literature when available. Thermodynamic properties for many chloro-oxy-carbon species have not, however, been previously measured or calculated. These have been calculated here using the techniques of group additivity<sup>4</sup> and the "THERM" computer code<sup>23,24</sup>. Bond dissociation energies (BE) from the literature<sup>37</sup> and bond dissociation (BD) groups developed by Lay et.al.<sup>38</sup> to calculate the respective radicals are included. These thermodynamic properties involved in the OH radical with vinyl chloride reaction system are listed in Table 5.1.

The potential energy diagram and input parameters for the chemical activation calculations, both  $\alpha$  - and  $\beta$  - addition (to the CD/Cl/H and CD/H<sub>2</sub> carbons respectively), are shown in Fig.5.1, 5.2 and Table 5.2, 5.3. respectively. The parameters in Table 5.2, 5.3 are referenced to the ground (stabilized) state of the complex because this is the formalism used in QK Theory.

**Table 5.1 Thermodynamic Property Data**

Species	Hf	S	Cp300	400	500	600	800	1000
OH	9.49	43.88	7.16	7.08	7.05	7.05	7.15	7.33
C <sub>2</sub> H <sub>3</sub> Cl	5.0	63.10	12.78	15.58	17.88	19.77	22.56	24.44
CH <sub>2</sub> O	-26.40	52.26	8.45	9.46	10.49	11.49	13.34	14.86
CH <sub>2</sub> Cl	29.10	59.60	9.22	10.18	11.14	12.13	14.10	15.83
CHClO	-39.30	61.80	11.12	12.46	13.55	14.42	15.70	16.58
CH <sub>2</sub> OHC.HCl	-14.60	78.32	18.15	21.22	23.74	25.86	29.23	31.71
CH <sub>2</sub> O.CH <sub>2</sub> Cl	-7.74	73.60	16.19	19.89	23.00	25.58	29.54	32.34
CHClOHC.H <sub>2</sub>	-9.63	77.81	18.20	20.95	22.55	25.21	29.97	32.17
CHClO.CH <sub>3</sub>	-6.21	73.53	17.14	20.14	21.97	24.91	30.24	32.90
CH <sub>2</sub> CHOH	-29.51	64.71	13.60	25.89	18.14	20.23	23.74	26.33
CH <sub>3</sub> CHO	-39.18	63.13	13.22	15.71	18.22	20.47	24.22	26.97

. represents radical site

## 5.4 Addition Reactions

### 5.4.1 $\alpha$ - Addition

The rate constant (high pressure limit) for addition at the  $\alpha$ - site  $k_1$  ( $k$  defined in Table 5.2), is assigned as follows:  $A_1$  is 0.5 that for 1,2 dichloroethylene + OH because the probability of OH addition to the CD/Cl/H carbon is half of what that of 1,2 dichloroethylene.  $E_1 = -0.14$  assigned same as 1,2 dichloroethylene + OH. The reverse reaction  $k_{-1}$  can be calculated from thermodynamics and microscopic reversibility:

$$\Delta G = -RT \ln K_{eq} = \Delta H - T\Delta S \quad \text{for the reaction}$$

$$\Delta H/RT - \Delta S/R = (E_f - E_r)/RT - \ln(A_f / A_r)$$

where f and r denote forward and reverse reaction.

Transforms above equation to standard states expressed in concentration units.

$$(\Delta H_c + \Delta nRT)/RT - (\Delta S_c + \Delta nR \ln(R'T))/R = (E_f - E_r)/RT - \ln(A_f / A_r)$$

where  $\Delta n$  is the mole change in the reaction.

$$(E_f - E_r) = \Delta H_c$$

$$\ln(A_f / A_r) = \Delta S_c/R + \Delta n \ln(eR'T)$$

where  $E$ ,  $A$ ,  $R'$ ,  $T$  are the activation energy, Arrhenius pre-exponential factor, gas constant ( $82.06 \text{ cm}^3\text{atm/mole/K}$ ) and mean temperature respectively.

The isomerization reaction  $k_3$  (see Table 5.2) is obtained from unimolecular TST. Including the loss of two rotors,  $\Delta S$  can be estimated as -8.5. Then

$$A_3 = (ek_B T/h) \exp(\Delta S/R) = 6.06E+11 \quad \text{at } T = 298K$$

where  $k_B$ ,  $h$ ,  $R$  are the Boltzman, Planck's and gas constant respectively;  $e = 2.718$ .

Activation energy of this isomerization  $E_3$  can be calculated from:

$$E_3 = \text{ring strain} + E_{abs} + \Delta H_{rxn} = 39.42 \text{ Kcal/mole}$$

where the ring strain for four member ring is 26 Kcal/mole, abstraction energy of H atom by a primary carbon,  $E_{abs}$ , is 10 Kcal/mole, and  $\Delta H_{rxn}$  of isomerization is 3.42 Kcal/mole.

Dissociations to products  $k_2$ ,  $k_4$ ,  $k_5$  (see Table 5.2) are obtained from application

of thermodynamics and microscopic reversibility to the reverse addition reactions. The rate constants, both forward and reverse used the references to the combination rates are listed in Table 5.2. The high pressure limit input parameters of  $\alpha$ - addition reaction for the chemical activation calculation are listed in Table 5.2.

The  $\alpha$ - addition reaction forms the  $\text{CHClOHC.H}_2^\#$  energized adduct. Further unimolecular reaction (isomerization) of this adduct is endothermic and relative small fractions of the adduct will isomerize and further react at higher temperature due to the tight transition state. The obvious presence of the low energy channel for the  $\alpha$ - addition adduct is Cl atom elimination.



This makes vinyl alcohol as the dominate product for all conditions (temperature and pressure) of this adduct formation path.

**Table 5.2. Input parameters for the QK Calculation  $\text{C}_2\text{H}_3\text{Cl} + \text{OH}$   $\alpha$ - addition**

Reaction	A	Ea <sup>a</sup>
k1 $\text{C}_2\text{H}_3\text{Cl} + \text{OH} \longrightarrow \text{CHClOHC.H}_2$ .	6.05E+11	-0.14
k-1 $\text{CHClOHC.H}_2 \longrightarrow \text{C}_2\text{H}_3\text{Cl} + \text{OH}$	2.16E+13	23.96
k2 $\text{CHClOHC.H}_2 \longrightarrow \text{Cl} + \text{CH}_2\text{CHOH}$	2.15E+13	9.52
k3 $\text{CHClOHC.H}_2 \longrightarrow \text{CHClO.CH}_3$	6.06E+11	39.42
K-3 $\text{CHClO.CH}_3 \longrightarrow \text{CHClOHC.H}_2$ .	5.52E+12	36.00
K4 $\text{CHClO.CH}_3 \longrightarrow \text{CHClO} + \text{CH}_3$	2.74E+14	10.02
K5 $\text{CHClO.CH}_3 \longrightarrow \text{Cl} + \text{CH}_3\text{CHO}$	4.25E+14	1.06
<sup>a</sup> units are $\text{cm}^3 \text{ mole sec}$ and $\text{Kcal/mole}$ $\langle v \rangle = 1086.89 \text{ cm}^{-1}$ (from CPFIT <sup>7</sup> )		
k1 A <sub>1</sub> factor taken as 0.5 that for $\text{CHClCHCl} + \text{OH}$ (A= 1.21E+12, Ea=-0.14) (ref. Abbatt et.al., J.Phys.Chem. 95,2382,1991)		
k-1 thermodynamics and microscopic reversibility <mr>		
k2 A <sub>2</sub> from A <sub>-2</sub> = 8.0E+12, E <sub>-2</sub> =0.5 from $\text{Cl} + \text{C}_2\text{H}_4$ ( Kerr,J.A. and Moss, 1981)		
k3 A <sub>3</sub> = (ekT/h)exp(S/R) x degeneracy (S=-8.5) E <sub>3</sub> = ring strain + Eabs + H= 26 + 10 + 3.42 = 39.42		
k-3 thermodynamics and microscopic reversibility <mr>		
k4 A <sub>4</sub> from A <sub>-4</sub> = 3.16E+11, E <sub>-4</sub> = 8.0 from 0.5 for $\text{CH}_3 + \text{C}_2\text{H}_4$ (Kerr and Moss, 1981)		
k5 A <sub>5</sub> from A <sub>-5</sub> = 1.78E+13, E <sub>5</sub> = 1.06 (Kerr and Moss, 1981)		
$\langle v \rangle = 1136.93 \text{ cm}^{-1}$ (from CPFIT <sup>24</sup> ); Lennard-Jones parameters: $\sigma = 4.55 \text{ \AA}$ , $\epsilon/k = 576.7 \text{ K}$		

#### 5.4.2 $\beta$ - addition

The rate constant for addition at the  $\beta$ - site,  $k'_1$  (see Table 5.3), is assigned as 0.4 ( $0.5 \times 0.78 = 0.38 \approx 0.4$ ) that for ethylene + OH where the probability of OH adding to CD/H2 carbon is half that of C<sub>2</sub>H<sub>4</sub> and 0.78 accounts for reduced volume fraction<sup>39</sup>. The reverse reaction  $k'_{-1}$  is calculated from thermodynamics and the microscopic reversibility method described previously.

The unimolecular isomerization reaction  $k'_2$  (see Table 5.3) is analyzed by TST where  $\Delta S = -8.5$  (includes loss of two rotors) and  $E_2 = \text{ring strain} + E_{\text{abs}} + \Delta H_{\text{rxn}} = 26 + 10 + 6.9 = 42.9$  Kcal/mole. Dissociation reaction  $k'_3$  to products (CH<sub>2</sub>O + CH<sub>2</sub>Cl) is obtained from the reverse combination and microscopic reversibility. The high pressure limit input parameters and literature references are listed in Table 5.3.

The  $\beta$ - addition reaction forms the CH<sub>2</sub>OHCHCl<sup>#</sup> energized adduct. Further unimolecular reaction (isomerization) of this adduct is, however, endothermic when ring strain + Ea of H abstraction +  $\Delta H_{\text{rxn}}$  are considered. A relatively small fraction of the adduct will isomerize and further react at higher temperatures due to high barrier energies (above the enthalpy change) and the tight transition state. The adduct is, therefore, either stabilized or it dissociates back to the initial reactants (C<sub>2</sub>H<sub>3</sub>Cl + OH), as this is the lowest energy dissociation channel.

Geometric mean frequencies were obtained from heat capacity estimates<sup>24</sup>, and Lennard-Jones parameters were obtained from tabulations<sup>40</sup> and a calculation method based on molar volumes and compressibility<sup>41</sup>.

**Table 5.3 Input parameters for the QK Calculation C<sub>2</sub>H<sub>3</sub>Cl + OH β - addition**

Reaction	A	Ea <sup>a</sup>
k1 C <sub>2</sub> H <sub>3</sub> Cl + OH ---> CH <sub>2</sub> OHCHCl.	2.17E+12	-0.14
k-1 CH <sub>2</sub> OHCHCl. ---> C <sub>2</sub> H <sub>3</sub> Cl + OH	6.03E+13	28.96
k2 CH <sub>2</sub> OHCHCl. ---> CH <sub>2</sub> O.CH <sub>2</sub> Cl	6.06E+11	42.9
K-2 CH <sub>2</sub> O.CH <sub>2</sub> Cl ---> CH <sub>2</sub> OHCHCl	7.17E+12	36.0
K3 CH <sub>2</sub> O.CH <sub>2</sub> Cl ---> CH <sub>2</sub> O + CH <sub>2</sub> Cl	1.18E+14	17.1
<sup>a</sup> units are cm <sup>3</sup> mole sec and Kcal/mole		
k1 A <sub>1</sub> factor taken as 0.4 that for C <sub>2</sub> H <sub>4</sub> + OH(A=5.42E+12), (Tsang,W. and Hampson,R.F., J.Phys.Chem.Ref.Data,15,1087, 1986). Ea same as CHClCHCl + OH.		
k-1 thermodynamics and microscopic reversibility <mr>		
k2 A <sub>2</sub> = (ekT/h)exp(S/R) x degeneracy (S=-8.5), E <sub>2</sub> = ring strain + Eabs + H= 26 + 10 + 6.9 = 42.9		
k-2 thermodynamics and microscopic reversibility <mr>		
k3 A <sub>3</sub> from A <sub>-3</sub> = 1.6E+11, E <sub>-3</sub> = 8.0 from C <sub>2</sub> H <sub>5</sub> + C <sub>2</sub> H <sub>4</sub> (Kerr,J.A. and Moss 1981)		
<v> = 1136.93 cm <sup>-1</sup> (from CPFIT <sup>24</sup> )		
Lennard-Jones parameters: σ = 4.55 Å, ε/k = 576.7 K		

### 5.5 Transition-State-Theory Calculations for Abstraction Reaction

The calculation of pre-exponential A factors for the bimolecular abstraction reactions using Transition-State-Theory (TST) is described in detail by Cohen and coworkers.<sup>42-45</sup> They developed a procedure for obtaining activation entropies without the need for a fully characterized potential energy surface. The fundamental equation of TST is<sup>44</sup>:

$$k(T) = \kappa (RT/N_a h) * [Q(AB^\#)/Q(A)Q(B)] \exp(-E/RT)$$

where  $\kappa$  is the transmission coefficient, R, N<sub>a</sub>, and h are the ideal gas, Avogadro's, and Planck's constant respectively. Q's are the partition functions for the activated complex AB<sup>#</sup> and reagents A and B. This equation can be expressed in practical thermochemical units as:

$$k(T) = 1.3E+13 * T^2 \exp(\Delta S^\# / R) \exp(-E/RT) * g$$

where k in cc/mol/sec unit and g is degeneracy.

Transition-State-Theory, as described by Cohen et al.<sup>44</sup>, will allow calculation only of the entropy of activation not the activation energy. A widely used method for predicting activation energy is offered by Evans and Polanyi<sup>22</sup>:

$$E = a\Delta H + b$$

where E is the experimental activation energy,  $\Delta H$  is the enthalpy change of reaction, and a and b are constants. The enthalpy change of reaction is assumed to be proportional to the bond dissociation energy (BE, in Kcal/mole) for a homologous series of species :

$$E/R = a' BE + b'$$

where  $E/R = -d(\ln k) / d(1/T)$  at 300K.

A modified Evans-Polanyi plot of OH abstraction of H atom from chlorinated hydrocarbons (CHCs) is illustrated in Fig. 5.3. The experimental E/R values are obtained from data in reference 44 and BEs are from Lay et.al.<sup>38</sup> The regression result shows that  $E/R = 149.3 (BE - 89.1)$

The bond dissociation energies evaluated for  $\alpha$ - and  $\beta$ - abstraction (from the CD/Cl/H and CD/H<sub>2</sub> carbons respectively) are 107 and 110 Kcal/mole (1.5 and 3.5 Kcal/mole resonance stabilization energy respectively); thus we calculate activation energies from the above correlation (Fig 5.3.) are 5.31 and 6.2 Kcal respectively.

The calculation for entropy of activation,  $\Delta S^\ddagger$ , requires knowledge of the activated complex (its bond lengths and angles, vibrational frequencies, internal rotor parameters, electronic degeneracy, and symmetry properties) along with similar parameters of the reactants (C<sub>2</sub>H<sub>3</sub>Cl and OH).

Consider abstraction of H by reaction of OH with C<sub>2</sub>H<sub>3</sub>Cl:



$$\Delta S^\ddagger = S^\ddagger - S_{C_2H_3Cl} - S_{OH}$$

where  $S^\ddagger$  = entropy of TST complex ( $^\ddagger$  denote as TST complex).

Begin with C<sub>2</sub>H<sub>3</sub>Cl as a model compound and then make corrections to the various degrees of freedom to obtain  $\Delta S^\ddagger$  as indicated below:

$$S^{\#} = S_{\text{C}_2\text{H}_3\text{Cl}} + \Delta S_{\text{trans}} + \Delta S_{\text{vib}} + \Delta S_{\text{rot}} + \Delta S_{\text{ir}} + \Delta S_{\text{e}} + \Delta S_{\text{n}} + \Delta S_{\sigma}$$

where the  $\Delta S$  terms represent the corrections required in adjusting the properties (translation, vibration, rotation, internal rotation, electronic, optical isomer, symmetry) of the model compound to those of the activated complex.

Define C...H as a one electron-bond in the TST structure and assume that the C...H, H...O and O-H bond lengths and C...H...O and H...O-H bond angles are 1.7Å, 1.5Å, 0.9Å, 180°, and 105° respectively. From this data, we can calculate the product of moments of inertia of the complex  $I^{\#3}$  then

$$\Delta S_{\text{rot}} = 0.5R \ln (I^{\#3}/I^3)$$

$$= 0.5R \ln [(14.29 \times 744.13 \times 757.83)/(15.15 \times 133.64 \times 148.79)] = 3.27 \text{ cal/mole/K}$$

$\Delta S_{\text{trans}}$  is given by  $1.5R \ln (M^{\#}/M) = 0.72 \text{ cal/mole/K}$  where  $M$  is molecular weight of species. The electronic degeneracy of the activated complex is 2 so that

$$\Delta S_{\text{e}} = R \ln(2) = 1.38 \text{ cal/mole/K.}$$

The external symmetry is assumed to be the same as the model compound, but one optical isomer exists in the TST, so

$$\Delta S_{\text{n}} = R \ln(n^{\#}/n) = R \ln(2) = 1.38 \text{ cal/mole/K.}$$

The calculation results are listed in Table 5.4.

The contribution of the vibrational frequencies  $\Delta S_{\text{vib}}$  and internal rotations  $\Delta S_{\text{ir}}$  to entropies and heat capacities of the activated complex can be calculated by using the "RADICALC" computer code developed by Bozzelli and Ritter<sup>38</sup>. The frequency changes are obtained from tables in Benson<sup>22</sup> and Cohen<sup>44</sup>. Corrections to the entropy due to changes in the barrier to rotation are interpolated from tables developed by Pitzer and coworkers<sup>46</sup>. Cohen and Benson<sup>44</sup> analyzed the reactions of OH with haloalkanes and proposed that the entropy of free rotation about the C...H bond is 4.5 cal/mol/K and H...O bond is 4.3 for halomethanes. They report values of 4.7 and 4.6 cal/mol/K for C...H and H...O bonds respectively in haloethanes. The average value of halomethanes and haloethanes for the C...H bond is used:



$$(\Delta S_{C...H} = [4.5+4.7]/2 = 4.6)$$

and the H...O bond

$$(\Delta S_{H...O} = [4.3+4.6]/2 = 4.45).$$

Unlike the haloethanes, there is no internal rotation about the C=C bond.

Hence

$$\Delta S_{ir} = \Delta S_{C...H} + \Delta S_{H...O} = (4.5+4.7)/2 + (4.3+4.6)/2 = 9.05 \text{ cal/mol/K at 300K.}$$

The entropy of activation,  $\Delta S^\ddagger$ , is obtained from the sum of the  $\Delta S$  terms minus entropy of OH radical as shown in Table 5.3.

$$\Delta S^\ddagger = \Sigma \Delta S - S_{OH}$$

Values of  $\Delta S$  for specific translation, vibration, rotation, internal rotation, electronic, and optical isomer are listed in Table 5.4. The activation energy and an entropy of activation for both abstraction channels are:

$$k_a = 1.40E+07 * T^2 \exp(-5310/RT)$$

$$k_b = 2.54E+07 * T^2 \exp(-6200/RT)$$

$$\begin{aligned} k_b / k_a &= (A_b / A_a) \exp(E_a/RT - E_b/RT) \\ &= 1.81 \exp(-488/T) \end{aligned}$$

where  $k_a$ ,  $k_b$  are the rate constants for  $\alpha$ - and  $\beta$ -abstraction channels respectively.

**Table 5.4 Calculated Contribution to  $\Delta S^\ddagger$  for OH + C2H3Cl Abstraction Reaction**

Types	$\Delta S_{trans}$	$\Delta S_{vib}$	$\Delta S_{rot}$	$\Delta S_{ir}$	$\Delta S_e$	$\Delta S_n$	$\Sigma \Delta S$	$\Delta S^\ddagger$
CD/Cl/H	0.72	0.8	3.27	9.05	1.38	1.38	16.58	-27.3
CD/H2	0.72	0.6	3.27	9.05	1.38	1.38	16.38	-27.5

A second method to estimate the Arrhenius A factors for specific H atom sites is to modify the observed experimental value for represents all H atoms into a sum where each term represents specific H atom sites. Cohen<sup>42</sup> had indicated that a reasonable approximation for abstraction of a specific H atom from a molecule is that: "The probability of OH colliding with H is proportional to a total cross section divided by

number of available H atoms"

In this case, we are dealing with the cross section observed for vinyl chloride, so the pre-exponential A factors for  $\alpha$ - and  $\beta$ -abstraction are proportional to number of H atom.

$$A_{\beta} / A_{\alpha} = 2$$

It is interesting to compare this rate constant ratio for relative number of H atom estimation with that of the TST method. The ratio of the pre-exponential A factors for  $\alpha$ - and  $\beta$ -abstraction from this empirical counting method is only slightly higher than the TST method (2.0 versus 1.8).

## 5.6 Results and Discussion

Howard<sup>33</sup> has predicted that elimination of Cl and formation of vinyl alcohol dominates for the  $\alpha$ - addition. Perry et al.<sup>34</sup> estimated that the rate constant of this channel is about  $6.0\text{E}+11 \text{ cm}^3\text{mol}^{-1}\text{s}^{-1}$  at room temperature which is about 15% of the total rate constant. The present calculation shows that the  $\alpha$ - addition to the CD/Cl/H carbon appears to be a similar fraction of that for  $\beta$ - addition to the CD/H<sub>2</sub> carbon, 10 - 20%, in agreement with the estimation of Perry et al.<sup>34</sup> This  $\beta$ - channel behaves much differently than  $\alpha$ - addition due to the lower energy (exothermic) reaction channel available to the  $\alpha$ -adduct - unimolecular elimination of Cl, forming vinyl alcohol + Cl. This product slate dominates for the  $\alpha$ - addition for all pressures with stabilization important at higher pressure (7600 torr).

Fig. 5.4 presents a plot of rate constants for the various channels of  $\alpha$ -addition at 760 torr. The apparent rate parameters to the specific product channels are listed in Table 5.5. The vinyl alcohol + Cl channel dominates the reaction in the temperature range 300 - 1200K. As temperature increases, other product channels (excluding stabilization) start to become more important; but are still 5 orders of magnitude below the major product channel: vinyl alcohol + Cl. The stabilization rate constant is 1% of that for the vinyl

alcohol + Cl channel at 300K and decreases with increasing temperature.

A plot of rate constants for  $\beta$ -addition product channels is shown in Fig. 5.5. The stabilization channel dominate the reaction by more than 4 orders of magnitude in the temperature range 300 - 1200K. The apparent rate parameters to the specific product channels are listed in Table 5.5.

Fig 5.6 shows the rate constants versus pressure at 300 K for all addition reaction channels. The  $\beta$ -addition channel dominates the reaction at high pressure and through the fall off regime as suggested by previous researchers<sup>33,34,35</sup>. The vinyl alcohol + Cl from  $\alpha$ -addition becomes dominate when pressure is decreased below than 1 torr.

**Table 5.5 Apparent Rate Constants for OH + C<sub>2</sub>H<sub>3</sub>Cl at 760 torr**

$k = A \cdot T^n \cdot \exp(-E_a/RT)$ , units in cc mole-sec,  $E_a$  in Kcal/mole

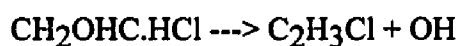
Reaction	A	n	E <sub>a</sub>	remark
OH+C <sub>2</sub> H <sub>3</sub> Cl --->H <sub>2</sub> O+CH <sub>2</sub> CCl	1.40E+07	2.0	5.31	$\alpha$ -abstraction
OH+C <sub>2</sub> H <sub>3</sub> Cl--->H <sub>2</sub> O+CHClCH.	2.54E+07	2.0	6.2	$\beta$ -abstraction
OH+C <sub>2</sub> H <sub>3</sub> Cl--->CHClOHCH <sub>2</sub> .	2.83E+18	-3.191	0.938	$\alpha$ -addition
OH+C <sub>2</sub> H <sub>3</sub> Cl--->Cl+CH <sub>2</sub> CHOH	7.49E+11	-0.029	-0.108	
OH+C <sub>2</sub> H <sub>3</sub> Cl--->CHClO.CH <sub>3</sub>	2.51E-11	4.028	8.874	
OH+C <sub>2</sub> H <sub>3</sub> Cl--->CHClO+CH <sub>3</sub>	5.34E-19	7.901	6.441	
OH+C <sub>2</sub> H <sub>3</sub> Cl--->Cl+CH <sub>3</sub> CHO	1.94E-11	5.893	8.488	
OH+C <sub>2</sub> H <sub>3</sub> Cl--->CH <sub>2</sub> OHCHCl.	1.33E+32	-6.638	5.718	$\beta$ -addition
OH+C <sub>2</sub> H <sub>3</sub> Cl--->CH <sub>2</sub> O.CH <sub>2</sub> Cl	9.45E+18	-3.828	15.804	
OH+C <sub>2</sub> H <sub>3</sub> Cl--->CH <sub>2</sub> O+CH <sub>2</sub> Cl	8.91E+10	-0.177	14.37	

Fig. 5.7 illustrates a plot of calculated and observed rate constant over the temperature range 300 - 1200 K at 760 torr. At low temperature, the  $\beta$ -addition channel dominates the reaction, as reported by Liu et.al.<sup>35</sup> At high temperature, however, the reverse reaction - dissociation of the adduct to vinyl chloride + OH (experimentally observed as reduced reaction rate) dominates over addition. A small, near constant (15%) fraction of the reactions proceed via  $\alpha$ -addition to products C<sub>2</sub>H<sub>3</sub>OH + Cl. The Quantum Kassel calculation does not include abstraction which is calculated separately by the TST

method described previously. The apparent rate constants of the two abstraction channels calculated by Transition-State-Theory are also shown in Fig. 5.7. One can see that total abstraction reaction ( $k_a + k_b$ ) becomes important above 850 K, while Liu et.al.<sup>35</sup> report that it dominates above 723 K. The total rate constant - addition and abstraction - is slightly over predicted when compared to experimental data in the temperature range 600 to 1000K at 760 torr. Here the absolute rate constant difference is within a factor of 2 for the worst case (600 to 1000K), but it is still reasonable compared to the literature.

Fig. 5.8 shows a comparison of the calculated results for important addition and abstraction channels with the experimental data of other researchers. At room temperature, the rate constants for the addition reaction channels only vary over a wide pressure range. Howard<sup>18</sup> extrapolated his experimental data (0.7 to 7 torr) for the reaction of OH radicals with  $C_2H_3Cl$  using a curved Lindemann plot and estimated a value for  $k \approx 4.20E+12 \text{ cm}^3 \text{ mole}^{-1} \text{ s}^{-1}$  in the high pressure limit (ca. 100 torr) while Perry et.al.<sup>19</sup> proposed that their work at 50 torr were at the high pressure limit and estimated a value of  $k \approx 3.97E+12 \text{ cm}^3 \text{ mole}^{-1} \text{ s}^{-1}$ . The current model is in good agreement with both research groups, as shown in Fig 5.8. but predicts the high pressure limit to be more near 760 torr with only 5% increase between 100 and 760 torr as illustrated in Fig. 5.8.

It is interesting to compare the QK calculation<sup>6,7,36</sup> to RRKM<sup>47</sup> theory. The reverse reaction of  $\beta$ - addition ( $k'_{-1}$ ), a unimolecular dissociation, will be used for this comparison.



because the  $\beta$ - addition channel dominates the reaction at low temperature. The Quantum Kassel calculation shows that this unimolecular dissociation ( $k'_{-1}$ ) dominates over stabilization at 1 atm and high temperature which is experimentally observed as reduced reaction rate. The input parameters for the RRKM calculation are listed in Table 5.6 which is run with the UNIMOLE code of Gilbert<sup>47</sup>.

**Table 5.6 Input parameters for RRKM calculation**

	Reactant molecule	Transition State
critical energy at 298K	28.9 (Kcal/mole)	
external symmetry number	1	1
collision diameter (Å)	4.55	
well depth (K)	576.7	
overall rotation ( $\text{cm}^{-1}$ )	0.19	0.15
moments of inertia ( $\text{amu Å}^2$ )	88.737	112.4
dimensions of adiabatic rotation	3	3
frequencies and degeneracies	3400, 3000(3),1300, 700,1150(3), 400(2), 1400(2),1050(3), 1200,730	3400,3000(3), 1650, 700, 1050(4), 420(2), 1400, 500, 600,

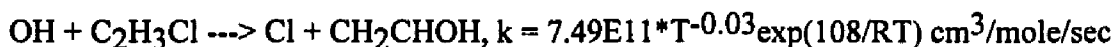
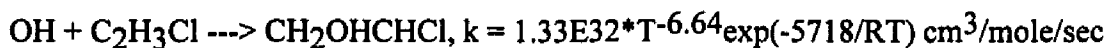
Fig. 5.9 shows a plot of rate constant versus  $1/T$  at 760 torr for the two different calculations. The unimolecular dissociation rate constant increases with increasing temperature for 16 orders of magnitude in the temperature range 300 to 1000K. One can see that calculation results from two techniques are in good agreement.

Fig. 5.10 illustrates a plot of the two calculated rate constants versus pressure at 300K and 1000K. At atmospheric condition (300K), the unimolecular reaction reaches its high pressure limit at 760 torr as predicted by QK and RRKM calculations. Both calculation techniques give the same high pressure limit rate constant,  $1.90\text{E-}8 \text{ sec.}^{-1}$ . The difference of only 2% is purely coincidental, as no changes were made in the vibration frequencies or moment of inertia from the initial calculation. The difference between two technique for low pressure limit rate constant is due to the complete omission of the Beta Collision ( $B_c$ ), the weak collision assumption in the RRKM calculation, while  $B_c$  is fully included in the QK and is calculated via the method of Troe<sup>48</sup>. Here the low pressure values are offset in pressure by the  $B_c$  factor between the two calculations, as they should be. The  $B_c$  (at 1200K and 760 torr,  $B_c = 0.13$ ) was not used in the RRKM calculation but to compare the results in this manner. The offset in the two calculations resulting from  $B_c$  will effectively increase the pressure in the QK result over the RRKM result by the  $B_c$

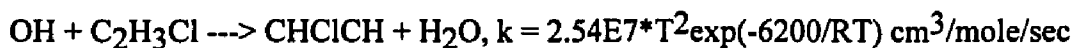
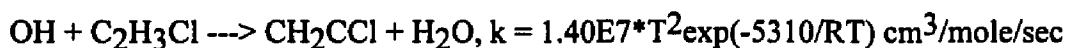
factor at the low pressure limit. This offset will decrease as pressure is increased to a point at the high pressure limit where the offset will be zero. In combustion environment, both the QK and the RRKM calculations show that dissociation reaction is still in the fall-off regime.

### 5.7 Summary

The addition reactions of vinyl chloride with hydroxy radical have been analyzed using thermochemical analysis and a statistical chemical activation formalism based on the Quantum Kassel Theory. Rate constant and reaction paths are predicted versus temperature and pressure and compared to experimental data where possible. Good agreement was obtained with the experimental data in the literature. The two abstraction paths have been analyzed by using an Evans-Polanyi relation for the activation energy of abstraction and Transition-State-Theory. The calculations serve as useful estimates for rate constants and reaction paths in applications of combustion and atmospheric modeling (pressure and temperature), where experimentally data are not available. Rate constants over a wide pressure and temperature range for OH addition and OH abstraction of H atom from the two distinct sites on vinyl chloride molecule are evaluated and recommended. The important addition reaction and rate constants at 760 torr pressure are:



Abstraction reactions are not dependent on pressure. The recommended rate constants for each of the channels are:



Extension of these analysis technique should allow reasonable estimation of the expected product distributions for a variety of addition reactions of hydroxy radicals to other halogenated ethylenes.

## CHAPTER 6

### THERMAL REACTIONS OF $\text{CH}_2\text{Cl}_2$ IN $\text{O}_2/\text{H}_2$ MIXTURES : IMPLICATIONS FOR CHLORINE INHIBITION OF CO CONVERSION TO $\text{CO}_2$

#### 6.1 Background

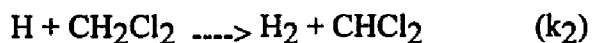
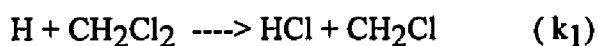
Reasonable methods for effective destruction of chlorinated hydrocarbons include: (a) conversion to HCl and  $\text{CO}_2$  by oxidation (e.g. incineration), and (b) conversion to HCl and hydrocarbons by pyrolysis in a hydrogen or methane rich atmosphere<sup>49</sup>. The presence of these chlorocarbons has long been known to slow the oxidation rate of hydrocarbons through studies of flame velocity, temperature, and flame stability. Westbrook<sup>2</sup> has modeled the inhibition of hydrocarbon oxidation in laminar flames by halogenated compounds. He suggested that the halogenated species serve to catalyze the recombination of H atoms into relatively nonreactive  $\text{H}_2$  molecules, reducing the available radical pool, specifically H atoms, and thereby lowering the overall rate of chain branching. Senkan et. al.<sup>3,4</sup> have developed mechanisms for  $\text{CH}_3\text{Cl}$ ,  $\text{C}_2\text{H}_3\text{Cl}$ , and HCl-doped CO oxidation flame systems. These later studies reached similar conclusions, suggesting that the reaction of  $\text{H} + \text{HCl} \rightarrow \text{H}_2 + \text{Cl}$  is responsible for the inhibition of CO conversion to  $\text{CO}_2$  in the oxidations.

Alternately, Benson and Weissman<sup>5</sup> and Senkan et. al.<sup>3</sup> have reported that use of  $\text{CH}_3\text{Cl}$  in  $\text{CH}_4$  or in  $\text{CH}_4$  plus 2-3%  $\text{O}_2$  respectively accelerated  $\text{CH}_4$  conversion to higher hydrocarbons. They concluded that this might lead to effective methods for converting  $\text{CH}_4$  to useful higher molecular weight hydrocarbons without either soot or excessive oxidation occurring<sup>3</sup>. Both acceleration and inhibition effects are apparent in hydrocarbon reaction systems with a chlorinated hydrocarbon present. Therefore, there is a significant need to develop quantitative insights into the mechanism of chlorocarbon

pyrolysis and oxidation in order to better understand and ultimately to optimize these reaction processes, especially for the conversion of chlorocarbons by incineration.

Tsao<sup>8</sup> studied the thermal decomposition of DCM with hydrogen over the temperature range of 973 - 1173K, in a 1 atm total pressure tubular flow apparatus. Activation energies of the global bulk and wall reactions on hydrogen reaction with DCM were 50.0 Kcal/mol, 57.8 Kcal/mole, with Arrhenius A factors of  $2.84\text{E}+10$  and  $2.65\text{E}+10 \text{ sec.}^{-1}$  respectively reported. The major products of reaction of DCM in the temperature range 973 to 1073 K were methane and methyl chloride. The minor products were ethylene, acetylene and HCl. Trace amounts of ethane, chloroethylene, 1,2-dichloroethylene, trichloroethylene, benzene were also observed. No chlorocarbons were found over 1223K and one second residence time where the only products were methane, hydrogen chloride, acetylene, ethane and benzene.

Huang<sup>9</sup> studied the kinetics of the reaction of atomic hydrogen with DCM in a flow system at a pressure of 2.1 to 2.7 mm Hg and room temperature. The major products observed were hydrogen chloride and methane. The extent of conversion of DCM increases first to a maximum and then decreases with increasing concentration of DCM. Through the modeling of the reaction scheme and comparison with experimental data, the rate constant of the initial steps were determined as follows :



where

$$k_1 = 3.63 \text{ E}+9 \text{ cm}^3/\text{mole}/\text{sec} , 298 \text{ K}$$

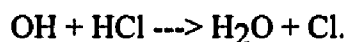
$$k_2 = 2.08\text{E}+7 \text{ cm}^3/\text{mole}/\text{sec} , 298 \text{ K}$$

Won<sup>10</sup> investigated the decomposition of dichloromethane/1,1,1-trichloroethane mixtures in a hydrogen bath gas. These experiments were carried out at one atmosphere total pressure in a tubular flow reactor. In his study, he demonstrated that selective formation of HCl can result from thermal reaction of chlorocarbon mixture and showed



that synergistic effects of 1,1,1--trichloroethane decomposition accelerate the rate of DCM decomposition. There is significant interaction of the decay products from 1,1,1--trichloromethane with the parent dichloromethane.

In this chapter, an experimental study on  $\text{CH}_2\text{Cl}_2$  reactions in  $\text{H}_2/\text{O}_2$  atmospheres and a detailed chemical kinetic mechanism developed from fundamental thermochemical principles are presented. The model is based on reactant and product profiles and shows good agreement with a wide range of experimental data. Sensitivity analysis on the mechanism provides insights into the effects of chlorocarbons in pyrolysis and oxidation environments. One such insight is that a major cause of the chlorocarbon induced inhibition of CO conversion to  $\text{CO}_2$  is loss of OH radical through the reaction:



## 6.2 Experimental Result

The thermal decomposition of  $\text{CH}_2\text{Cl}_2$  in  $\text{H}_2/\text{O}_2$  mixtures in an Ar bath gas was studied at 1 atmosphere total pressure in tubular flow reactors of different surface to volume (S/V) ratios. Data at different S/V ratios were used to decouple the apparent wall and bulk phase decomposition rates. The reaction systems were analyzed systematically over a temperature range from 883 to 1093°K, with average residence times ranging from 0.1 to 2.0 seconds. Three different size (0.4, 1.05, and 1.6 cm ID) flow reactors were used to study five different feeds, as listed in Table 6.1. Residence times and global kinetic parameters were determined using methods and analysis described by Chang and Bozzelli<sup>50</sup>.

**Table 6.1 Reactant Feed Ratios**

Feed	Mole Percent CH <sub>2</sub> Cl <sub>2</sub> : H <sub>2</sub> : O <sub>2</sub> : Ar				Equiv. Ratio	Cl/H Ratio
1.	1	1	1	97	1.5	0.5
2.	1	2	2	95	1.0	0.33
3.	1	3	1	95	2.5	0.25
4.	1	1	3	95	0.5	0.5
5.	1	1	98	0	0.015	0.5

Experimental results on the decomposition of CH<sub>2</sub>Cl<sub>2</sub> are shown in Fig 6.1 and 6.2. The normalized concentration ( $C/C_0$ ) is presented as a function of the average residence time for several temperatures and two widely varying initial reagent ratios in the 1.05 cm reactor; O<sub>2</sub>:H<sub>2</sub>:CH<sub>2</sub>Cl<sub>2</sub>:Ar = 1:1:1:97 and 98:1:1:0 respectively. It was found that complete decay (99%) of the CH<sub>2</sub>Cl<sub>2</sub> at 1 second residence time occurs at 1093°K for all the reactant ratio sets. The continuity in the measured species levels plotted for a single residence time versus temperature provides an indication of the consistency in our experimental procedures. This is because our experiments were performed by varying flow times and feed conditions at a single oven temperature profile. The data at varied temperature, therefore, represents experiments performed over time periods of months.

The major products for CH<sub>2</sub>Cl<sub>2</sub> decomposition at our conditions as shown in Fig 6.3 are CH<sub>3</sub>Cl, CH<sub>4</sub>, CO, CO<sub>2</sub>, and HCl. The minor hydrocarbon products as shown in Fig 6.4, having concentrations below 5%, include C<sub>2</sub>H<sub>4</sub>, C<sub>2</sub>H<sub>2</sub>, 1,1 and 1,2 C<sub>2</sub>H<sub>2</sub>Cl<sub>2</sub>, C<sub>2</sub>HCl<sub>3</sub>, and C<sub>2</sub>H<sub>3</sub>Cl. The sum of chlorocarbon products and CH<sub>2</sub>Cl<sub>2</sub> reactant decreases with increasing temperature and residence time. The major products when CH<sub>2</sub>Cl<sub>2</sub> conversion is above 90% are HCl and nonchlorinated species: CH<sub>4</sub>, C<sub>2</sub>H<sub>2</sub>, C<sub>2</sub>H<sub>4</sub>, CO, and CO<sub>2</sub>. Mass balance determinations for carbon and chlorine were within ±8% and ±7% respectively for all experiments.

The importance of  $O_2$  in our system depends strongly on experimental conditions. As shown in Fig 6.5, oxygen has almost no effect on the decay of  $CH_2Cl_2$  when conversion is below 50% (less than 1023°K, 1 sec. residence time) and/or the initial  $O_2$  concentration is below about 5%. When conversion of  $CH_2Cl_2$  is close to 1, almost all carbon is present as CO and  $CO_2$ . The CO concentration, as shown in Fig 6.6, is much higher than  $CO_2$ . At higher  $O_2$  to  $H_2$  ratios, more CO is converted to  $CO_2$ . At temperatures above 1033°K,  $O_2$  plays a more significant role in conversion. The higher the ratio of  $O_2$  to  $H_2$ , the lower the temperature needed to observe the formation of CO and  $CO_2$ .

An increase in the S/V ratio of the reactor was observed to accelerate the  $CH_2Cl_2$  decomposition as shown in Fig 6.7. The relative magnitude of this effect, however, was small. For a 60% increase in S/V between the 1.05 and 1.6 cm ID flow tubes, there was only a 5% difference in conversion rate, with no effect on the relative distribution of principal products observed. Hence, while a surface effect exists, its magnitude is small relative to bulk (homogeneous) reaction. The relative change in decomposition of  $CH_2Cl_2$  (acceleration in this case) is much larger for the 0.4 cm ID reactor. Analysis of our results on the several hundred kinetic runs lead us to strongly recommend a minimum reactor ID of 1.0 cm for data analysis on these chlorocarbon studies.

A first order plug flow model was utilized to analyze the overall (global) experimental data on  $CH_2Cl_2$  loss. In addition, the homogeneous and wall rate constants were decoupled and separately evaluated. The Arrhenius rate expressions in Table 6.2 were found to fit the overall homogeneous reaction systems studied. The average contribution from wall reaction was less than 6% of the homogeneous reaction.

**Table 6.2 Global Rate Constants ( $K_{\text{exp}}$ ) for  $\text{CH}_2\text{Cl}_2/\text{O}_2/\text{H}_2$  in Ar**

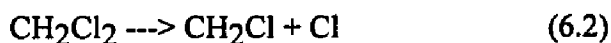
Ar:O <sub>2</sub> :H <sub>2</sub> :CH <sub>2</sub> Cl <sub>2</sub>	$K_{\text{exp}}$
97 : 1 : 1 : 1	$3.76 \times 10^{14} \times \exp(-69982/RT)$
95 : 2 : 2 : 1	$5.00 \times 10^{12} \times \exp(-60405/RT)$
95 : 3 : 1 : 1	$2.25 \times 10^{15} \times \exp(-72645/RT)$
95 : 1 : 3 : 1	$4.25 \times 10^{13} \times \exp(-64969/RT)$

Clearly, these global rate constants are valid only for the specific reactant conditions. A detailed elementary reaction mechanism which explains the data at all reactant ratios is therefore preferred.

### 6.3 Kinetic Mechanism and Modeling

We have, therefore, developed a detailed elementary reaction mechanism (Appendix B) to model the  $\text{CH}_2\text{Cl}_2$  pyrolysis/oxidation reaction systems. The principles of thermochemical kinetics have been applied. The inclusion of chlorine adds a fourth element to conventional hydrocarbon oxidation mechanisms and significantly increases overall complexity. In addition, the thermochemical parameters including enthalpy of formation, entropy, and heat capacities for many chloro-oxy-carbon products and intermediates have not been previously measured or calculated and they are required for input to detailed modeling codes. We have developed thermodynamics for a number of these compounds using the techniques of group additivity and the "THERM"<sup>23</sup> computer code.

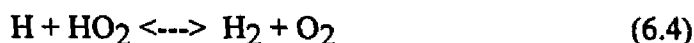
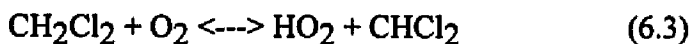
The initiation steps of this reaction system involve unimolecular decomposition of  $\text{CH}_2\text{Cl}_2$  or bimolecular reaction of  $\text{H}_2$  or  $\text{CH}_2\text{Cl}_2$  with  $\text{O}_2$ . The possible unimolecular reactions include:



We base our estimate of the A factor for reaction (6.1) on Transition State Theory (1000°K). The  $E_a$  is from analysis of reactions of  $^1\text{CH}_2$  which is widely shown to insert into hydrocarbons with an  $E_a$  of 0.0 and on insertion of  $^1\text{CCl}_2$  into HCl, which we have experimentally measured<sup>51</sup> to be 15 kcal/mole, using  $\Delta H_f^{298} (^1\text{CCl}_2)$  of 39 Kcal/mole as recommended by NIST. An extrapolation to the insertion of  $^1\text{CHCl}$  into HCl yields a value of 7.5 kcal/mole. This trend is in agreement with OH radical addition reactions to chloro-olefins, Abbatt and Anderson<sup>52</sup>. Similar results were also determined by Blake et. al.<sup>53</sup> who show a 12 Kcal/mole Gibbs Free Energy barrier (suggested as mostly entropic in nature) for insertion of  $^1\text{CCl}_2$  into ethylene. Setser<sup>54</sup> recommends an  $E_a$  of 8 Kcal/mol for insertion of  $^1\text{CF}_2$  into HCl. One possible reason for this apparent activation energy is that the electrons from the Cl atom(s) may reduce the ability of the unoccupied orbital on the singlet methylene to combine with bonding electrons in the molecule undergoing insertion. In developing this mechanism, we have used the  $H_f^{298}$  of 39.0 Kcal/mol for  $^1\text{CCl}_2$  as recommended by Lias et al.<sup>55-57</sup> There are a number of widely different values for this  $H_f^{298}$  ranging up to 52 Kcal/mol in a very recent publication<sup>58</sup>. The  $E_a$ 's for rate constants involving  $^1\text{CCl}_2$  are based on the 39.0 Kcal/mol value; where the reverse reaction rate constants calculated in the CHEMKIN<sup>59</sup> code from thermodynamics and micro-reversibility have been considered in all cases. Use of different thermo parameters in this mechanism will dramatically alter the reverse rate constants specific to this species. Rates calculated using Quantum Rice- Ramsperger-Kassel (QRRK)<sup>6,7</sup> analysis will be similar if the input parameters are correctly scaled to account for the different  $H_f$  value. We are working on adjustments to the mechanism to account for this higher  $H_f^{298}$  for those researchers electing to use this value in their codes. We recommend the mechanism in this paper be used with thermo properties consistent with data in Appendix A and look forward to further studies clarifying the  $H_f$  of  $^1\text{CCl}_2$ .

It is observed that step (6.2) dominates the dissociation by more than three orders of magnitude because of its lower  $E_a$  and high  $A$  factor.

Reactions with  $O_2$  include :



We note that the relative rates of reaction of  $CH_2Cl_2$  and  $H_2$  with  $O_2$  are a strong function of conversion. At close to initial conditions, these reactions contribute to initiation. At medium to high conversions, sensitivity analysis of the mechanism indicates that these reactions proceed in reverse.

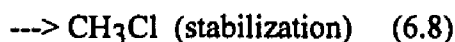
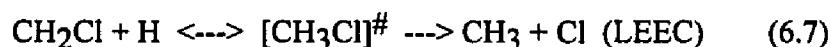
The  $CH_2Cl$  radical formed in reaction (6.2) will abstract H atom from  $H_2$  and form  $CH_3Cl$ :



H atom is produced from steps (6.5) and (6.6)



The  $CH_2Cl$  radical also rapidly reacts with H atoms, which are present at significant concentrations in our system, forming a chemically activated adduct  $[CH_3Cl]^\#$ :

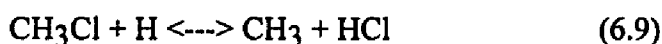


where LEEC represents a Low Energy Exit Channel for the  $CH_3 + Cl$  products relative to the  $CH_2Cl + H$  reactants. The fraction of  $[CH_3Cl]^\#$  which decomposes to reactants, lower energy products  $CH_3 + Cl$ , or to stabilized  $CH_3Cl$  is a function of energy distribution in the initially formed  $[CH_3Cl]^\#$  adduct (temperature), stabilizing collisions (pressure), as well as unimolecular and stabilization rate constants.

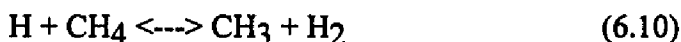
We treat these non-elementary reactions systems such as (6.7),(6.8) with the bimolecular Quantum Rice-Ramsperger-Kassel (QRRK) theory<sup>6,7</sup> as modified by Ritter et. al.<sup>60</sup> The energy level diagram and input parameters for the chemical activation

calculations of the reaction of  $\text{CH}_2\text{Cl} + \text{H}$  are shown in Fig 6.8 and Appendix C. The QRRK analysis clearly indicates that at atmospheric pressure and the temperatures of interest, stabilization represents only about 1% of the reaction channel. Essentially all of the reaction proceeds to the Low Energy Exit Channel for the energized complex dissociation.

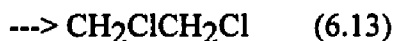
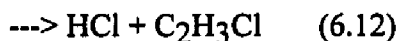
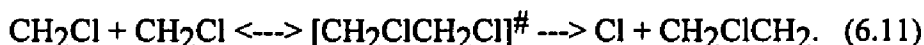
Sensitivity analysis tells us that the significant route to  $\text{CH}_3$  radical in our reaction system is



The formation of  $\text{CH}_4$  as one of the major products results from reaction of  $\text{CH}_3$  with the  $\text{H}_2$  reagent.



Radicals such as  $\text{CH}_3$ ,  $\text{CH}_2\text{Cl}$ , and  $\text{CHCl}_2$  will combine to form energized complexes. At our temperatures (ca. 1000°K), these adducts rapidly react to lower energy products before stabilization. An example is the  $\text{CH}_2\text{Cl} + \text{CH}_2\text{Cl}$  system, whose energy level diagram and QRRK input parameters are shown in Fig 6.9 and listed Appendix III.



The  $\text{CH}_2\text{ClCH}_2$  radical rapidly decomposes by beta scission to  $\text{Cl} + \text{C}_2\text{H}_4$  because of the weak C-Cl bond, relative to the stronger C-C bond formed. The dominant reaction path in combination reactions of  $\text{CH}_2\text{Cl} + \text{CH}_2\text{Cl}$  is a function of both pressure and temperature. At one atmosphere pressure and low temperature, formation of the stable adduct (1,2 dichloroethane) dominates - ca 70%. This channel decreases with increasing temperature where reverse reaction (dissociation of the adduct to reactants - non reaction) is the other important channel here. At the temperatures of this study and 1 atm, reaction to  $\text{Cl} +$  ethyl radical and to  $\text{HCl} +$  ethylene are more important, with the  $\text{Cl} +$  chloroethyl radical path slightly favored over  $\text{HCl}$  elimination. Stabilization becomes less important as the

pressure is decreased. The Cl elimination from the energized adduct can dominate because: i, sufficient energy is available to it and ii, this channel has the higher Arrhenius A factor. The primary unimolecular reaction for the stabilized 1,2 dichloroethane is HCl elimination, because it is the lower energy channel.

The methyl and chloro-methyl radical combination pathways are significantly more important in the formation of C<sub>2</sub> hydrocarbons (HC) and chloro-hydrocarbons (CHC) in reaction systems with Cl present, than in HC oxidations alone. This is a result of atomic Cl being formed at early reaction times. The Cl reacts very rapidly with the reactant fuel molecules, which at early time are present at high levels. The important reaction paths at combustion temperature are abstraction of H by the Cl to form the corresponding HC radical and HCl. These abstraction reactions by Cl are fast, they have high Arrhenius A factors, usually greater than 1.0 E+13, with relatively low Ea's, typically just a few Kcal/mole, (if the reaction is endothermic the Ea is just a few kcal/mole over  $\Delta H_{rxn}$ ).

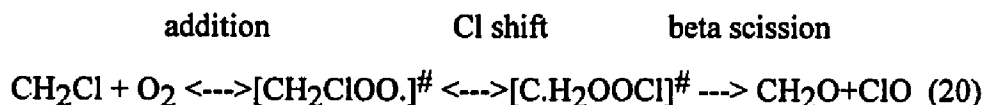
The result is a rapid, nearly - catalytic production of HC and ClC radicals early in the reaction, where there is recycle of a significant fraction of the HCl to Cl. This represents an acceleration of the fuel decay to the corresponding radicals. C<sub>1</sub> radical reactions with molecular oxygen are not as rapid as with C<sub>2</sub> and larger radicals. Conversion of the C<sub>1</sub> radicals into C<sub>2</sub>'s via combination is now very important. The oxidation and pyrolysis pathways of C<sub>2</sub> hydrocarbons are, therefore, also more important in this reaction system than in CH<sub>4</sub> oxidation when no Cl or HCl is present.

We note that our input parameters to the bimolecular QRRK<sup>6,7</sup> calculation on these chemical activation reaction systems (listed in Appendix C) are significantly different from those of Senkan and Karra<sup>61</sup> (over one order of magnitude in several cases). Our calculated results reflect these differences, which might result from use of different thermodynamic properties - enthalpies, entropies and heat capacities for the



relevant species. A listing of the thermodynamic properties of the stable chemical compounds and the radicals used in our mechanism is included in Appendix A.

Other important reactions involve the  $\text{CH}_3$ ,  $\text{CH}_2\text{Cl}$ , and  $\text{CHCl}_2$  radical reactions with  $\text{O}_2$ ; for example,



A potential energy level diagram and input parameters for the QRRK calculations, including reference, for the above reaction system are illustrated in Fig 6.10 and Appendix C. The energized complex can be stabilized, decompose back to initial reactants, or be further isomerized by Cl shift to  $[\text{C.H}_2\text{OOC}]^\#$ . This second complex immediately dissociates to lower energy products  $\text{CH}_2\text{O}$  and  $\text{ClO}$ . Bimolecular QRRK calculations show that only a small fraction of the collisions of  $\text{CH}_2\text{Cl}$  radicals with  $\text{O}_2$  form  $\text{CH}_2\text{O}$  and  $\text{ClO}$ . More than 95% of the energized complex formed decomposes back to initial reactants at temperatures of 873°K and 1073°K.

The kinetic reaction mechanism used in this study (Appendix II) includes 281 elementary reaction steps involving 61 stable compounds and free radical species. All addition and recombination reactions are analyzed by the CHEMACT<sup>7,60</sup> computer code based on bimolecular QRRK theory<sup>6,7</sup>. All unimolecular reactions including beta scission, simple dissociation, isomerization, and elimination are treated with unimolecular QRRK analysis. Further details on specific procedures followed in our bimolecular QRRK analysis has been discussed in chapter 4,5 and in the tables of input parameters in Appendix C.

Experimental data are compared with model predictions in Figs 6.11 to 6.13 for reagent decomposition and product distribution between 973 and 1073°K. The calculated mole fractions for  $\text{CH}_2\text{Cl}_2$  are in very good agreement with those determined experimentally. For  $\text{CO}$  and  $\text{CO}_2$ , model predictions are also in reasonable accord with the experimental data. The model predicts the mole fraction levels of  $\text{CH}_4$  and  $\text{CH}_3\text{Cl}$

versus time and temperature reasonably well, but it slightly over-predicts  $\text{CH}_4$  at higher temperature. The model predicts the low concentration (1-4%) chlorinated  $\text{C}_2$  products reasonably well. It is worthwhile to point out that the scale is amplified (x25), and is not a log scale as used in many model comparisons.

$\text{CH}_2\text{Cl}_2$  decay along with intermediate and final product formation at 1053°K is plotted versus reaction time in Fig 6.14 to 6.16 as opposed to temperature in the figures above. Again one can see that the agreement between the model and experiment is very good.

It is valuable to compare both our experimental data for  $\text{CH}_2\text{Cl}_2$  reactions as well as our model calculations with the data of other researchers. Fig 6.17 illustrates that our model predictions are in agreement with other experimental data on methylene chloride pyrolysis and oxidation (details in Table 6.3).

**Table 6.3 Comparison with Other Researcher's Experimental Conditions**

Temp Range °K	Reactant Conditions	Ref
973 - 1223	20% $\text{CH}_2\text{Cl}_2$ in $\text{H}_2$	8
748 - 1083	4% $\text{CH}_2\text{Cl}_2$ + 4% 1,1,1 $\text{C}_2\text{H}_3\text{Cl}_3$ in $\text{H}_2$	10
1023 - 1273	6.7% $\text{CH}_2\text{Cl}_2$ in ( $\text{CH}_4/\text{Ar}$ : 50/50)	62
1023 - 1273	1.2% $\text{CH}_2\text{Cl}_2$ + 1.2% $\text{C}_2\text{HCl}_3$ in ( $\text{CH}_4/\text{Ar}$ : 50/50)	62
absolute pressure = 1 atm (all cases)		

The small deviation shown in Fig 6.17 between our model and the data of Won<sup>10</sup> at low temperatures is due to synergistic effects resulting from the decomposition of the co-reagent 1,1,1  $\text{C}_2\text{H}_3\text{Cl}_3$  to  $\text{Cl} + 1,1\text{-C}_2\text{H}_3\text{Cl}_2$  radical. We note that less than 1% of the decomposition of the 1,1,1  $\text{C}_2\text{H}_3\text{Cl}_3$  parent follows this chain branching pathway. The major path is decomposition to  $\text{HCl} + 1,1\text{-C}_2\text{H}_2\text{Cl}_2$ . A separate model<sup>63</sup> for 1,1,1

$C_2H_3Cl_3$  verifies the importance of this step and other important reactions of 1,1,1 trichloroethane which we not included in this study.

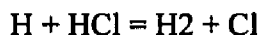
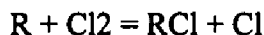
**Table 6.4. Sensitivity analysis relative to  $CO_2$  formation at 1053°K**

Reaction	Residence Time (sec)			
	0.5	1.0	1.5	2.0
$CH_2Cl_2=CH_2Cl+Cl$	1.12E00	1.23E00	1.67E00	2.64E-1
$CH_2Cl_2+H=HCl+CH_2Cl$	-1.77E-1	-3.08E-2	2.12E-1	1.78E-1
$CH_2Cl_2+Cl=HCl+CHCl_2$	-2.02E-1	-1.84E-1	-1.88E-1	-4.26E-2
$CH_2Cl_2+OH=CHCl_2+H_2O$	-1.78E-1	-1.45E-1	-8.05E-2	-2.28E-2
$CH_2Cl+CH_2Cl=C_2H_3Cl+HCl$	-1.39E-1	-1.66E-1	-2.96E-1	-5.54E-2
$CH_2Cl+CHCl_2=CH_2CCl_2+HCl$	-1.49E-1	-1.85E-2	-2.07E-1	-5.06E-2
$CHCl_2+CHCl_2=C_2HCl_3+HCl$	-1.25E-1	-1.44E-1	-1.29E-1	-3.38E-2
$CH_2Cl+CHCl_2=CHClCHCl+HCl$	-5.54E-1	-6.77E-1	-9.06E-1	-1.98E-1
$CH_2Cl+O_2=CH_2O+ClO$	1.35E00	1.55E00	2.06E00	4.36E-1
$CH_2Cl+ClO=CHClO+HCl$	-1.61E-1	-1.97E-1	2.21E-1	-3.14E-2
$H+O_2=O+OH$	6.94E-1	9.38E-1	2.31E00	2.27E-1
$H+H_2O=H_2+OH$	-2.35E-1	-2.10E-1	-8.51E-2	-9.64E-2
$OH+HCl=H_2O+Cl$	-6.44E-2	-1.45E-1	-3.07E-1	-4.36E-1
$H+HCl=H_2+Cl$	1.19E-1	1.40E-1	1.73E-1	3.61E-2
$HOCl=Cl+OH$	1.42E-1	2.65E-1	4.52E-1	6.32E-1
$CO+ClO=CO_2+Cl$	1.50E-1	8.77E-2	2.04E-2	1.29E-2
$CO+OH=CO_2+H$	5.18E-1	5.58E-1	5.32E-1	3.43E-1
$CO+HO_2=CO_2+OH$	3.05E-1	3.01E-1	2.78E-1	3.49E-1

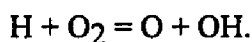
The faster decay of  $CH_2Cl_2$  in the data of Tsao<sup>8</sup>, Fig 6.17, results from higher  $CH_2Cl_2$  concentrations leading to more chain branching and not from the  $H_2$  bath gas. The slower decay (higher temperature requirement) for  $CH_2Cl_2$  in  $CH_4/Ar$  bath gas results from the slower reactions of  $Cl$  with  $CH_4$  relative to  $H_2$  and slower reactions of  $CH_3$  relative to  $H$  atoms, where  $H_2$  was present. Methane is, in addition, an intermediate product in  $CH_2Cl_2/H_2$  pyrolysis and large  $CH_4$  levels shift several of the  $CH_4$  production channels toward the reverse.

The sensitivity computer code SENS<sup>64</sup> was utilized to determine the relative importance of the reactions in the mechanism to various products, and specifically to reactions effective in inhibiting CO conversion to CO<sub>2</sub>. As shown in Table 6.4, the results indicate that the reaction  $\text{OH} + \text{HCl} \rightarrow \text{H}_2\text{O} + \text{Cl}$  is a major OH sink, which depletes OH and effectively stops the CO conversion via  $\text{CO} + \text{OH} \rightarrow \text{CO}_2 + \text{H}$ . The OH reaction with HCl is faster than  $\text{OH} + \text{CO}_2$  and depletes the OH when chlorocarbons, which lead to HCl levels comparable to those of CO, are present. Reactions with HO<sub>2</sub> and ClO are now the primary mechanism for CO conversion to CO<sub>2</sub> e.g. via  $\text{CO} + \text{HO}_2 \rightarrow \text{CO}_2 + \text{OH}$ .

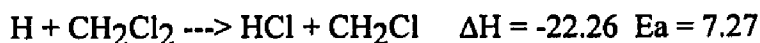
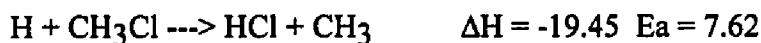
Westbrook<sup>3</sup> reports an important mechanism of chlorinated hydrocarbon inhibition as:



with the net result of these reactions being  $\text{H} + \text{H} = \text{H}_2$ . This "catalyzed" recombination of H atom reportedly results in a reduction in chain branching reactions such as



We have used the sensitivity code and our mechanism to evaluate the importance of these abstraction reactions in our system and do not find high sensitivity. We have evaluated the literature data to select the most accurate rate constants for H atom abstraction of Cl from RCl and determined that these reactions have relatively high activation energies ( $E_a$ 's). A best fit Evans-Polanyi relationship of  $E_a = \Delta H/4 + 12.58$  is obtained for the  $H_{\text{rxn}} = -50$  to  $-10$  Kcal/mol range. For example:

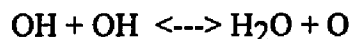
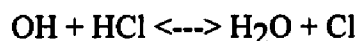


We find very little  $\text{Cl}_2$  produced. Molecular chlorine has a relative weak bond, and its reactions with hydrocarbon radicals, H, OH, and O are all exothermic. The  $\text{Cl}_2$  reactions, while rapid, are not indicated to be significant by the sensitivity analysis for our conditions, and  $\text{OH} + \text{HCl}$  is the most important inhibition reaction.

We have, in addition, used the sensitivity code with our mechanism to model more typical incineration conditions:  $\text{CH}_4$  (4%) with 0.4%  $\text{CH}_2\text{Cl}_2$ , 16%  $\text{O}_2$  in Ar, 1400°K. The results continue to show that the reaction of  $\text{OH} + \text{HCl} \rightarrow \text{H}_2\text{O} + \text{Cl}$  dominates the inhibition, with  $\text{H} + \text{HCl} \rightarrow \text{H}_2 + \text{Cl}$  also active, but less important as an inhibition mechanism. The Cl atoms produced, however, react rapidly with any  $\text{H}_2$  or hydrocarbon present to produce HCl and a radical, thus continuing the chain. This accelerates the reaction under fuel rich or low conversion conditions. Under CO burnout conditions, however, HCl depletes OH and the Cl produced then competes for hydrogen with oxygen and oxy species where the thermodynamics for H abstraction are favorable. Our conclusions on the importance of  $\text{OH} + \text{HCl}$  to inhibition are in agreement with those of Barat et. al.<sup>48</sup> in Well Stirred Reactor studies of  $\text{CH}_3\text{Cl}$  inhibition in ethylene/ $\text{O}_2$  flames. We also note that Roessler et. al.<sup>49</sup> report  $\text{H} + \text{HCl} = \text{H}_2 + \text{Cl}$  as the most important, but  $\text{OH} + \text{HCl}$  as the next most important inhibition reaction for CO oxidation in  $\text{H}_2/\text{O}_2$  mixtures with HCl present.

The reaction of  $\text{Cl} + \text{HO}_2$ , part of which goes to  $\text{HCl} + \text{O}_2$  (termination), now becomes an important part of the inhibition process. The lower degree of CO burnout decreases the system temperature, resulting in higher concentrations of  $\text{HO}_2$ .

The model indicates another interesting component relating to the effects of chlorocarbon inhibition. The addition of limited quantities of high temperature  $\text{H}_2\text{O}$  to the oxidation system, where Cl or oxygen atoms are present, shifts the reactions



to the left. This increases the OH concentrations and improves CO conversion during the reaction of chlorocarbons in  $\text{CH}_4/\text{O}_2/\text{HCl}$  atmospheres.

We also observe that chlorinated hydrocarbons initiate reactions in the fuel rich regions of chlorocarbon/hydrocarbon/ $\text{O}_2$  mixtures faster than during the normal oxidation of hydrocarbons<sup>65</sup>. This results in pyrolysis or molecular weight growth reactions in the fuel rich zones and increased possibility of soot formation. The reason for the increased hydrocarbon reactions is again the presence of chlorine. Carbon-chlorine bonds are known to be weaker than carbon-hydrogen, carbon-carbon, or carbon-oxygen bonds. Therefore, the C-Cl bond can break at lower temperatures, resulting in chain branching. The Cl atoms generated will rapidly abstract H atom from the hydrocarbons due to low activation energies and relatively high Arrhenius A factors, thus propagating the chain.

#### 6.4 Summary

A detailed kinetic reaction mechanism based upon fundamental thermochemical and kinetic principles, Transition State Theory, and evaluated literature rate constant data was developed. The mechanism was used to model results obtained from our experiments, in addition to results from other studies, on the thermal reactions of  $\text{CH}_2\text{Cl}_2$ . Reactions which demonstrated high sensitivity to CO burnout (inhibition) were evaluated. Here results indicate that the reaction  $\text{OH} + \text{HCl} \rightarrow \text{H}_2\text{O} + \text{Cl}$  is a major cause of OH loss. This decrease in OH effectively stops CO burnout. The reaction  $\text{H} + \text{HCl} \rightarrow \text{H}_2 + \text{Cl}$  is also important when  $\text{H}_2$  concentrations are low. The lower temperatures resulting from decreased CO conversion caused the  $\text{Cl} + \text{HO}_2$  reaction channel to  $\text{HCl} + \text{O}_2$ , termination, to become an important contributor to inhibition.

Sensitivity analysis indicates that the reaction  $\text{OH} + \text{OH} \rightleftharpoons \text{H}_2\text{O} + \text{O}$ , which usually forms  $\text{H}_2\text{O}$  during hydrocarbon incineration, reacts in the reverse direction when HCl is present at concentrations comparable to CO due to the large extent of OH depletion. The addition of moderate levels of high temperature steam is predicted to help

CO conversion by shifting the equilibrium to produce more OH for this and the  $\text{OH} + \text{HCl} \rightleftharpoons \text{H}_2\text{O} + \text{Cl}$  reaction.

## CHAPTER 7

### KINETIC STUDY ON PYROLYSIS AND OXIDATION OF $\text{CH}_3\text{Cl}$ IN $\text{Ar}/\text{H}_2/\text{O}_2$ MIXTURES

#### 7.1 Background

In recent years incineration has become a preferred method of destruction applicable to combustible organic wastes, with particular reference to the important family of hazardous wastes termed chlorinated hydrocarbons. The simplest subgroup within this family is the chlorinated methanes, which are widely used as industrial solvents. Reasonable methods for effective destruction of chlorinated hydrocarbons include: (a) conversion to  $\text{H}_2\text{O}$ ,  $\text{HCl}$ , and  $\text{CO}_2$  by oxidation (e.g. incineration), and (b) conversion to  $\text{HCl}$  and hydrocarbons by pyrolysis in a hydrogen or methane rich atmosphere<sup>5</sup>.

There are no other studies on reactions of chloromethane in  $\text{H}_2/\text{O}_2$  atmospheres to our knowledge. There are a number of studies on  $\text{CH}_3\text{Cl}$  oxidation or pyrolysis<sup>3,5,20</sup> in other atmospheres, including methane. These studies conclude that the  $\text{CH}_3\text{Cl}$  tends to initiate methane degradation faster, when present, and that the facile production of methyl radicals leads to relatively efficient formation of  $\text{C}_2$  species, i.e. molecular weight growth.

Earlier kinetic studies on methyl chloride pyrolysis were reported in 1959 by Shilov and Sabirova<sup>11</sup>. Measurements were made at initial  $\text{CH}_3\text{Cl}$  pressures of 10.1-34.3 torr, temperatures of 1062K-1147K, and at contact times of 0.4- 5.0 seconds; They found  $\text{HCl}$ ,  $\text{CH}_4$ , and  $\text{C}_2\text{H}_2$  in the ratios of 3:1:0.6. They also reported that the measured apparent first-order rate constants increased with increasing pressure. This data has been re-analyzed by Holbrook<sup>12</sup> and Fost et al.<sup>13</sup> to test Slater and RRKM theories. The calculated rate constants were, however, 20 to 30 times smaller than those experimentally measured. Our present analysis indicates that the experiments incurred significant chain continuation reaction due to rapid atomic chlorine abstraction of hydrogen from hydrocarbons.



Data on the pyrolysis of  $\text{CH}_3\text{Cl}$  at a high degree of conversion were reported by LeMoan<sup>15</sup>. The reaction was run at 993K for 30 hours in a batch reactor yielded conversions larger than 95%. The gas phase contained  $\text{HCl}$ ,  $\text{CH}_4$ , and small quantities of  $\text{H}_2$ , benzene, and toluene. Low transient concentrations of  $\text{CH}_2\text{Cl}_2$ ,  $\text{C}_2\text{H}_6$ , and  $\text{C}_2\text{H}_5\text{Cl}$  were detected at the beginning of the pyrolysis. In the liquid phase, benzene (72%), toluene (11%), xylene (1%), and monochlorobenzene (12%) were identified. There were two distinct solid phases: carbon in the reactor and naphthalene and soot at the exit from the reactor. The reaction mechanism, despite the large number of products identified, was considered to be schematically simple. It was proposed that, initially,  $\text{CH}_3\text{Cl}$  would decompose into  $\text{HCl}$  and  $^1\text{CH}_2$ , which would dimerize into  $\text{C}_2\text{H}_4$  or decompose into  $\text{CH} + \text{H}$  or  $\text{C} + \text{H}_2$ . The combination of two  $\text{CH}$  radicals would form acetylene. Acetylene would combine, then cyclize to form benzene, from which the identified higher molecular weight compounds would be formed. The hydrogenation of  $\text{CH}_2$  radicals would lead to methane. As we shall see later, this mechanism is not plausible.

$\text{CH}_3\text{Cl}$  decomposition was also studied by Weissman and Benson<sup>5</sup> using a flow system to generate product distributions at temperatures of 1260 and 1310K and over the pressure range 180 - 370 torr. They measured  $\text{CH}_4$ ,  $\text{C}_2\text{H}_2$ ,  $\text{C}_2\text{H}_4$ , and  $\text{HCl}$  as the major products with lower quantities of aromatic hydrocarbons and soot using Gas Chromatography and Mass Spectrometry techniques.

Miller et al.<sup>17</sup> and Senkan et al.<sup>16</sup> have both examined flames from  $\text{CH}_3\text{Cl}/\text{CH}_4/\text{O}_2$  mixtures. They presented kinetic modeling of the combustion of  $\text{CH}_3\text{Cl}$  in flames and suggested that the presence of chlorine decreases the concentration of ethane species and promotes soot formation by simultaneously increasing the rate of formation of  $\text{C}_2\text{H}_3$  and  $\text{C}_2\text{H}_2$ , which enhances the rate of nucleation and surface growth processes.

Roesler et al.<sup>18</sup> studied moist  $\text{CO}$  oxidation chemistry inhibited by  $\text{HCl}$  experimentally and numerically with dilute mixtures of  $\text{CO}$  (~1%),  $\text{H}_2\text{O}$  (~0.5%),  $\text{O}_2$  and

PLEASE NOTE

Page(s) not included with original material  
and unavailable from author or university.  
Filmed as received.

65-114

University Microfilms International

### 10.5.2 Fuel Lean Equivalence ratio 0.8 at in the PSR.

The major PICS calculated in this system, before addition of combustion modifiers, are  $\text{Cl}_2$ , Cl atom, HOCl, and Phosgene, and these range in mole fraction from  $1.0 \times 10^{-4}$  to  $1.0 \times 10^{-14}$ . Chloro-formaldehyde, trichloroethylene, and vinyl chloride concentrations are also calculated, but are at lower levels than the phosgene. Specifics are described below.

Figures 10.5 and 10.6 show the Cl atom mole fraction versus reaction time in the burnout and the low temperature cool-down regions respectively. Cl atom mole fraction at the PSR exit is at relatively high levels, probably super equilibrium. It decreases exponentially throughout the burnout and cool down zones.

The independent effects of adding 1% steam, hydrogen peroxide and formaldehyde at the beginning of the burnout zone are also illustrated in figure 10.5. Steam reduces the Cl mole fraction in the burnout region, i.e. it shifts the



equilibrium to the right, also increasing OH.

Formaldehyde addition at the 1% level increases Cl - creating a slightly higher temperature (initiates secondary combustion) and higher levels of the radical pool. Adding smaller amounts of  $\text{CH}_2\text{O}$ , (0.1 and 0.01 %) leaves the Cl level at that of the non-additive case. Cl in the cool down region, figure 10.6, shows similar trends but less difference in the Cl levels, for all additives.

The inlet of additives modifies the fuel equivalence ratio, as they are an added mass flow; the addition reduces the initial mole fraction of product species by 1 to 3 percent. The addition of 1 % formaldehyde for example increases the fuel equivalence ratio from 0.80 to 0.85.

Molecular chlorine levels in the cool down region are shown in Figure 10.7, where they are observed to increase from mole fraction of near 0.05 to 7.0 (xE-05) in 0.2

seconds for the non-additive case. Steam and H<sub>2</sub>O<sub>2</sub> effect a reduction of ca 15 % and formaldehyde effects a reduction of ca 30 % in the effluent Cl<sub>2</sub> levels.

HCl mole fractions throughout the reactor are shown in figure 10.8. HCl levels increase rapidly upon exit from the PSR and remain nearly constant throughout the cool-down region. Note that the abscissa scale in figure 10.8 is highly amplified and the differences in HCl through the cool-down region are all less than 2 %. All additives at the 1 % level show ca 1 % decreases in the HCl level, but this is the effect of increasing the total mole fraction while keeping the HCl nearly constant. The effluent HCl levels effectively remain unchanged for the different additives, in this fuel lean efficient combustion system.

Phosgene levels from the PSR through the higher temperature PFR are shown to decrease in the burnout region from mole fraction 1.0E-10 to 1.0E-14, figure 10.9. They increase, however, in the cool down region to ca. 1.2E13 as shown in figure 10.10. One percent CH<sub>2</sub>O added in the burnout region effects a more rapid decay of phosgene in this zone, but results in a slightly higher steady state level. Injection of H<sub>2</sub>O vapor results in the lowest mole fraction phosgene in the burnout region, while hydrogen peroxide effects the lowest overall level at the exit of the cool-down region.

### 10.5.3 Effects on CO/CO<sub>2</sub> Ratio

The CO/CO<sub>2</sub> ratio or level of CO emission is often used in the combustion community for determination of efficiency. We evaluate this ratio for both fuel rich and fuel lean conditions, and the conditions of 1 % water vapor, hydrogen peroxide, formaldehyde and oxygen added to the burnout region.

### 10.5.4 CO / CO<sub>2</sub> Fuel Rich Initial Conditions

Figures 10.11 and 10.12 correspond to the fuel rich system, which serves as a validation of the modeling. Clearly this fuel rich system,  $\phi = 1.5$ , is oxygen starved, and anything

that serves to increase the oxidant will significantly benefit this inadequate combustion system. The CO/CO<sub>2</sub> ratio is used as an indicator of combustion efficiency for 10,000 ppm, 1.2%, CH<sub>3</sub>Cl in the feed.

The Figures 10.11 and 10.12 show that addition of oxygen - 1 %, has the most dramatic effect, while hydrogen peroxide has a significant benefit, in agreement with the data of Cooper. It does not, however, equal the improvement of O<sub>2</sub>, because one of the two oxygen atoms in each H<sub>2</sub>O<sub>2</sub> is needed to form H<sub>2</sub>O, the sink for H's from the peroxide. Steam has some benefit in CO/CO<sub>2</sub> ratio, at the expense of H<sub>2</sub> formation, while formaldehyde further inhibits the combustion system. While these improvements with added O<sub>2</sub> are expected, they are an important check on the model and suggest that the model is representative of the chemistry occurring. The quantitative predictions we are calculating might not be 100 % accurate, but the qualitative trends should exist, and a combustor operator could look for these trends in optimization.

#### 10.5.5 CO / CO<sub>2</sub> Ratio Fuel Lean Initial Conditions - Equivalence ratio 0.8

The effect of steam addition, 0 to 0.4 mole fraction, on the CO / CO<sub>2</sub> effluent ratio, at two initial CH<sub>3</sub>Cl to CH<sub>4</sub> ratios, 1:4 and 1:10, is illustrated in figure 10.13. The initial CO and CO/CO<sub>2</sub> ratio is observed to be higher in the CH<sub>3</sub>Cl/CH<sub>4</sub> ratio 1:4 than for ratio 1:10.

$$1:4 = (\text{CH}_3\text{Cl}:\text{CH}_4:\text{O}_2 = 1.61:6.44:19.12)$$

$$1:10 = (\text{CH}_3\text{Cl}:\text{CH}_4:\text{O}_2 = 0.69:6.9:19.25)$$

A dramatic improvement - reduction in CO level and CO/CO<sub>2</sub> ratio, occurs as steam is added initially for the above CH<sub>3</sub>Cl / CH<sub>4</sub> ratios. CO mole fractions first decrease by more than one half, then rise as the mole fraction H<sub>2</sub>O added increases above 0.2. CO/CO<sub>2</sub> levels also decrease, then increase, but this ratio starts to increase faster than the CO.

The calculated effects from separate addition of steam, H<sub>2</sub>O<sub>2</sub> and CH<sub>2</sub>O, at the

1% level are illustrated in figures 10.14 and 10.15 for burnout and cool-down regions respectively. 1% formaldehyde increases the CO/CO<sub>2</sub> ratio in the burnout and at the start of the cooldown zone; but the 1% formaldehyde and the non-additive case are identical at the effluent point. This CO increase is primarily due to changes in the fuel equivalence ratio. 0.01 % CH<sub>2</sub>O added has no effect. H<sub>2</sub>O and H<sub>2</sub>O<sub>2</sub> addition show a small benefit at this one percent level.

The fraction change, X<sub>c</sub> reported as:

$$X_c = (\text{Concentration} - \text{additive}) / (\text{Concentration} - \text{non additive}) \text{ conditions}$$

for the PICs: phosgene, OH radical, H<sub>2</sub>, CO, Cl<sub>2</sub> and Cl atom, is illustrated in figure 10.16, for addition of: 1% steam, 1% H<sub>2</sub>O<sub>2</sub> and 0.01% CH<sub>2</sub>O at the 320 K effluent point. A value of 1 corresponds to no change.

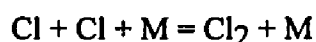
#### 10.5.6 Discussion

The temperature of the additives injected is relatively "cold", 400 K, compared to the near 2000 K temperature in the burnout zone. A decrease in temperature in the burnout region can result from injection of large quantities of additives and may reduce CO burnout. Super heated steam may be a better choice for an additive here.

Cl atoms add to CO in a stepwise process, in two steps, to form phosgene.



Two Cl atoms also combine to form chlorine gas.



These appear to be the mechanism of phosgene and Cl<sub>2</sub> formation in the relatively low Cl to H ratio and ideal, well mixed, fuel lean combustion studies reported in this paper. Here the POHC is effectively completely destroyed at the end of the adiabatic burnout region, and the levels of chlorocarbon PIC's are not high enough to account for the phosgene formation.

The phosgene formation mechanism may be very different in non well mixed systems, in systems where there is higher chlorine loadings, or where the POHC or Chlorinated PICs are present in significant concentrations. This is most likely the case, for example, in the studies on phosgene formation reported by the Koshland or Sawyer research groups at Berkeley<sup>19</sup>.

The fuel rich calculation results are an important check on the model and help support the model as representative of the chemistry occurring. We indicate that the quantitative predictions might not be 100 % accurate, but that the qualitative trends should be present.

### 10.6 Conclusions

We have illustrated several examples of the presently available analysis of combustion systems using a detailed mechanism and the assumption of complete mixing.

Under fuel rich conditions, addition of steam, hydrogen peroxide, and oxygen will improve CO/CO<sub>2</sub> ratio. Oxygen is the most effective here. Additions of formaldehyde or methane to the burnout region will produce more CO in a stepwise process which may increase CO/CO<sub>2</sub> ratio.

Under fuel lean conditions, formation of CO is low. Additions of steam and hydrogen peroxide to the burnout region slightly improve the CO/CO<sub>2</sub> ratio. Addition of CH<sub>2</sub>O under fuel lean conditions may decrease other PICs while slightly increasing formation of CO and COCl<sub>2</sub>, unless an oxygen source is co-added. Formaldehyde addition at lower equivalence ratios should be more beneficial.

These results are specific to the conditions in this study and we note that that a fuel equivalence ration lower than 0.8 was calculated to yield lower pollutant levels and more efficient combustion.

## **APPENDIX A**

### **THERMODYNAMIC PROPERTIES**



SPECIES	HF(298)	S (298)	CP300	CP500	CP800	CP1000	CP1500	CP2000	Ref
AR	0.00	36.98	4.97	4.97	4.97	4.97	4.97	4.97	a
C(S)	0.00	21.83	2.06	3.50	4.74	5.15	5.65	5.89	a
Cl	28.90	39.50	5.20	5.40	5.35	5.30	5.24	3.40	b
H <sub>2</sub>	0.00	31.21	6.90	6.99	7.10	7.21	7.72	8.17	a
H	52.10	27.36	4.97	4.97	4.97	4.97	4.97	4.97	a
HCl	-22.07	44.64	6.96	6.99	7.29	7.56	8.10	8.40	c
Cl <sub>2</sub>	0.00	53.30	8.10	8.59	8.91	8.99	9.10	9.16	b
CH <sub>2</sub>	92.35	46.32	8.28	8.99	10.15	10.88	12.22	13.00	a
<sup>1</sup> CH <sub>2</sub>	101.44	44.15	8.28	8.99	10.15	10.88	12.22	13.00	a
CH <sub>3</sub>	35.12	46.38	9.26	10.81	12.90	14.09	16.26	17.56	a
CH <sub>4</sub>	-17.90	44.48	8.51	11.10	15.00	17.20	20.61	22.61	a
C <sub>2</sub> H <sub>2</sub>	54.19	48.01	10.60	13.08	15.31	16.29	18.31	19.57	a
C <sub>2</sub> H <sub>3</sub>	70.40	56.20	10.89	13.87	17.16	18.73	21.34	23.20	e
C <sub>2</sub> H <sub>4</sub>	12.54	52.39	10.28	14.91	20.03	22.45	26.21	28.35	a
C <sub>2</sub> H <sub>5</sub>	28.36	57.90	12.26	17.13	22.85	25.74	30.54	33.31	e
C <sub>2</sub> H <sub>6</sub>	-20.24	54.85	12.58	18.68	25.80	29.33	34.91	38.37	a
CHCl	76.62	56.17	8.80	10.13	12.11	13.22	14.78	14.96	f
CH <sub>2</sub> Cl	29.10	59.60	9.32	11.14	14.10	15.83	18.31	18.93	h
CCl <sub>2</sub>	51.10	49.00	11.09	12.52	13.61	14.09	15.41	15.84	f
CHCl <sub>2</sub>	23.50	67.40	13.11	14.68	16.83	17.98	19.80	21.20	h
CH <sub>3</sub> Cl	-19.59	56.01	9.77	13.20	17.02	18.87	21.80	23.40	i
CH <sub>2</sub> Cl <sub>2</sub>	-22.80	64.59	12.26	15.88	19.36	20.81	22.90	24.00	c
CHCl <sub>3</sub>	-24.20	70.66	15.77	19.31	21.96	22.82	24.21	24.60	c
C <sub>2</sub> HCl	52.10	58.10	13.17	15.18	16.88	17.55	18.80	19.55	j
C <sub>2</sub> H <sub>3</sub> Cl	5.00	63.09	12.33	17.73	22.47	24.26	26.88	28.80	b
CH <sub>2</sub> CCl <sub>2</sub>	0.62	69.25	15.81	20.56	24.68	26.19	28.21	29.60	j
CHClCHCl	0.75	69.25	15.81	20.56	24.68	26.19	28.21	29.60	j
CHClCH	61.83	64.46	11.39	16.35	21.23	23.38	26.87	28.80	j
CH <sub>2</sub> CCl	60.40	64.46	11.39	16.35	21.23	23.38	26.87	28.80	j
CCl <sub>2</sub> CH	58.20	68.88	17.52	22.16	25.74	26.90	28.60	29.85	j
C <sub>2</sub> HCl <sub>3</sub>	-1.40	77.63	19.22	23.75	26.80	27.60	28.98	30.10	j
CH <sub>2</sub> ClCH <sub>2</sub>	21.18	68.50	14.01	20.09	25.88	28.98	33.44	34.21	j
CH <sub>3</sub> CHCl	17.68	67.31	14.10	19.79	25.42	27.99	32.50	34.70	h
CH <sub>3</sub> CCl <sub>2</sub>	11.50	73.60	17.28	22.86	28.09	30.18	33.09	35.01	j
CHCl <sub>2</sub> CH <sub>2</sub>	16.04	74.30	17.35	22.95	28.03	30.29	33.07	34.55	j
CH <sub>2</sub> ClCHCl	11.49	75.80	16.81	22.56	27.67	29.75	33.21	34.50	j
CH <sub>2</sub> ClCCl <sub>2</sub>	7.05	83.20	20.21	25.68	30.14	31.77	34.50	36.10	j
C <sub>2</sub> H <sub>2</sub> Cl <sub>3</sub>	8.50	83.10	20.21	25.68	30.14	31.77	34.50	36.10	j
C <sub>2</sub> H <sub>5</sub> Cl	-26.83	66.03	15.06	21.67	28.43	31.47	36.27	39.17	j
CH <sub>3</sub> CHCl <sub>2</sub>	-31.10	73.05	18.29	24.81	30.87	33.44	37.80	40.16	g
CH <sub>2</sub> ClCH <sub>2</sub> Cl	-30.60	74.16	18.99	24.74	30.32	33.06	38.79	40.77	g
CH <sub>3</sub> CCl <sub>3</sub>	-33.84	76.55	22.52	28.45	33.70	35.73	38.91	41.60	c

C2H2Cl4	-37.20	86.01	25.23	31.32	36.05	37.59	39.82	41.10	g
C2HCl4	5.80	87.90	23.50	28.76	32.52	33.68	35.70	36.30	j
CH2ClCHCl2	-34.70	81.50	21.01	27.67	33.26	35.36	38.91	41.10	c
O	59.55	38.47	5.23	5.08	5.01	5.01	4.98	4.98	a
O2	0.0	49.01	7.02	7.44	8.04	8.35	8.73	9.04	a
OH	9.49	43.88	7.16	7.05	7.15	7.33	7.87	8.27	a
H2O	-57.80	45.10	8.02	8.41	9.24	9.85	11.23	12.20	a
HO2	3.50	54.73	8.37	9.48	10.78	11.43	12.47	13.23	a
H2O2	-32.53	55.66	10.42	12.35	14.30	15.21	16.85	17.88	a
CO	-26.42	47.21	6.96	7.13	7.61	7.94	8.41	8.67	a
CHO	10.40	53.66	8.27	9.27	10.73	11.51	12.55	13.15	a
ClO	24.20	54.10	7.50	8.21	8.69	8.81	9.00	9.10	b
Cl2O	19.71	63.66	11.41	12.76	13.46	13.55	13.81	13.85	b
ClO2	25.00	61.50	9.99	11.72	12.97	13.32	13.80	13.86	b
CClO	-4.00	63.50	10.80	11.70	12.50	12.90	13.40	13.70	b
HOCl	-17.80	56.50	8.91	10.08	11.13	11.58	12.40	12.80	b
COCl2	-52.60	67.80	13.81	16.26	17.97	18.45	19.21	19.50	b
CHClO	-39.30	61.80	11.12	13.55	15.70	16.58	18.11	18.80	j
CO2	-94.05	51.07	8.90	10.65	12.30	12.97	13.93	14.45	a
CH2O	-26.00	52.26	8.45	10.49	13.34	14.86	16.95	18.14	a
CH3O	3.90	53.25	9.01	12.22	16.28	18.38	21.56	23.13	a
CH2OH	-2.60	59.61	9.72	12.58	15.99	17.60	19.80	21.00	a
CH2CO	-11.74	57.79	12.98	16.92	20.31	21.61	23.80	25.55	a
CH3OH	-48.06	57.28	10.48	14.34	19.00	21.35	24.96	27.25	b
HCCO	41.36	60.62	11.82	14.63	17.13	18.09	19.38		b
CH2ClO	2.16	63.27	11.22	15.05	18.65	20.33	22.40	23.70	j
CH2ClOO	3.50	73.11	15.84	17.98	22.92	24.57	27.10	28.40	j
CH2OOC1	10.00	78.60	17.50	22.10	27.10	28.80	31.70	33.30	j

Unit: Hf, Kcal/mol; S and Cp, cal/(mol °K)

### References for Thermodynamic Properties

- a. JANAF Thermochemical Tables, 3rd Edition, NSRDS-NBS 37 (1986)
- b. Benson, S.W., Thermochemical Kinetics, John Wiley and Son, 1976
- c. Stull, D.R., Westrum, R.F., and Sinke, G.C., The Chemical Thermodynamics of Organic Compounds, Robert E. Kreger Publishing Co., 1987
- d. Orlov, Y.D., Lebedev, Y.A., and Korsunskii, B.L., Russ. J. Chem., 1424, 1985
- e. Brouard, M., Lightfoot, P.D., and Pilling, M.J.; J. Phys. Chem., 90, 445, 1986

- f. Lias, S.G.; Bartmess, J.E.; Liebman, J.F.; Holmes, J.L.; Levin, R.D.; Mallard, G.W.; J. Phys. Chem. Ref. Data, 17, Suppl. 1, 1988
- g. Pedley, J.B.; Naylor, R.O.; Kirby, S.P.; Thermodynamic Data of Organic Compounds, Chapman and Hall, New York, 1987
- h. Tschuikow-Roux, E. and Chen, Y.; J. Am. Chem. Soc., 111, 1511 1989.
- i. Rogers, A.S.; Selected Values for Thermodynamic Properties of Chemical Compounds, Thermodynamic Research Center, Texas A&M Univ. 1982
- j. Estimated by Group Additivity and NJIT bond energy.

## APPENDIX B

### DETAILED MECHANISM FOR CH<sub>2</sub>Cl<sub>2</sub> AND CH<sub>3</sub>Cl PYROLYSIS AND OXYDATION

$$k = A \times T^n \times \exp(-E_a/RT)$$

units for A: cm<sup>3</sup>/mole-sec and sec<sup>-1</sup>; E<sub>a</sub>: Kcal/mole

ΔH<sub>rxn</sub> taken as from stabilized adduct.

CH<sub>2</sub>S : singlet methylene, <sup>1</sup>CH<sub>2</sub>

DISSOC: apparent rate constant from DISSOC computer code  
(QRRK unimolecular dissociation calculation, high pressure limit k listed above.  
DISSOC values used in kinetic code)

QRRK : apparent rate constant from CHEMACT computer code  
high pressure limit k listed in Appendix C

Reaction	A	n	Ea	source
CH <sub>2</sub> Cl <sub>2</sub> = CHCl + HCl	1.42E+14	0.0	105.	1
	1.82E+37	-7.43	85.7	DISSOC
CH <sub>2</sub> Cl <sub>2</sub> = CH <sub>2</sub> Cl + Cl	1.02E+16	0.0	75.8	2,3
	1.60E+40	-7.84	83.6	DISSOC
CH <sub>2</sub> Cl <sub>2</sub> + H = CH <sub>2</sub> Cl + HCl	7.00E+13	0.0	7.1	4
CH <sub>2</sub> Cl <sub>2</sub> + Cl = CHCl <sub>2</sub> + HCl	2.79E+13	0.0	2.94	4
CH <sub>2</sub> Cl <sub>2</sub> + CH <sub>3</sub> = CH <sub>4</sub> + CHCl <sub>2</sub>	6.76E+10	0.0	7.2	4
CH <sub>2</sub> Cl <sub>2</sub> + CH <sub>3</sub> = CH <sub>3</sub> Cl + CH <sub>2</sub> Cl	1.40E+11	0.0	4.9	4
CH <sub>2</sub> Cl <sub>2</sub> + O <sub>2</sub> = CHCl <sub>2</sub> + HO <sub>2</sub>	1.35E+13	0.0	51.8	20
CH <sub>2</sub> Cl <sub>2</sub> + HO <sub>2</sub> = CHCl <sub>2</sub> + H <sub>2</sub> O <sub>2</sub>	6.67E+12	0.0	18.27	21
CH <sub>2</sub> Cl <sub>2</sub> + OH = CHCl <sub>2</sub> + H <sub>2</sub> O	2.83E+12	0.0	2.09	19
CH <sub>2</sub> Cl <sub>2</sub> + O = CHCl <sub>2</sub> + OH	6.00E+12	0.0	5.76	40
CH <sub>3</sub> Cl = CH <sub>3</sub> + Cl	1.28E+15	0.0	83.0	15,30
	1.31E+37	-6.92	90.65	DISSOC
CH <sub>3</sub> Cl = CH <sub>2</sub> S + HCl				
	1.10E+28	-5.15	109.67	DISSOC
CH <sub>3</sub> Cl + H = CH <sub>3</sub> + HCl	6.64E+13	0.0	7.62	4
CH <sub>3</sub> Cl + Cl = CH <sub>2</sub> Cl + HCl	3.16E+13	0.0	3.3	4
CH <sub>3</sub> Cl + O <sub>2</sub> = CH <sub>2</sub> Cl + HO <sub>2</sub>	2.02E+13	0.0	54.2	22
CH <sub>3</sub> Cl + O = CH <sub>2</sub> Cl + OH	1.70E+13	0.0	7.3	4
CH <sub>3</sub> Cl + OH = CH <sub>2</sub> Cl + H <sub>2</sub> O	2.45E+12	0.0	2.7	4
CH <sub>3</sub> Cl + ClO = CH <sub>2</sub> Cl + HOCl	3.03E+11	0.0	10.7	38,19
CH <sub>3</sub> Cl + HO <sub>2</sub> = CH <sub>2</sub> Cl + H <sub>2</sub> O <sub>2</sub>	1.00E+13	0.0	21.66	45
CH <sub>3</sub> Cl + CH <sub>3</sub> = CH <sub>4</sub> + CH <sub>2</sub> Cl	3.30E+11	0.0	9.4	4
CH <sub>2</sub> Cl + H <sub>2</sub> = CH <sub>3</sub> Cl + H	3.90E+12	0.0	14.06	4,6
CH <sub>2</sub> Cl + O <sub>2</sub> = CH <sub>2</sub> O + ClO	1.91E+14	-1.27	3.81	QRRK
CH <sub>2</sub> Cl + O <sub>2</sub> = CH <sub>2</sub> ClOO	2.73E+33	-7.5	4.44	QRRK
CH <sub>2</sub> Cl + O = CH <sub>2</sub> ClO	1.29E+15	-1.98	1.1	QRRK
CH <sub>2</sub> Cl + O = CH <sub>2</sub> O + Cl	5.59E+13	-0.13	0.71	QRRK
CH <sub>2</sub> Cl + OH = CH <sub>2</sub> O + HCl	1.24E+22	-2.72	3.86	QRRK
CH <sub>2</sub> Cl + OH = CH <sub>2</sub> OH + Cl	2.00E+12	0.29	3.27	QRRK
CH <sub>2</sub> Cl + HO <sub>2</sub> = CH <sub>2</sub> ClO + OH	1.00E+13	0.0	0.0	25,12
CH <sub>2</sub> Cl + ClO = CHClO + HCl	4.13E+19	-2.22	2.36	QRRK
CH <sub>2</sub> Cl + ClO = CH <sub>2</sub> ClO + Cl	4.15E+12	0.07	11.1	QRRK
CH <sub>2</sub> Cl + CH <sub>2</sub> O = CH <sub>3</sub> Cl + CHO	3.56E+11	0.0	6.2	24,4
CH <sub>2</sub> Cl + CH <sub>2</sub> Cl = C <sub>2</sub> H <sub>4</sub> Cl <sub>2</sub>	7.84E+45	-10.21	13.15	QRRK
CH <sub>2</sub> Cl + CH <sub>2</sub> Cl = CH <sub>2</sub> ClCH <sub>2</sub> + Cl	9.34E+29	-4.94	14.07	QRRK
CH <sub>2</sub> Cl + CH <sub>2</sub> Cl = C <sub>2</sub> H <sub>3</sub> Cl + HCl	3.75E+35	-6.73	13.16	QRRK
CH <sub>2</sub> Cl + CHCl <sub>2</sub> = C <sub>2</sub> H <sub>3</sub> Cl <sub>3</sub>	6.41E+33	-10.22	12.91	QRRK
CH <sub>2</sub> Cl + CHCl <sub>2</sub> = CH <sub>2</sub> CCl <sub>2</sub> + HCl	3.75E+36	-7.22	13.62	QRRK
CH <sub>2</sub> Cl + CHCl <sub>2</sub> = CHClCHCl + HCl	1.22E+37	-7.20	13.64	QRRK
CH <sub>2</sub> Cl + CH <sub>3</sub> = C <sub>2</sub> H <sub>5</sub> Cl	3.27E+40	-8.49	10.59	QRRK

Reaction	A	n	Ea	source
CH <sub>2</sub> Cl + CH <sub>3</sub> = C <sub>2</sub> H <sub>4</sub> + HCl	3.50E+29	-4.49	9.18	QRRK
CH <sub>2</sub> Cl + CH <sub>3</sub> = C <sub>2</sub> H <sub>5</sub> + Cl	9.27E+19	-2.07	10.13	QRRK
CH <sub>2</sub> Cl + H = CH <sub>3</sub> Cl	3.04E+25	-4.47	3.49	QRRK
CH <sub>2</sub> Cl + H = CH <sub>3</sub> + Cl	5.12E+14	-0.22	0.31	QRRK
CH <sub>2</sub> Cl + H = CH <sub>2</sub> S + HCl	9.48E+04	1.91	2.6	QRRK
CHCl <sub>2</sub> + CH <sub>3</sub> = CH <sub>3</sub> CHCl <sub>2</sub>	2.28E+41	-8.68	11.62	QRRK
CHCl <sub>2</sub> + CH <sub>3</sub> = C <sub>2</sub> H <sub>3</sub> Cl + HCl	1.35E+30	-4.96	11.55	QRRK
CHCl <sub>2</sub> + CH <sub>3</sub> = CH <sub>3</sub> CHCl + Cl	2.74E+25	-3.45	12.81	QRRK
CHCl <sub>2</sub> + CHCl <sub>2</sub> = C <sub>2</sub> H <sub>2</sub> Cl <sub>4</sub>	9.08E+45	-10.56	13.17	QRRK
CHCl <sub>2</sub> + CHCl <sub>2</sub> = C <sub>2</sub> H <sub>2</sub> Cl <sub>3</sub> + Cl	1.36E+30	-5.23	14.18	QRRK
CHCl <sub>2</sub> + CHCl <sub>2</sub> = C <sub>2</sub> HCl <sub>3</sub> + HCl	6.72E+35	-7.11	13.21	QRRK
CHCl <sub>2</sub> + H = CH <sub>2</sub> Cl <sub>2</sub>	4.81E+26	-4.82	3.81	QRRK
CHCl <sub>2</sub> + H = CH <sub>2</sub> Cl + Cl	1.25E+14	-0.03	0.57	QRRK
CHCl <sub>2</sub> + H <sub>2</sub> = CH <sub>2</sub> Cl <sub>2</sub> + H	4.30E+12	0.0	15.3	4,5
CCl <sub>3</sub> + CH <sub>3</sub> = C <sub>2</sub> H <sub>3</sub> Cl <sub>3</sub>	9.54E+46	-10.66	11.74	QRRK
CCl <sub>3</sub> + CH <sub>3</sub> = CH <sub>2</sub> CCl <sub>2</sub> + HCl	1.62E+30	-5.33	8.64	QRRK
CCl <sub>3</sub> + CH <sub>3</sub> = CH <sub>3</sub> CCl <sub>2</sub> + Cl	3.98E+22	-2.63	7.09	QRRK
CCl <sub>3</sub> + CH <sub>2</sub> Cl = C <sub>2</sub> H <sub>2</sub> Cl <sub>4</sub>	4.01E+45	-10.15	10.67	QRRK
CCl <sub>3</sub> + CH <sub>2</sub> Cl = C <sub>2</sub> HCl <sub>3</sub> + HCl	4.74E+30	-5.08	8.81	QRRK
CCl <sub>3</sub> + CH <sub>2</sub> Cl = C <sub>2</sub> H <sub>2</sub> Cl <sub>3</sub> + Cl	5.90E+23	-2.84	8.96	QRRK
CCl <sub>3</sub> + H <sub>2</sub> = CHCl <sub>3</sub> + H	5.01E+12	0.0	14.3	49
CCl <sub>3</sub> + CH <sub>4</sub> = CHCl <sub>3</sub> + CH <sub>3</sub>	5.00E+12	0.0	14.9	49
CHCl + CHCl = CHClCHCl	4.00E+12	0.0	0.0	50
CHCl + O <sub>2</sub> = CHClO + O	1.50E+13	0.0	2.86	50
CHCl + O = CHClO	1.00E+13	0.0	0.0	50
CHCl + O <sub>2</sub> = CO + HOCl	1.20E+11	0.0	0.0	50
C <sub>2</sub> H <sub>3</sub> Cl + H = CH <sub>2</sub> ClCH <sub>2</sub>	5.01E+23	-4.21	8.47	QRRK
C <sub>2</sub> H <sub>3</sub> Cl + H = C <sub>2</sub> H <sub>4</sub> + Cl	1.55E+13	-0.02	5.84	QRRK
C <sub>2</sub> H <sub>3</sub> Cl + H = C <sub>2</sub> H <sub>3</sub> + HCl	1.20E+12	0.0	15.0	36
C <sub>2</sub> HCl <sub>3</sub> + H = CH <sub>2</sub> ClCCl <sub>2</sub>	1.51E+23	-4.18	7.52	QRRK
C <sub>2</sub> HCl <sub>3</sub> + H = C <sub>2</sub> H <sub>2</sub> Cl <sub>3</sub>	2.87E+22	-4.09	10.89	QRRK
C <sub>2</sub> HCl <sub>3</sub> + H = CH <sub>2</sub> CCl <sub>2</sub> + Cl	1.45E+13	-0.01	5.83	QRRK
C <sub>2</sub> HCl <sub>3</sub> + H = CHClCHCl + Cl	7.37E+12	-0.01	9.22	QRRK
CH <sub>2</sub> CCl <sub>2</sub> + H = C <sub>2</sub> H <sub>3</sub> Cl + Cl	7.21E+12	0.0	7.51	QRRK
CHClCHCl + H = C <sub>2</sub> H <sub>3</sub> Cl + Cl	3.44E+13	0.03	5.89	QRRK
CHClCHCl = C <sub>2</sub> HCl + HCl	7.26E+13	0.0	69.09	50
CH <sub>2</sub> CCl <sub>2</sub> = C <sub>2</sub> HCl + HCl	1.45E+14	0.0	69.22	50
C <sub>2</sub> HCl <sub>3</sub> = C <sub>2</sub> Cl <sub>2</sub> + HCl	7.26E+13	0.0	74.44	50
C <sub>2</sub> HCl + H = HCl + C <sub>2</sub> H	1.00E+13	0.0	17.03	50
C <sub>2</sub> HCl + H = C <sub>2</sub> H <sub>2</sub> + Cl	2.00E+13	0.0	2.1	50
C <sub>2</sub> H <sub>4</sub> Cl <sub>2</sub> = C <sub>2</sub> H <sub>3</sub> Cl + HCl	3.98E+13	0.0	58.0	30
	6.76E+19	-1.93	58.71	DISSOC

Reaction	A	n	Ea	source
CH <sub>3</sub> CHCl <sub>2</sub> = C <sub>2</sub> H <sub>3</sub> Cl + HCl	2.80E+13	0.0	57.65	30
	2.94E+21	-2.37	59.46	DISSOC
CH <sub>3</sub> CHCl <sub>2</sub> = CH <sub>3</sub> CHCl + Cl	6.65E+15	0.0	80.7	3,23
	3.17E+42	-8.10	92.67	DISSOC
C <sub>2</sub> H <sub>3</sub> Cl <sub>3</sub> = CHClCHCl + HCl	1.39E+20	-2.03	60.45	DISSOC
C <sub>2</sub> H <sub>3</sub> Cl <sub>3</sub> = CH <sub>2</sub> CCl <sub>2</sub> + HCl	3.13E+19	-2.02	60.33	DISSOC
C <sub>2</sub> H <sub>2</sub> Cl <sub>4</sub> = C <sub>2</sub> HCl <sub>3</sub> + HCl	8.62E+21	-2.57	51.87	DISSOC
C <sub>2</sub> H <sub>5</sub> Cl = C <sub>2</sub> H <sub>4</sub> + HCl	7.81E+19	-2.0	60.66	DISSOC
C <sub>2</sub> H <sub>5</sub> Cl = C <sub>2</sub> H <sub>5</sub> + Cl	2.35E+43	-8.5	96.98	DISSOC
C <sub>2</sub> H <sub>5</sub> Cl + Cl = HCl + CH <sub>3</sub> CHCl	3.55E+13	0.0	15.0	4
C <sub>2</sub> H <sub>5</sub> Cl + Cl = HCl + CH <sub>2</sub> ClCH <sub>2</sub>	1.12E+13	0.0	15.0	4
C <sub>2</sub> H <sub>5</sub> Cl + H = HCl + C <sub>2</sub> H <sub>5</sub>	1.00E+14	0.0	7.9	4
C <sub>2</sub> H <sub>3</sub> Cl = C <sub>2</sub> H <sub>2</sub> + HCl	3.16E13	0.0	45.27	30
	1.62E+28	-4.29	75.78	DISSOC
C <sub>2</sub> H <sub>3</sub> Cl = C <sub>2</sub> H <sub>3</sub> + Cl	3.98E+15	0.0	87.0	26
	1.71E+38	-7.13	96.37	DISSOC
C <sub>2</sub> H <sub>6</sub> = C <sub>2</sub> H <sub>5</sub> + H	1.30E+16	0.0	100.7	7
	6.22E+47	-9.76	111.25	DISSOC
C <sub>2</sub> H <sub>6</sub> = CH <sub>3</sub> + CH <sub>3</sub>	8.00E+16	0.0	90.4	7
	5.34E+54	-11.12	112.21	DISSOC
C <sub>2</sub> H <sub>6</sub> + H = C <sub>2</sub> H <sub>5</sub> + H <sub>2</sub>	6.61E+13	0.0	3.6	4
C <sub>2</sub> H <sub>6</sub> + Cl = C <sub>2</sub> H <sub>5</sub> + HCl	4.37E+13	0.0	0.1	19
C <sub>2</sub> H <sub>6</sub> + O = C <sub>2</sub> H <sub>5</sub> + OH	2.51E+13	0.0	6.4	4
C <sub>2</sub> H <sub>6</sub> + OH = C <sub>2</sub> H <sub>5</sub> + H <sub>2</sub> O	8.85E+09	1.04	1.81	36
C <sub>2</sub> H <sub>5</sub> = C <sub>2</sub> H <sub>4</sub> + H	5.01E+13	0.0	40.9	7
	1.83E+39	-7.75	52.82	DISSOC
C <sub>2</sub> H <sub>5</sub> + H = CH <sub>3</sub> + CH <sub>3</sub>	1.35E+22	-2.17	7.0	QRRK
C <sub>2</sub> H <sub>5</sub> + O = CH <sub>2</sub> O + CH <sub>3</sub>	1.00E+13	0.0	0.0	18
C <sub>2</sub> H <sub>5</sub> + O <sub>2</sub> = C <sub>2</sub> H <sub>4</sub> + HO <sub>2</sub>	2.00E+12	0.0	4.99	11
C <sub>2</sub> H <sub>5</sub> + HO <sub>2</sub> = C <sub>2</sub> H <sub>4</sub> + H <sub>2</sub> O <sub>2</sub>	3.01E+11	0.0	0.0	36
C <sub>2</sub> H <sub>4</sub> + O <sub>2</sub> = C <sub>2</sub> H <sub>3</sub> + HO <sub>2</sub>	4.22E+13	0.0	57.62	36
C <sub>2</sub> H <sub>4</sub> + CH <sub>3</sub> = C <sub>2</sub> H <sub>3</sub> + CH <sub>4</sub>	4.20E+11	0.0	11.11	11
C <sub>2</sub> H <sub>4</sub> + OH = C <sub>2</sub> H <sub>3</sub> + H <sub>2</sub> O	1.58E+04	2.75	4.173	36
C <sub>2</sub> H <sub>4</sub> + H = C <sub>2</sub> H <sub>3</sub> + H <sub>2</sub>	6.92E+14	0.0	14.5	8
C <sub>2</sub> H <sub>4</sub> + Cl = C <sub>2</sub> H <sub>3</sub> + HCl	2.39E+13	0.0	2.6	30
C <sub>2</sub> H <sub>4</sub> = C <sub>2</sub> H <sub>2</sub> + H <sub>2</sub>	2.95E+17	0.0	79.28	11
	8.52E+43	-8.32	121.24	DISSOC
C <sub>2</sub> H <sub>4</sub> = C <sub>2</sub> H <sub>3</sub> + H	2.00E+16	0.0	110.0	7
	8.53E+30	-5.87	118.24	DISSOC
C <sub>2</sub> H <sub>3</sub> + H = C <sub>2</sub> H <sub>2</sub> + H <sub>2</sub>	9.26E+13	0.0	0.0	36
C <sub>2</sub> H <sub>3</sub> = C <sub>2</sub> H <sub>2</sub> + H	3.16E+12	0.0	38.3	7
	6.24E+29	-5.29	46.5	DISSOC

Reaction	A	n	Ea	source
C2H3 + O2 = C2H2 + HO2	1.21E+11	0.0	0.0	36
C2H3 + O2 = CHO + CH2O	3.97E+12	0.0	-0.25	47
C2H2 + H2 = C2H3 + H	2.41E+12	0.0	65.0	36
C2H2 + HO2 = CH2CO + OH	6.03E+09	0.0	7.95	36
C2H2 + Cl = C2H + HCl	1.58E+14	0.0	16.9	30
C2H2 + O2 = C2H + HO2	1.21E+11	0.0	0.0	36
C2H2 + O = CH2 + CO	4.10E+08	1.5	1.69	11
C2H2 + O = HCCO + H	1.02E+07	2.0	1.9	13
C2H2 + OH = CH2CO + H	3.20E+11	0.0	0.2	13
C2H2 + OH = C2H + H2O	1.45E+04	2.68	12.04	36
C2H2 + H = C2H + H2	6.00E+13	0.0	23.66	11
C2H + O2 = CO + CH2	2.41E+12	0.0	0.0	36
C2H + H2 = C2H2 + H	1.15E+13	0.0	2.88	36
C2H + CH4 = C2H2 + CH3	1.81E+12	0.0	0.5	36
C2H + OH = CH2 + CO	1.81E+13	0.0	0.0	36
C2H + OH = C2H2 + O	1.81E+13	0.0	0.0	36
HCCO + H = CH2S + CO	3.00E+13	0.0	0.0	11
CH2CO + O = CH2 + CO2	1.74E+12	0.0	1.35	13
CH2CO + M = CH2 + CO + M	3.00E+15	0.0	75.98	13
CH2CO + H = HCCO + H2	5.00E+13	0.0	8.0	13
CH2CO + O = HCCO + OH	1.00E+13	0.0	8.0	13
CH2CO + OH = HCCO + H2O	7.50E+12	0.0	2.0	13
CH2CO + OH = CHO + CH2O	1.00E+13	0.0	0.0	11
CH2CO + H = CH3 + CO	7.00E+12	0.0	3.01	11
CH4 = CH3 + H	1.00E+16	0.0	105.0	7
	1.03E+33	-5.58	111.8	DISSOC
CH4 + H = CH3 + H2	1.55E+14	0.0	11.0	4
CH4 + Cl = CH3 + HCl	3.09E+13	0.0	3.6	46
CH4 + O2 = CH3 + HO2	4.04E+13	0.0	56.91	36
CH4 + O = CH3 + OH	1.02E+09	1.5	8.6	36
CH4 + OH = CH3 + H2O	1.93E+05	2.4	2.11	36
CH4 + HO2 = CH3 + H2O2	2.00E+13	0.0	18.0	9
CH4 + ClO = CH3 + HOCl	6.03E+11	0.0	15.0	37,19
CH3 + O2 = CH2O + OH	4.35E+13	-0.45	17.26	QRRK
CH3 + O2 = CH3O + O	2.86E+15	-0.315	30.86	QRRK
CH3 + O = CH2O + H	7.00E+13	0.0	0.0	10,11
CH3 + OH = CH3O + H	3.87E+12	-0.19	13.74	8
CH3 + HO2 = CH3O + OH	2.00E+13	0.0	0.0	12,36
CH3 + ClO = CH2O + HCl	3.47E+18	-1.80	2.07	QRRK
CH3 + ClO = CH3O + Cl	3.33E+11	0.46	0.03	QRRK
CH3O + M = CH2O + H + M	1.00E+14	0.0	25.1	36
CH3O + O2 = CH2O + HO2	6.62E+10	0.0	2.6	36



Reaction	A	n	Ea	source
CH <sub>3</sub> O + CO = CO <sub>2</sub> + CH <sub>3</sub>	1.57E+13	0.0	11.8	36
CH <sub>3</sub> O + HO <sub>2</sub> = CH <sub>2</sub> O + H <sub>2</sub> O <sub>2</sub>	3.01E+11	0.0	0.0	36
CH <sub>3</sub> O + CH <sub>3</sub> = CH <sub>4</sub> + CH <sub>2</sub> O	2.41E+13	0.0	0.0	36
CH <sub>3</sub> O + O = OH + CH <sub>2</sub> O	6.03E+12	0.0	0.0	36
CH <sub>3</sub> O + OH = H <sub>2</sub> O + CH <sub>2</sub> O	1.81E+13	0.0	0.0	36
CH <sub>3</sub> O + H = H <sub>2</sub> + CH <sub>2</sub> O	1.99E+13	0.0	0.0	36
CH <sub>3</sub> O + Cl = HCl + CH <sub>2</sub> O	4.00E+14	0.0	0.0	36
CH <sub>3</sub> O + ClO = CH <sub>2</sub> O + HOCl	2.41E+13	0.0	0.0	31,36
CH <sub>2</sub> O + ClO = CHO + HOCl	5.50E+03	2.81	5.86	32,36
CH <sub>2</sub> O + CH <sub>3</sub> = CH <sub>4</sub> + CHO	1.00E+11	0.0	6.09	11
CH <sub>2</sub> O + H = CHO + H <sub>2</sub>	2.50E+13	0.0	3.99	10,11
CH <sub>2</sub> O + O = CHO + OH	3.50E+13	0.0	3.51	10,11
CH <sub>2</sub> O + OH = CHO + H <sub>2</sub> O	3.00E+13	0.0	1.19	10
CH <sub>2</sub> O + HO <sub>2</sub> = CHO + H <sub>2</sub> O <sub>2</sub>	1.00E+12	0.0	8.0	9,16
CH <sub>2</sub> O + Cl = CHO + HCl	5.00E+13	0.0	0.5	19
CH <sub>2</sub> O + O <sub>2</sub> = CHO + HO <sub>2</sub>	2.05E+13	0.0	38.95	36
CH <sub>2</sub> O + M = CHO + H + M	5.00E+16	0.0	76.2	11
CH <sub>2</sub> OH + M = CH <sub>2</sub> O + H + M	1.00E+14	0.0	25.1	13
CH <sub>2</sub> OH + OH = H <sub>2</sub> O + CH <sub>2</sub> O	2.41E+13	0.0	0.0	13
CH <sub>2</sub> OH + CH <sub>3</sub> = CH <sub>4</sub> + CH <sub>2</sub> O	2.41E+12	0.0	0.0	13
CH <sub>2</sub> OH + O = OH + CH <sub>2</sub> O	4.22E+13	0.0	0.0	13
CH <sub>2</sub> OH + HO <sub>2</sub> = H <sub>2</sub> O <sub>2</sub> + CH <sub>2</sub> O	1.21E+13	0.0	0.0	13
CH <sub>2</sub> OH + Cl = HCl + CH <sub>2</sub> O	4.00E+14	0.0	0.0	36
CH <sub>2</sub> OH + H = H <sub>2</sub> + CH <sub>2</sub> O	6.03E+12	0.0	0.0	13
CH <sub>2</sub> OH + O <sub>2</sub> = HO <sub>2</sub> + CH <sub>2</sub> O	5.00E+10	0.0	0.0	13
CHO + M = H + CO + M	2.50E+14	0.0	16.79	11
CHO + H = CO + H <sub>2</sub>	2.00E+14	0.0	0.0	10,11
CHO + O <sub>2</sub> = CO + HO <sub>2</sub>	5.12E+13	0.0	1.69	36
CHO + O = CO + OH	3.01E+13	0.0	0.0	36
CHO + O = H + CO <sub>2</sub>	3.01E+13	0.0	0.0	36
CHO + OH = CO + H <sub>2</sub> O	3.01E+13	0.0	0.0	36
CH <sub>2</sub> + O <sub>2</sub> = CH <sub>2</sub> O + O	1.00E+14	0.0	3.7	8
CH <sub>2</sub> + CH <sub>4</sub> = CH <sub>3</sub> + CH <sub>3</sub>	1.81E+05	0.0	0.0	36
CH <sub>2</sub> + CH <sub>3</sub> Cl = CH <sub>3</sub> + CH <sub>2</sub> Cl	9.10E+04	0.0	0.0	51
CH <sub>2</sub> + H <sub>2</sub> = CH <sub>3</sub> + H	3.01E+09	0.0	0.0	36
CH <sub>2</sub> + H <sub>2</sub> O = CH <sub>3</sub> + OH	9.64E+07	0.0	0.0	36
CH <sub>2</sub> S + M = CH <sub>2</sub> + M	1.00E+13	0.0	0.0	13
CH <sub>2</sub> S + O <sub>2</sub> = CO + H <sub>2</sub> O	2.41E+11	0.0	0.0	13
CH <sub>2</sub> S + CH <sub>4</sub> = C <sub>2</sub> H <sub>5</sub> + H	9.43E+12	-0.13	6.62	QRRK
CH <sub>2</sub> S + CH <sub>4</sub> = CH <sub>3</sub> + CH <sub>3</sub>	3.45E+22	-2.48	7.46	QRRK
CH <sub>2</sub> S + CH <sub>4</sub> = C <sub>2</sub> H <sub>6</sub>	5.78E+46	-10.31	12.83	QRRK
CH <sub>2</sub> S + CH <sub>3</sub> Cl = C <sub>2</sub> H <sub>5</sub> Cl	7.85E+31	-6.15	5.83	QRRK

Reaction	A	n	Ea	source
CH <sub>2</sub> S + CH <sub>3</sub> Cl = C <sub>2</sub> H <sub>4</sub> + HCl	1.60E+18	-1.47	2.71	QRRK
CH <sub>2</sub> S + CH <sub>3</sub> Cl = C <sub>2</sub> H <sub>5</sub> + Cl	3.09E+07	1.7	0.52	QRRK
CH <sub>2</sub> S + H <sub>2</sub> = CH <sub>4</sub>	3.82E+25	-4.47	3.77	QRRK
CH <sub>2</sub> S + H <sub>2</sub> = CH <sub>3</sub> + H	1.27E+14	-0.08	0.13	QRRK
CO + OH = CO <sub>2</sub> + H	4.40E+06	1.5	-0.741	13
CO + HO <sub>2</sub> = CO <sub>2</sub> + OH	5.80E+13	0.0	22.934	36
CO + O <sub>2</sub> = CO <sub>2</sub> + O	2.50E+12	0.0	47.8	13
CO + ClO = Cl + CO <sub>2</sub>	6.03E+11	0.0	17.4	19
CO + O + M = CO <sub>2</sub> + M	6.17E+14	0.0	3.0	36
H + O <sub>2</sub> = O + OH	1.69E+17	-0.9	17.39	36
H + O <sub>2</sub> + M = HO <sub>2</sub> + M	7.00E+17	-0.8	0.0	11
O + H <sub>2</sub> = H + OH	1.08E+04	2.8	5.92	36
O + H <sub>2</sub> O = OH + OH	1.50E+10	1.14	17.24	10
H + H <sub>2</sub> O = H <sub>2</sub> + OH	4.60E+08	1.6	18.56	10
H + OH + M = H <sub>2</sub> O + M	2.22E+22	-2.0	0.0	36
O <sub>2</sub> + M = O + O + M	1.20E+14	0.0	107.55	13
H + O + M = OH + M	4.71E+18	-1.0	0.0	36
HO <sub>2</sub> + M = H + O <sub>2</sub> + M	1.21E+19	-1.18	48.61	36
H + HO <sub>2</sub> = OH + OH	1.69E+14	0.0	0.87	36
H + HO <sub>2</sub> = H <sub>2</sub> + O <sub>2</sub>	6.62E+13	0.0	2.13	36
O + HO <sub>2</sub> = OH + O <sub>2</sub>	2.00E+13	0.0	0.0	10,11
OH + HO <sub>2</sub> = H <sub>2</sub> O + O <sub>2</sub>	2.00E+13	0.0	0.0	10
O + HCl = OH + Cl	5.24E+12	0.0	6.4	4
OH + HCl = Cl + H <sub>2</sub> O	2.45E+12	0.0	1.1	4
H + H + M = H <sub>2</sub> + M	6.40E+17	-1.0	0.0	4
Cl + Cl + M = Cl <sub>2</sub> + M	2.34E+14	0.0	-1.8	4
H + Cl + M = HCl + M	1.00E+17	0.0	0.0	17
H + HCl = Cl + H <sub>2</sub>	2.30E+13	0.0	3.5	4
H + Cl <sub>2</sub> = HCl + Cl	8.51E+13	0.0	1.0	4
Cl + HO <sub>2</sub> = HCl + O <sub>2</sub>	1.08E+13	0.0	-0.338	19
Cl + HO <sub>2</sub> = ClO + OH	2.47E+13	0.0	0.89	19
Cl + H <sub>2</sub> O <sub>2</sub> = HCl + HO <sub>2</sub>	6.62E+12	0.0	1.95	19
H <sub>2</sub> O <sub>2</sub> + M = OH + OH + M	1.29E+33	-4.86	53.25	36
H <sub>2</sub> O <sub>2</sub> + OH = HO <sub>2</sub> + H <sub>2</sub> O	1.75E+12	0.0	0.32	36
H <sub>2</sub> O <sub>2</sub> + O = HO <sub>2</sub> + OH	9.63E+06	2.0	3.97	36
H <sub>2</sub> O <sub>2</sub> + H = HO <sub>2</sub> + H <sub>2</sub>	4.82E+13	0.0	7.95	36
H <sub>2</sub> O <sub>2</sub> + H = H <sub>2</sub> O + OH	2.41E+13	0.0	3.97	36
H <sub>2</sub> O <sub>2</sub> + O <sub>2</sub> = HO <sub>2</sub> + HO <sub>2</sub>	5.42E+13	0.0	39.74	36
CH <sub>2</sub> ClO = CH <sub>2</sub> O + Cl	4.73E+12	0.0	7.6	7,27
	4.53E+31	-6.41	22.56	DISSOC
CH <sub>2</sub> ClO = CHClO + H	3.27E+13	0.0	14.3	7,28
	1.83E+27	-5.13	21.17	DISSOC

Reaction	A	n	Ea	source
CHClO = CHO + Cl	1.99E+15	0.0	77.6	7,29
	8.86E+29	-5.15	92.92	DISSOC
CHClO = CO + HCl	1.10E+30	-5.19	92.96	DISSOC
CHClO + H = CHO + HCl	8.33E+13	0.0	7.4	19
CHClO + H = CH <sub>2</sub> O + Cl	6.99E+14	-0.58	6.36	QRRK
CHClO + OH = CClO + H <sub>2</sub> O	7.50E+12	0.0	1.2	33,11
CHClO + O = CClO + OH	8.80E+12	0.0	3.5	34,11
CHClO + Cl = CClO + HCl	2.40E+13	0.0	0.5	35,19
CHClO + O <sub>2</sub> = CClO + HO <sub>2</sub>	4.50E+12	0.0	41.8	49
CHClO + ClO = CClO + HOCl	1.10E+13	0.0	0.5	49
CHClO + CH <sub>3</sub> = CClO + CH <sub>4</sub>	2.50E+13	0.0	6.0	49
CHClO + CH <sub>3</sub> = CH <sub>3</sub> Cl + CHO	1.50E+13	0.0	8.8	49
H <sub>2</sub> + ClO = H + HOCl	6.03E+11	0.0	14.1	39,19
O + Cl <sub>2</sub> = Cl + ClO	2.51E+12	0.0	2.72	48
H + Cl <sub>2</sub> = HCl + Cl	8.59E+13	0.0	1.17	48
HOCl + OH = ClO + H <sub>2</sub> O	1.81E+12	0.0	0.99	19
HOCl + H = HCl + OH	9.55E+13	0.0	7.62	4,44
HOCl + Cl = Cl <sub>2</sub> + OH	1.81E+12	0.0	0.26	19
HOCl + Cl = HCl + ClO	7.28E+12	0.0	0.1	4,41
HOCl + O = OH + ClO	6.03E+12	0.0	4.37	19
HOCl = Cl + OH	2.85E+15	0.0	54.2	42
	1.76E+20	-3.01	56.72	DISSOC
HOCl = H + ClO	1.76E+14	0.0	92.2	43
	8.12E+14	-2.09	93.69	DISSOC
CClO = CO + Cl	1.30E+14	0.0	8.0	49
CClO + OH = CO + HOCl	3.30E+12	0.0	0.0	49
CClO + O <sub>2</sub> = CO <sub>2</sub> + ClO	1.00E+13	0.0	0.0	49
CClO + Cl = CO + Cl <sub>2</sub>	4.00E+14	0.0	0.8	49
COCl <sub>2</sub> + M = CClO + Cl + M	1.20E+16	0.0	75.5	49
COCl <sub>2</sub> + OH = CClO + HOCl	1.00E+13	0.0	23.3	49
COCl <sub>2</sub> + O = CClO + ClO	2.00E+13	0.0	17.0	49
COCl <sub>2</sub> + H = CClO + HCl	5.00E+13	0.0	6.3	49
COCl <sub>2</sub> + Cl = CClO + Cl <sub>2</sub>	3.20E+14	0.0	23.5	49
COCl <sub>2</sub> + CH <sub>3</sub> = CClO + CH <sub>3</sub> Cl	1.90E+13	0.0	12.9	49

### Sources of Rate Constants

1.  $A = 10^{13.55} \times 4$ ,  $E_a = \Delta H_{\text{rxn}} + 7.5$ ; (detail see text)
2. A factor based on thermodynamics and microreversibility.  
 $A_1$  taken as that for  $\text{C}_2\text{H}_5 + \text{CH}_3$  ( $A = 2.0 \times 10^{13}$ )  
 $E_a = \text{BE} - RT$ . (this case Bond Energy is 77.8 Kcal)
3. Allara, D.L. and Shaw, R.J., J. Phys. Chem. Ref. Data, 9, 523, 1980.
4. Kerr, J.A. and Moss, S.J., Handbook of Bimolecular and Thermolecular Gas Reaction}, Vol. I & II, CRC Press Inc., 1981.
5. A factor taken as average that for  $\text{CH}_2\text{Cl} + \text{H}_2$  and  $\text{CCl}_3 + \text{H}_2$  ;  
 $E_a$  from Evans--Polanyi plot.
6. A factor taken as 2 that for  $\text{CH}_3 + \text{H}_2$  ( $A = 1.6 \times 10^{12}$ ) ;  
 $E_a$  from Evans--Polanyi plot.
7. Dean, A.M., J. Phys. Chem., 89, 4600 1985.
8. Olson, D.B. and Gardiner, W.C. Jr., Combust. Flame, 32, 151, 1978
9. Cathonnet, M., Gaillard, F., Boettner, J.C., Cambray, P., Kamed, D., and Bellet, J.C., Twentieth Symposium (International) on Combustion, The Combustion Institute, pp 819--829, 1984.
10. Warnatz, J., Bockhorn, H., Moser, A., and Wenz, H.W., Nineteenth Symposium (International) on Combustion, The Combustion Institute, pp 167--179, 1982.
11. Warnatz, J.; Combustion Chemistry ( W.C. Gardiner, Jr., Ed. ) Springer--Verlag, NY, 1984.
12. Hennessy, R.J., Robison, C., Smith, D.B., Twenty--first Symposium (International) on Combustion}/The Combustion Institute, pp. 761--772, 1986.
13. Miller, J.A., Mitchell, R.E., Smooke, M.D., and Kee, R.J., Nineteenth Symposium (International) on Combustion), The Combustion Institute, pp. 127--141, 1982.
14. Westbrook, C.K., and Dryer, F.A., Prog. Energy Combust. Sci., 10, 1 1984.
15. A factor taken as  $10^{15.4}$  (Benson 1984)  
 $E_a = \Delta H_{\text{rxn}} - RT$
16. Levy, J.M., Taylor, B.R., Longwell, J.P., and Sarofim, A.F., Nineteenth Symposium

- (International) on Combustion, The Combustion Institute, pp. 167--179, 1982.
17. Ritter, E., Bozzelli, J.W., and Dean, A.M.'s paper accepted in J. Phys. Chem. 1988.  
Note -- This reference incorrectly lists Kerr and Moss as source of this rate constant. The rate constant was determined by evaluation of literature data and kinetics studies in these laboratories.
  18. Cohen, N., Int. J. of Chem. Kinetics, Vol 18, 59-82, (1986).
  19. Demore, W.B., Molina, M.J., Waston, R.T., Golden, D.M., Hampson, R.F., Kurylo, M.J., Howard, C.J., AR Ravishankara, and Sander, S.P., Chemical Kinetic and Photochemical Data for use in Stratospheric Modeling, Evaluation No. 8, JPL Publication 87-41, 1987
  20. A factor taken as 1/3 that for  $\text{CH}_4 + \text{O}_2$ ;  $E_a = \Delta H_{\text{rxn}}$ .
  21. A factor taken as 1/3 that for  $\text{CH}_4 + \text{HO}_2$ ;  $E_a = H_{\text{rxn}} + 8$ .
  22. A factor taken as 3/4 that for  $\text{CH}_4 + \text{O}_2$ ;  $E_a = \Delta H_{\text{rxn}}$
  23. A factor based on thermodynamics and microreversibility.  
 $A_{-1}$  taken as that for  $\text{CH}_3 + \text{C}_3\text{H}_7$  ( $A = 2.0 \times 10^{13}$ ),  $E_a = \Delta H_{\text{rxn}}$
  24. A factor taken as 2 that for  $\text{CH}_3 + \text{CH}_2\text{O}$   
 $E_a = 6.2$
  25. A factor taken as 1/2 that for  $\text{CH}_3 + \text{HO}_2$
  26. Manion, J.A. and Louw, R., Recl. Trav. Chim. Pays-Bas 105, 442- 448, 1986.
  27. A factor based on thermodynamics and microreversibility.  
 $A_{-1}$  taken as that for  $\text{CH}_3 + \text{C}_2\text{H}_4$  ( $\log A = 11.5$ ),  $E_a = \Delta H_{\text{rxn}} + 6$
  28. A factor based on thermodynamics and microreversibility.  
 $A_{-1}$  taken as that for  $\text{H} + \text{C}_3\text{H}_6$  ( $\log A = 12.9$ ),  $E_a = \Delta H_{\text{rxn}} + 1$ .
  29. A factor based on thermodynamics and microreversibility.  
 $A_{-1}$  taken as that for  $\text{CH}_3 + \text{C}_2\text{H}_3$  ( $A = 1.84 \times 10^{13}$ ),  $E_a = \Delta H_{\text{rxn}}$
  30. Benson, S.W. and Weissman, M., Int'l J. Chem. Kin. Vol. 16, 307, (1984).
  31. Treated as  $\text{CH}_3\text{O} + \text{C}_2\text{H}_5$
  32. Treated as  $\text{CH}_2\text{O} + \text{C}_2\text{H}_5$

33. A factor taken as 1/4 that for  $\text{CH}_2\text{O} + \text{OH}$ ;  $E_a = 1.2$
34. A factor taken as 1/4 that for  $\text{CH}_2\text{O} + \text{O}$   
 $E_a = 3.5$
35. A factor taken as 1/4 that for  $\text{CH}_2\text{O} + \text{Cl}$   
 $E_a = 0.5$
36. Tsang, W. and Hampson, R.F., J. Phys. Chem. Ref. Data 1986, 15, 1087.
37. A factor refer from Demore et.al. 1987 (source 19);  $E_a = \Delta H_{\text{rxn}} + 4$
38. A factor taken as 1/2 that  $\text{CH}_4 + \text{ClO}$ ;  $E_a = \Delta H_{\text{rxn}} + 4$
39. A factor refer from Demore et.al. 1987 (source 19);  $E_a = \Delta H_{\text{rxn}} + 4$
40. Herron, J.T., J. Phys. Chem. Ref. Data 1988,17,967.
41. A factor taken as 1/6 that for  $\text{C}_2\text{H}_6 + \text{Cl}$ ;  $E_a = 0.1$
42. A factor based on thermodynamics and microreversibility.  
 $A_1$  taken as that for  $\text{CH}_3 + \text{CH}_3$   
 $E_a = \Delta H_{\text{rxn}} - RT$
43. A factor based on thermodynamics and microreversibility.  
 $A_1$  taken as that for  $\text{H} + \text{C}_2\text{H}_5$   
 $E_a = \Delta H_{\text{rxn}} - RT$
44. A factortaken as that for  $\text{CH}_3\text{Cl} + \text{H}$ ;  $E_a = 7.62$
45. A factor taken as 1/2 that for  $\text{CH}_4 + \text{HO}_2$ ;  $E_a = \Delta H_{\text{rxn}} + 8$ .
46. Parmar, S.S. and Benson, S.W.; J. Phys. Chem., 92, 2652, 1988.
47. Slagle, I.R., Park, J.Y., Heaven, M.C., and Gutman, D.; J. Am. Chem. Soc., 106, 4356, 1984.
48. Baulch, D.L., Duxbury, J., Grant, S.J., Montague, D.C.; J. Phys. Chem. Ref. Data, 10, Suppl.1,1, 1981.
49. Won., YangSoo, PhD Thesis, NJIT, 1991
50. Wu, Y.P., PhD Thesis, NJIT, 1992
51. A factor taken as 1/2 that for  $\text{CH}_4 + \text{CH}_2$

## **APPENDIX C**

### **CHEMACT INPUT DATA**

units for A : cm<sup>3</sup>/mol-sec and sec<sup>-1</sup>; Ea : Kcal/mole

$\Delta H_{\text{rxn}}$  taken as from stabilized adduct.

Activated complex Lennard-Jones parameters are estimated using critical property data tabulated in Reid, Prausnitz and Poling (The Properties and Gases and Liquids, 4th Ed.)

geometric mean frequencies are estimated using CPFIT computer code (Ritter, E.R., J. Chem. Inf. Comput. Sci. 31, 400-408,1991) and/or from "Table of Molecular Vibration Frequencies Consolidated Vol.I, Natl. Stand. Ref. Data Ser."; Shimanouchi, T., (U.S. Natl. Bur. Stand.) 1972, NSRDS--NBS 39.

**Table C.1. CH<sub>2</sub>Cl + H QRRK calculation input parameters**

	Reaction	A	Ea
k1	CH <sub>2</sub> Cl + H → CH <sub>3</sub> Cl	1.0E+14	0.0
k-1	CH <sub>3</sub> Cl → CH <sub>2</sub> Cl + H	8.9E+15	100.8
k2	CH <sub>3</sub> Cl → <sup>1</sup> CH <sub>2</sub> + HCl	3.6E+13	101.7
k3	CH <sub>3</sub> Cl → CH <sub>3</sub> + Cl	1.2E+15	81.6

k1 A<sub>1</sub> factor taken as that for 1-C<sub>3</sub>H<sub>7</sub> + H,  
(Allara,D.L. and Shaw, R.J., J. Phys. Chem. Ref. Data, 9,523, 1980)

k-1 thermodynamics and microreversibility <mr>

k2 Ea = H<sub>rxn</sub> + 3.75 (evaluated literature for HCl eliminations)  
A = (ekT/h) exp<sup>S/R</sup> (Transition State Theory) S = 0.0

k3 A<sub>3</sub> factor based on thermodynamics and microreversibility.

A<sub>3</sub> taken as that for C<sub>2</sub>H<sub>5</sub> + CH<sub>3</sub> (Allara & Shaw)

Ea = H<sub>rxn</sub> - RT

<v> = 1575.0 cm<sup>-1</sup>

Lennard-Jones parameters : σ = 4.18 Å, ε/k = 350.0 K

**Table C.2. CH<sub>2</sub>Cl + CH<sub>2</sub>Cl QRRK calculation input parameters**

	Reaction	A	Ea
k1	CH <sub>2</sub> Cl + CH <sub>2</sub> Cl → CH <sub>2</sub> ClCH <sub>2</sub> Cl	4.0E+12	0.0
k-1	CH <sub>2</sub> ClCH <sub>2</sub> Cl → CH <sub>2</sub> Cl + CH <sub>2</sub> Cl	4.8E+17	89.2
k2	CH <sub>2</sub> ClCH <sub>2</sub> Cl → CH <sub>2</sub> ClCH <sub>2</sub> + Cl	6.0E+15	80.7
k3	CH <sub>2</sub> ClCH <sub>2</sub> Cl → C <sub>2</sub> H <sub>3</sub> Cl + HCl	1.9E+13	55.4

k1. A<sub>1</sub> factor taken as that for 1-C<sub>3</sub>H<sub>7</sub> + 1-C<sub>3</sub>H<sub>7</sub>  
(Allara,D.L. and Shaw, R.J., J. Phys. Chem. Ref. Data, 9,523, 1980)

k-1 thermodynamics and microreversibility <mr>.

k2. A<sub>2</sub> factor based on thermodynamics and microreversibility.

A<sub>2</sub> taken as that for C<sub>3</sub>H<sub>7</sub> + CH<sub>3</sub> (Allara & Shaw)

Ea = H<sub>rxn</sub> - RT

k3 Ea = H<sub>rxn</sub> + 38 (evaluated HCl eliminate rate data)

A = (ekT/h) exp<sup>S/R</sup> (Transition State Theory) x Degeneracy

S = -4.0

<v> = 797.2 cm<sup>-1</sup>

Lennard-Jones parameters : σ = 5.12 Å, ε/k = 471.2 K



**Table C.3. CH<sub>2</sub>Cl + OH QRRK calculation input parameters**

	Reaction	A	Ea
k1	CH <sub>2</sub> Cl + OH → CH <sub>2</sub> ClOH	1.6E+13	0.0
k-1	CH <sub>2</sub> ClOH → CH <sub>2</sub> Cl + OH	2.4E+16	91.0
k2	CH <sub>2</sub> ClOH → CH <sub>2</sub> OH + Cl	5.5E+15	81.2
k3	CH <sub>2</sub> ClOH → CH <sub>2</sub> O + HCl	7.6E+13	40.6

k1 A<sub>1</sub> factor taken as that for CH<sub>2</sub>Cl + CH<sub>3</sub>

(Allara, D.L. and Shaw, R.J., J. Phys. Chem. Ref. Data, 9, 523, 1980)

k-1 thermodynamics and microreversibility.

k2 A<sub>3</sub> factor based on thermodynamics and microreversibility.

A<sub>3</sub> taken as that for C<sub>2</sub>H<sub>5</sub> + CH<sub>3</sub> (Allara & Shaw)

$$E_a = H_{\text{rxn}} - RT$$

k3 E<sub>a</sub> = H<sub>rxn</sub> + 38 (evaluated HCl eliminate rate data)

$$A = (ekT/h) \exp^{S/R} \text{ (Transition State Theory) } \times \text{Degeneracy}$$

$$S = -4.0$$

$$\langle v \rangle = 1200.0 \text{ cm}^{-1}$$

Lennard-Jones parameters :  $\sigma = 4.61 \text{ \AA}$ ,  $\epsilon/k = 535.0 \text{ K}$

**Table C.4. CH<sub>2</sub>Cl + ClO QRRK calculation input parameters**

	Reaction	A	Ea
k1	CH <sub>2</sub> Cl + ClO → CH <sub>2</sub> ClOCl	6.5E+12	0.0
k-1	CH <sub>2</sub> ClOCl → CH <sub>2</sub> Cl + ClO	2.3E+16	86.3
k2	CH <sub>2</sub> ClOCl → CH <sub>2</sub> ClO + Cl	3.0E+15	64.0
k3	CH <sub>2</sub> ClOCl → CHClO + HCl	9.6E+12	34.0

k1 A<sub>1</sub> factor taken as 1/2 that for CH<sub>3</sub> + ClO (Table 9, k1)

k-1 thermodynamics and microreversibility.

k2 A = (ekT/h) exp<sup>S/R</sup>

(Benson, S.W., "Thermochemical Kinetics", John Wiley & Son, 2nd ed. N.Y., 1976.

CH<sub>3</sub>I → CH<sub>3</sub> + I) S = 9.0, E<sub>a</sub> = H<sub>rxn</sub> - RT

k3 E<sub>a</sub> = Ring Strain + abstraction + H<sub>rxn</sub>

$$A = (ekT/h) \exp^{S/R} \text{ (Transition State Theory) } \times \text{Degeneracy}$$

$$S = -4.0$$

$$\langle v \rangle = 797.2 \text{ cm}^{-1}$$

Lennard-Jones parameters :  $\sigma = 5.12 \text{ \AA}$ ,  $\epsilon/k = 471.2 \text{ K}$

Table C.5. CH<sub>2</sub>Cl + O QRRK calculation input parameters

CH <sub>2</sub> Cl + O $\rightleftharpoons$ [CH <sub>2</sub> ClO] <sup>#</sup> $\rightarrow$ Products			
	Reaction	A	E <sub>a</sub>
k1	CH <sub>2</sub> Cl + O $\rightarrow$ CH <sub>2</sub> ClO	2.0E+13	0.5
k-1	CH <sub>2</sub> ClO $\rightarrow$ CH <sub>2</sub> Cl + O	1.2E+16	84.5
k2	CH <sub>2</sub> ClO $\rightarrow$ CH <sub>2</sub> O + Cl	3.0E+13	7.0
k3	CH <sub>2</sub> ClO $\rightarrow$ CHO + HCl	7.3E+13	34.0

- k1. A<sub>1</sub> factor taken as 1/3 that for CH<sub>3</sub> + O  
(Washido & Bayes, J. Chem. Phys. 73, 1665, 1980)
- k<sub>-1</sub> thermodynamics and microreversibility.
- k2. A factor taken as that CCCC.  $\rightarrow$  C<sub>2</sub>H<sub>5</sub> + C=C  
(Dean, A.M., J. Phys. Chem. 1985)  
E<sub>a</sub> = H<sub>rxn</sub> + 7.0
- k3 E<sub>a</sub> = Ring Strain + abstraction + H<sub>rxn</sub>  
A = (ekT/h) exp<sup>S/R</sup> (Transition State Theory) x Degeneracy  
S = 0.0

$$\langle v \rangle = 1247.0 \text{ cm}^{-1}$$

Lennard-Jones parameters :  $\sigma = 4.61 \text{ \AA}$ ,  $\epsilon/k = 535.0 \text{ K}$

Table C.6. CH<sub>2</sub>Cl + O<sub>2</sub> QRRK calculation input parameters

CH <sub>2</sub> Cl + O <sub>2</sub> $\rightleftharpoons$ [CH <sub>2</sub> ClOO] <sup>#</sup> $\rightleftharpoons$ [C.H <sub>2</sub> OOCl] <sup>#</sup> $\rightarrow$ CH <sub>2</sub> O + ClO			
	Reaction	A	E <sub>a</sub>
k1	CH <sub>2</sub> Cl + O <sub>2</sub> $\rightarrow$ CH <sub>2</sub> ClOO.	4.0E+12	0.0
k-1	CH <sub>2</sub> ClOO. $\rightarrow$ CH <sub>2</sub> Cl + O <sub>2</sub>	3.5E+15	25.4
k2	CH <sub>2</sub> ClOO. $\rightarrow$ C.H <sub>2</sub> OOCl	4.8E+12	26.0
k-2	C.H <sub>2</sub> OOCl $\rightarrow$ CH <sub>2</sub> ClOO.	3.0E+11	19.0
k3	C.H <sub>2</sub> OOCl $\rightarrow$ CH <sub>2</sub> O + ClO	5.0E+13	1.00

- k1 A<sub>1</sub> factor taken as that for 1-C<sub>3</sub>H<sub>7</sub> + O<sub>2</sub>  
(Mark et.al. Chem. Phys. Lett. vol. 132, p417, 1986)
- k-1 thermodynamics and microreversibility <mr>.
- k2 A = (ekT/h) exp<sup>S/R</sup> (Transition State Theory) S = -4.0, Estimate a barrier of 26 Kcal/mol ( 19 Kcal for ring strain and 7 Kcal for ROO. abstraction of Cl)
- k-2 <mr>
- k3 A<sub>3</sub> factor based on <mr>; A<sub>3</sub> taken as 1/2 that for CH<sub>2</sub>O + OH  
(Dean, A.M. and Westmoreland, P.R. Int'l. J. of Chem. Kinetics, Vol. 19, 207-228, 1987) E<sub>a</sub> = 1.0
- $$\langle v \rangle = 1116.0 \text{ cm}^{-1}$$
- Lennard-Jones parameters :  $\sigma = 4.90 \text{ \AA}$ ,  $\epsilon/k = 356.0 \text{ K}$

Table C.7.  $\text{CH}_2\text{Cl} + \text{CH}_3$  QRRK calculation input parameters

	Reaction	A	Ea
k1	$\text{CH}_2\text{Cl} + \text{CH}_3 \rightarrow \text{CH}_2\text{ClCH}_3$	$2.00\text{E}+13$	0.0
k-1	$\text{CH}_2\text{ClCH}_3 \rightarrow \text{CH}_2\text{Cl} + \text{CH}_3$	$1.63\text{E}+17$	90.6
k2	$\text{CH}_2\text{ClCH}_3 \rightarrow \text{C}_2\text{H}_4 + \text{HCl}$	$3.24\text{E}+13$	56.6
k3	$\text{CH}_2\text{ClCH}_3 \rightarrow \text{C}_2\text{H}_5 + \text{Cl}$	$2.17\text{E}+15$	84.1

k1  $A_1$  factor taken as that for  $\text{C}_3\text{H}_7 + \text{CH}_3$  ( $A = 2.0 \text{E}+13$ ) (Allara, D.L. and Shaw, R.J., J. Phys. Chem. Ref. Data, 9, 523, 1980) (Bond energy ref: Weissman, M and Benson, S.W., J. Phys. Chem., 87, 243, 1983)

k-1 thermodynamics and microreversibility.  $E_a = 0.0$ ,

k2 Benson, S.W., "Thermochemical Kinetics", John Wiley & Son, 2nd ed. N.Y., 1976

k3  $A_3$  based on  $\langle m \rangle$ ,  $A_{-3}$  taken as that  $\text{CH}_3\text{CH}_2 + \text{CH}_3$  ( $A = 2.0 \text{E}+13$ )

$$E_a = \Delta H_r - RT$$

$$\langle v \rangle = 1265.3 \text{ cm}^{-1}$$

Lennard-Jones parameters :  $\sigma = 4.90 \text{ \AA}$ ,  $\epsilon/k = 300.0 \text{ K}$

Table C.8.  $\text{CH}_2\text{Cl} + \text{CHCl}_2$  QRRK calculation input parameters

	Reaction	A	Ea
k1	$\text{CH}_2\text{Cl} + \text{CHCl}_2 \rightarrow \text{CH}_2\text{ClCHCl}_2$	$3.97\text{E}+12$	0.0
k-1	$\text{CH}_2\text{ClCHCl}_2 \rightarrow \text{CH}_2\text{Cl} + \text{CHCl}_2$	$5.28\text{E}+17$	90.1
k2	$\text{CH}_2\text{ClCHCl}_2 \rightarrow \text{CH}_2\text{CCl}_2 + \text{HCl}$	$4.80\text{E}+12$	52.2
k3	$\text{CH}_2\text{ClCHCl}_2 \rightarrow \text{CHClCHCl} + \text{HCl}$	$1.92\text{E}+13$	52.6

k1  $A_1$  factor as 1/2 that for  $\text{C}_4\text{H}_9 + 2\text{-C}_3\text{H}_7$  ( $A = 7.94 \text{E}+12$ ) (Allara, D.L. and Shaw) (Bond energy ref: Weissman, M and Benson, S.W., J Phys. Chem., 87, 243, 1983)

k-1 thermodynamics and microreversibility.  $E_a = 0.0$ ,

k2  $E_a = H_{\text{rxn}} + 38.5$  (evaluated HCl eliminate rate data)

$A = (ekT/h) \exp^{S/R}$  (Transition State Theory) x Degeneracy

$$S = -4.0$$

k3  $A_3 = 10^{13.72} * 10^{(-4/4.6)} * 4$

$$E_a = \Delta H + 38.5$$

$$\langle v \rangle = 678.7 \text{ cm}^{-1}$$

Lennard-Jones parameters :  $\sigma = 5.72 \text{ \AA}$ ,  $\epsilon/k = 498.9 \text{ K}$

**Table C.9. CH<sub>3</sub> + ClO QRRK calculation input parameters**

	Reaction	A	Ea
k1	CH <sub>3</sub> + ClO → CH <sub>3</sub> OCl	1.3E+13	0.0
k-1	CH <sub>3</sub> OCl → CH <sub>3</sub> + ClO	3.7E+15	90.3
k2	CH <sub>3</sub> OCl → CH <sub>3</sub> O + Cl	3.0E+15	63.8
k3	CH <sub>3</sub> OCl → CH <sub>2</sub> O + HCl	1.4E+13	34.0

k1 A<sub>1</sub> factor taken as 1/2 that for CH<sub>3</sub> + OH

(Dean et al. Int'l J. Chem. Kin., 19, 207, 1987.)

k-1 thermodynamics and microreversibility.

k2 A = (ekT/h) exp<sup>S/R</sup>

(ref: Benson CH<sub>3</sub>I → CH<sub>3</sub> + I) S = 9.0

Ea = H<sub>rxn</sub> - RT

k3 Ea = Ring Strain + abstraction + H<sub>rxn</sub>

A = (ekT/h) exp<sup>S/R</sup> (Transition State Theory) x Degeneracy

S = -4.0

<v> = 1111.0 cm<sup>-1</sup>

Lennard-Jones parameters : σ = 5.12 Å, ε/k = 537.0 K

**Table C.10. CH<sub>3</sub> + CHCl<sub>2</sub> QRRK calculation input parameters**

	Reaction	A	Ea
k1	CH <sub>3</sub> + CHCl <sub>2</sub> → CH <sub>3</sub> CHCl <sub>2</sub>	1.5E+12	0.0
k-1	CH <sub>3</sub> CHCl <sub>2</sub> → CH <sub>3</sub> + CHCl <sub>2</sub>	2.0E+17	91.9
k2	CH <sub>3</sub> CHCl <sub>2</sub> → CH <sub>3</sub> CHCl + Cl	3.9E+15	76.8
k3	CH <sub>3</sub> CHCl <sub>2</sub> → C <sub>2</sub> H <sub>3</sub> Cl + HCl	4.0E+13	55.4

k1 A<sub>1</sub> factor taken as that for CH<sub>3</sub> + 2-C<sub>4</sub>H<sub>9</sub>

(Allara, D.L. and Shaw, R.J., J. Phys. Chem. Ref. Data, 9, 523, 1980)

k-1 thermodynamics and microreversibility.

k2 A<sub>2</sub> factor based on <mr>, A<sub>2</sub> taken as that for C<sub>3</sub>H<sub>7</sub> + CH<sub>3</sub> (Allara & Shaw)

Ea = H<sub>rxn</sub> - RT

k3 Ea = H<sub>rxn</sub> + 38 (evaluated HCl eliminate rate data)

A = (ekT/h) exp<sup>S/R</sup> (Transition State Theory) x Degeneracy

S = -4.0

<v> = 797.2 cm<sup>-1</sup>

Lennard-Jones parameters : σ = 5.12 Å, ε/k = 471.2 K

**Table C.11.  $\text{CHCl}_2 + \text{CHCl}_2$  QRRK calculation input parameters**

	Reaction	A	Ea
k1	$\text{CHCl}_2 + \text{CHCl}_2 \rightarrow \text{CHCl}_2\text{CHCl}_2$	$1.2\text{E}+12$	0.0
k-1	$\text{CHCl}_2\text{CHCl}_2 \rightarrow \text{CHCl}_2 + \text{CHCl}_2$	$5.9\text{E}+17$	88.6
k2	$\text{CHCl}_2\text{CHCl}_2 \rightarrow \text{CHCl}_2\text{CHCl} + \text{Cl}$	$6.7\text{E}+15$	74.6
k3	$\text{CHCl}_2\text{CHCl}_2 \rightarrow \text{C}_2\text{HCl}_3 + \text{HCl}$	$1.9\text{E}+13$	51.1

k1  $A_1$  factor taken as 1/4 that for  $1\text{-C}_4\text{H}_9 + 1\text{-C}_4\text{H}_9$

(Allara, D.L. and Shaw, R.J., J. Phys. Chem. Ref. Data, 9,523, 1980)

k-1 thermodynamics and microreversibility.

k2  $A_2$  factor based on  $\langle \text{mr} \rangle$ ,  $A_2$  taken as that for  $\text{C}_4\text{H}_9 + \text{CH}_3$  (Allara & Shaw)

$$E_a = H_{\text{rxn}} - RT$$

k3  $E_a = H_{\text{rxn}} + 38$  (evaluated HCl eliminate rate data)

$$A = (ekT/h) \exp^{S/R} \text{ (Transition State Theory) } \times \text{Degeneracy}$$

$$S = -4.0$$

$$\langle v \rangle = 578.0 \text{ cm}^{-1}$$

Lennard-Jones parameters :  $\sigma = 5.91 \text{ \AA}$ ,  $\epsilon/k = 525.9 \text{ K}$

**Table C.12.  $\text{CH}_2\text{CHCl} + \text{H}$  QRRK calculation parameters**

	Reaction	A	Ea
k1	$\text{C}_2\text{H}_3\text{Cl} + \text{H} \rightarrow \text{CH}_2\text{CH}_2\text{Cl}$	$1.33\text{E}+13$	5.8
k-1	$\text{CH}_2\text{CH}_2\text{Cl} \rightarrow \text{C}_2\text{H}_3\text{Cl} + \text{H}$	$1.27\text{E}+13$	45.1
k2	$\text{CH}_2\text{CH}_2\text{Cl} \rightarrow \text{C}_2\text{H}_4 + \text{Cl}$	$3.13\text{E}+13$	20.7
k3	$\text{CH}_2\text{CH}_2\text{Cl} \rightarrow \text{C}_2\text{H}_3 + \text{HCl}$	$9.60\text{E}+12$	62.3

k1  $A_1$  factor taken as 1/3 that for  $\text{CH}_2\text{CH}_2 + \text{H}$  ( $A=4.0 \text{ E}+13, E_a=2.6$ ) (Allara and Shaw)

$E_a$  taken as average of  $\text{C}_2\text{H}_4 + \text{H}$  and  $\text{C}_2\text{Cl}_4 + \text{H}$

(Tsang, W. and Walker, J.A., proceeding 23rd Symposium on Combustion Int'l Combustion Inst. p139, 1991;  $\text{C}_2\text{Cl}_4 + \text{H}$ ,  $E_a=9.0$ )

k-1 thermodynamics and microreversibility.

k2  $A_2$  from  $\langle \text{mr} \rangle$ ,  $A_2$  taken as that for  $\text{CH}_2\text{CH}_2 + \text{Cl}$  ( $A = 1.6 \text{ E}+13, E_a = 0.0$ )

(Kerr, J.A. and Moss, S.J., "Handbook of Bimolecular and Termolecular Gas Reaction Vol. I & II", CRC Press Inc., 1981)

k3  $E_a = H_{\text{rxn}} + 38$  (evaluated HCl eliminate rate data)

$$A = (ekT/h) \exp^{S/R} \text{ (Transition State Theory) } \times \text{Degeneracy}$$

$$S = -4.0$$

$$\langle v \rangle = 1265.3 \text{ cm}^{-1}$$

Lennard-Jones parameters :  $\sigma = 4.9 \text{ \AA}$ ,  $\epsilon/k = 300.0 \text{ K}$

**Table C.13. CH<sub>2</sub>CCl<sub>2</sub> + H QRRK calculation parameters**

CH <sub>2</sub> CCl <sub>2</sub> + H $\rightleftharpoons$ [CH <sub>2</sub> CHCl <sub>2</sub> ] <sup>#</sup> $\rightarrow$ Products			
	Reaction	A	Ea
k1	CH <sub>2</sub> CCl <sub>2</sub> + H $\rightarrow$ CH <sub>2</sub> CHCl <sub>2</sub>	7.00E+12	7.5
k-1	CH <sub>2</sub> CHCl <sub>2</sub> $\rightarrow$ CH <sub>2</sub> CCl <sub>2</sub> + H	8.08E+12	43.8
k2	CH <sub>2</sub> CHCl <sub>2</sub> $\rightarrow$ C <sub>2</sub> H <sub>3</sub> Cl + Cl	4.62E+14	22.4
k3	CH <sub>2</sub> CHCl <sub>2</sub> $\rightarrow$ CHClCH + HCl	2.40E+13	57.7

k1 A<sub>1</sub> factor taken as 1/2 that for C<sub>2</sub>Cl<sub>4</sub> + H (A=1.4 E+13)  
(Tsang, W. and Walker, J.A., Proceeding 23rd Symposium on Combustion Int'l  
Combustion Inst. p139, 1991)

k-1 thermodynamics and microreversibility.

k2 A<sub>2</sub> based upon <mr>, for CH<sub>2</sub>CHCl + Cl = CH<sub>2</sub>CHCl<sub>2</sub>

with A<sub>2</sub> = 2.0 E+13 and Ea<sub>2</sub> = 1.5

(Kerr, J.A. and Moss, S.J., "Handbook of Bimolecular and Termolecular Gas  
Reaction Vol. I & II", CRC Press Inc., 1981)

k3 Ea = H<sub>rxn</sub> + 38 (evaluated HCl eliminate rate data)

A = (ekT/h) exp<sup>S/R</sup> (Transition State Theory) x Degeneracy

S = -4.0

<v> = 736.0 cm<sup>-1</sup>

Lennard-Jones parameters : σ = 5.1 Å, ε/k = 435.9 K

**Table C.14. CHClCHCl + H QRRK calculation parameters**

CHClCHCl + H $\rightleftharpoons$ [CH <sub>2</sub> ClCHCl] <sup>#</sup> $\rightarrow$ Products			
	Reaction	A	Ea
k1	CHClCHCl + H $\rightarrow$ CH <sub>2</sub> ClCHCl	2.60E+13	5.8
k-1	CH <sub>2</sub> ClCHCl $\rightarrow$ CHClCHCl + H	1.41E+13	47.2
k2	CH <sub>2</sub> ClCHCl $\rightarrow$ C <sub>2</sub> H <sub>3</sub> Cl + Cl	1.72E+14	27.3
k3	CH <sub>2</sub> ClCHCl $\rightarrow$ CH <sub>2</sub> CCl. + HCl	2.40E+13	57.7

k1 A<sub>1</sub> factor taken as 2 that for C<sub>2</sub>H<sub>3</sub>Cl + H (A=1.3 E+13)

(Tsang, W. and Walker, J.A., Proceeding 23rd Symposium on Combustion Int'l  
Combustion Inst. p139, 1991)

k-1 thermodynamics and microreversibility.

k2 A<sub>2</sub> based upon <mr>, for CH<sub>2</sub>CHCl + Cl = CH<sub>2</sub>CHCl<sub>2</sub>

with A<sub>2</sub> = 2.0 E+13 and Ea<sub>2</sub> = 1.5 (Kerr, J.A. and Moss, S.J. 1981)

k3 Ea = H<sub>rxn</sub> + 38 (evaluated HCl eliminate rate data)

A = (ekT/h) exp<sup>S/R</sup> (Transition State Theory) x Degeneracy

S = -4.0

<v> = 736.0 cm<sup>-1</sup>

Lennard-Jones parameters : σ = 5.1 Å, ε/k = 435.9 K

**Table C.15.  $\text{CHClCCl}_2 + \text{H}$  QRRK calculation parameters**

	Reaction	A	Ea
k1	$\text{CHClCCl}_2 + \text{H} \rightarrow \text{CH}_2\text{ClCCl}_2$	$1.33\text{E}+13$	5.8
k-1	$\text{CH}_2\text{ClCCl}_2 \rightarrow \text{CHClCCl}_2 + \text{H}$	$1.18\text{E}+13$	49.5
k2	$\text{CH}_2\text{ClCCl}_2 \rightarrow \text{CH}_2\text{CCl}_2 + \text{Cl}$	$7.30\text{E}+13$	22.5
k3	$\text{CH}_2\text{ClCCl}_2 \rightarrow \text{C}_2\text{HCl}_2 + \text{HCl}$	$9.60\text{E}+12$	64.5

k1  $A_1$  factor taken as that for  $\text{C}_2\text{H}_3\text{Cl} + \text{H}$  ( $A=1.33 \text{ E}+13$ )

(Tsang, W. and Walker, J.A., Proceeding 23rd Symposium on Combustion Int'l  
Combustion Inst. p139, 1991;

k-1 thermodynamics and microreversibility.

k2  $A_2$  based upon  $\langle \text{mr} \rangle$ , for  $\text{C}_2\text{Cl}_4 + \text{Cl} = \text{C}_2\text{Cl}_5$

with  $A_2 = 1.26 \text{ E}+13$  and  $E_{a,2} = 0.0$  (Kerr, J.A. and Moss, S.J. 1981)

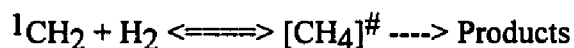
k3  $E_a = H_{\text{rxn}} + 38$  (evaluated HCl eliminate rate data)

$A = (ekT/h) \exp^{S/R}$  (Transition State Theory) x Degeneracy

$S = -4.0$

$\langle v \rangle = 666.62 \text{ cm}^{-1}$

Lennard-Jones parameters :  $\sigma = 5.6 \text{ \AA}$ ,  $\epsilon/k = 510.0 \text{ K}$

**Table C.16.  $^1\text{CH}_2 + \text{H}_2$  QRRK calculation parameters**

	Reaction	A	Ea
k1	$^1\text{CH}_2 + \text{H}_2 \rightarrow \text{CH}_4$	$7.0\text{E}+13$	0.0
k-1	$\text{CH}_4 \rightarrow ^1\text{CH}_2 + \text{H}_2$	$5.9\text{E}+15$	119.34
k2	$\text{CH}_4 \rightarrow \text{CH}_3 + \text{H}$	$1.0\text{E}+16$	105.0

k1 Miller, J.A. and Bowman, C.T., Prog. Energy. Combust. Sci., p 1, 1989.

k-1 thermodynamics and microreversibility.

k2 Dean, A. M., J. Phys. Chem., 89, 4600, 1985

$\langle v \rangle = 1957.0 \text{ cm}^{-1}$

Lennard-Jones parameters :  $\sigma = 3.76 \text{ \AA}$ ,  $\epsilon/k = 148.6 \text{ K}$

**Table C.17.  $^1\text{CH}_2 + \text{CH}_4$  QRRK calculation input data**

	Reaction	A	Ea
k1	$^1\text{CH}_2 + \text{CH}_4 \rightarrow \text{C}_2\text{H}_6$	4.00E+13	0.0
k-1	$\text{C}_2\text{H}_6 \rightarrow ^1\text{CH}_2 + \text{CH}_4$	1.46E+16	103.78
k2	$\text{C}_2\text{H}_6 \rightarrow \text{CH}_3 + \text{CH}_3$	8.00E+16	90.4
k3	$\text{C}_2\text{H}_6 \rightarrow \text{C}_2\text{H}_5 + \text{H}$	1.30E+16	100.7

k1 Miller, J.A. and Bowman, C.T., Prog. Energy. Combust. Sci., p 1, 1989.

k-1 thermodynamics and microreversibility.

k2 Dean, A. M., J. Phys. Chem., 89, 4600, 1985

k3 Dean, A. M., J. Phys. Chem., 89, 4600, 1985

$$\langle v \rangle = 1509.0 \text{ cm}^{-1}$$

Lennard-Jones parameters :  $\sigma = 4.342 \text{ \AA}$ ,  $\epsilon/k = 246.8 \text{ K}$

**Table C.18.  $^1\text{CH}_2 + \text{CH}_3\text{Cl}$  QRRK calculation input parameters**

	Reaction	A	Ea
k1	$^1\text{CH}_2 + \text{CH}_3\text{Cl} \rightarrow \text{C}_2\text{H}_5\text{Cl}$	2.00E+13	0.0
k-1	$\text{C}_2\text{H}_5\text{Cl} \rightarrow ^1\text{CH}_2 + \text{CH}_3\text{Cl}$	8.71E+15	108.68
k2	$\text{C}_2\text{H}_5\text{Cl} \rightarrow \text{C}_2\text{H}_4 + \text{HCl}$	3.24E+13	56.6
k3	$\text{C}_2\text{H}_6 \rightarrow \text{C}_2\text{H}_5 + \text{Cl}$	2.17E+15	84.1

k1  $A_1$  factor taken as that for  $^1\text{CH}_2 + \text{CH}_4$  ( $A = 4.0 \text{ E}+13$ )

k-1 thermodynamics and microreversibility.  $E_a = 0.0$ ,

k2 Benson, S.W., "Thermochemical Kinetics", John Wiley & Son, 2nd ed. N.Y., 1976

k3  $A_3$  based on thermodynamics and microreversibility.

$A_{-3}$  taken as that  $\text{CH}_3\text{CH}_2 + \text{CH}_3$  ( $A = 2.0 \text{ E}+13$ )

$E_a = \Delta H_r - RT$

$$\langle v \rangle = 1265.3 \text{ cm}^{-1}$$

Lennard-Jones parameters :  $\sigma = 4.898 \text{ \AA}$ ,  $\epsilon/k = 300.0 \text{ K}$



**APPENDIX D**

**EXPERIMENT AND MODELING RESULTS FIGURES**

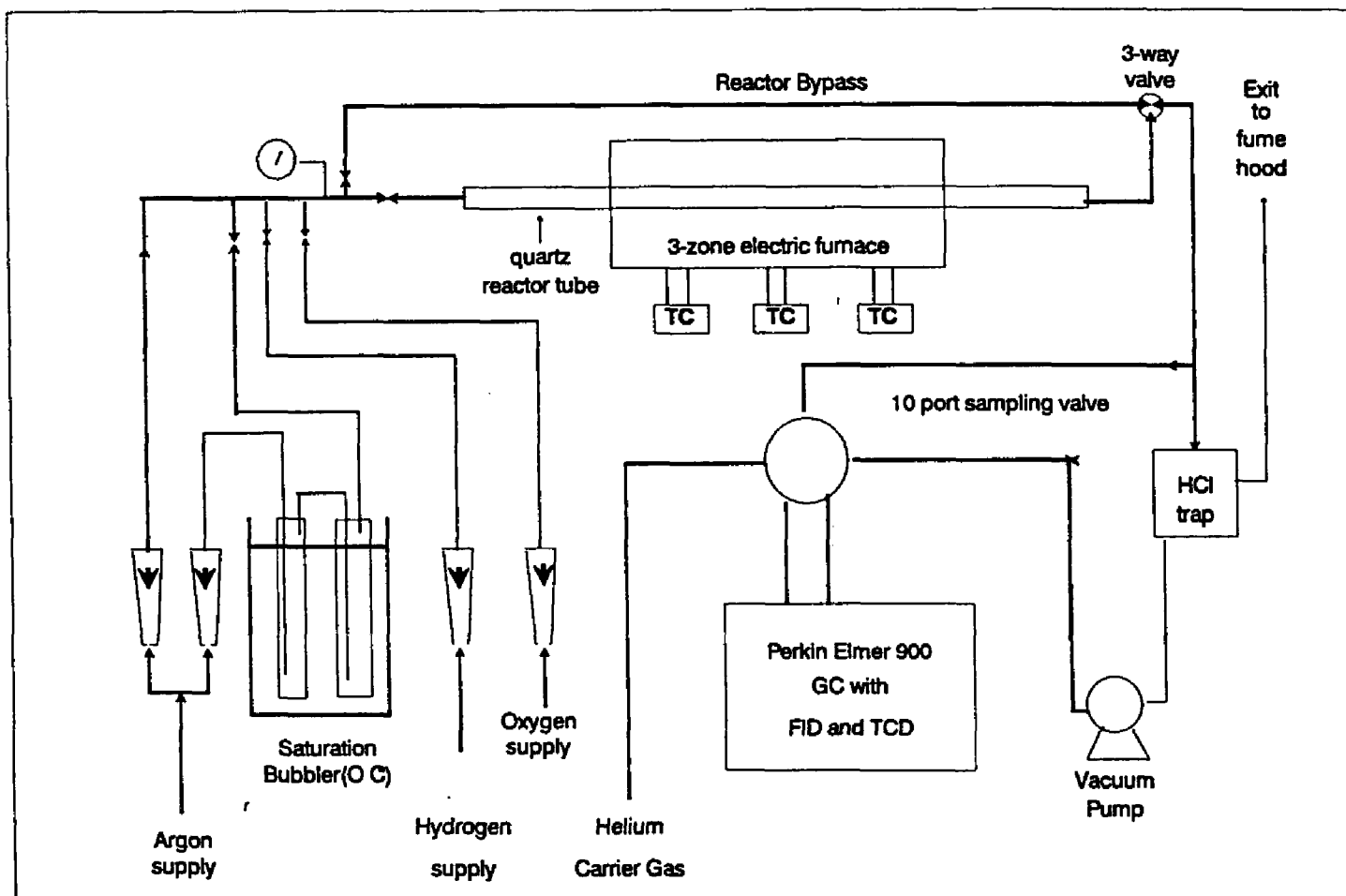


**Fig 2.1 Experimental Apparatus**

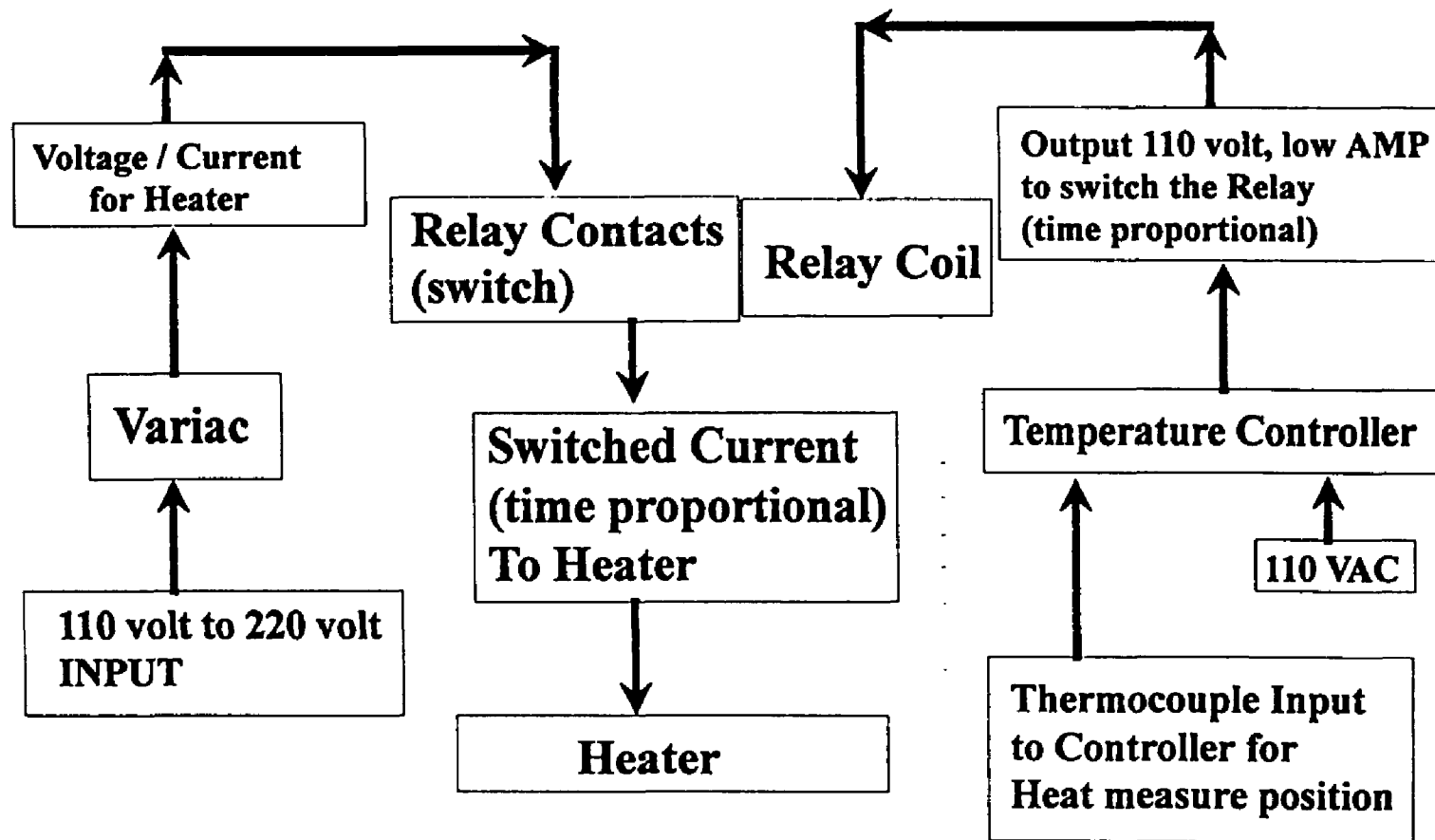


**Fig 2.2 Schematic of Voltage and Thermocouple Input to Temperature Controller**

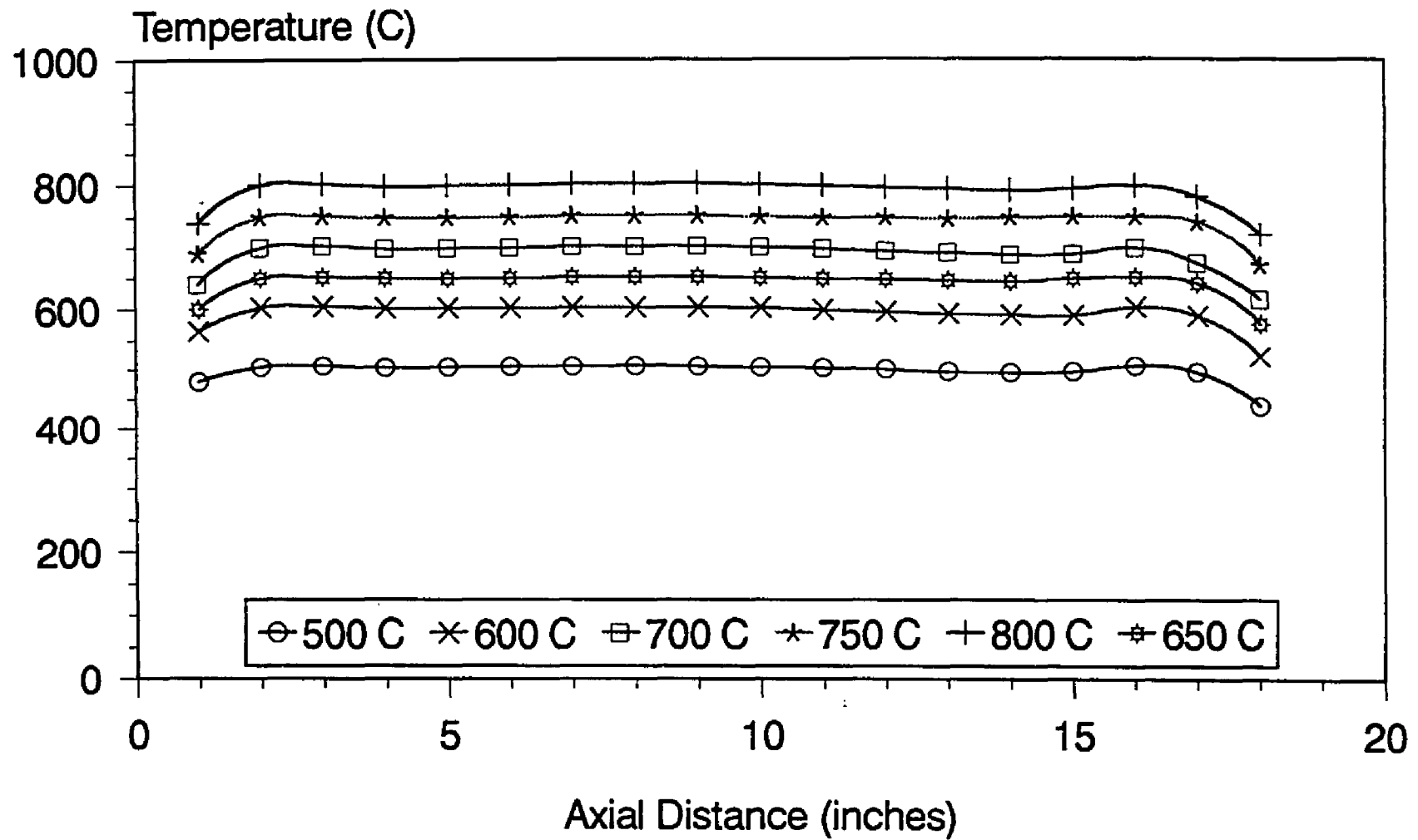


Fig 2.3 Temperature Profile

Column: 1.5m x 1/8" OD, 1% AT-1000 on Graphpac GB

Detector: FID, 250 C

Temperature: 35 C, 2 min, 15 C/min. to 200 C

Carrier Gas: He, 25 ml/min.

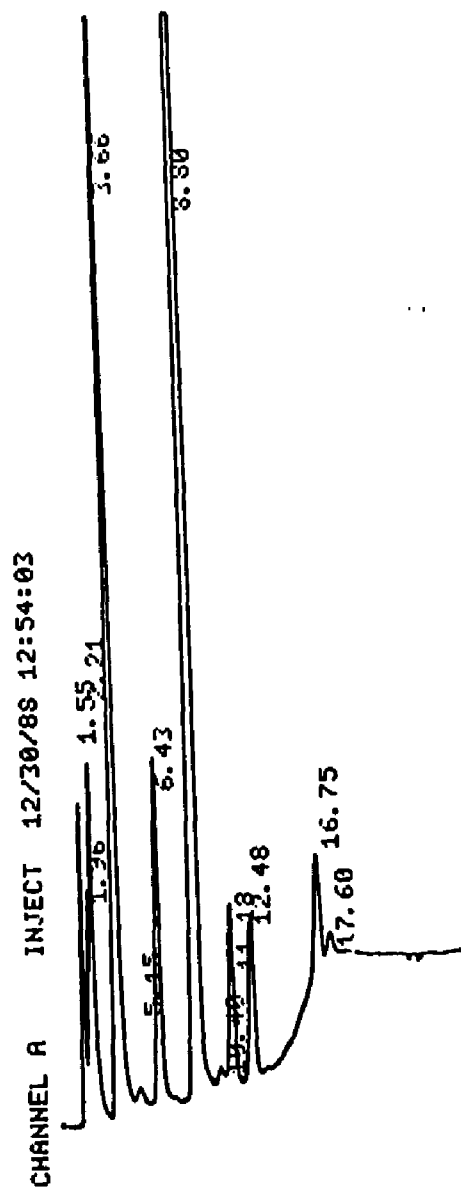


Figure 2.4 Sample Chromatogram of  $\text{CH}_2\text{Cl}_2/\text{O}_2/\text{H}_2$  Decomposition

Column: 1.8m x 1/8" OD, GCA-013 SPHEROCARB 100/200

Detector: TCD, 100 C, 175 mA

Temperature: 35 C, 2 min, 15 C/min. to 200 C

Carrier Gas: He, 30 ml/min.

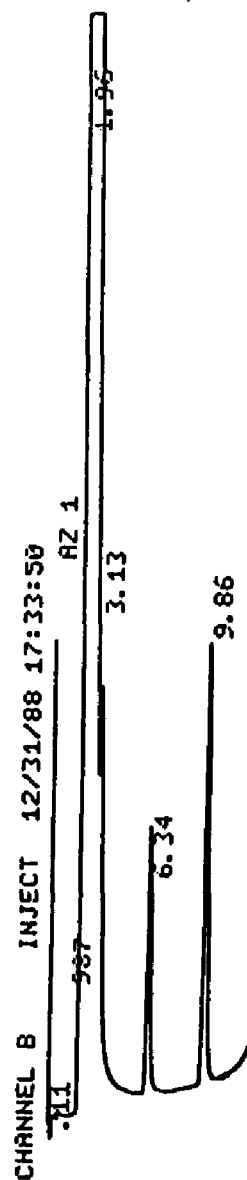


Figure 2.5 Sample Chromatogram of  $\text{CH}_2\text{Cl}_2/\text{O}_2/\text{H}_2$  Decomposition

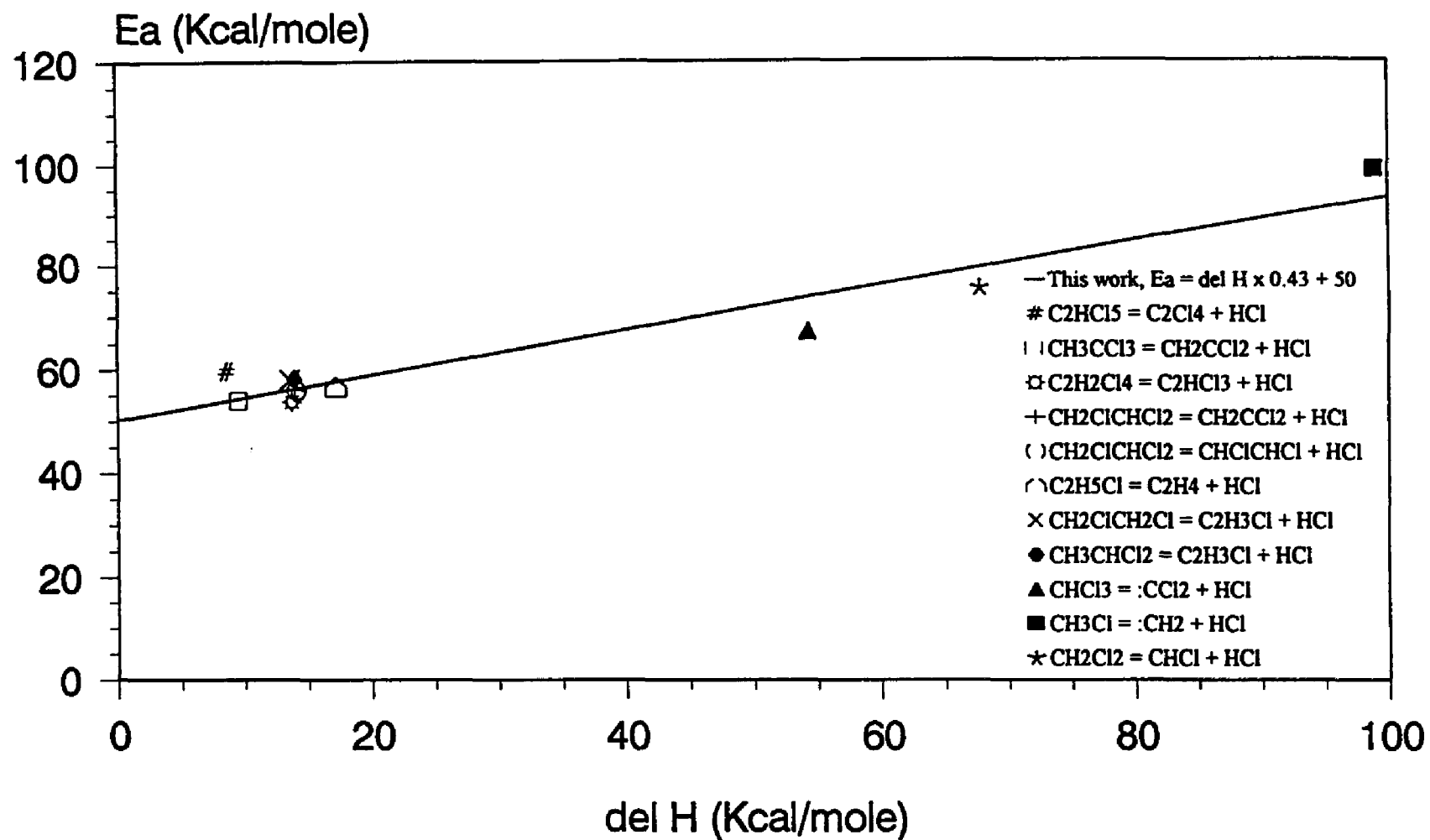


Fig. 4.1 Energy Barrier for HCl elimination

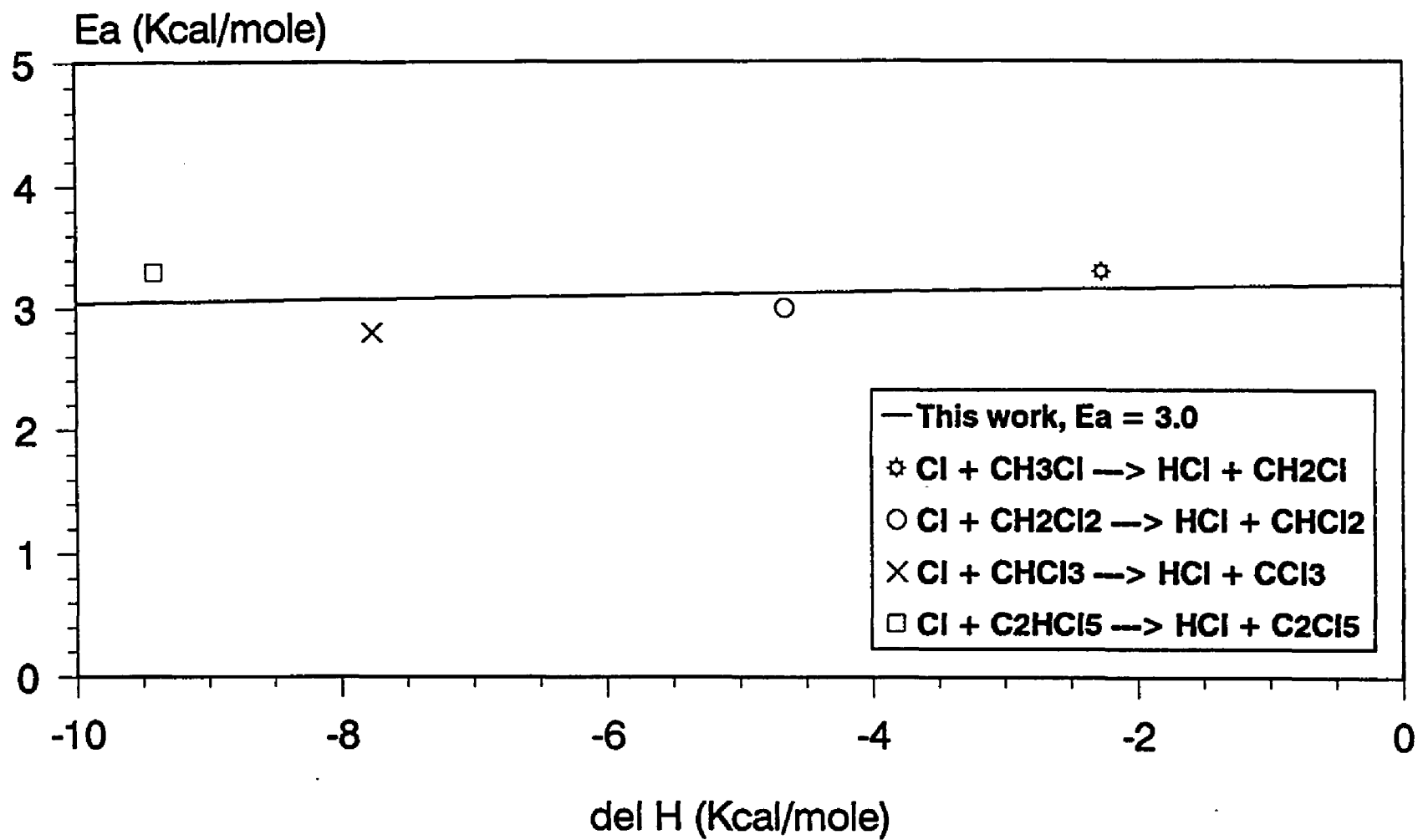


Fig 4.2 Evans-Polanyi Plot,  $\text{Cl} + \text{CHC} \rightarrow \text{HCl} + \text{R}'$ .



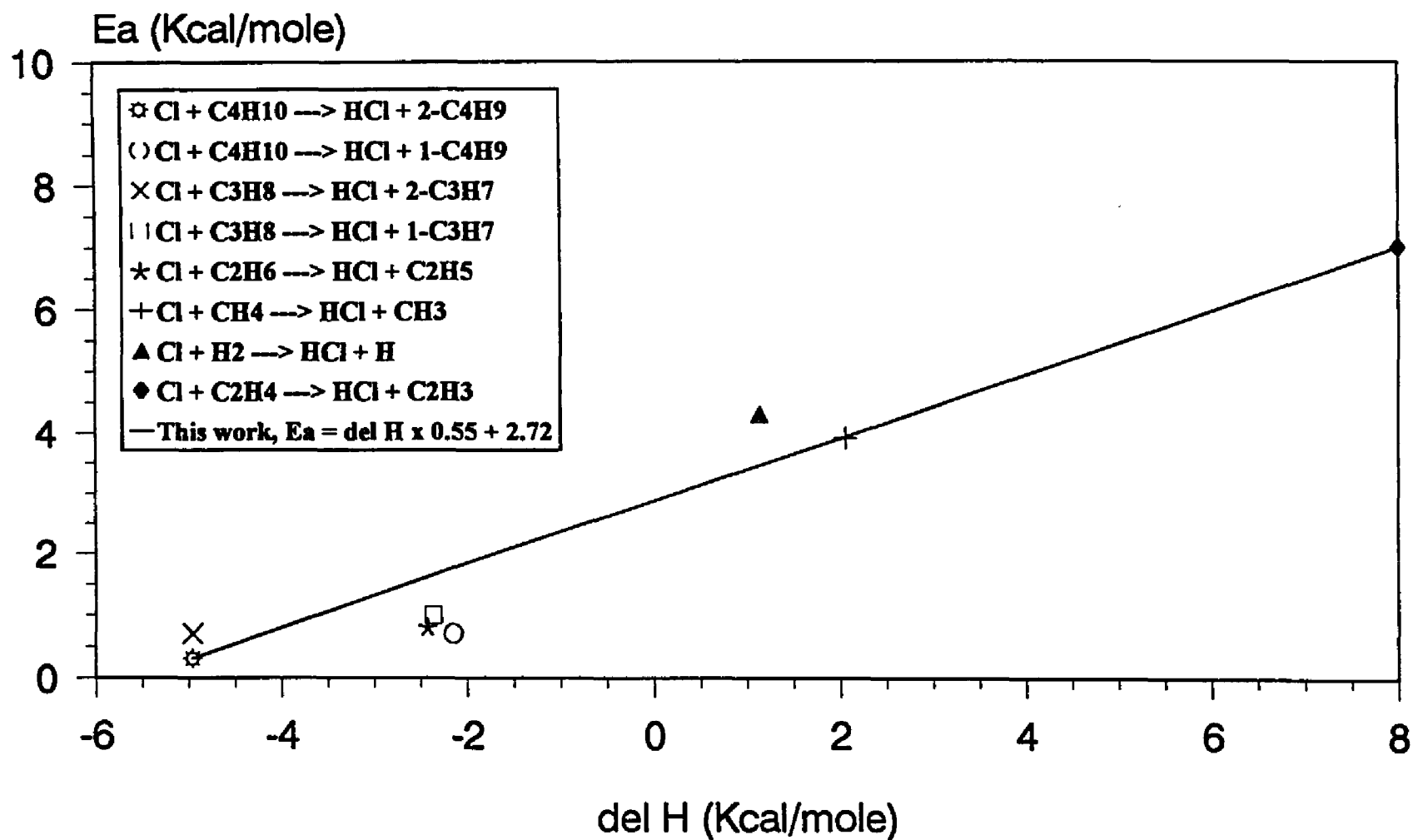


Fig. 4.3 Evans-Polanyi Plot,  $\text{Cl} + \text{RH} \longrightarrow \text{HCl} + \text{R}$ .

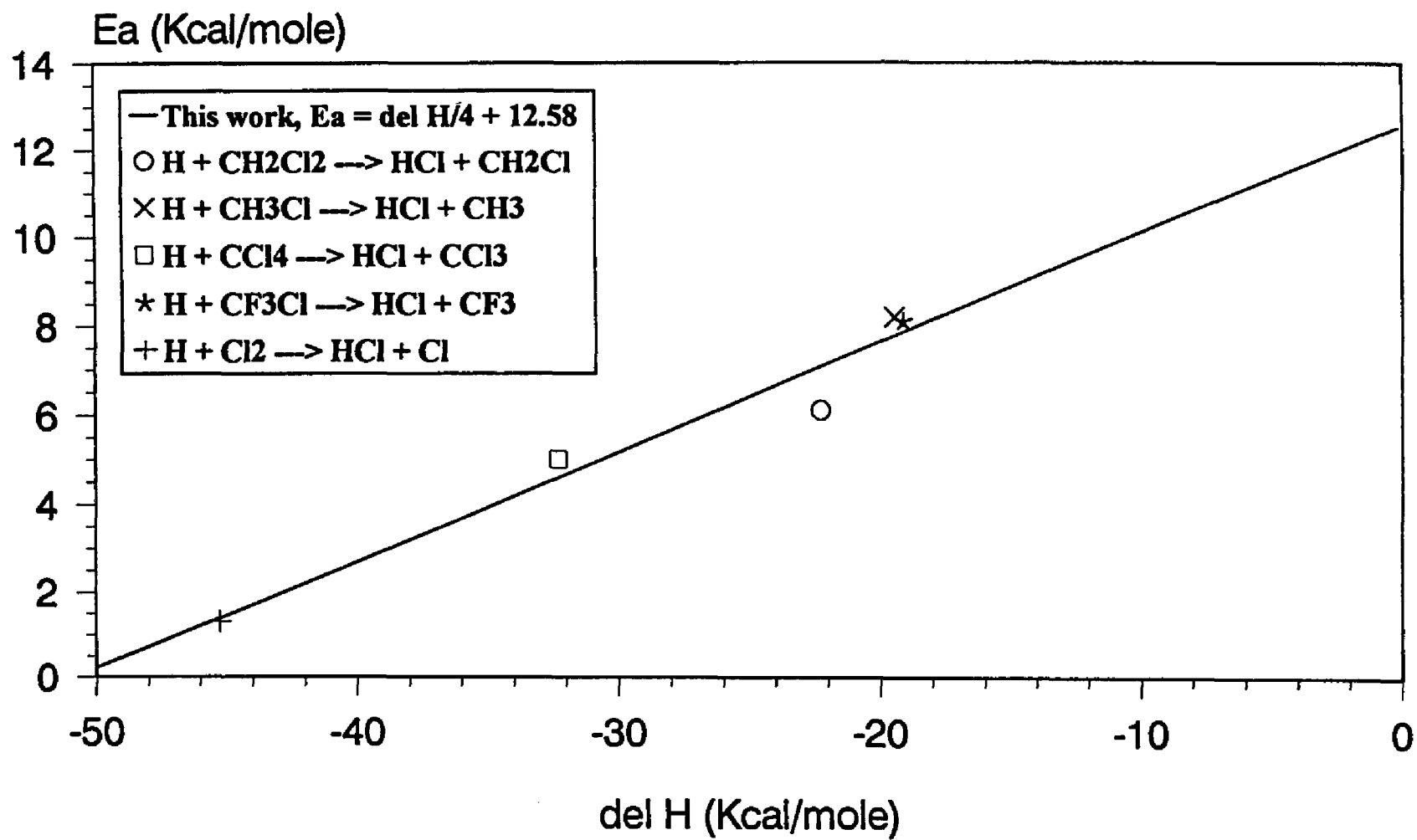


Fig. 4.4 Evans-Polanyi Plot,  $H + RCl \rightarrow HCl + R$ .

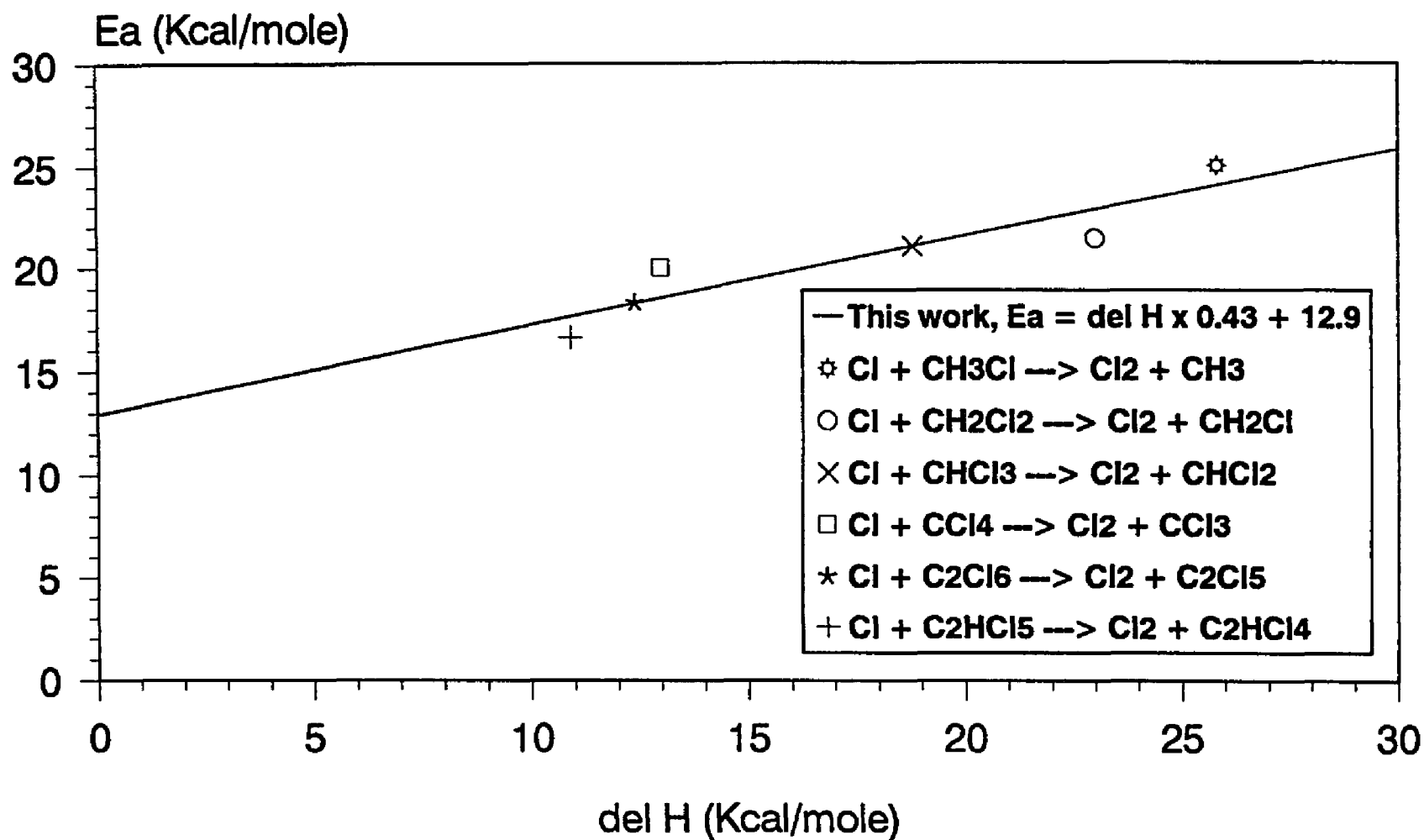


Fig. 4.5 Evans-Polanyi Plot,  $\text{Cl} + \text{RCl} \rightarrow \text{Cl}_2 + \text{R}$ .

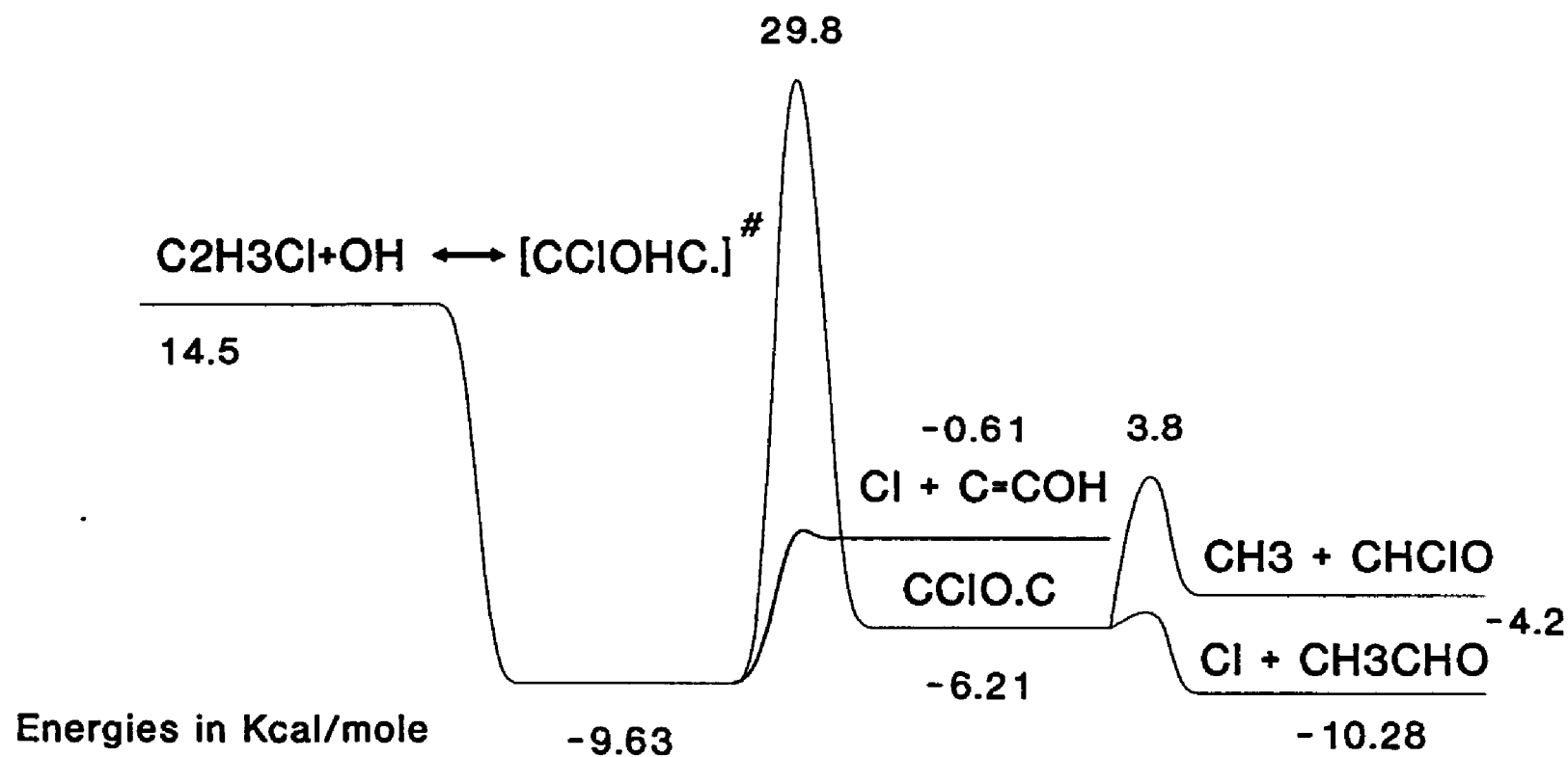


Fig 5.1 Energy level for  $\text{C}_2\text{H}_3\text{Cl} + \text{OH}$  alpha addition

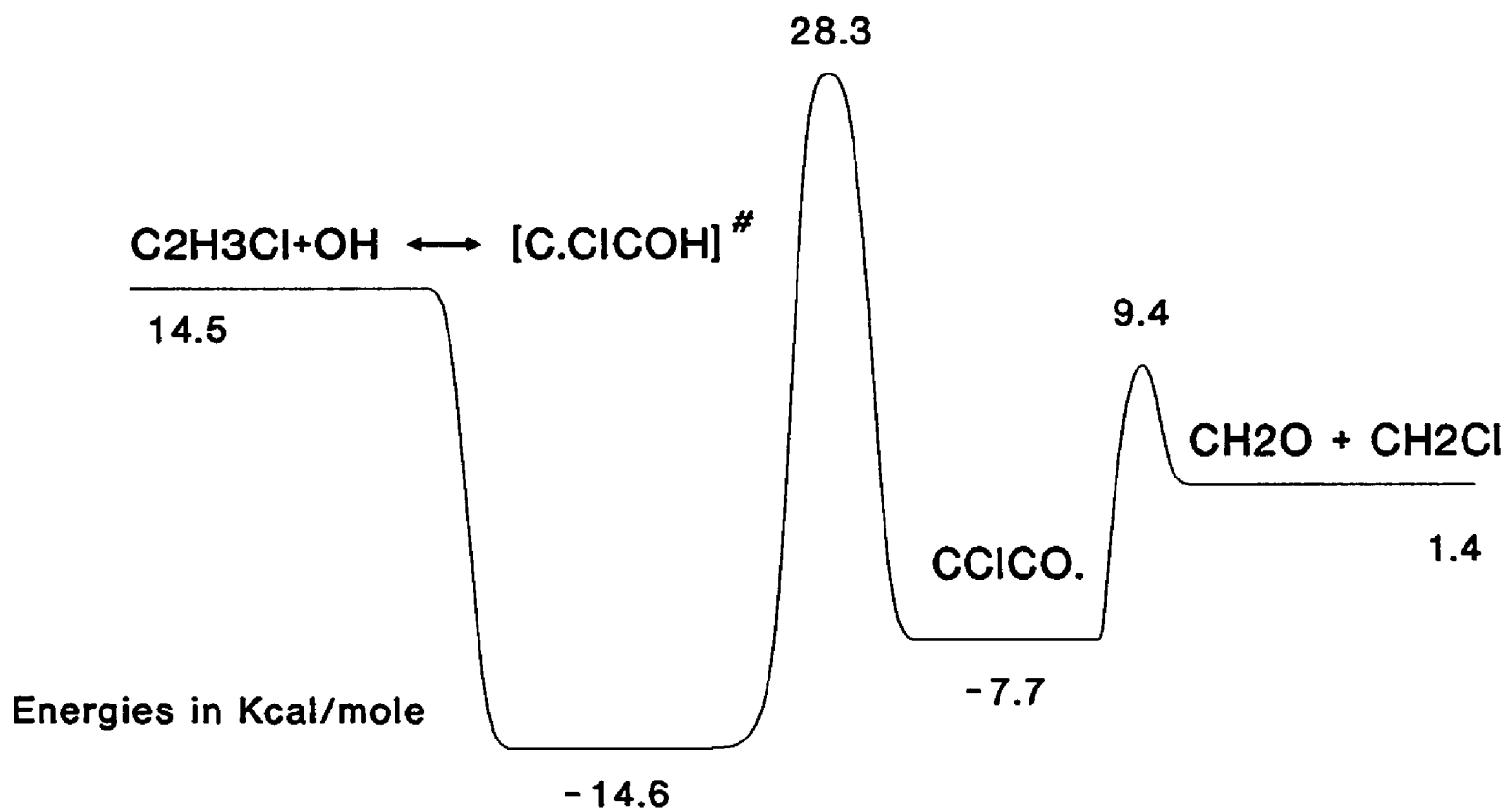
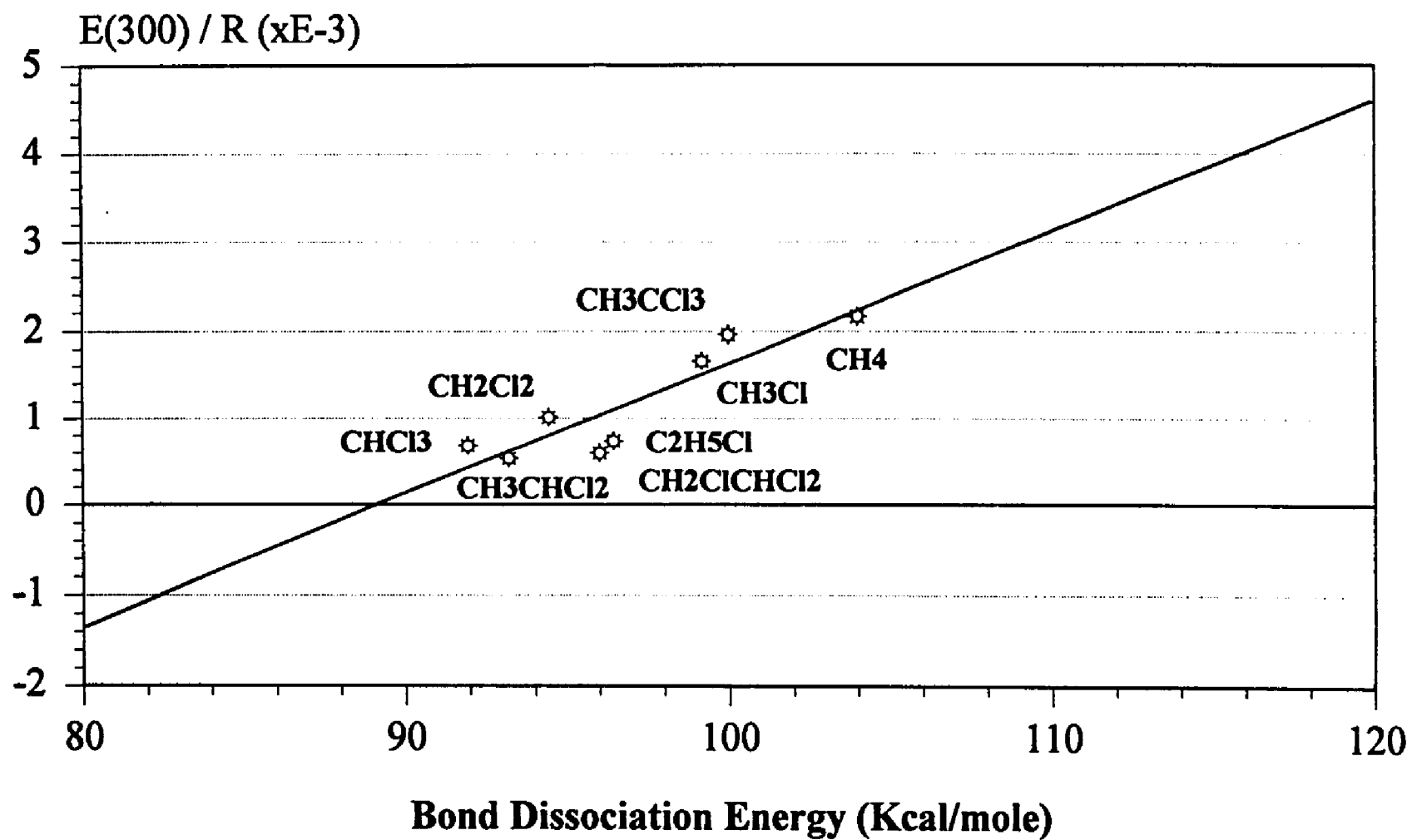


Fig 5.2 Potential energy diagram for  $\text{C}_2\text{H}_3\text{Cl} + \text{OH}$  beta addition



**Fig. 5.3** M<sup>O</sup>dified Evans-Polanyi plot of OH abstraction of H atom from CHC

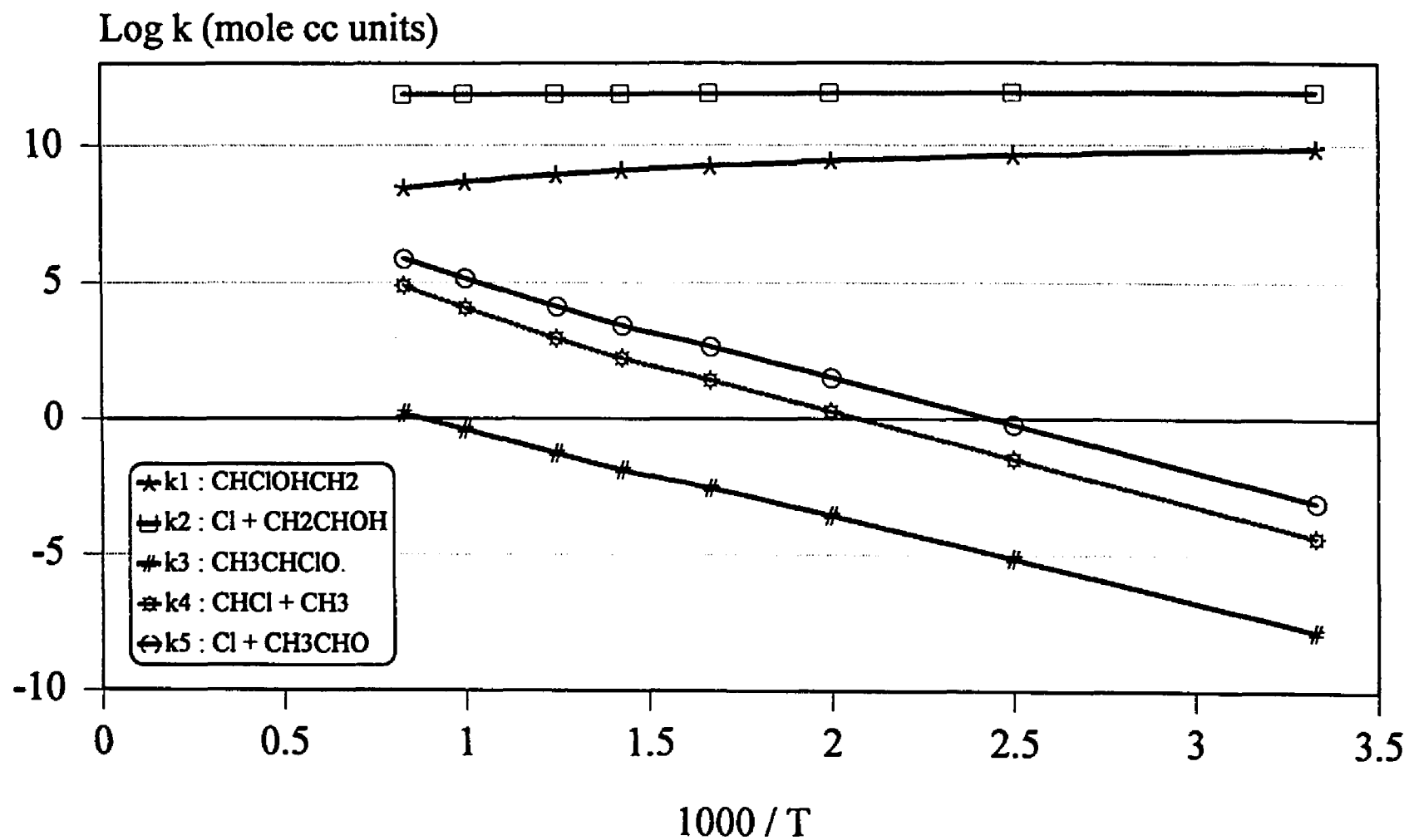


Fig. 5.4 Plot of the rate constants for alpha addition reaction versus 1000/T at 760 torr

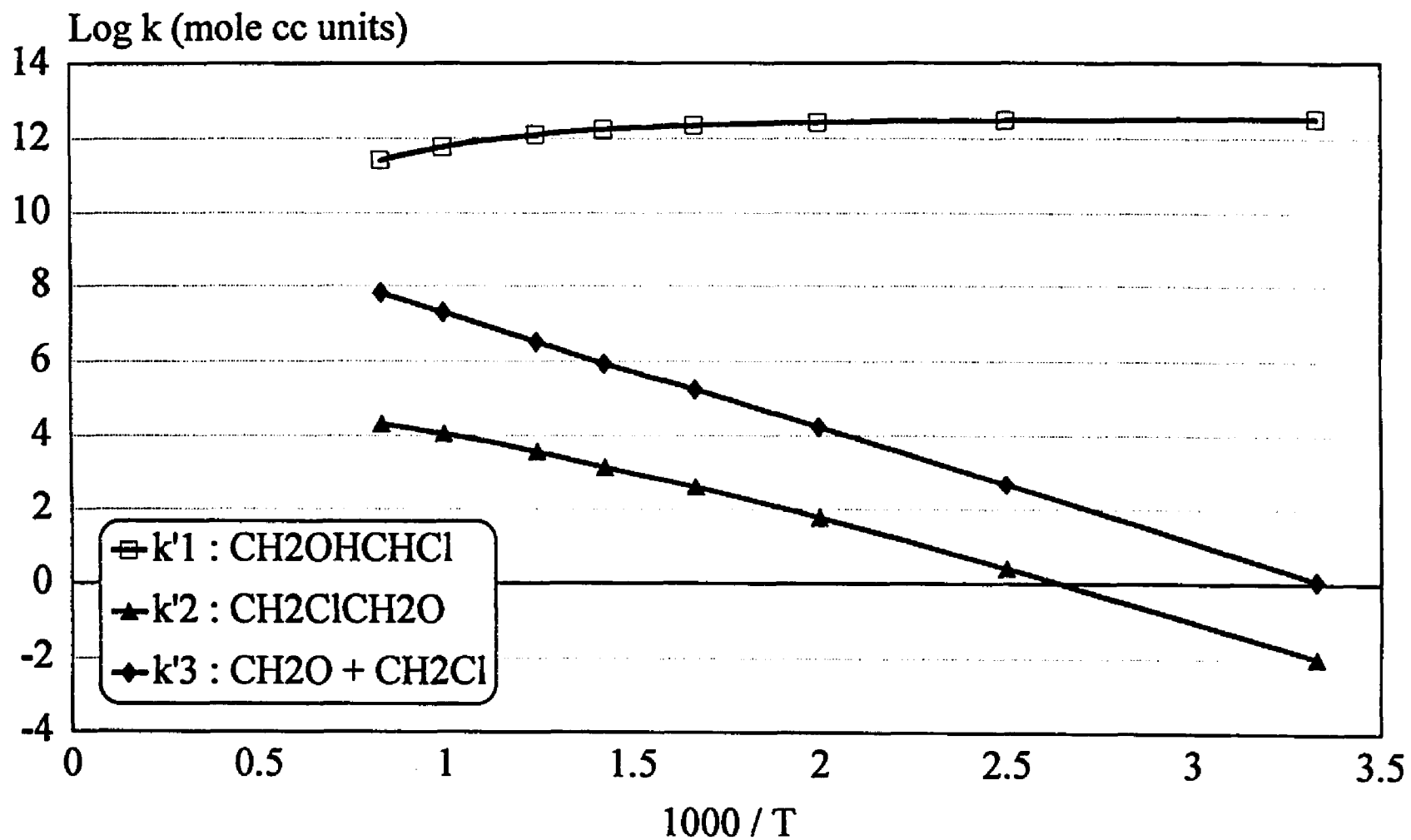


Fig. 5.5 Plot of the rate constants for beta addition reaction versus 1000/T at 760 torr



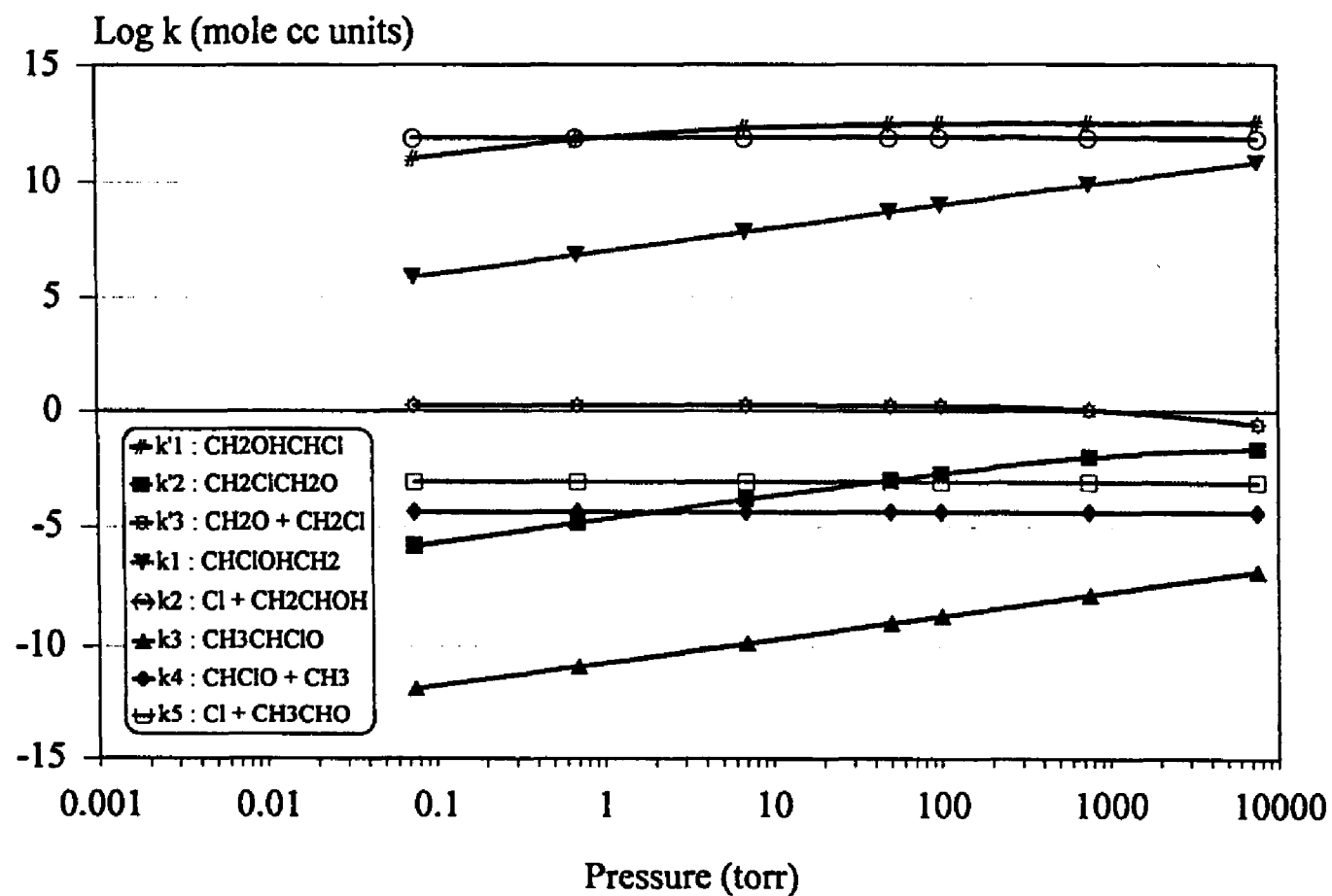


Fig 5.6 Major Reaction Products from The Reaction of Vinyl Chloride + OH Plotted versus Pressure at 300 K

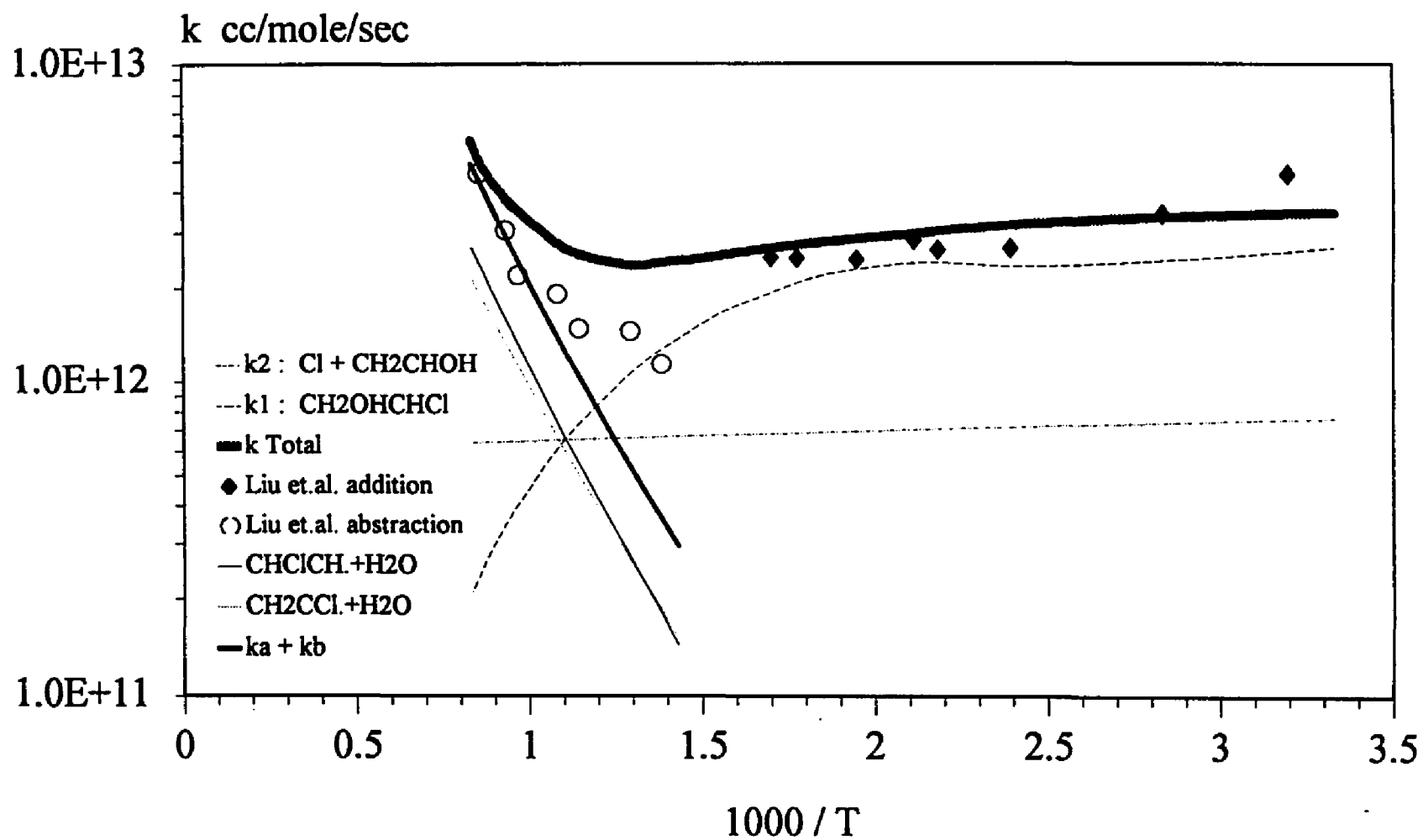


Fig. 5.7 Comparison of calculated results for  $\text{C}_2\text{H}_3\text{Cl} + \text{OH}$  to experimental data at 760 torr versus  $1000/T$

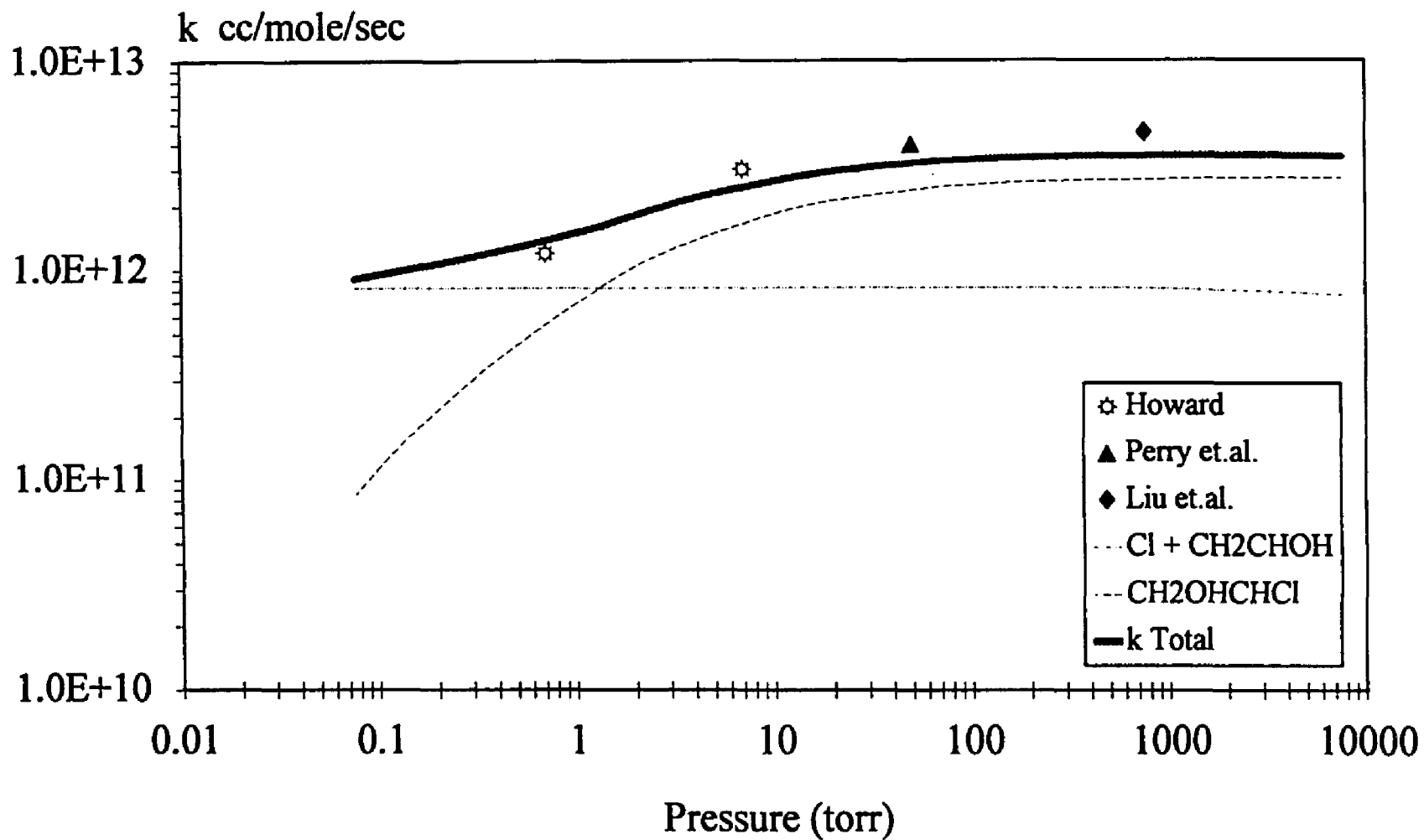


Fig. 5.8 Comparison of calculated results for C<sub>2</sub>H<sub>3</sub>Cl to experiments at room temperature versus pressure

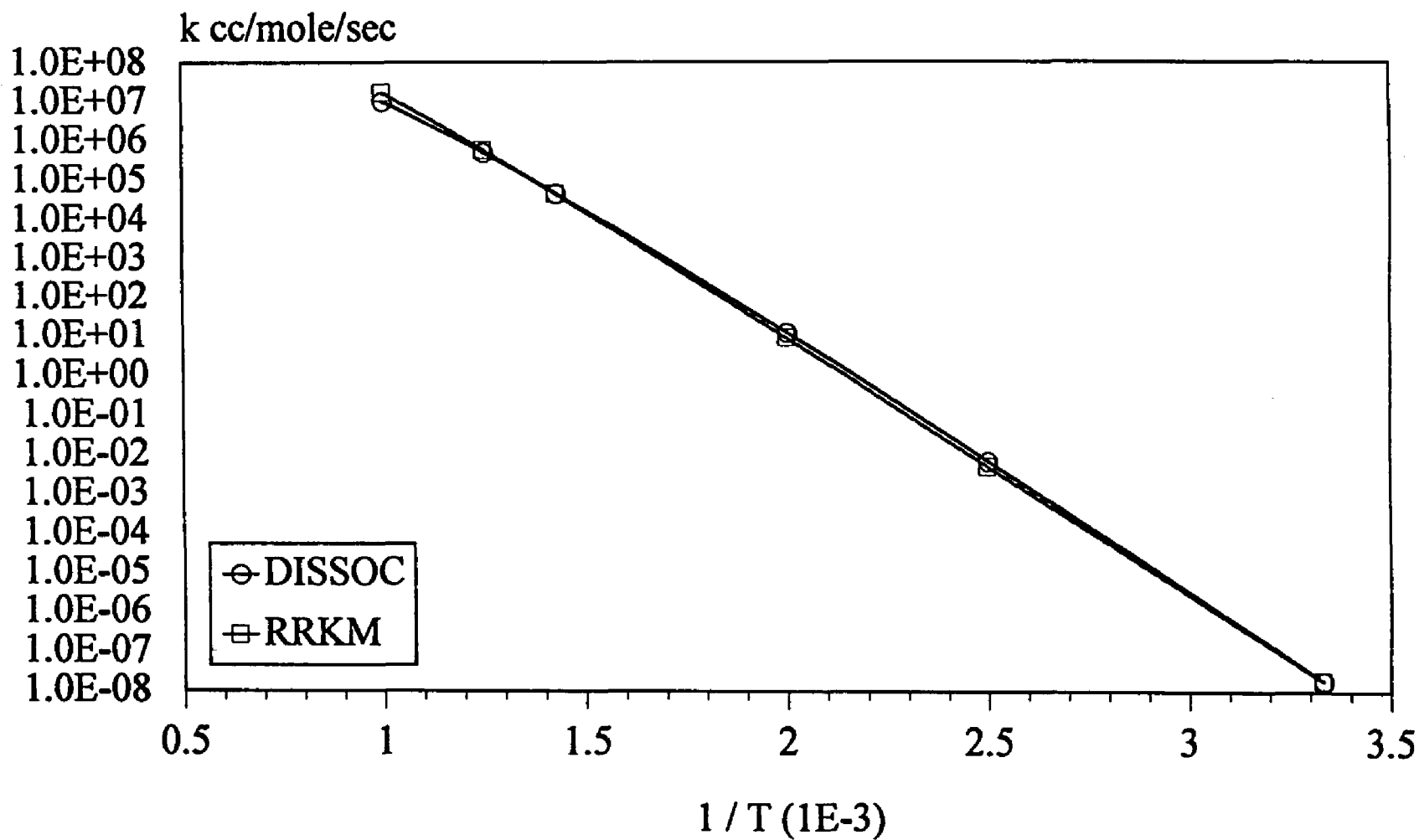


Fig. 5.9 Comparison of calculated results for  $\text{CH}_2\text{OHC.HCl} \rightarrow \text{C}_2\text{H}_3\text{Cl} + \text{OH}$  dissociation reaction at 760 torr versus  $1/T$

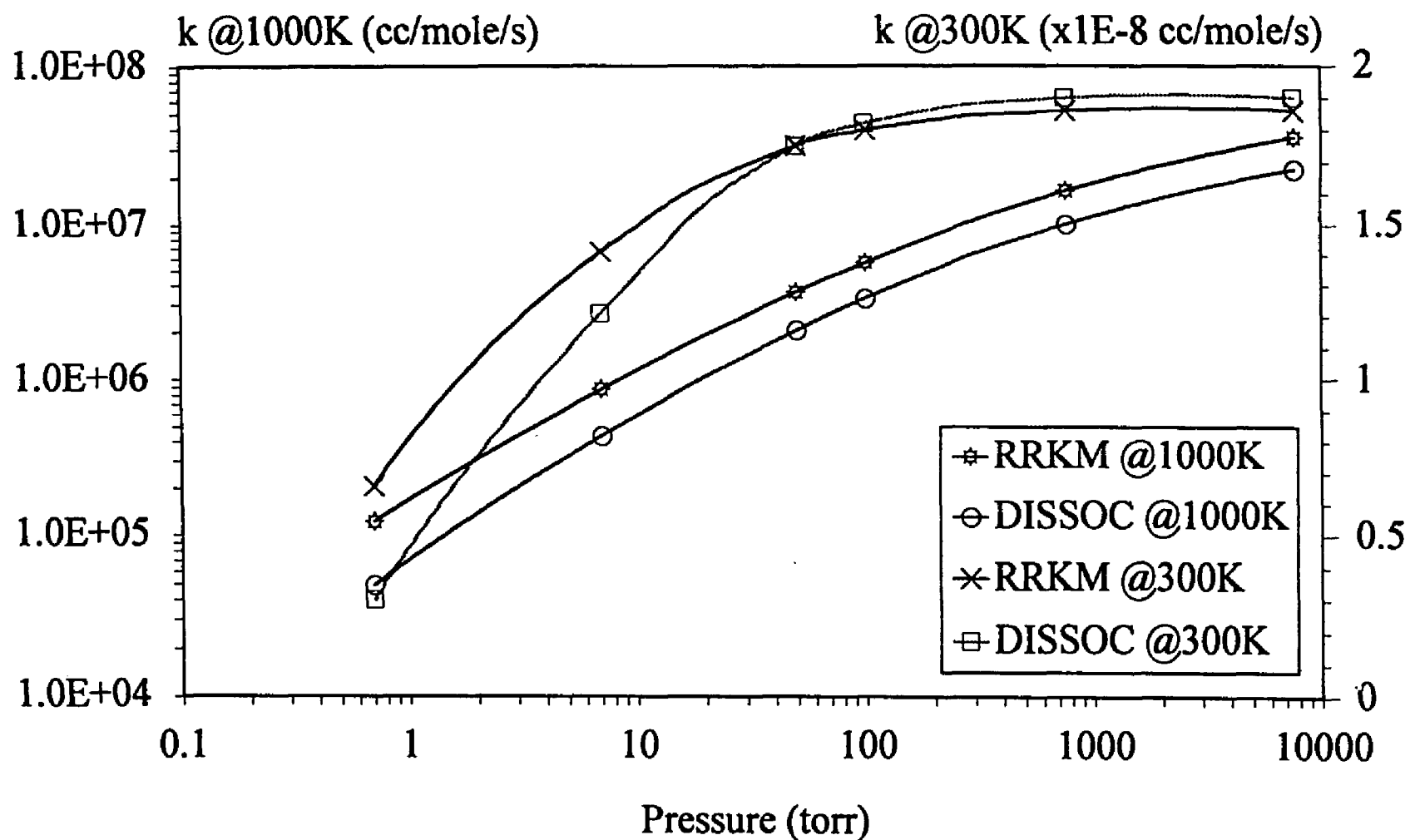


Fig. 5.10 Comparison of calculated results for  $\text{CH}_2\text{OHC.HCl} \rightarrow \text{C}_2\text{H}_3\text{Cl} + \text{OH}$  dissociation reaction versus pressure

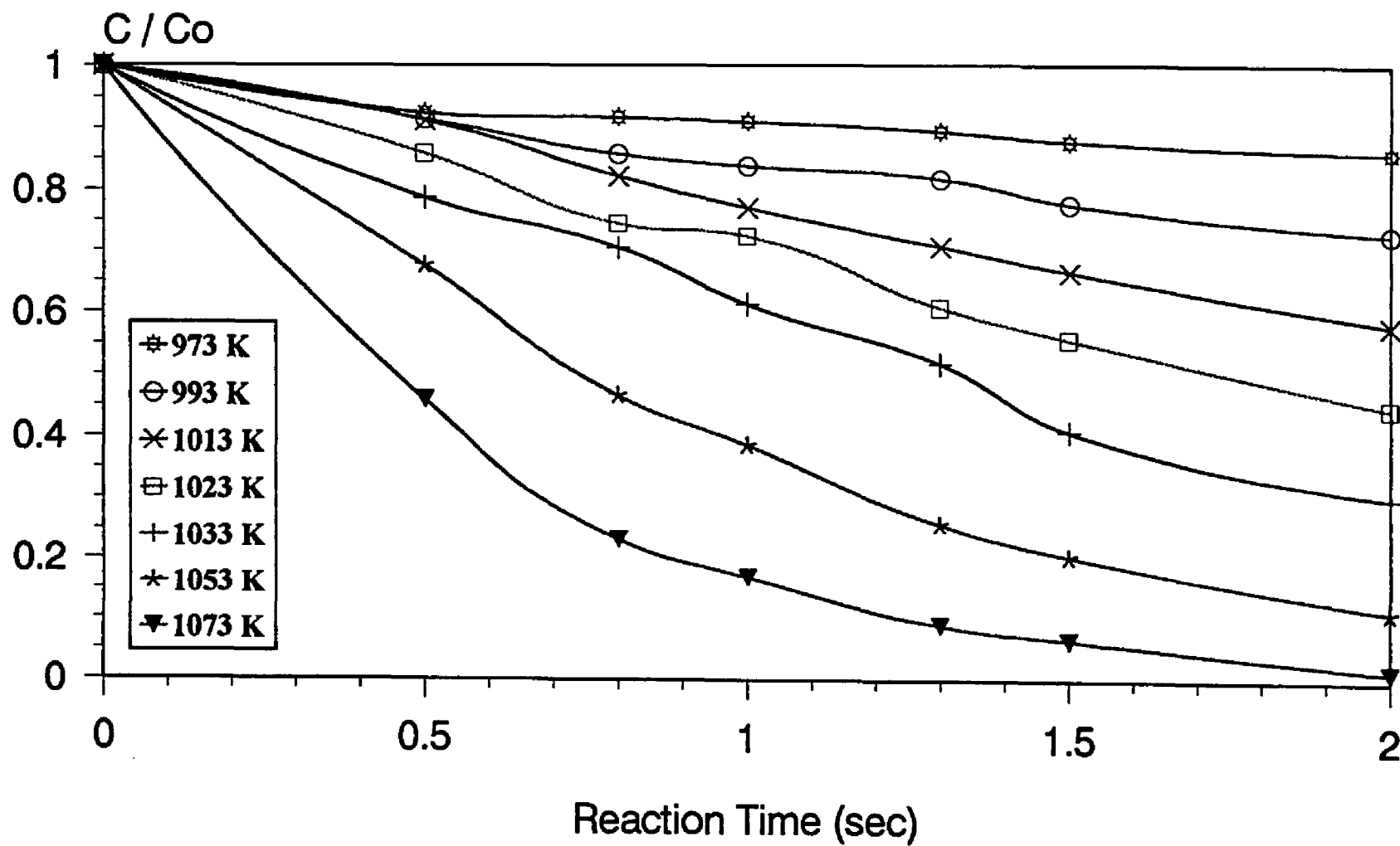


Fig 6.1  $\text{CH}_2\text{Cl}_2$  conversion versus time at different temperature. Reactant ratios:  $\text{O}_2:\text{H}_2:\text{CH}_2\text{Cl}_2:\text{Ar}=1:1:1:97$

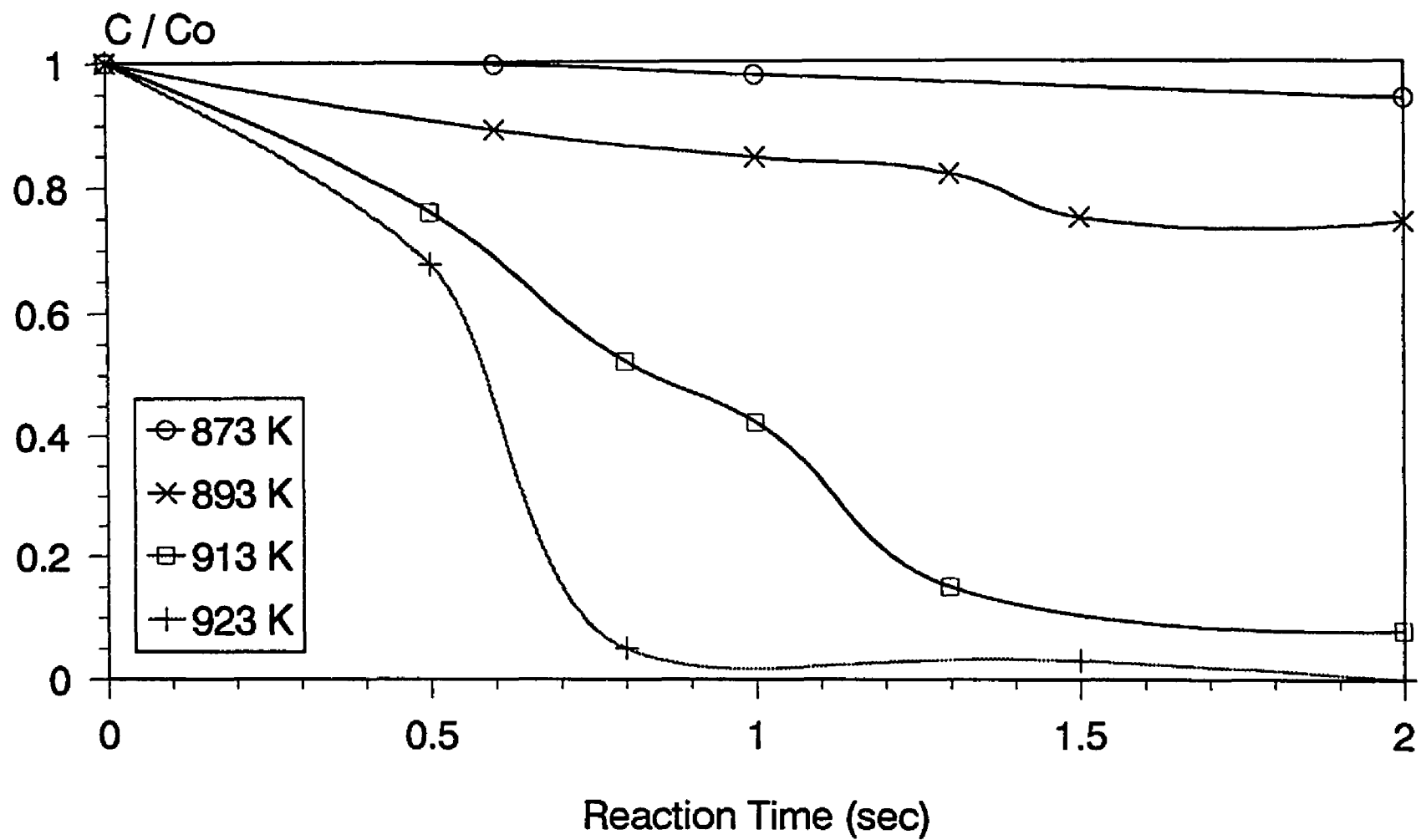


Fig 6.2  $\text{CH}_2\text{Cl}_2$  conversion versus time at different temperatures. Reactant ratios:  $\text{O}_2:\text{H}_2:\text{CH}_2\text{Cl}_2=98:1:1$

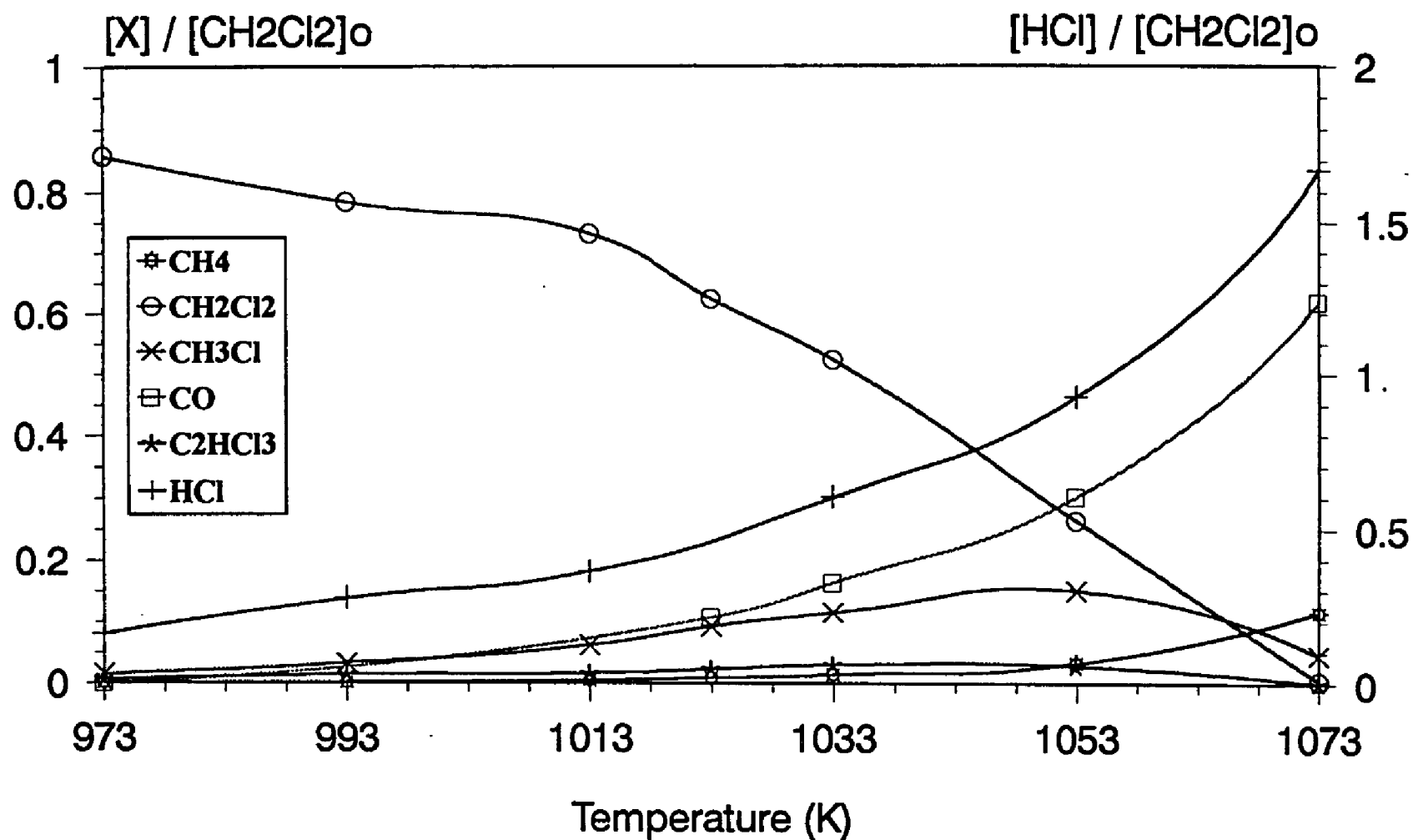


Fig 6.3 Major product distribution for CH<sub>2</sub>Cl<sub>2</sub> decomposition. 1 sec. residence time,  
 Reactant ratios: O<sub>2</sub>:H<sub>2</sub>:CH<sub>2</sub>Cl<sub>2</sub>:Ar=2:2:1:95



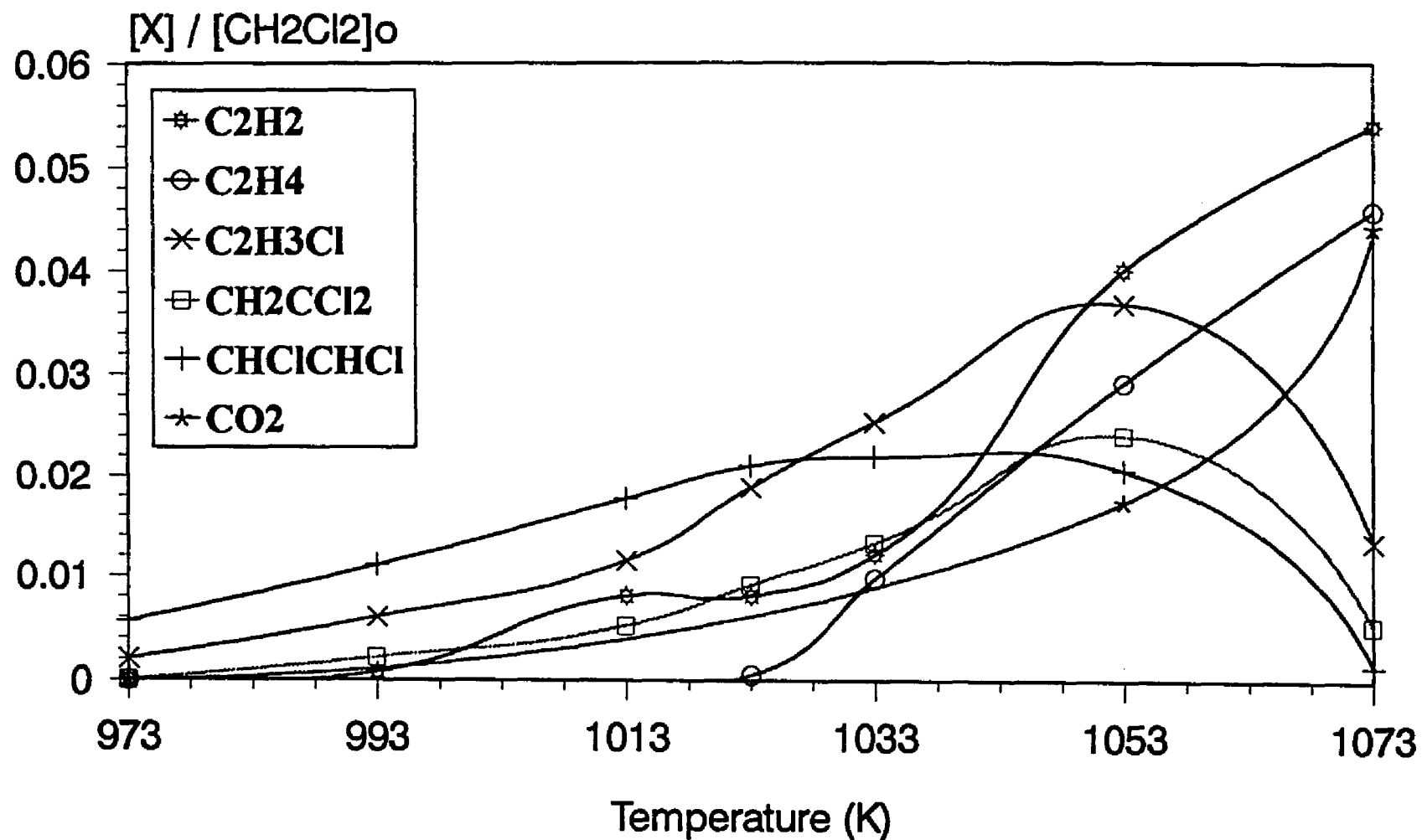


Fig 6.4 Minor product distribution for  $\text{CH}_2\text{Cl}_2$  decomposition. 1 sec. residence time,  
Reactant ratios:  $\text{O}_2:\text{H}_2:\text{CH}_2\text{Cl}_2:\text{Ar}=2:2:1:95$

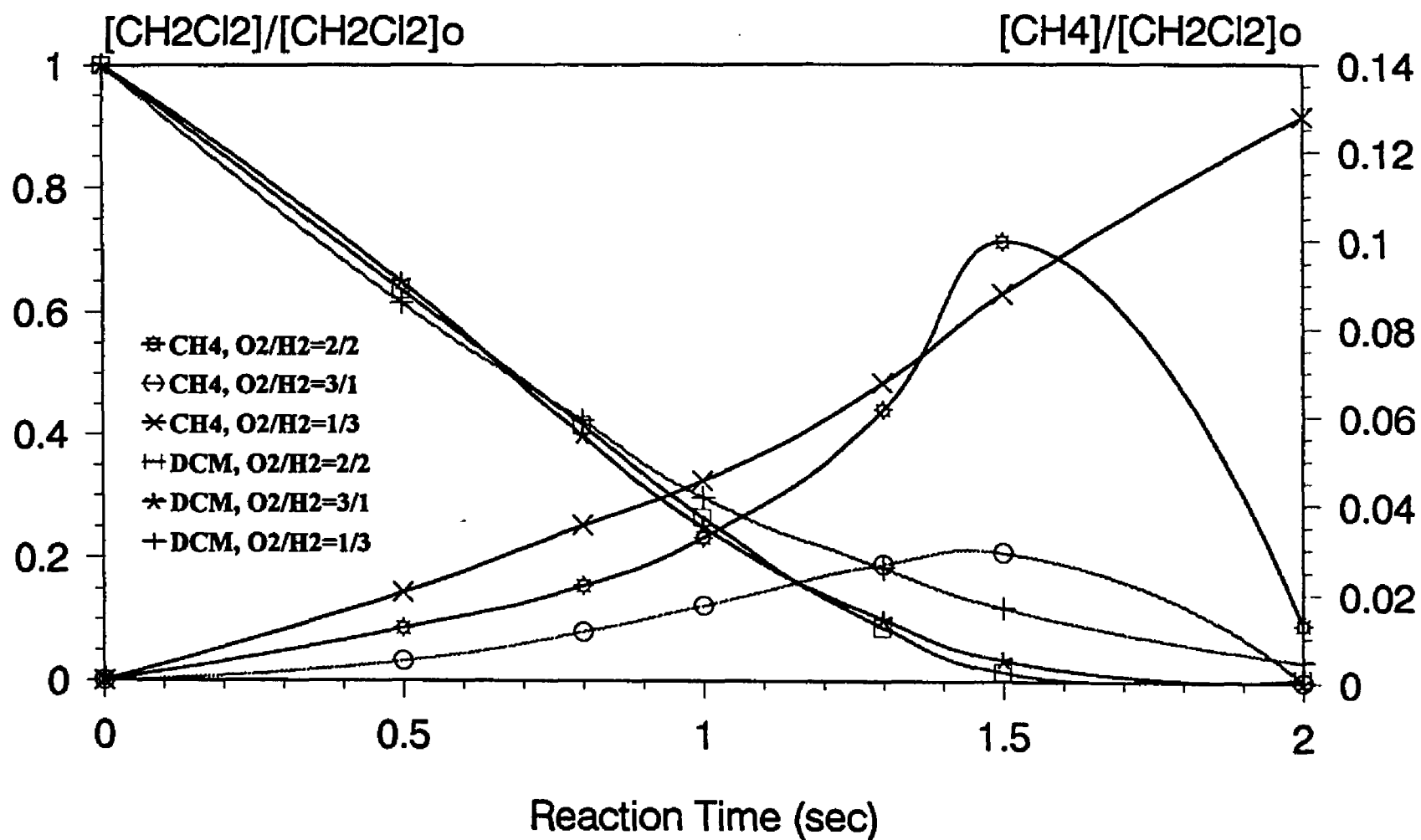


Fig 6.5 Comparison of CH<sub>2</sub>Cl<sub>2</sub> conversion and products at 1053K, 1% CH<sub>2</sub>Cl<sub>2</sub> with different O<sub>2</sub>/H<sub>2</sub> feed ratios

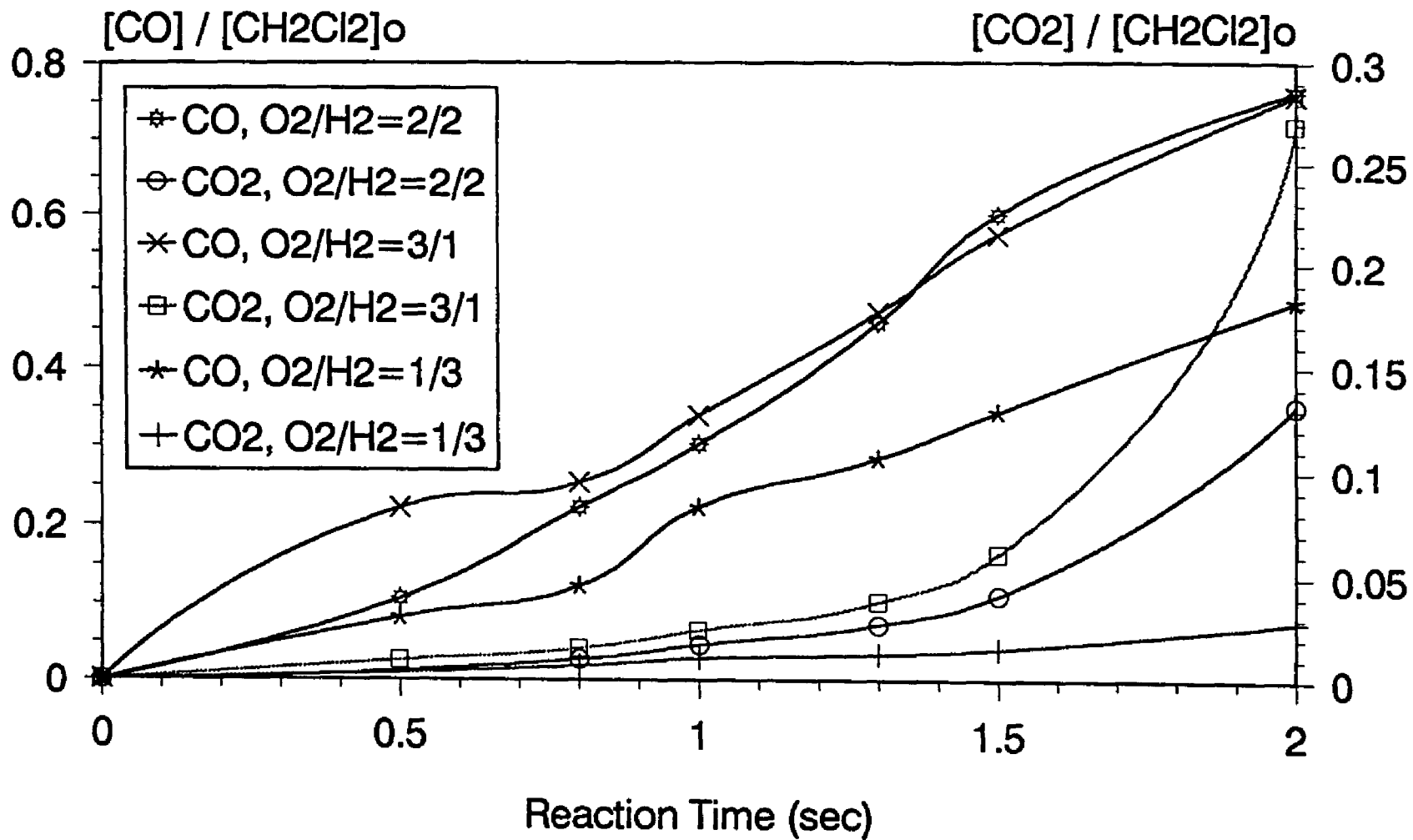


Fig 6.6 Comparison of CO and CO<sub>2</sub> production at 1053K, 1% CH<sub>2</sub>Cl<sub>2</sub> with different O<sub>2</sub>/H<sub>2</sub> feed ratios.

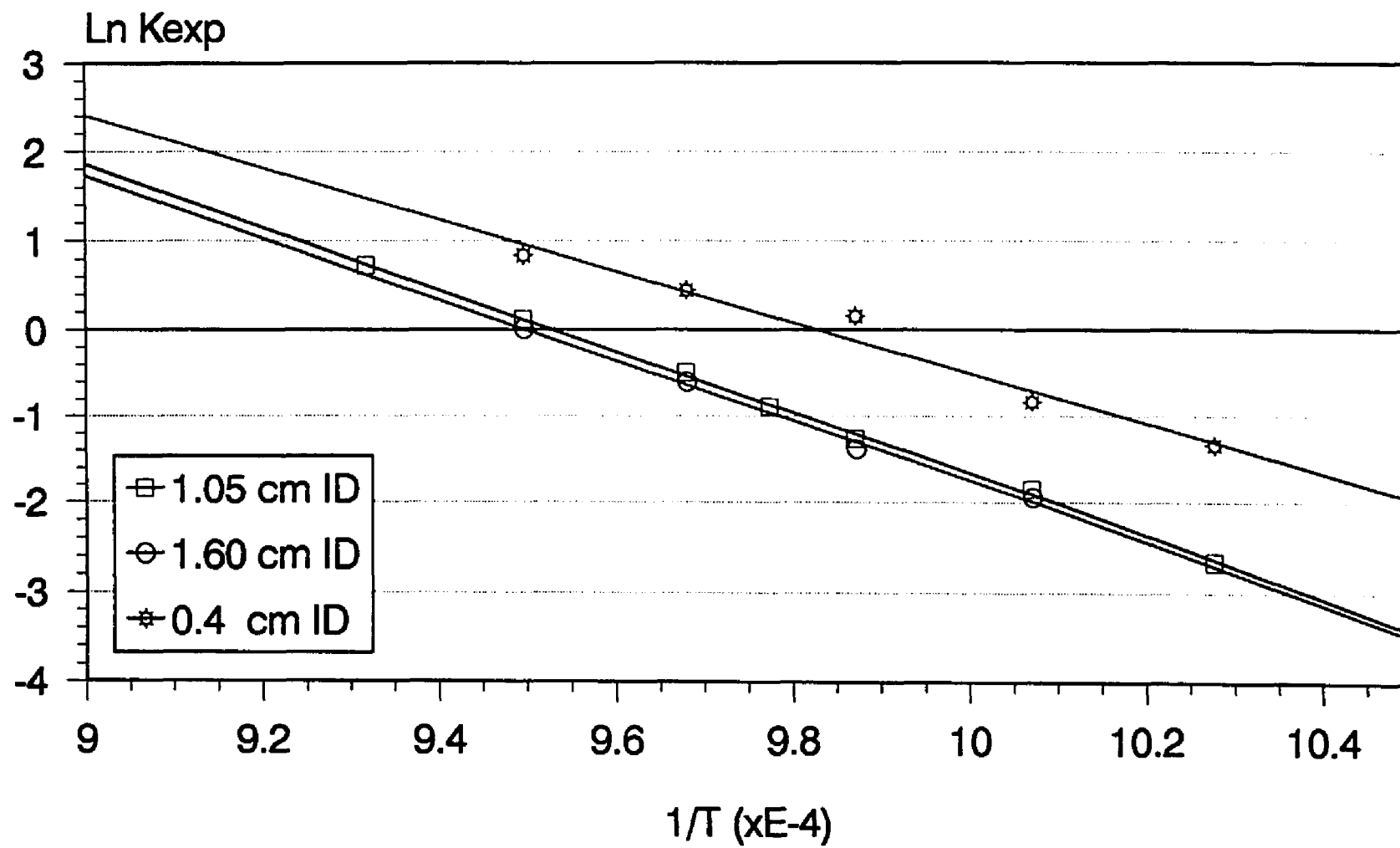
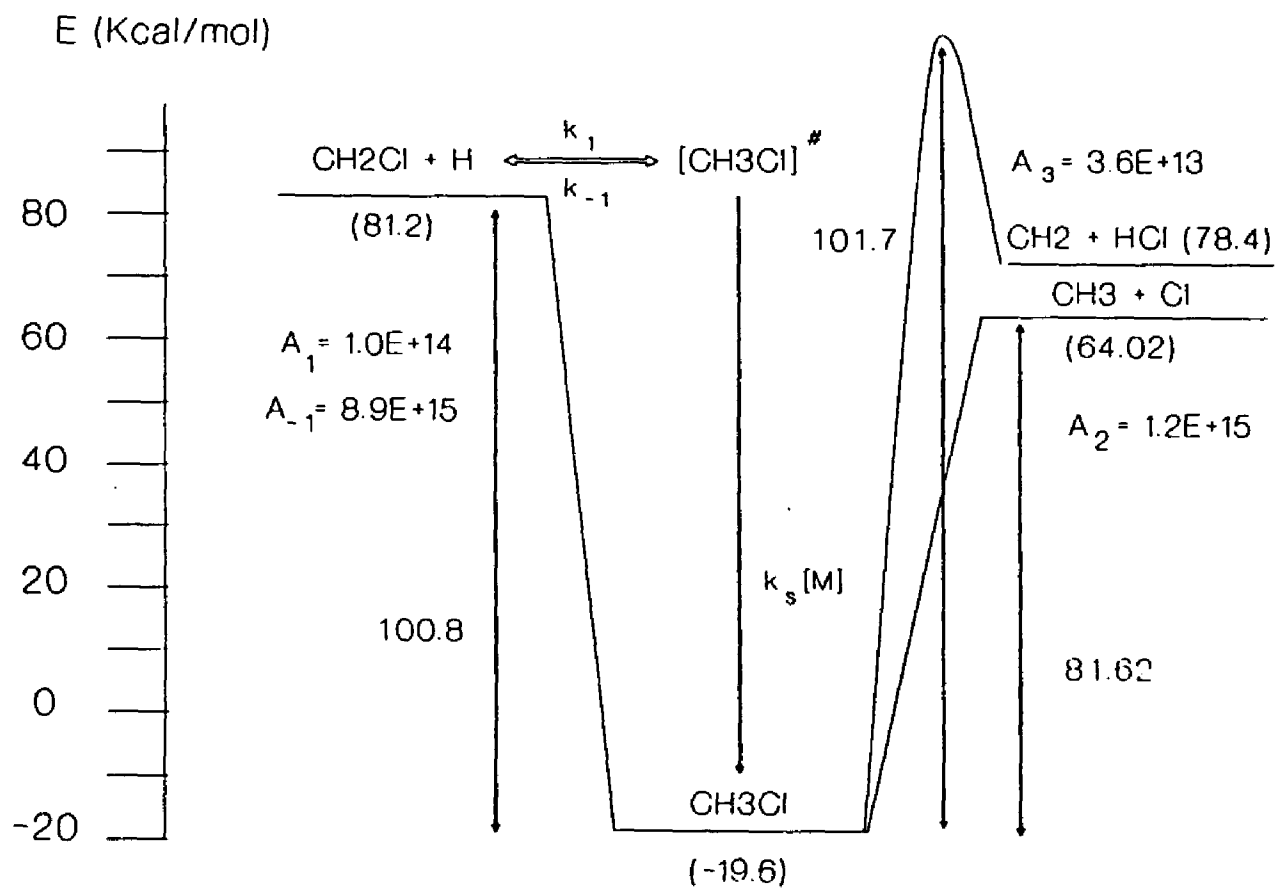


Fig 6.7 Arrhenius behavior of global  $K_{exp}$  for  $\text{CH}_2\text{Cl}_2/\text{O}_2/\text{H}_2$



**Fig 6.8 Energy Level for  $\text{CH}_2\text{Cl} + \text{H}$  Reaction**

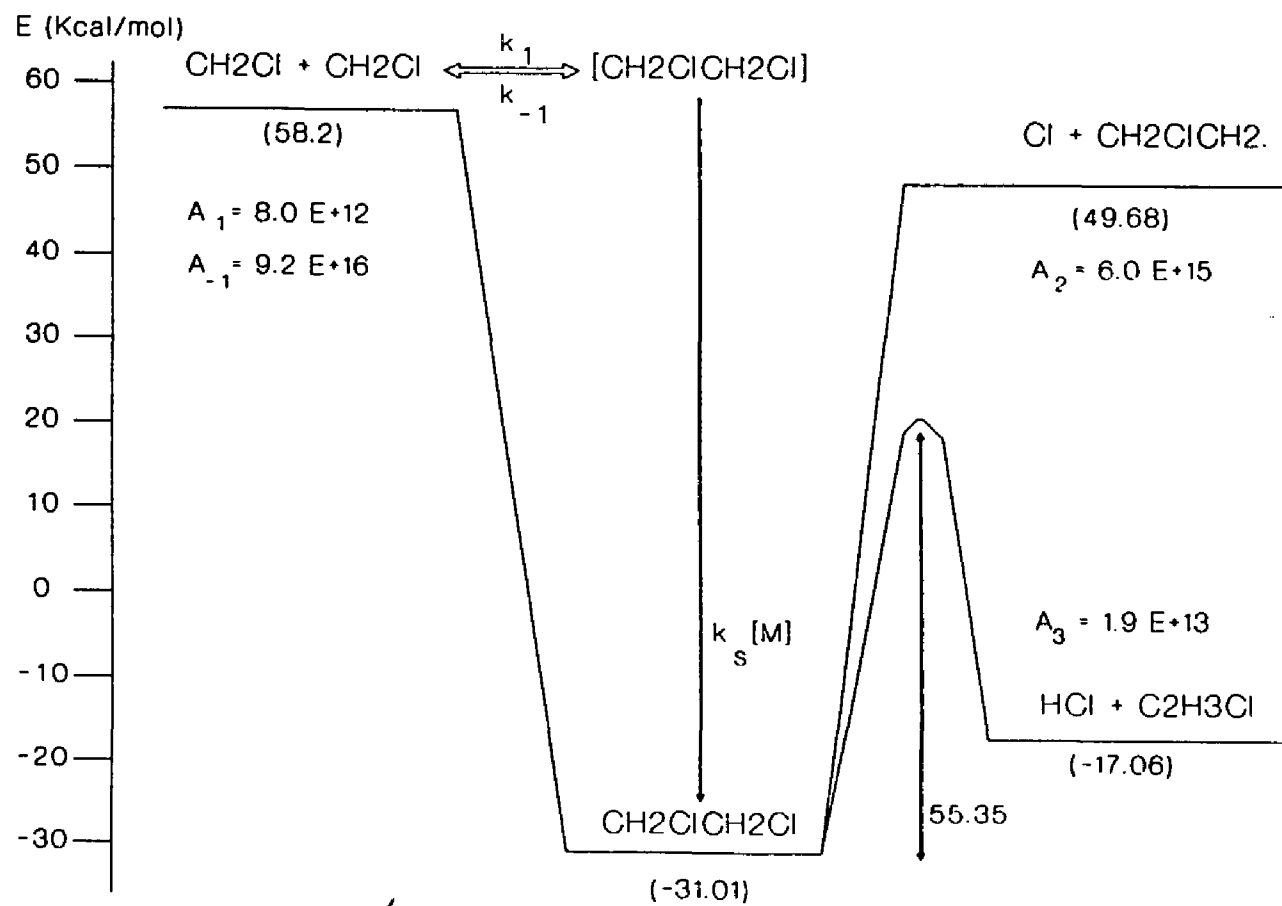


Fig 6.9 Energy Level for  $\text{CH}_2\text{Cl} + \text{CH}_2\text{Cl}$  Reaction

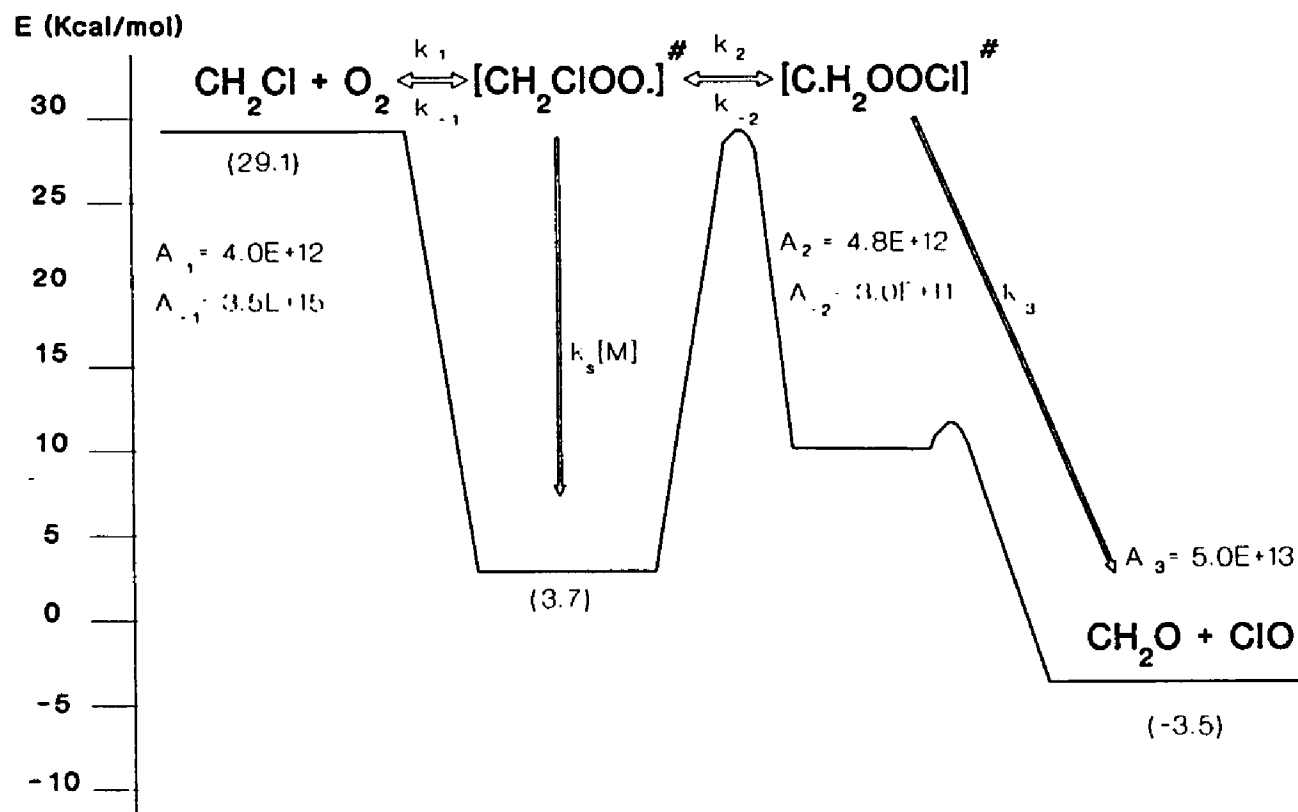


Fig 6.10 Energy Level for  $\text{CH}_2\text{Cl} + \text{O}_2$  Reaction

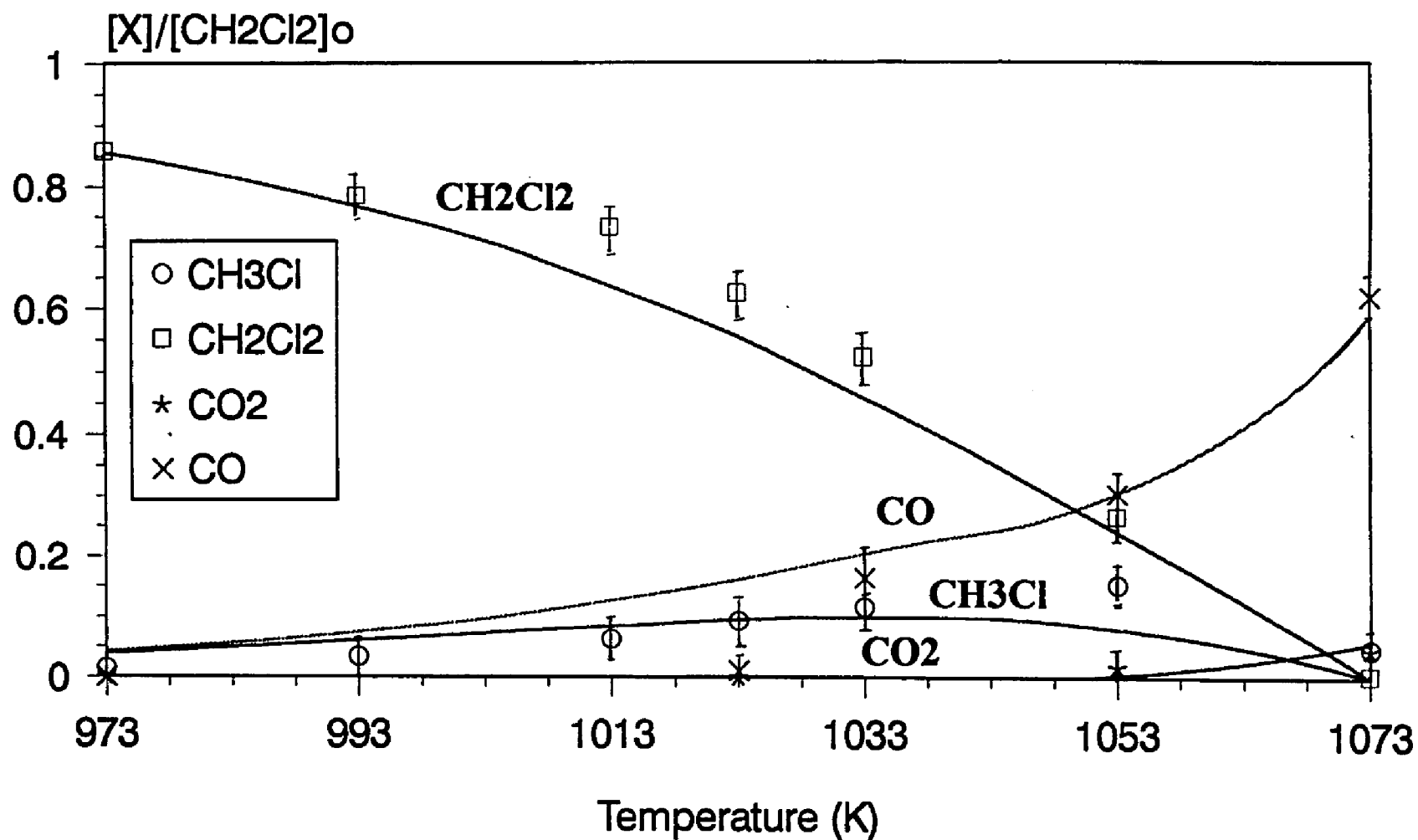


Fig 6.11 Comparison of calculated and experimental product distribution versus temperature. 1 sec. residence time, Reactant ratios:  $O_2:H_2:CH_2Cl_2:Ar=2:2:1:95$



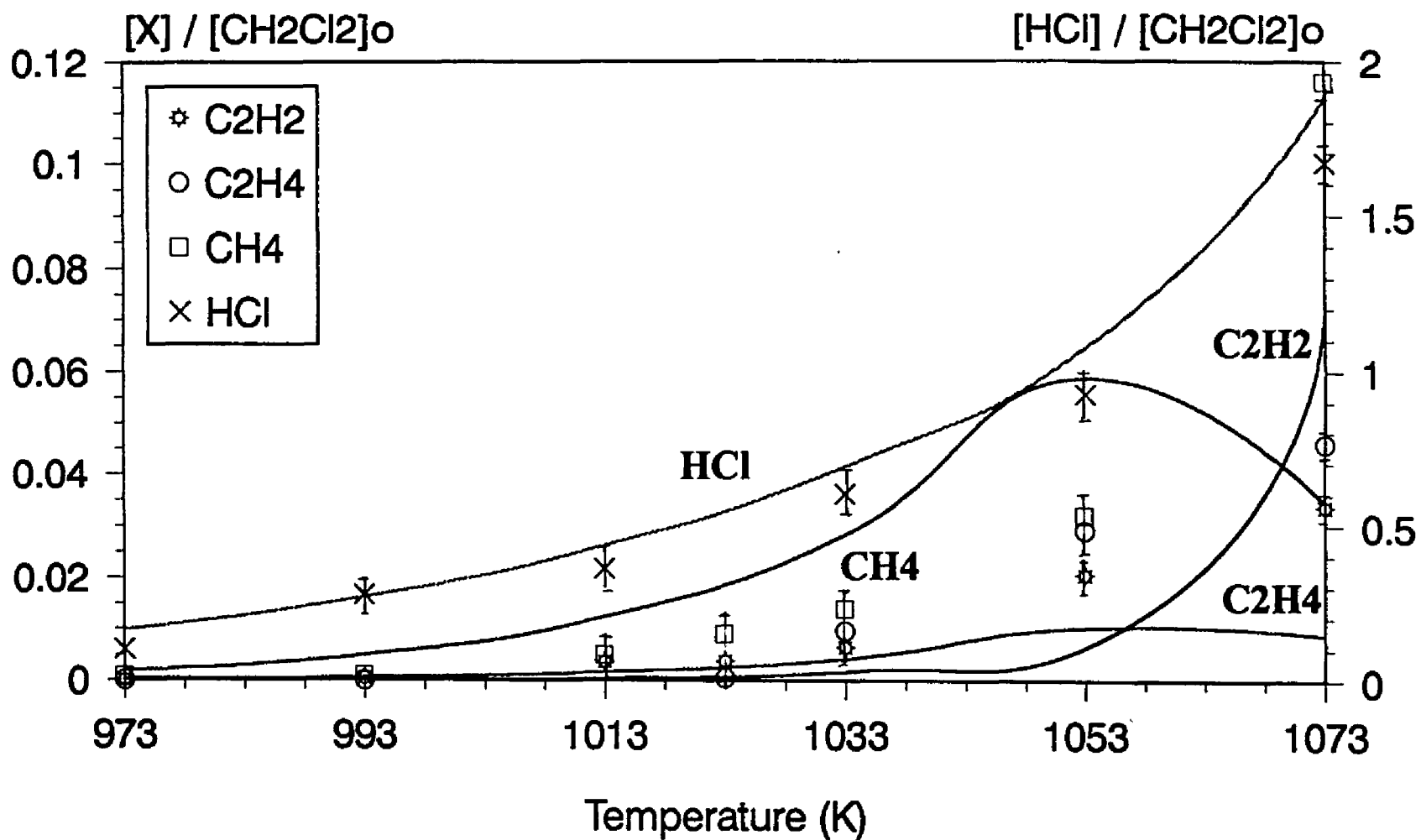


Fig 6.12 Comparison of calculated and experimental product distribution versus temperature. 1 sec. residence time, Reactant ratios:  $\text{O}_2:\text{H}_2:\text{CH}_2\text{Cl}_2:\text{Ar}=2:2:1:95$

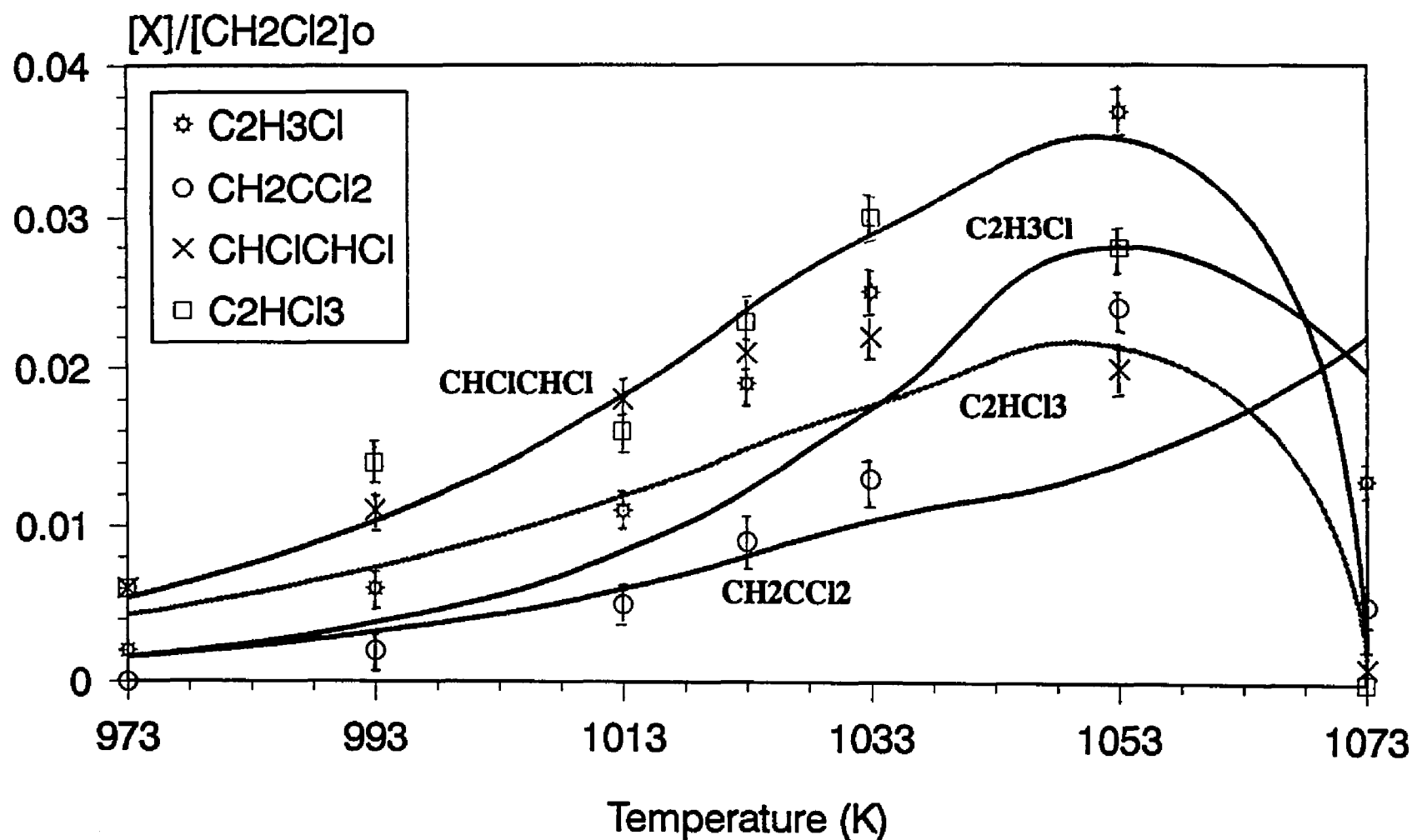


Fig 6.13 Comparison of calculated and experimental product distribution versus temperature. 1 sec. residence time, Reactant ratios:  $O_2:H_2:CH_2Cl_2:Ar=2:2:1:95$

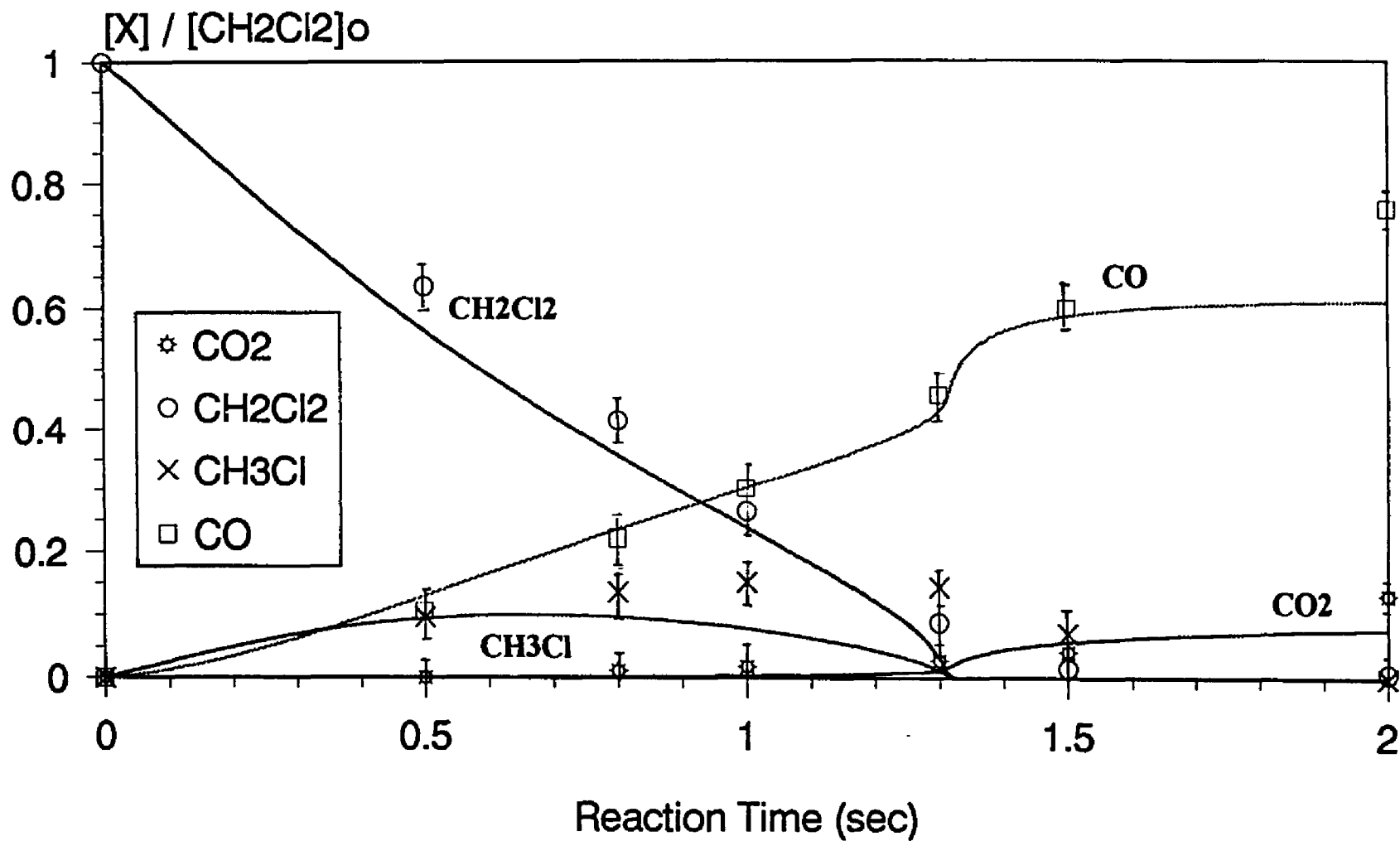


Fig 6.14 Comparison of calculated and experimental product distribution versus residence time at 1053K,  
Reactant ratios:  $\text{O}_2:\text{H}_2:\text{CH}_2\text{Cl}_2:\text{Ar}=2:2:1:95$

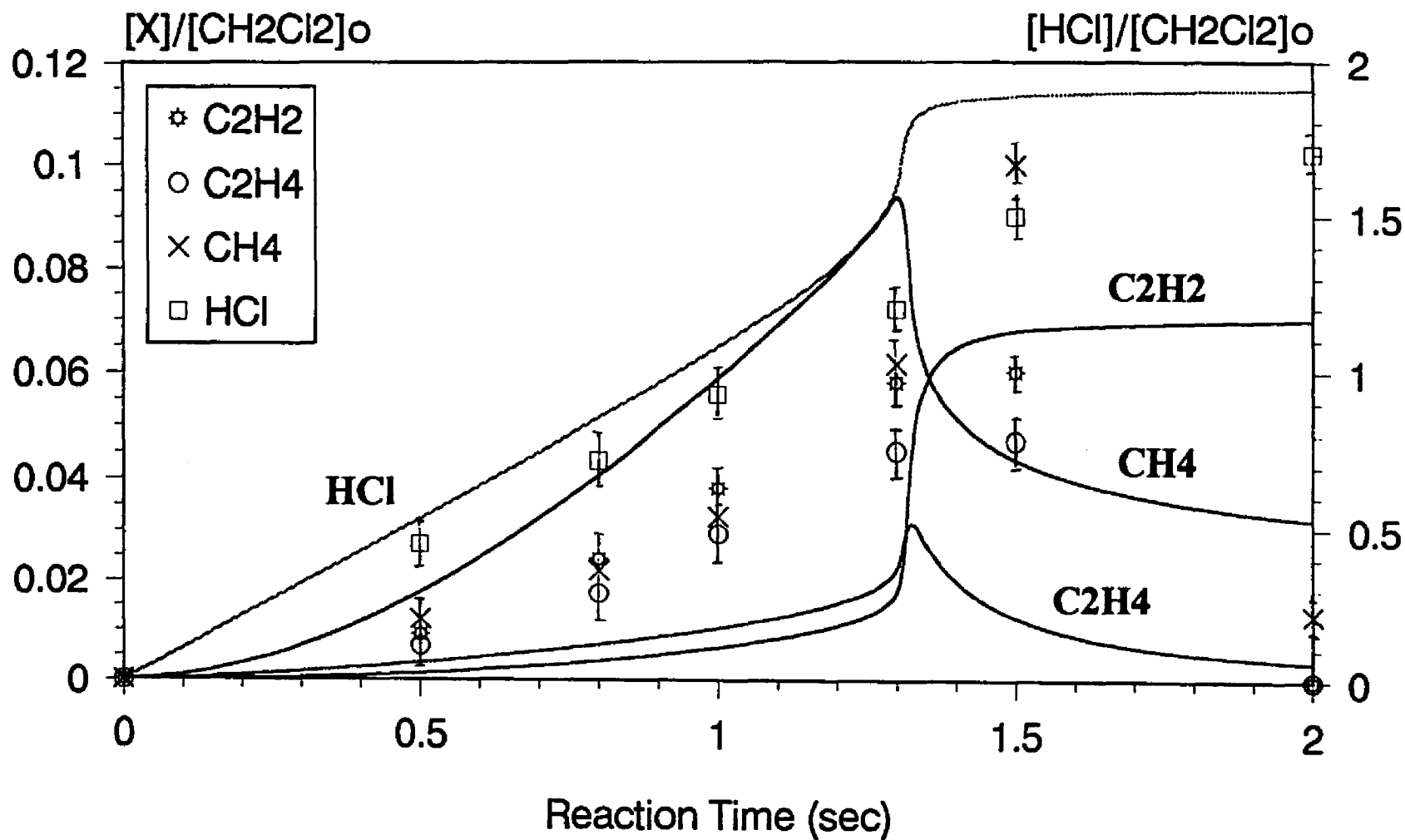


Fig 6.15 Comparison of calculated and experimental product distribution versus residence time at 1053K,  
Reactant ratios:  $\text{O}_2:\text{H}_2:\text{CH}_2\text{Cl}_2:\text{Ar}=2:2:1:95$

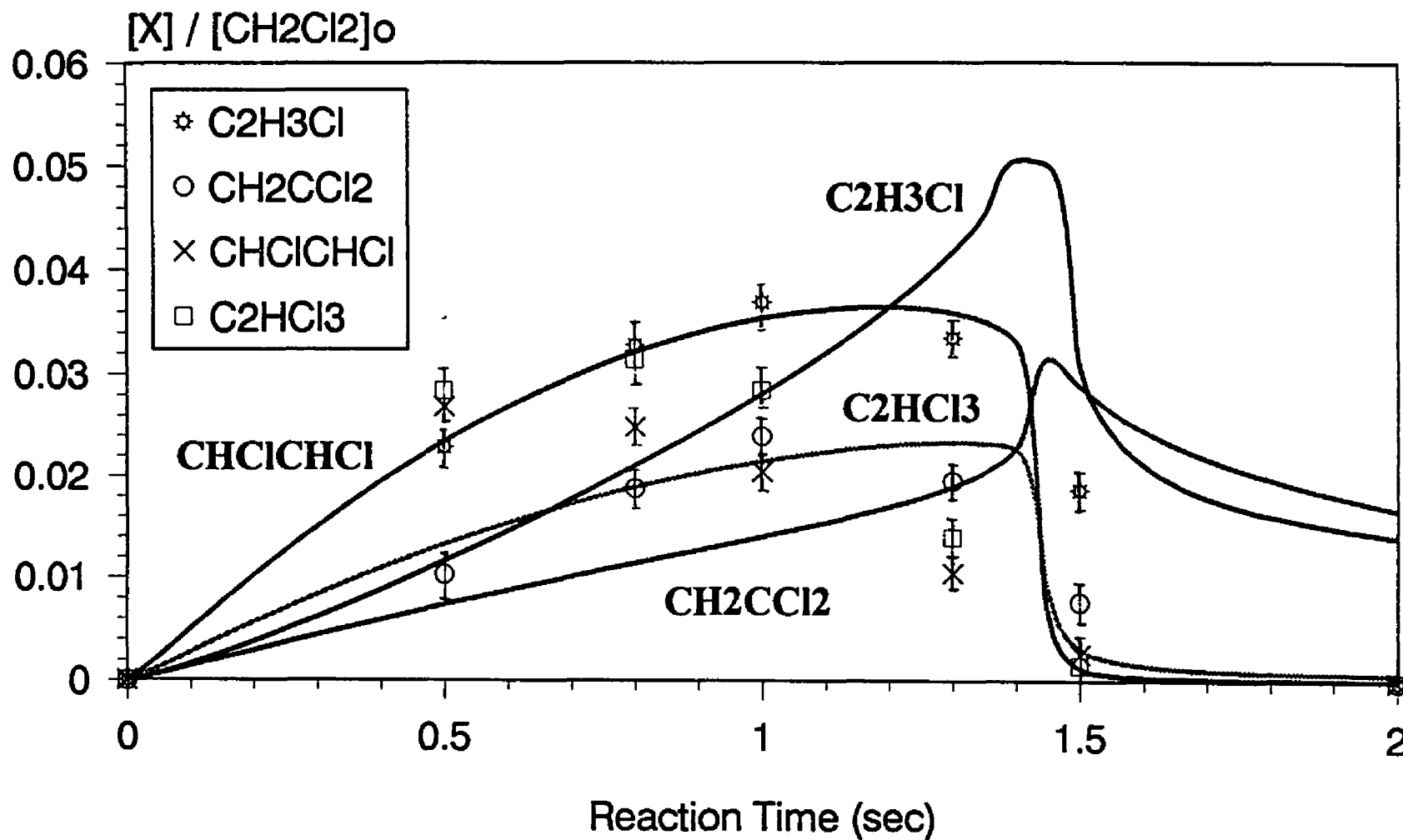
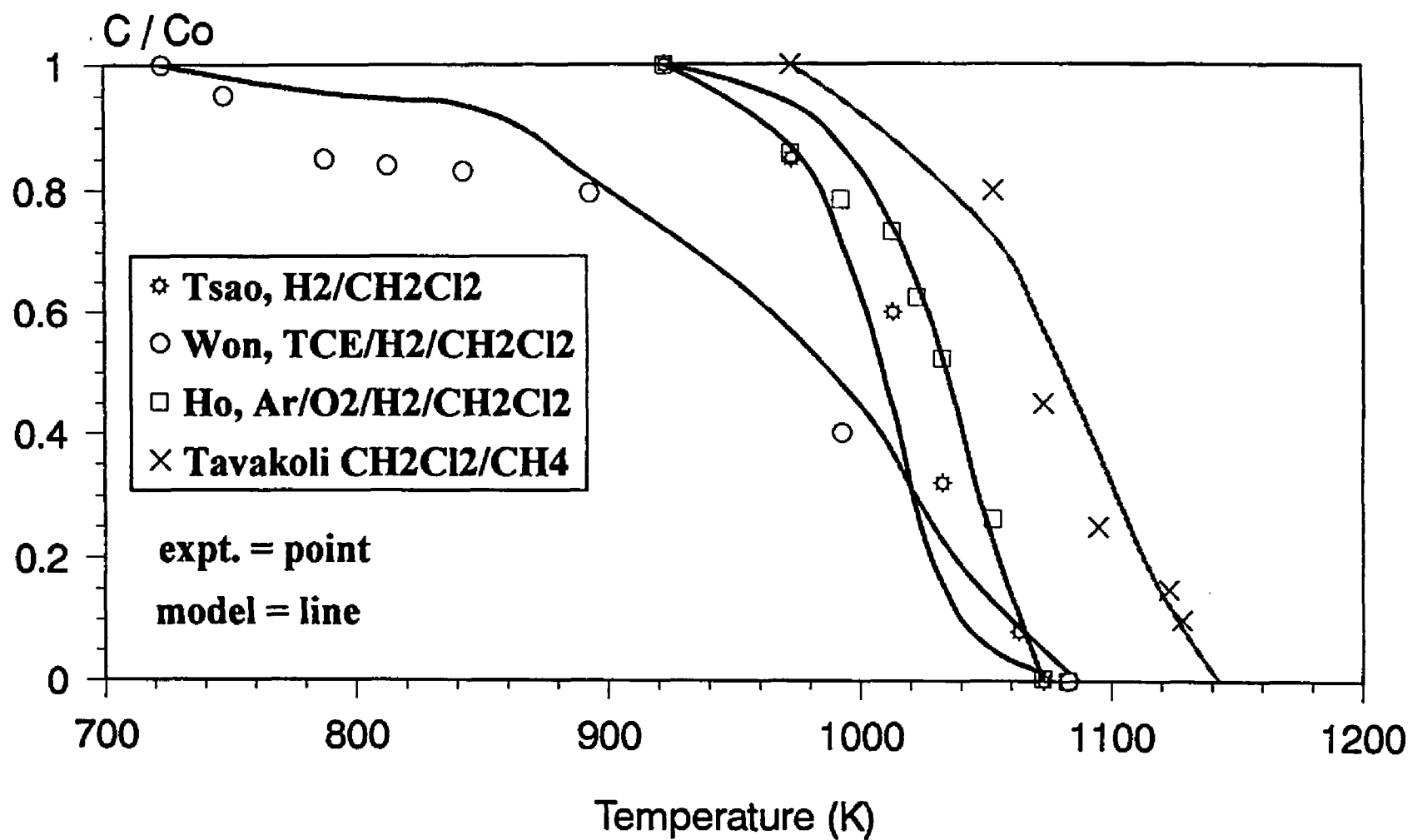


Fig 6.16 Comparison of calculated and experimental product distribution versus residence time at 1053K,  
Reactant ratios: O<sub>2</sub>:H<sub>2</sub>:CH<sub>2</sub>Cl<sub>2</sub>:Ar=2:2:1:95



**Fig 6.17 Comparison of experimental data and model predictions with data of other studies.**

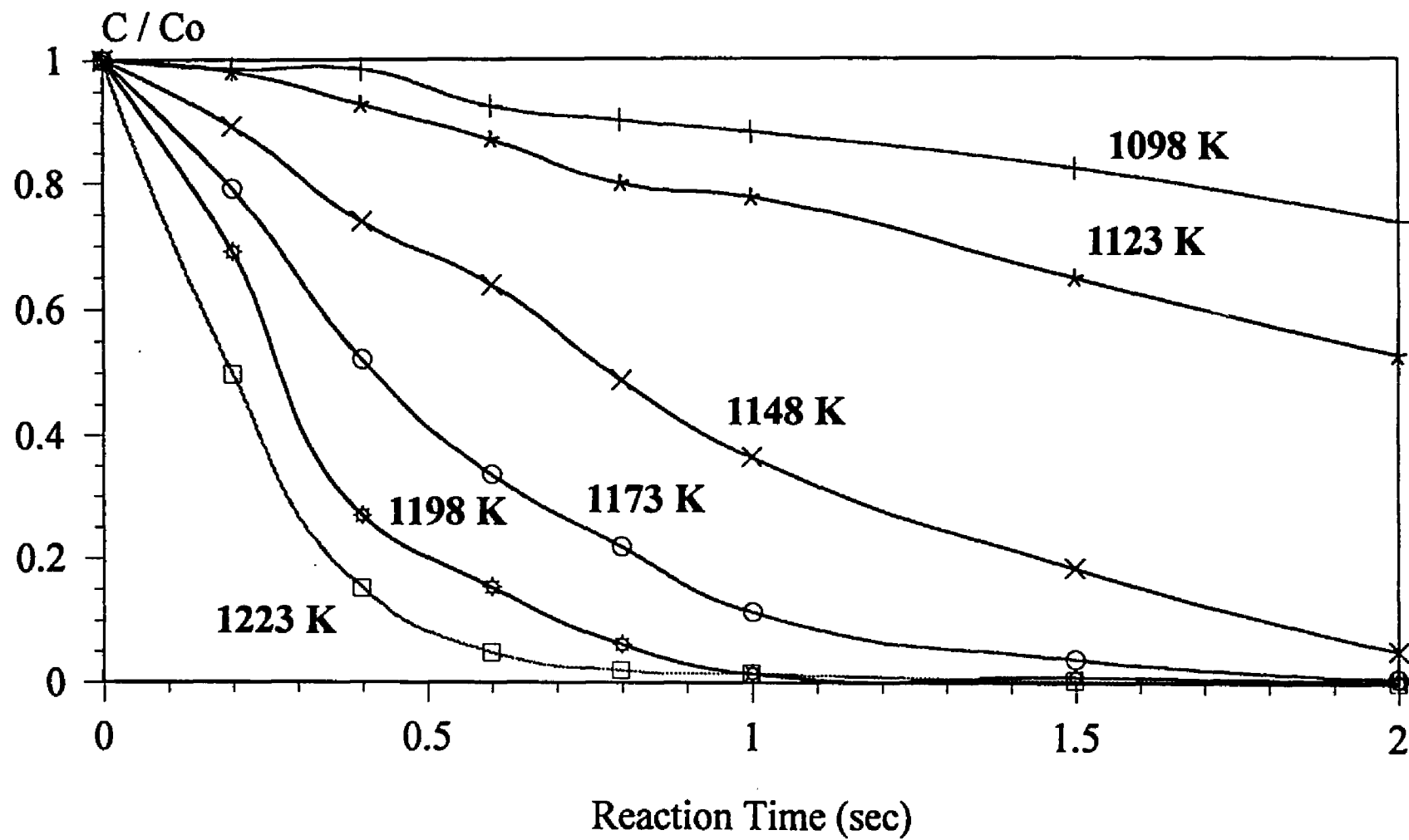


Fig 7.1 Conversion versus time at different temperature, Reactant ratios:  $O_2:H_2:CH_3Cl:Ar=1:1:2:96$

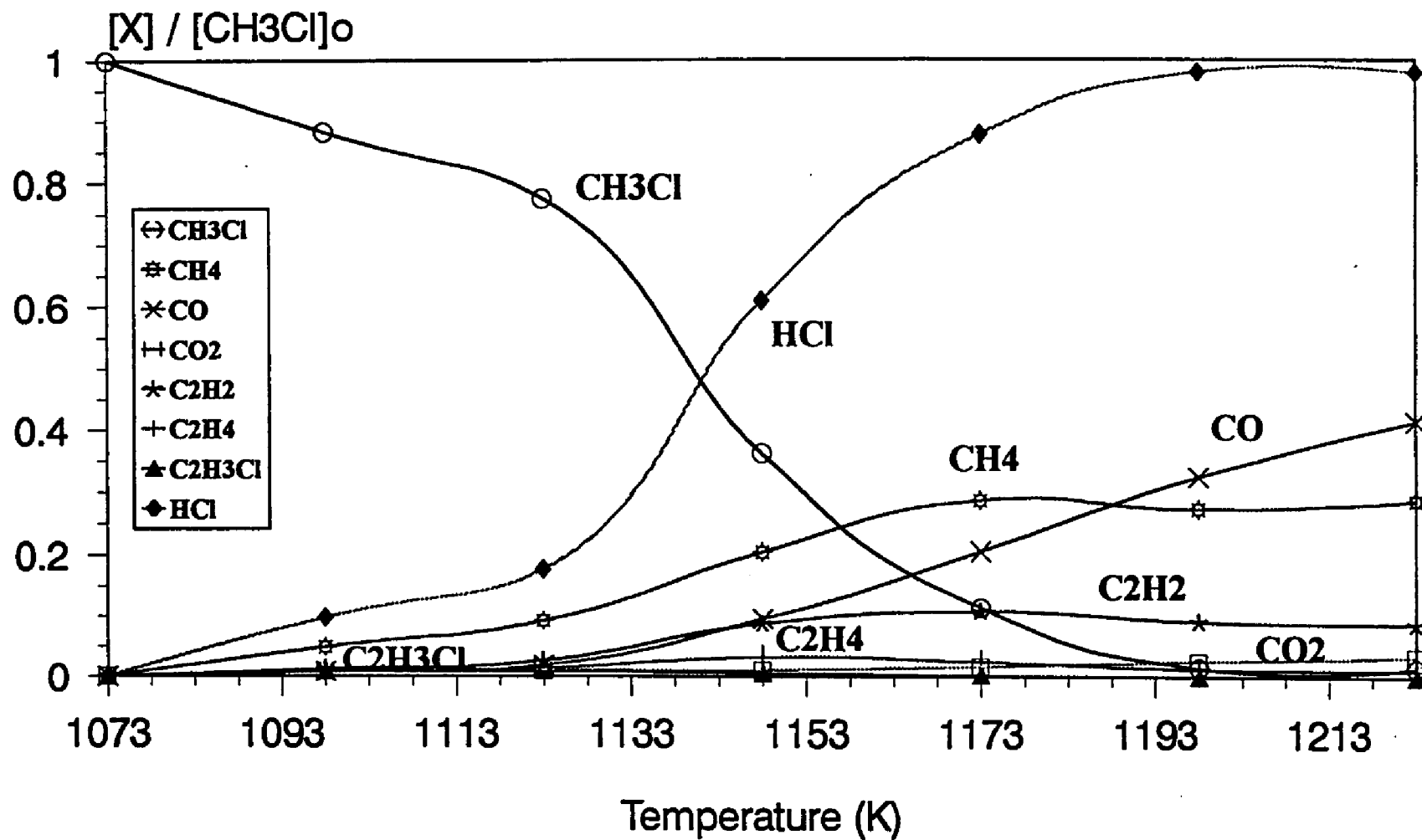


Fig 7.2 Product distribution for  $\text{CH}_3\text{Cl}$  decomposition versus temperature at 1 sec residence time.  
 Reactant ratios:  $\text{O}_2:\text{H}_2:\text{CH}_3\text{Cl}:\text{Ar}=1:1:2:96$



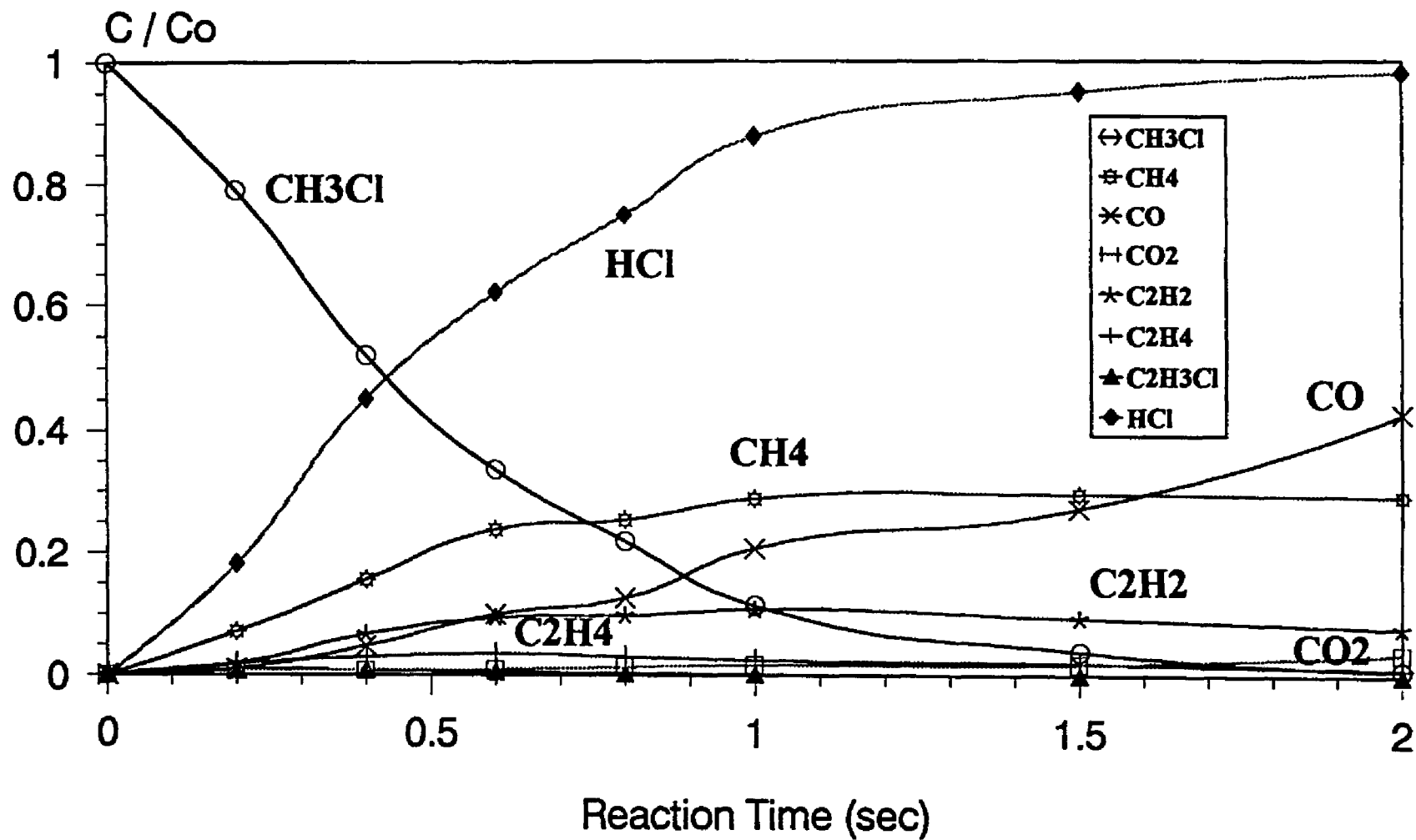


Fig 7.3 Product distribution for  $\text{CH}_3\text{Cl}$  decomposition versus residence time at 1148K.  
Reactant ratios:  $\text{O}_2:\text{H}_2:\text{CH}_3\text{Cl}:\text{Ar}=1:1:2:96$

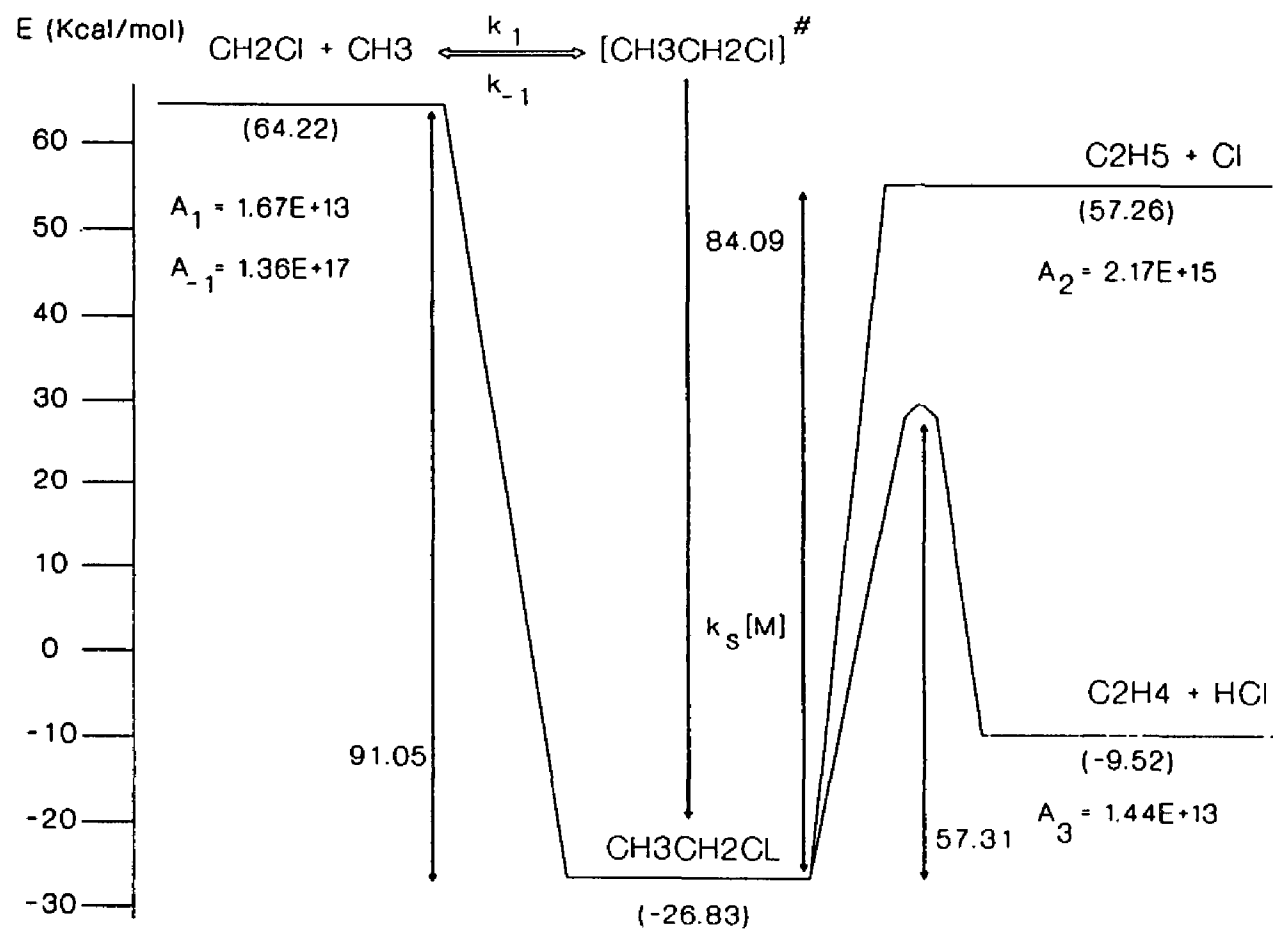


Fig 7.4 Energy Level for  $\text{CH}_2\text{Cl} + \text{CH}_3$  Reaction

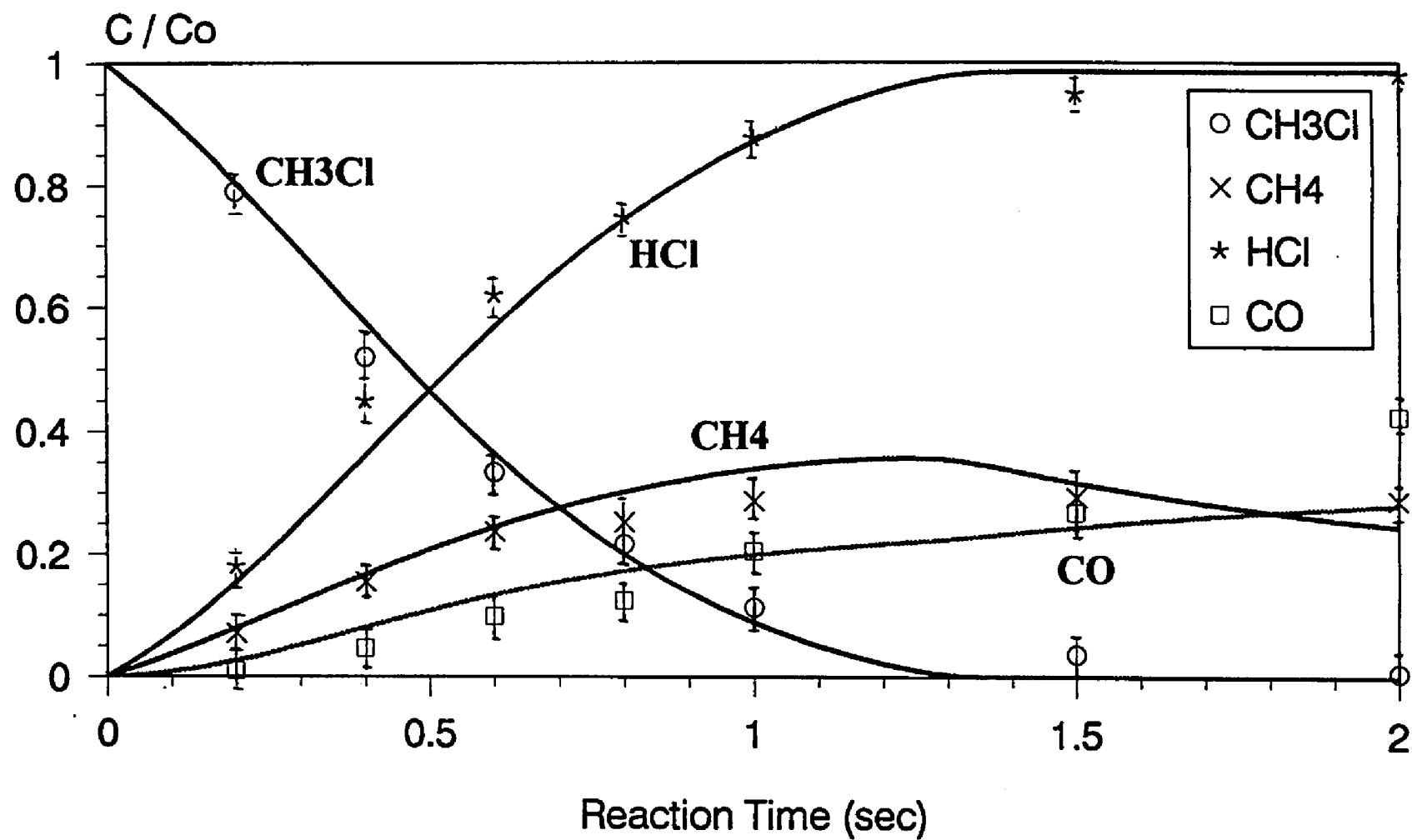


Fig 7.5 Comparison of calculated and experimental product distribution versus residence time at 1173K.  
 Reactant ratios:  $O_2:H_2:CH_3Cl:Ar=1:1:2:96$

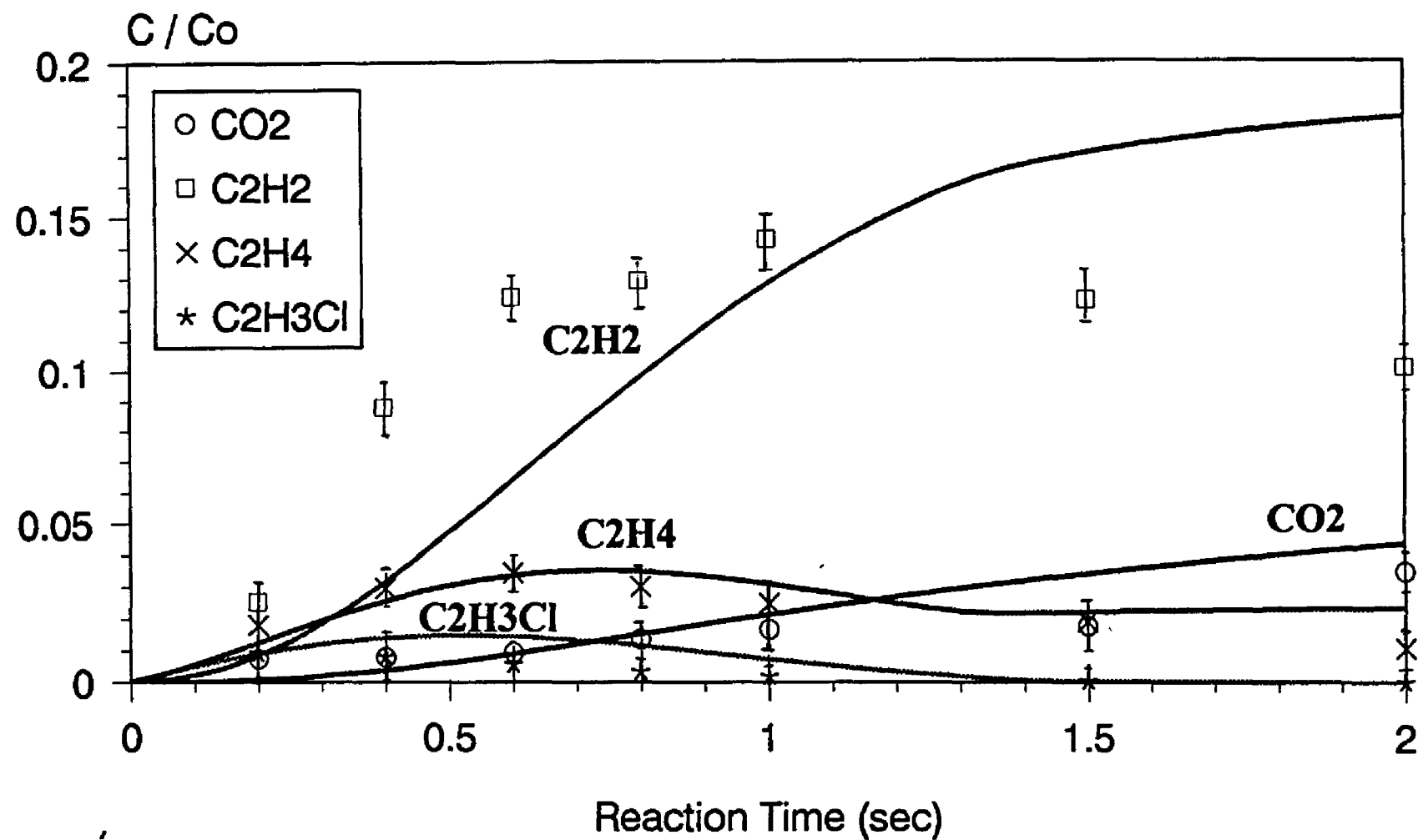


Fig 7.6 Comparison of calculated and experimental product distribution versus residence time at 1173K.  
 Reactant ratios:  $\text{O}_2:\text{H}_2:\text{CH}_3\text{Cl}:\text{Ar}=1:1:2:96$

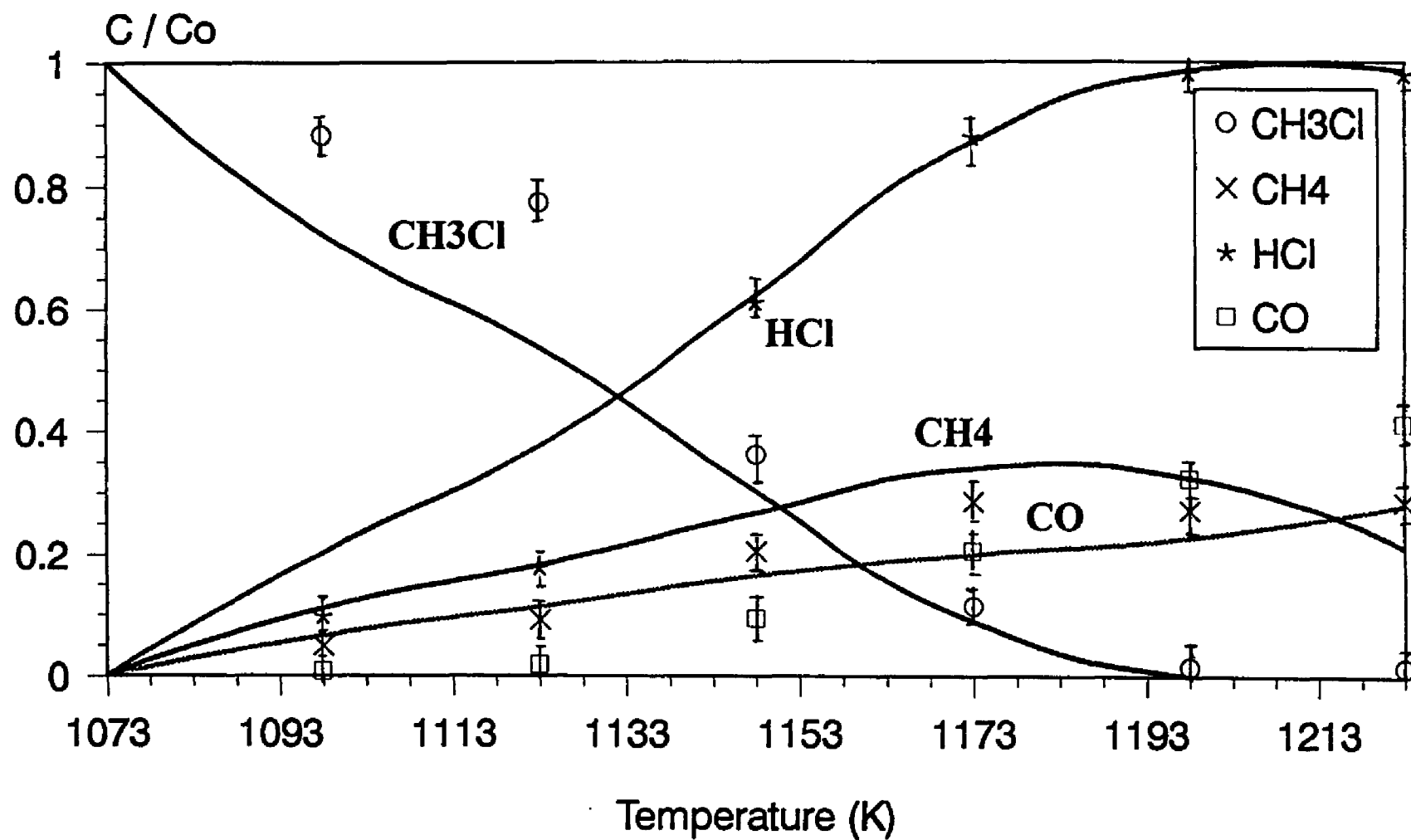


Fig 7.7 Comparison of calculated and experimental product distribution versus temperature at 1 sec. residence time.  
 Reactant ratios:  $\text{O}_2:\text{H}_2:\text{CH}_3\text{Cl}:\text{Ar}=1:1:2:96$

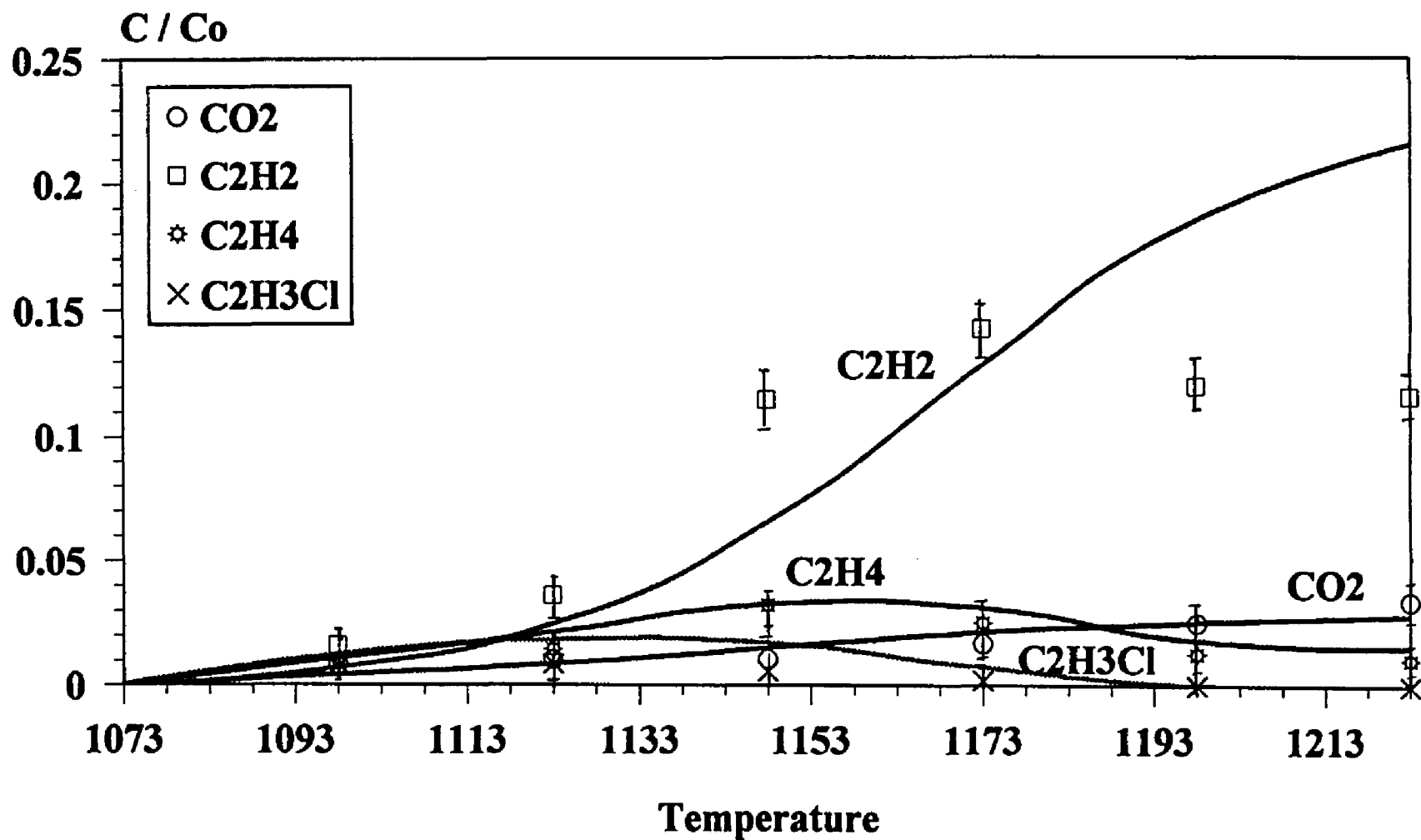


Fig 7.8 Comparison of calculated and experimental product distribution versus temperature at 1 sec. residence time.  
 Reactant ratios:  $\text{O}_2:\text{H}_2:\text{CH}_3\text{Cl}:\text{Ar}=1:1:2:96$

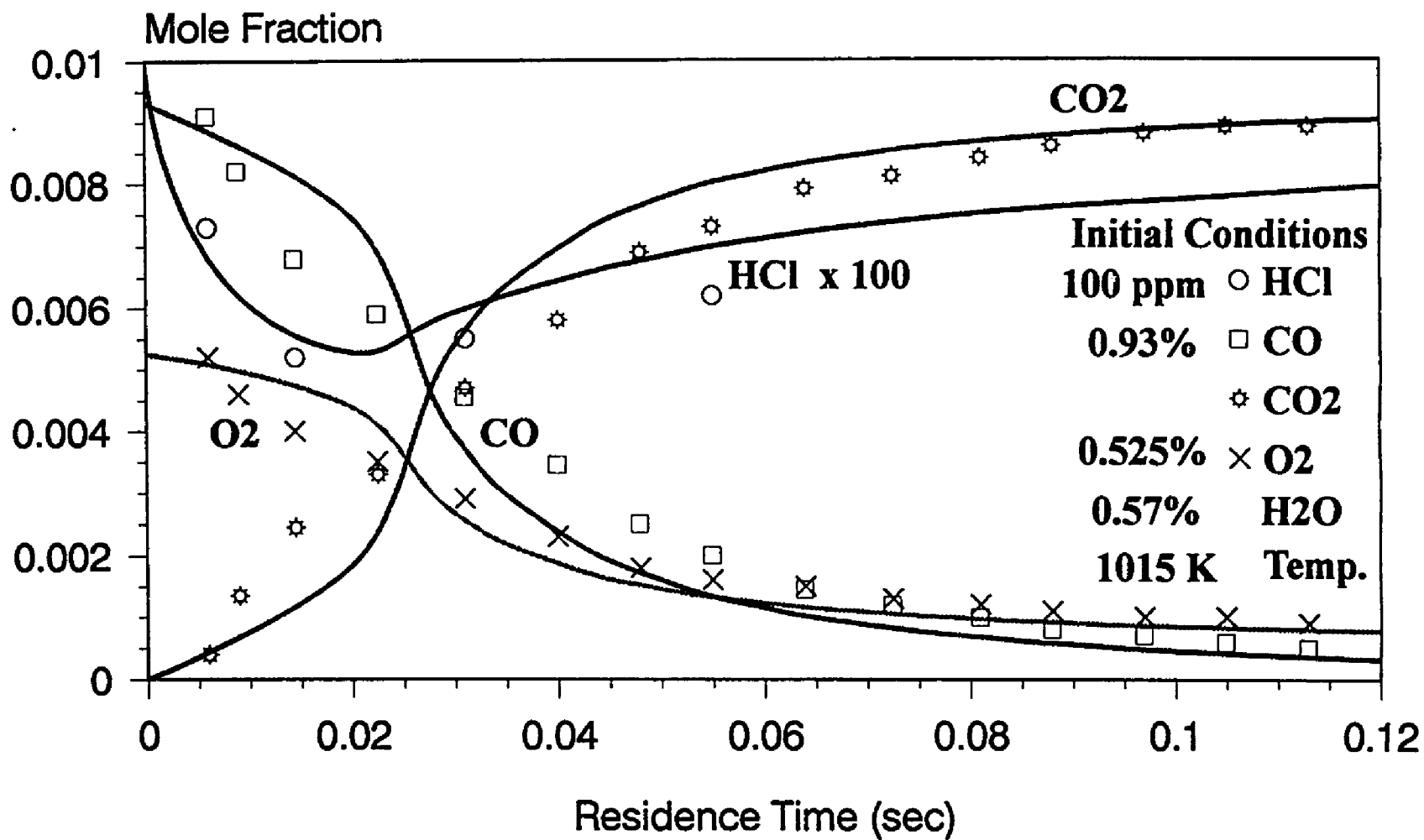


Fig 7.9 Comparison of our model with Princeton experimental data using temperature profile of princeton flow reactor.

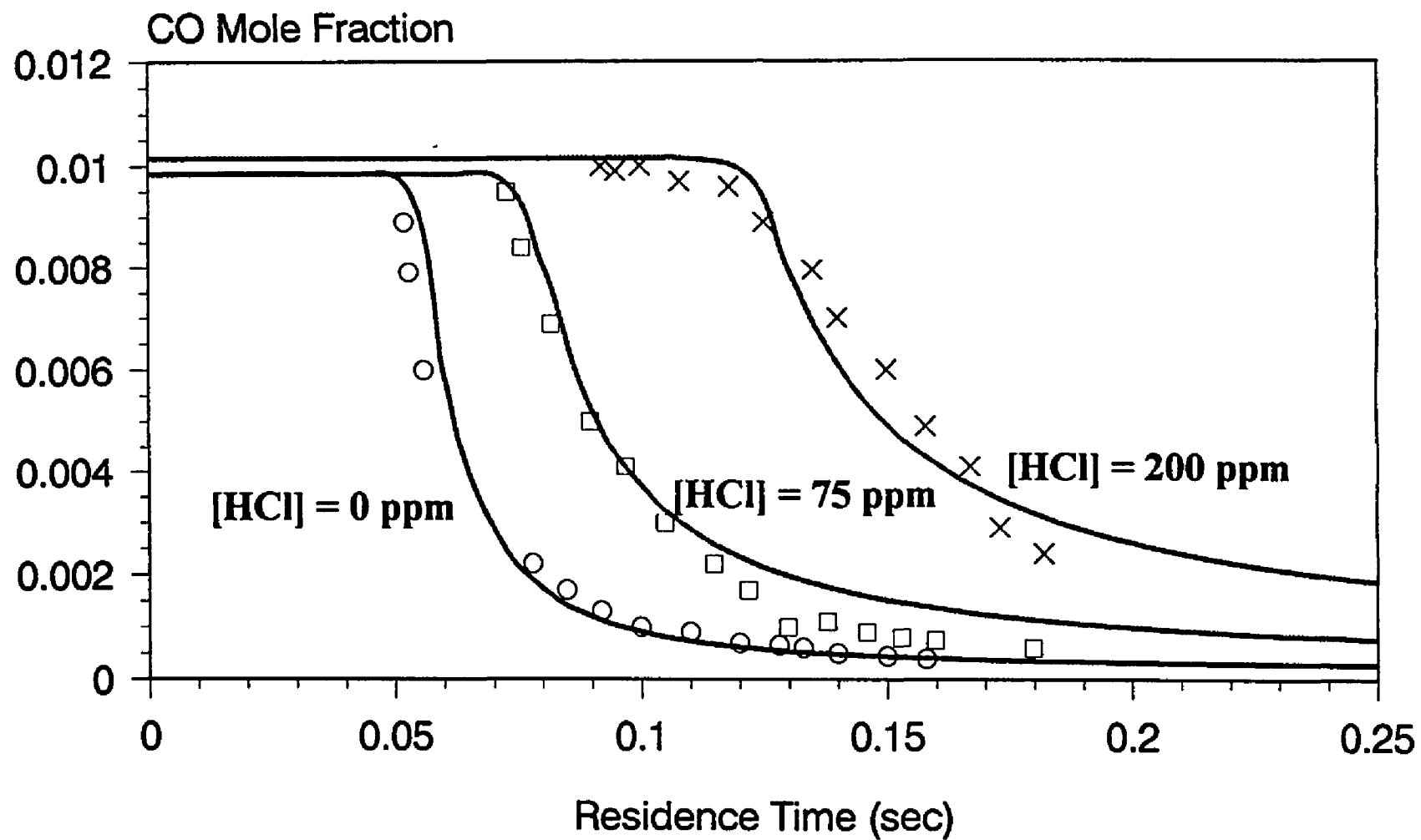


Fig 7.10 Comparison of model and experimental data for CO oxidation with different HCl concentration added.



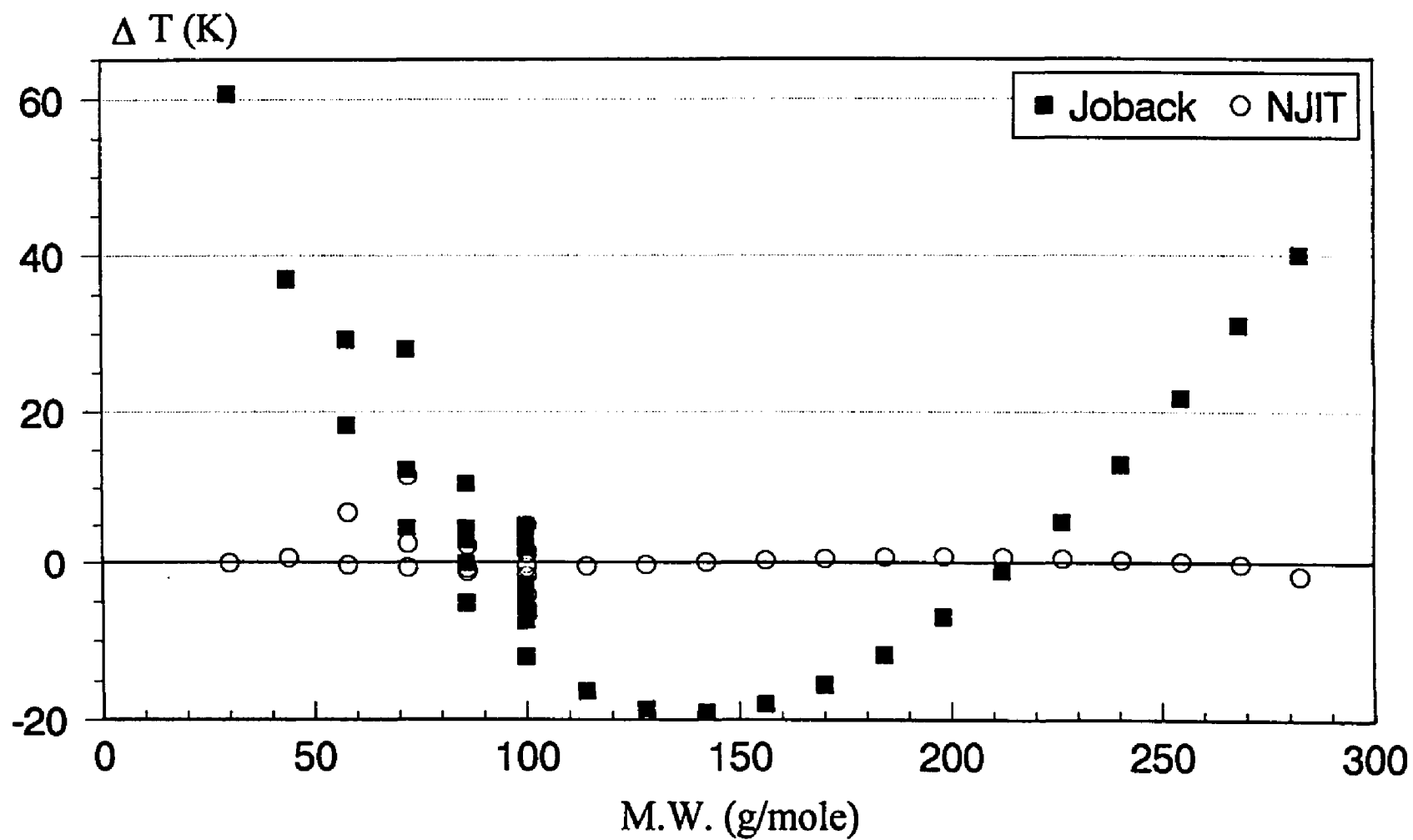


Fig 8.1 Plot of Residuals on Tb of Alkanes

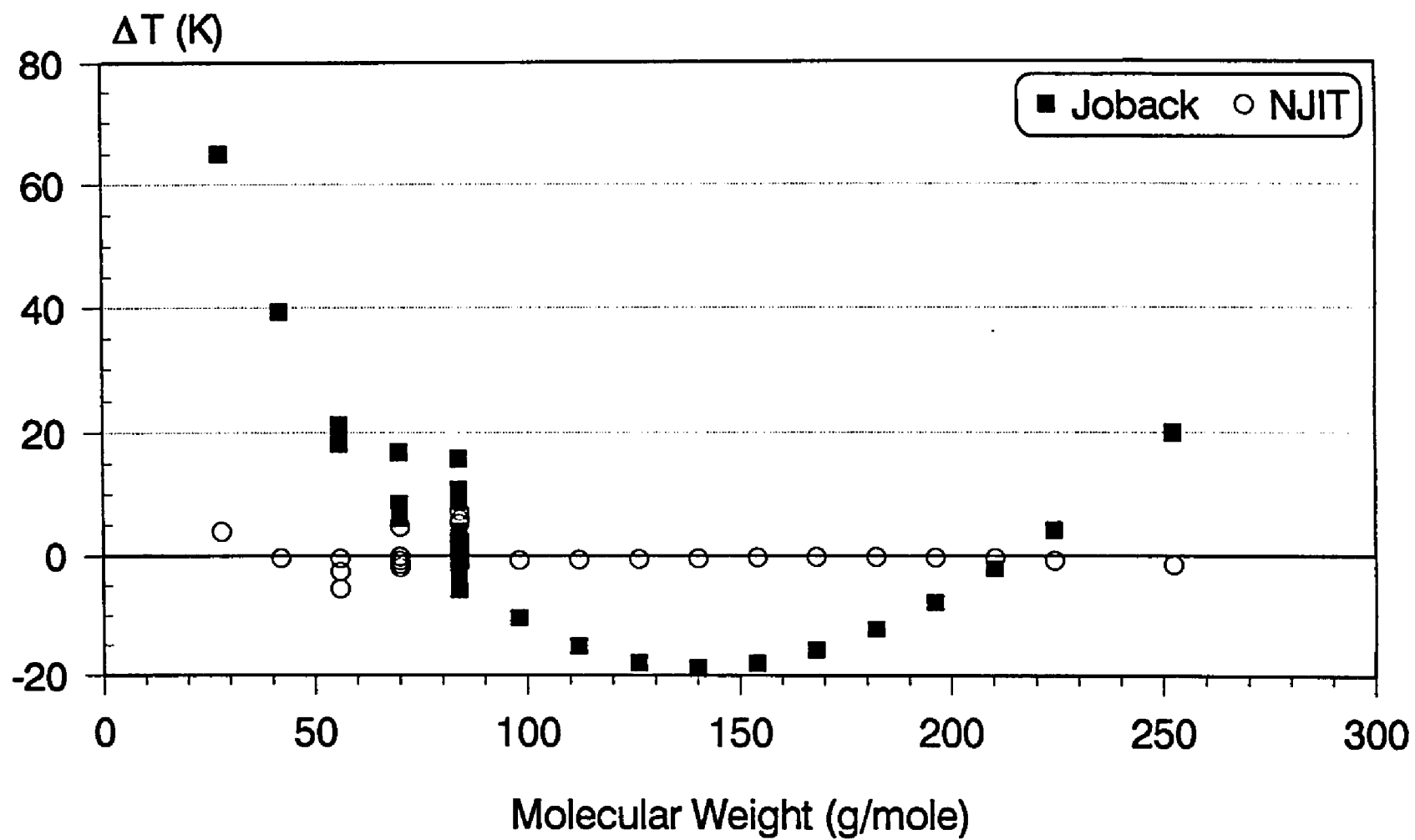


Fig 8.2 Plot of Residuals on Tb of Alkenes

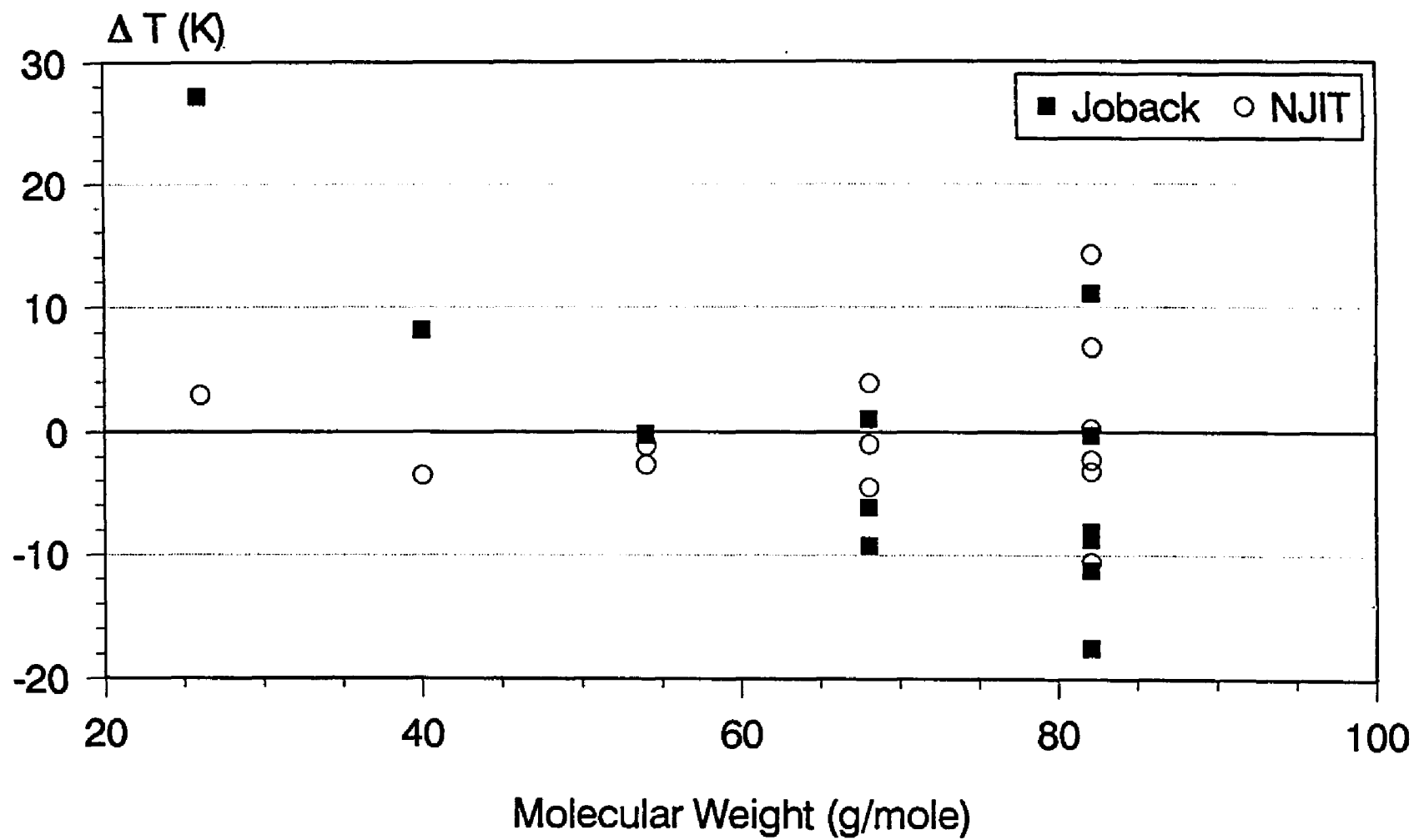


Fig 8.3 Plot of Residuals on Tb of Alkynes

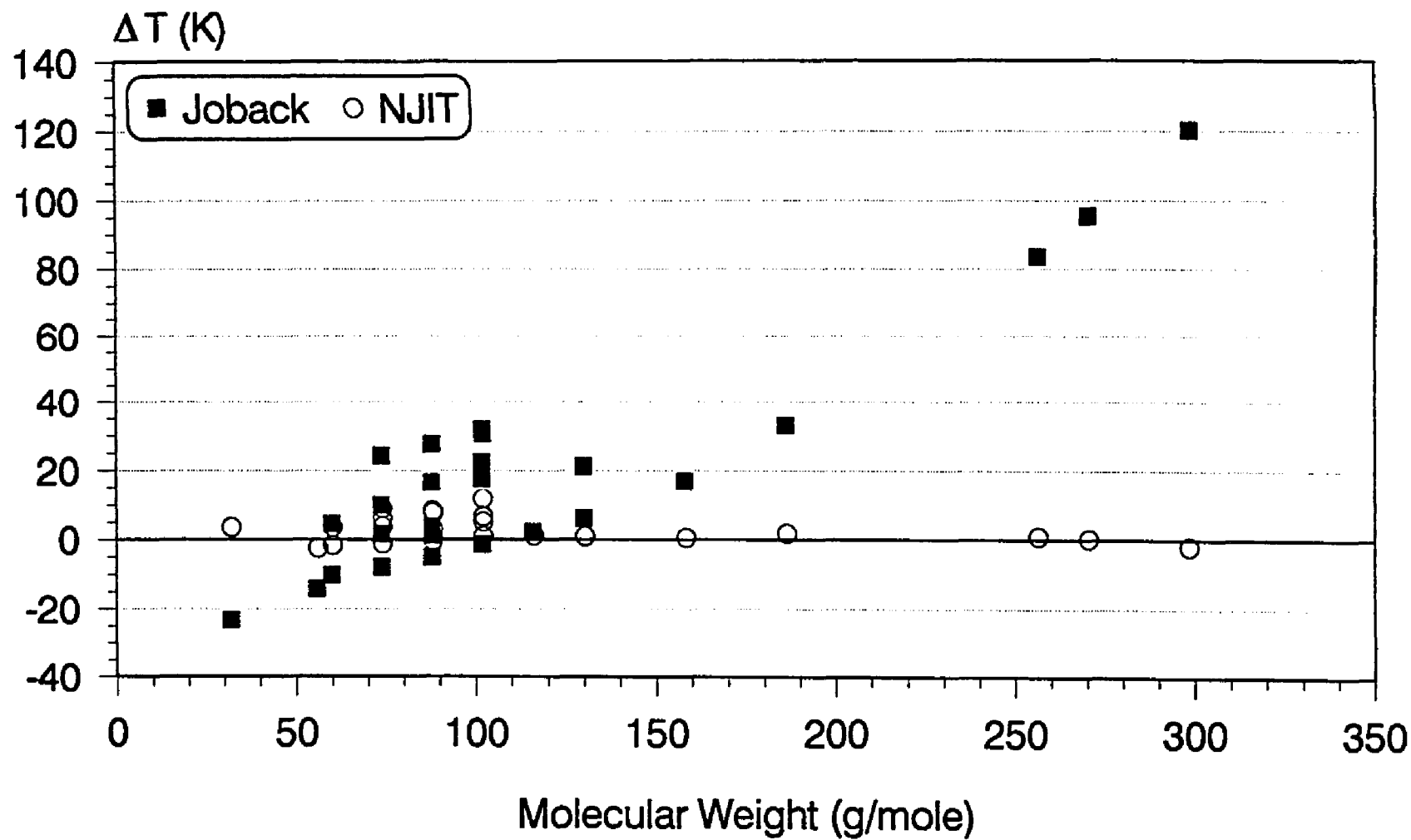


Fig 8.4 Plot of Residuals on Tb of Alcohols

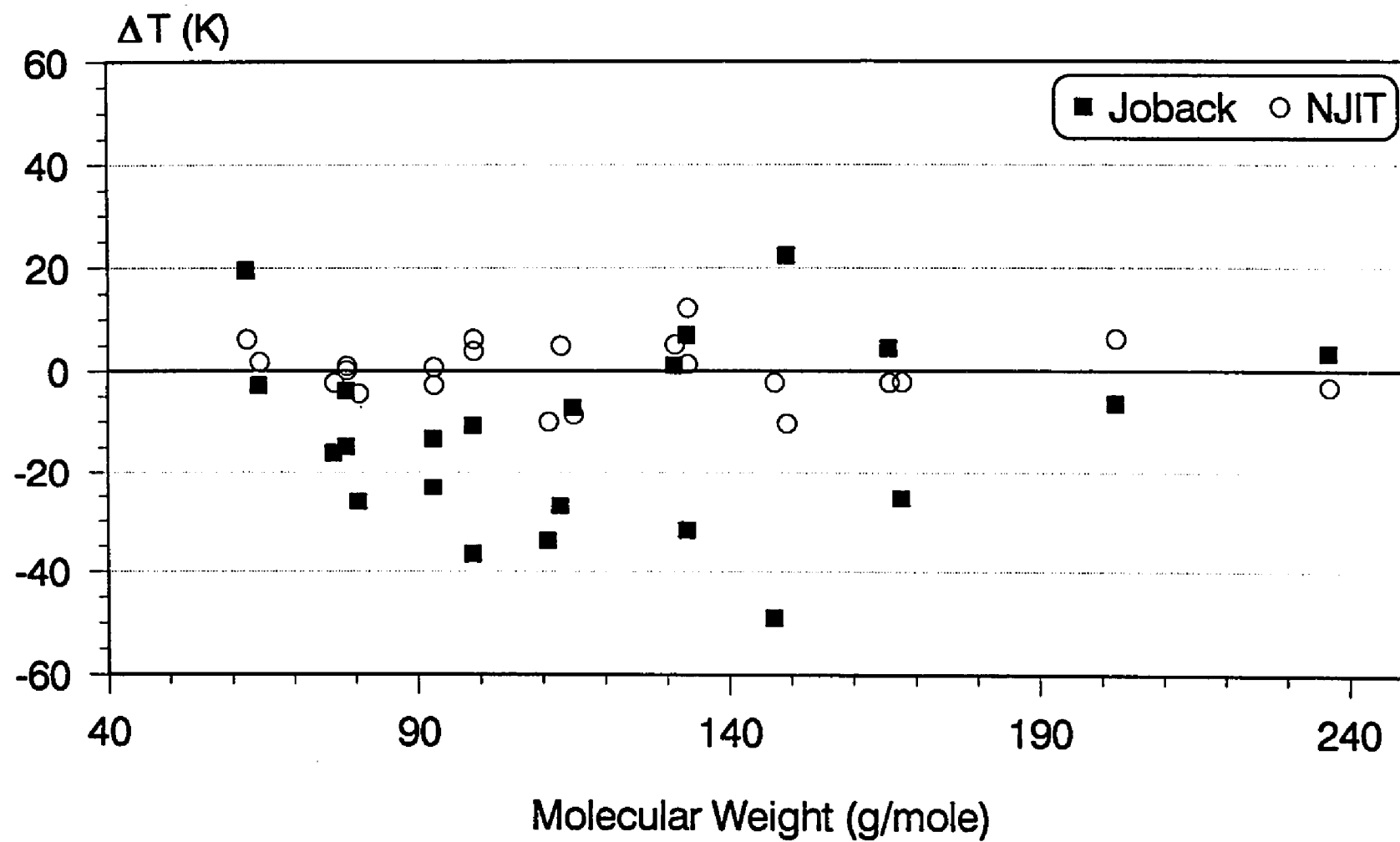


Fig 8.5 Plot of Residuals on Tb of Chlorocarbons

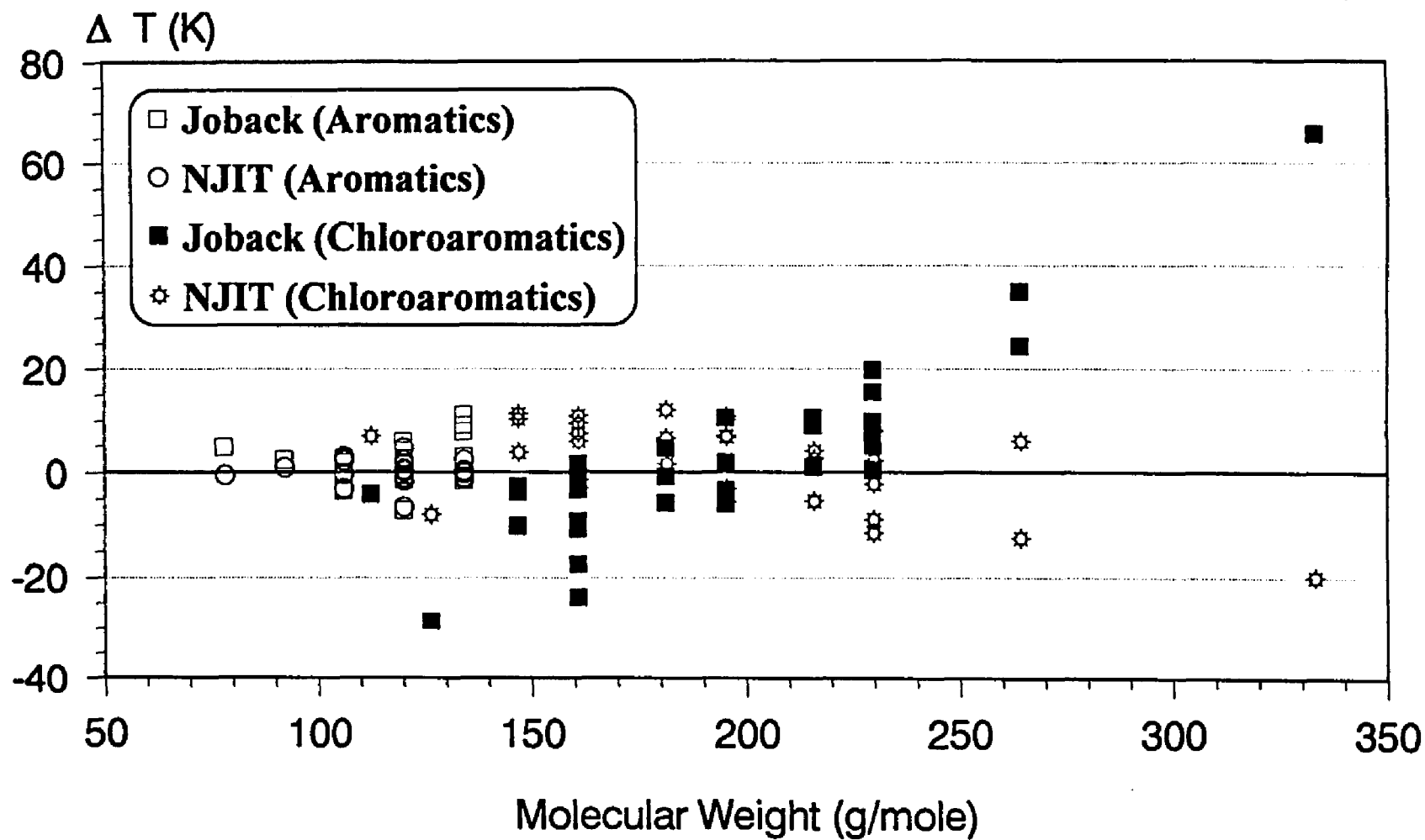


Fig 8.6 Plot of residuals on Tb of Aromatics

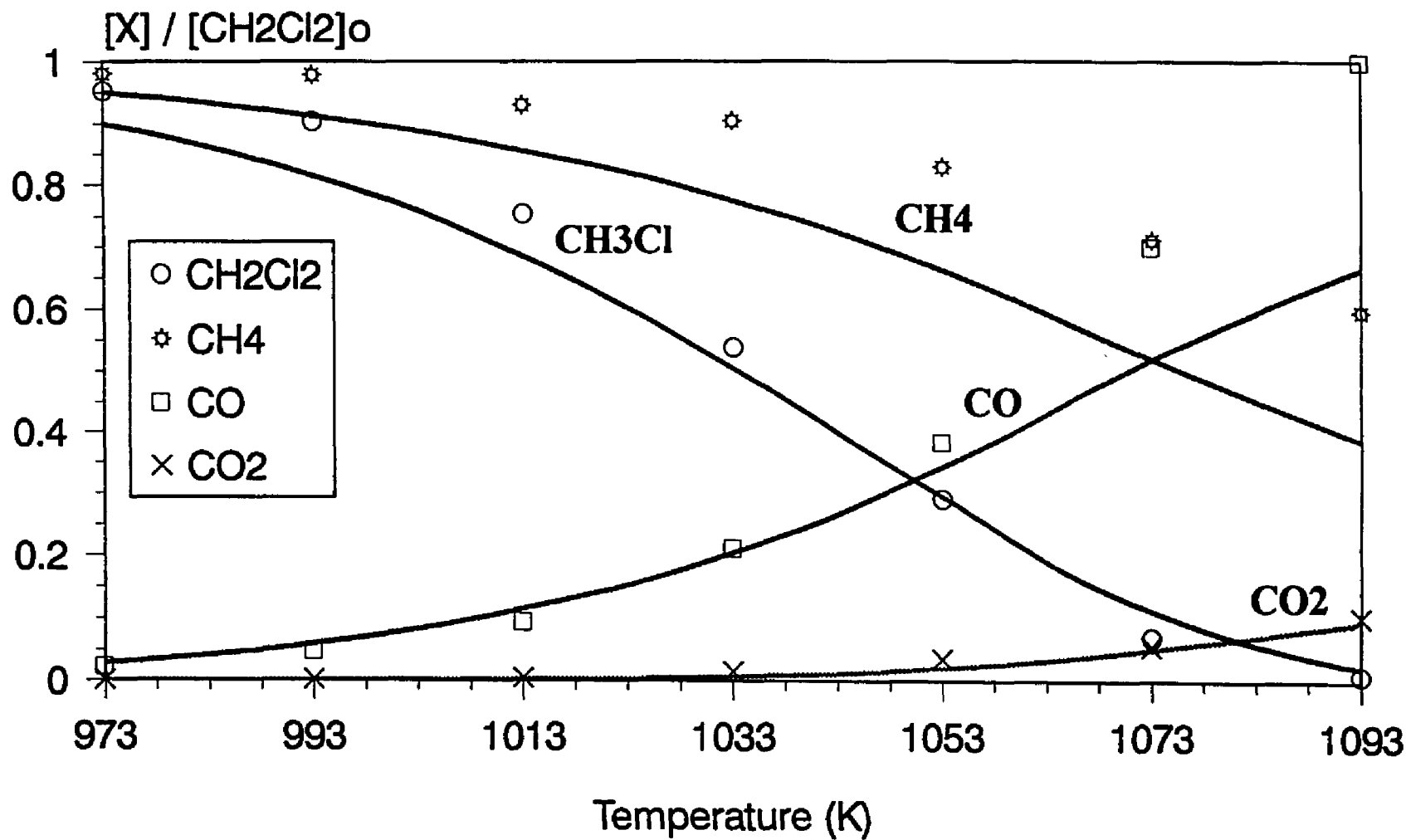
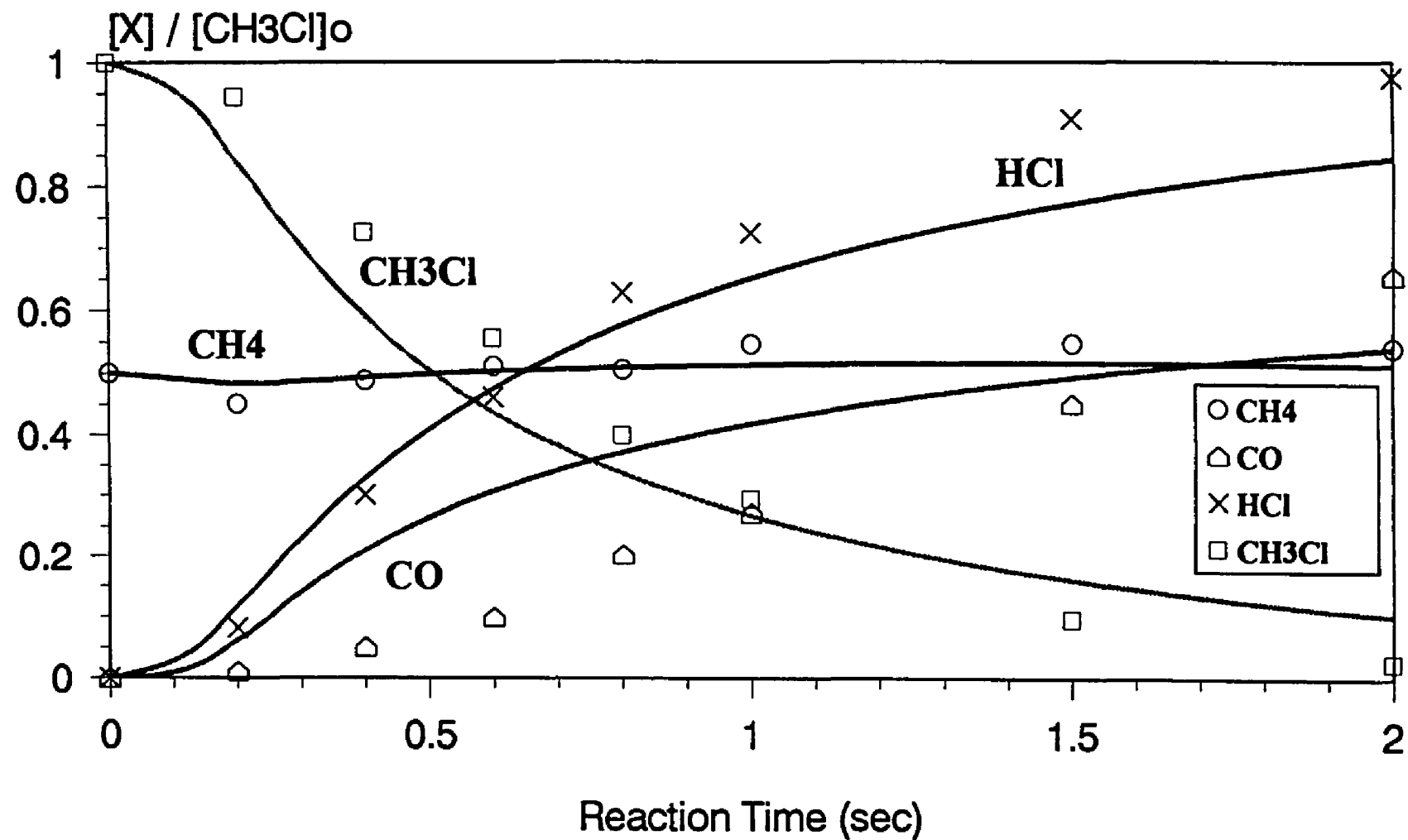


Fig 9.1 Comparison of calculated and experimental product distribution versus temperature at 1 sec. residence time.  
Reactant ratios:  $\text{O}_2:\text{CH}_4:\text{CH}_2\text{Cl}_2:\text{Ar}=4:1:1:94$



**Fig 9.2 Comparison of calculated and experimental product distribution versus residence time at 1173K.**  
**Reactant ratios:  $O_2:CH_4:CH_3Cl:Ar=2:1:2:95$**



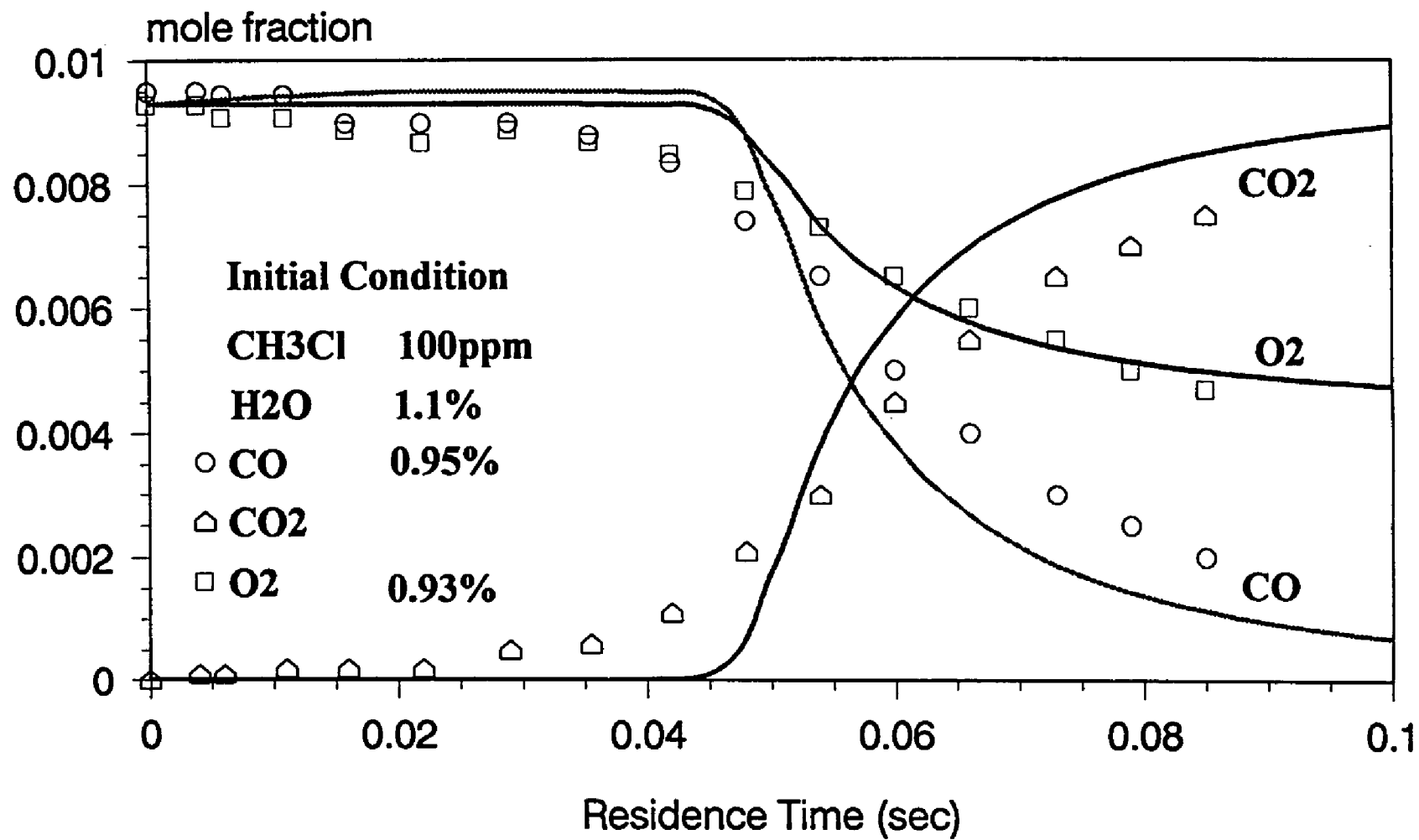
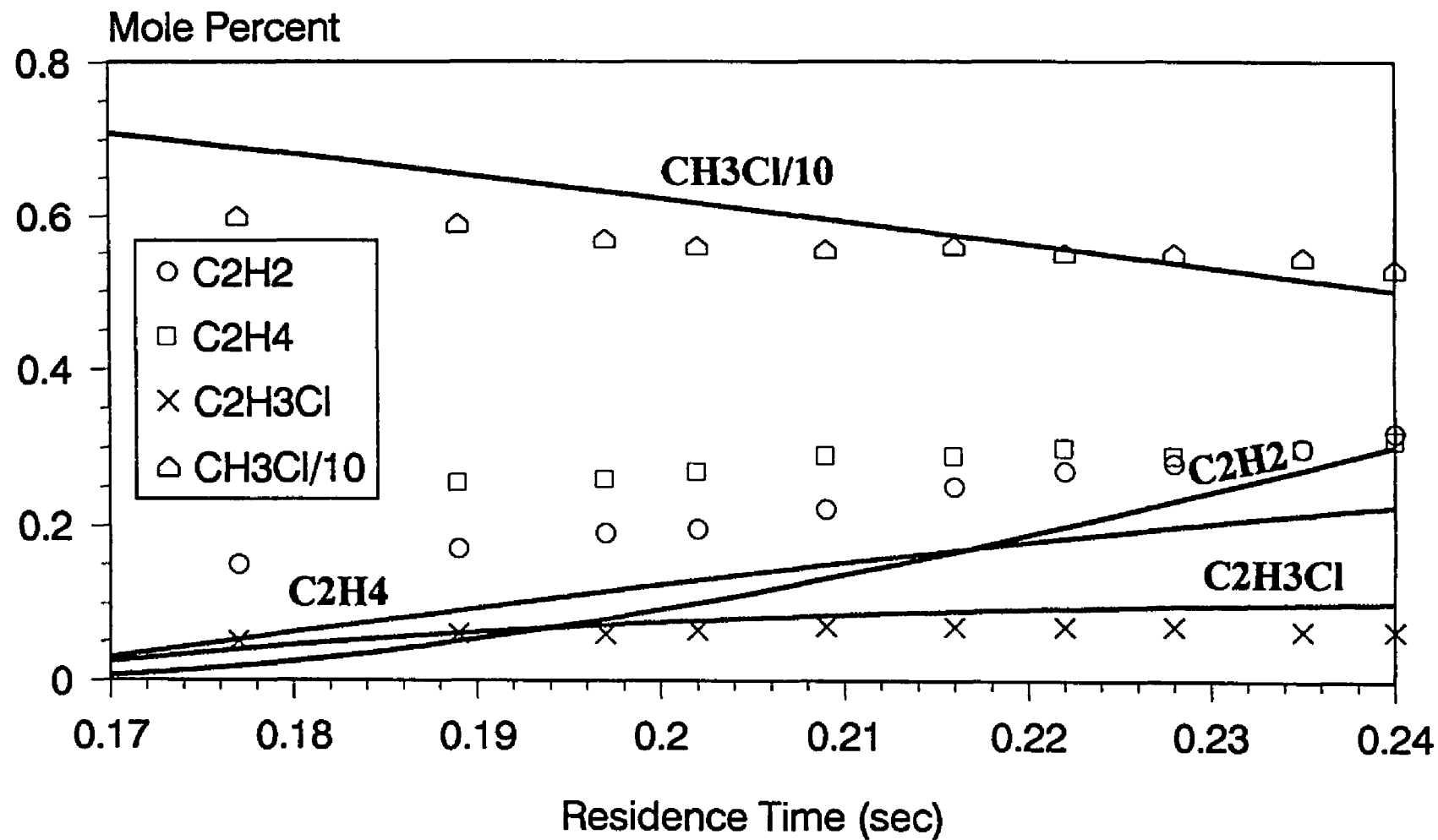


Fig 9.3 Comparison of our model with Roesler et al. experimental data.



**Fig 9.4 Comparison of calculated and experimental product distribution versus residence time at 1253K.**  
**Reactant ratios: O<sub>2</sub>:CH<sub>3</sub>Cl:Ar=2.05:7.32:90.6**

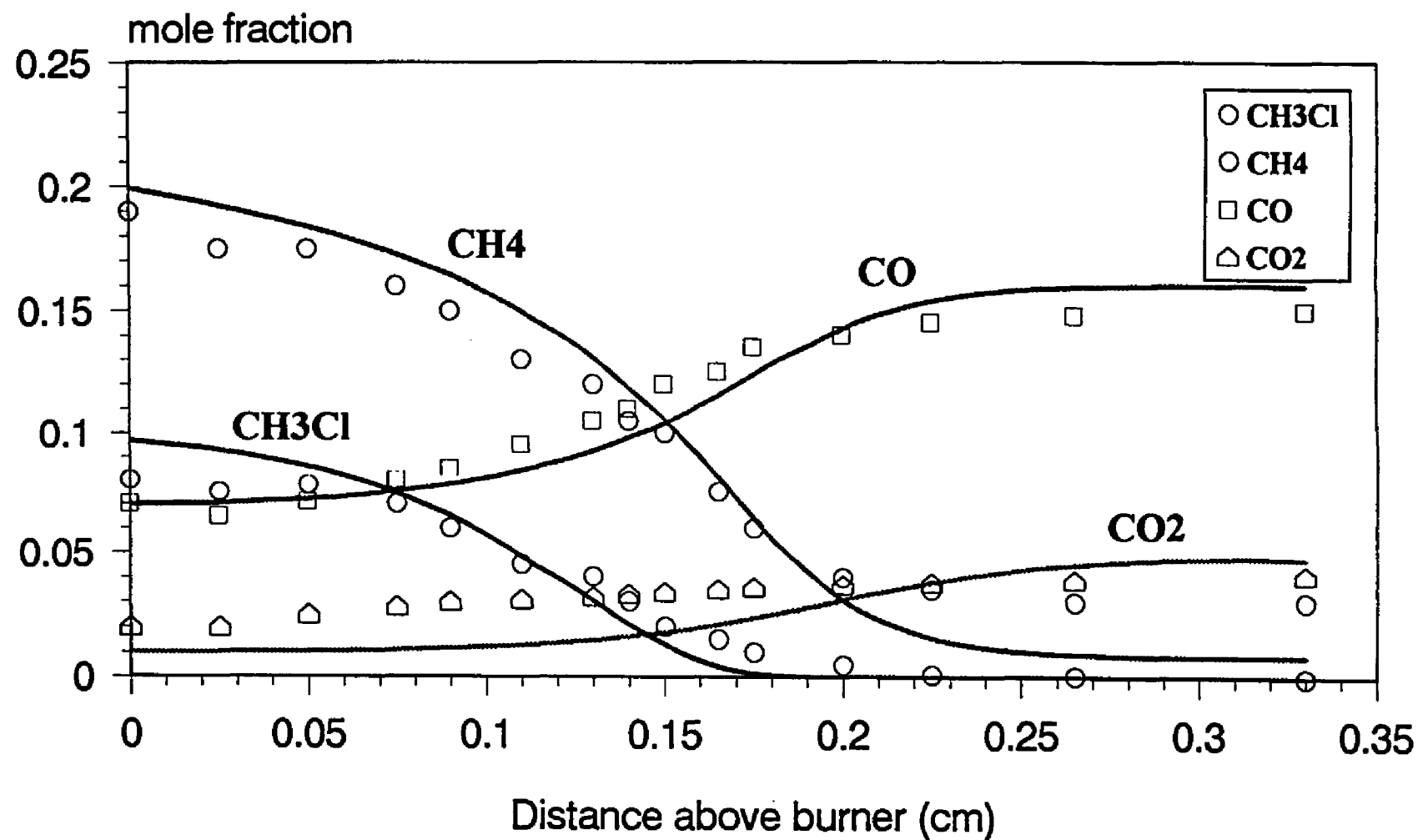


Fig 9.5 Comparison of our model with Karra et al. flame data

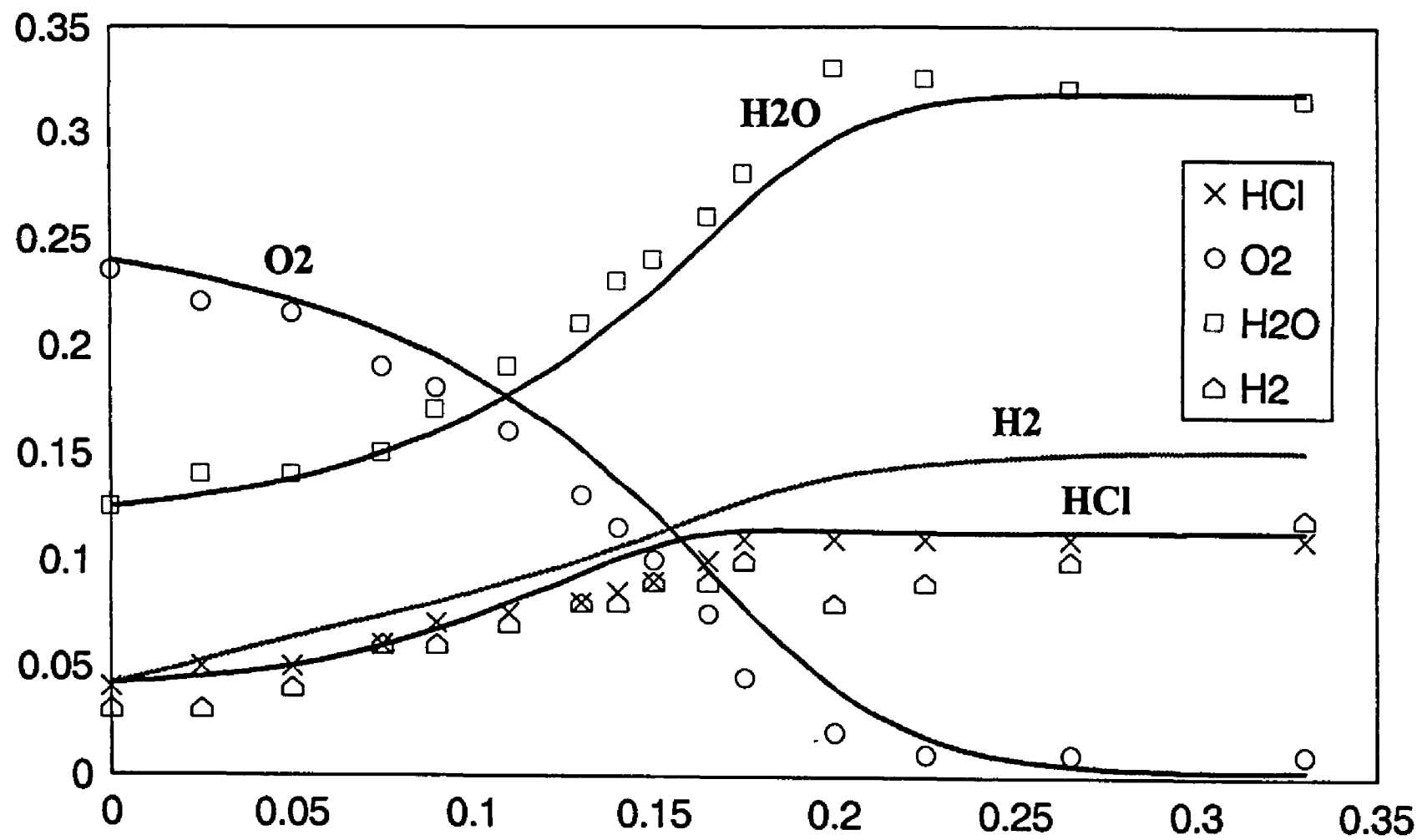


Fig 9.6 Comparison of our model with Karra et al. flame data

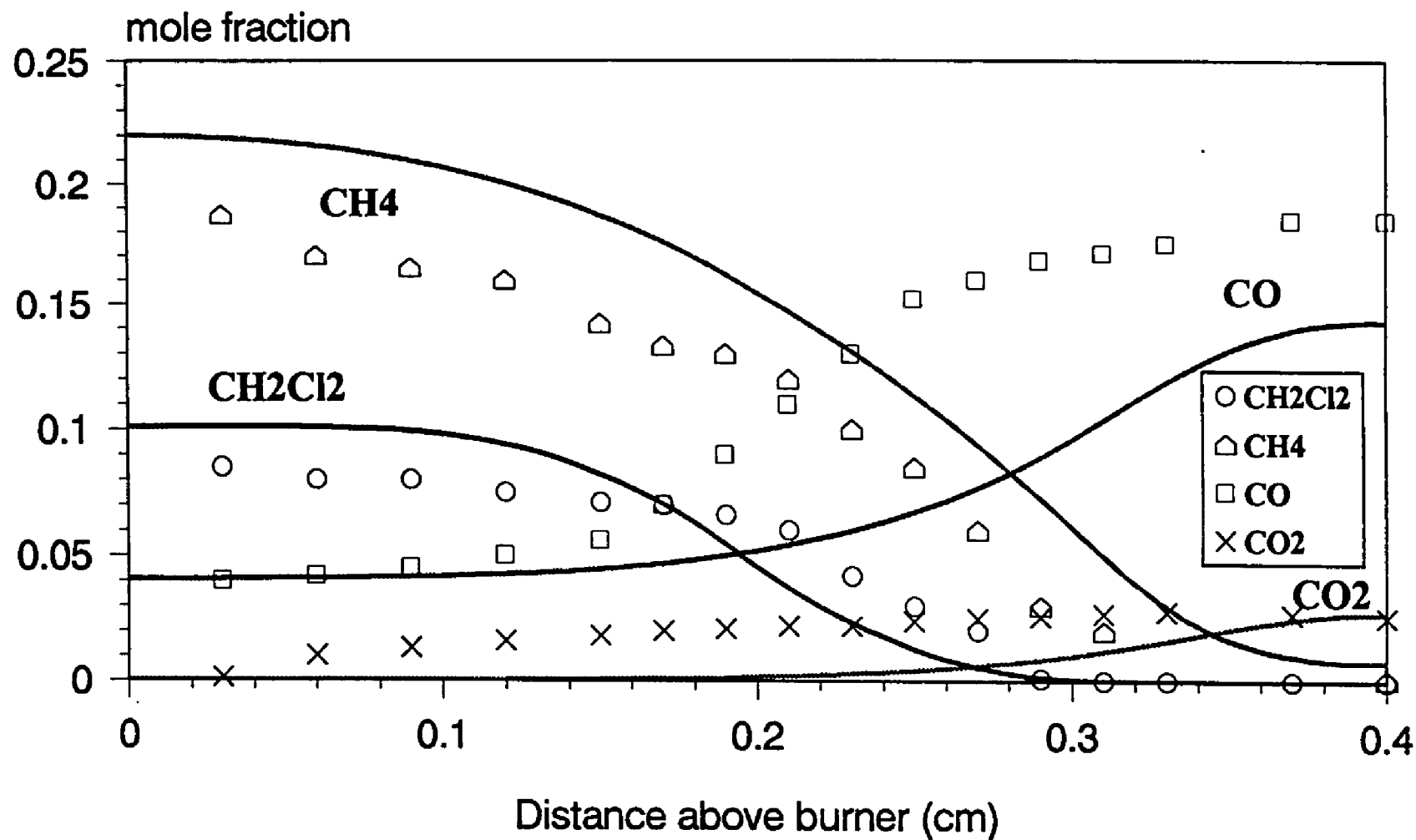


Fig 9.7 Comparison of our model with Qun et al. flame data

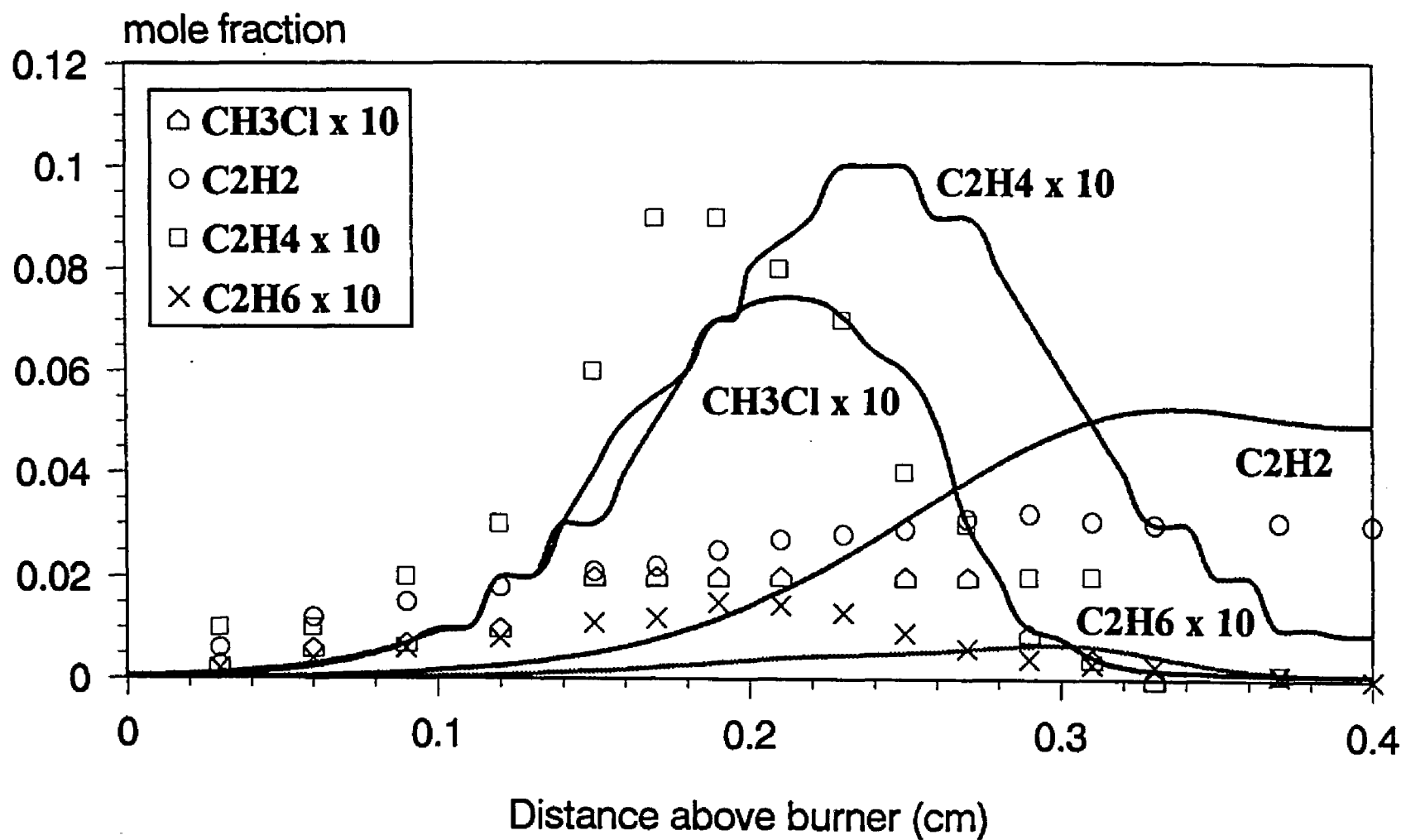


Fig 9.8 Comparison of our model with Qun et al. flame data

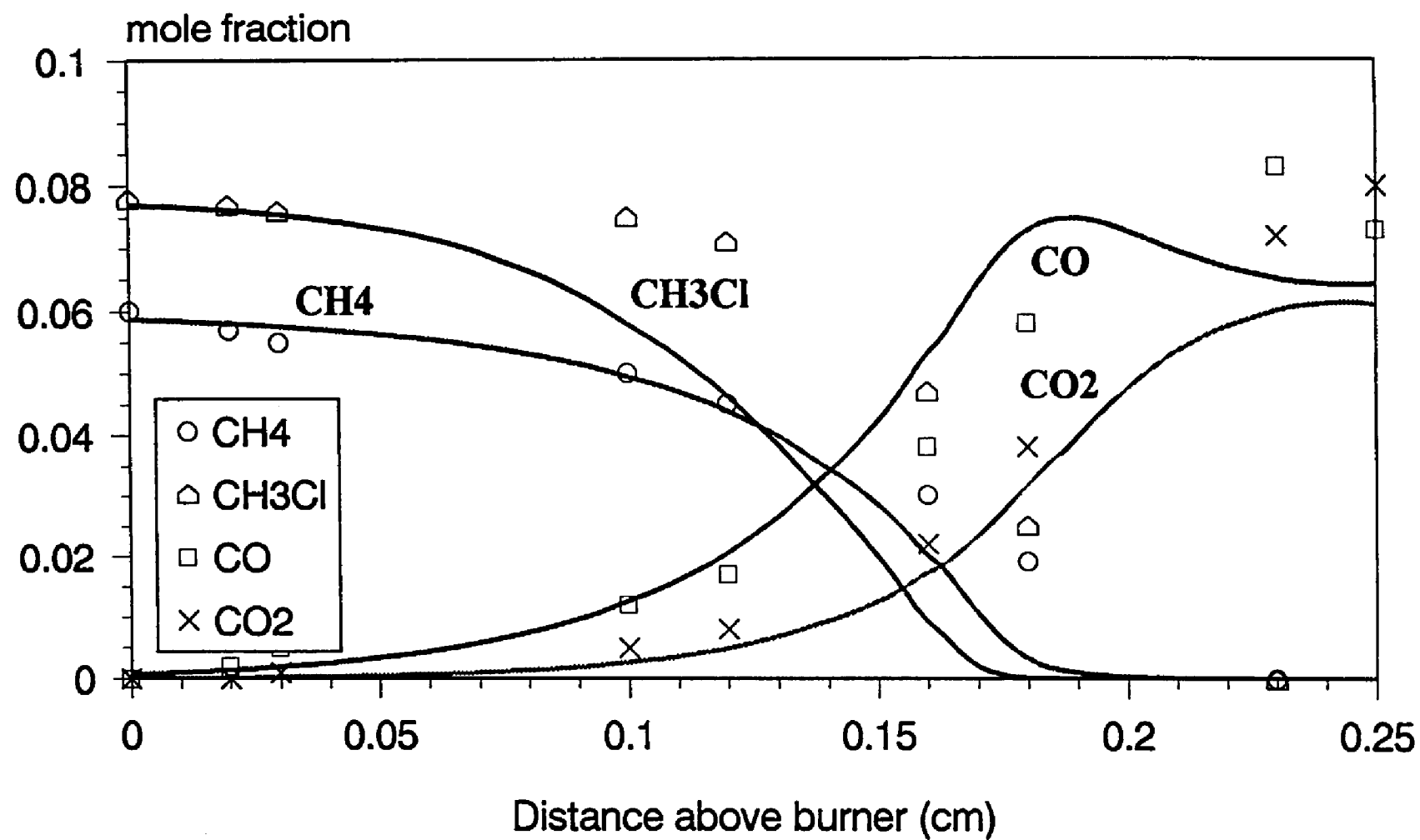


Fig 9.9 Comparison of our model with Miller et al. flame data

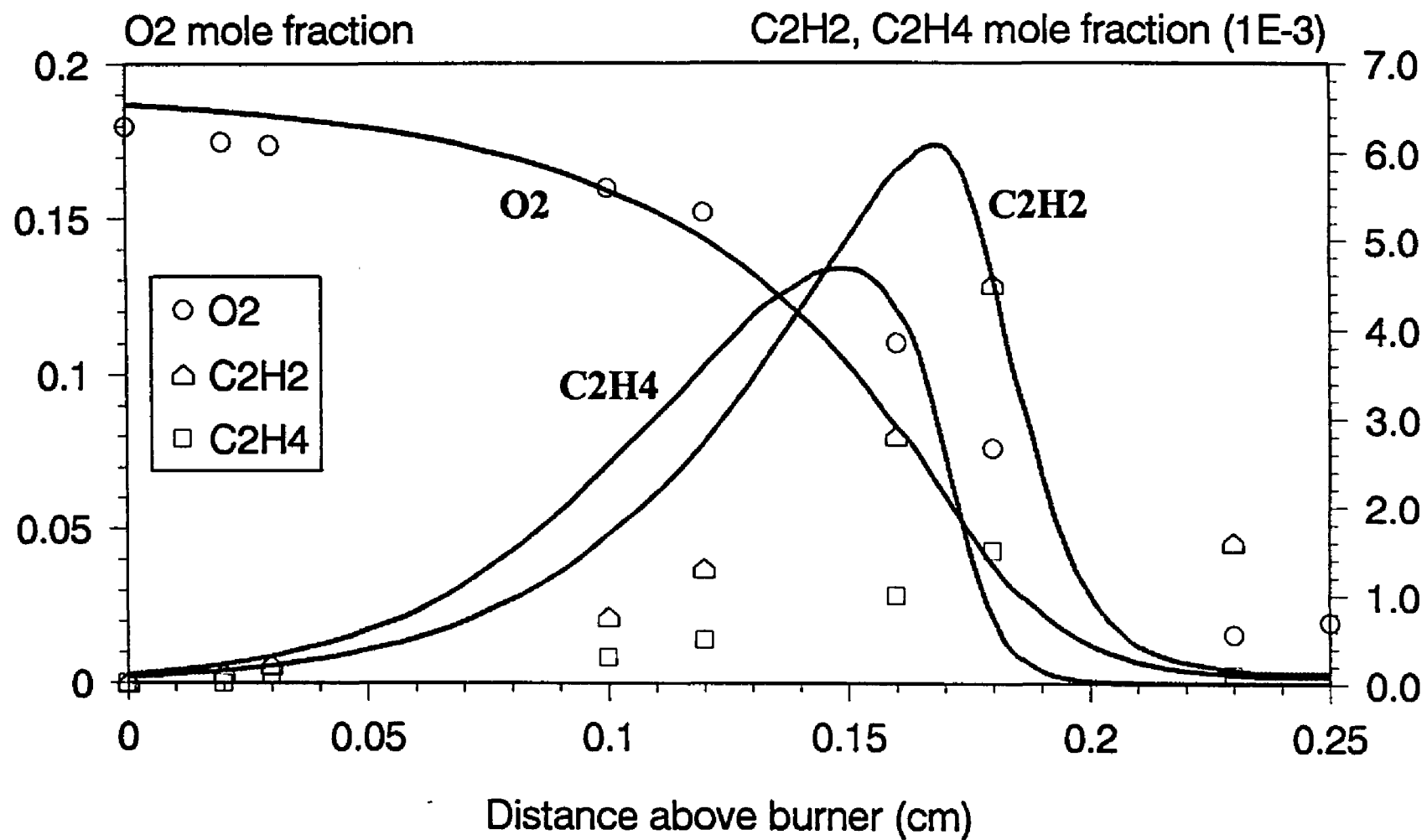
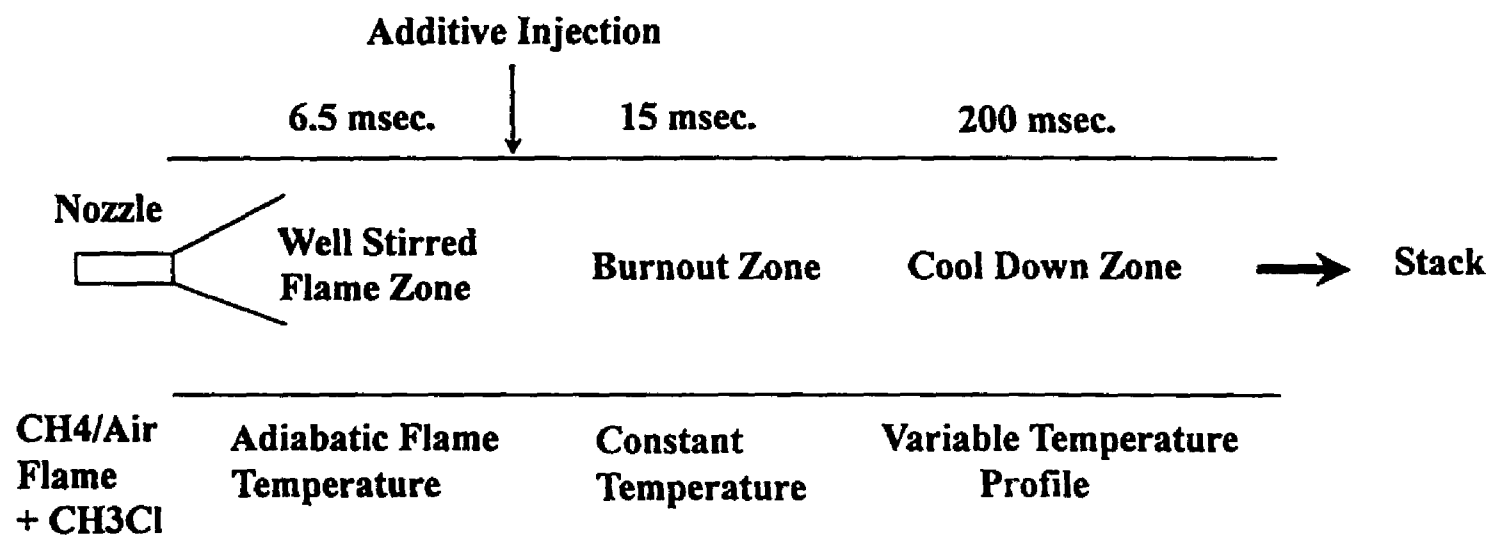


Fig 9.10 Comparison of our model with Miller et al. flame data





## MODEL

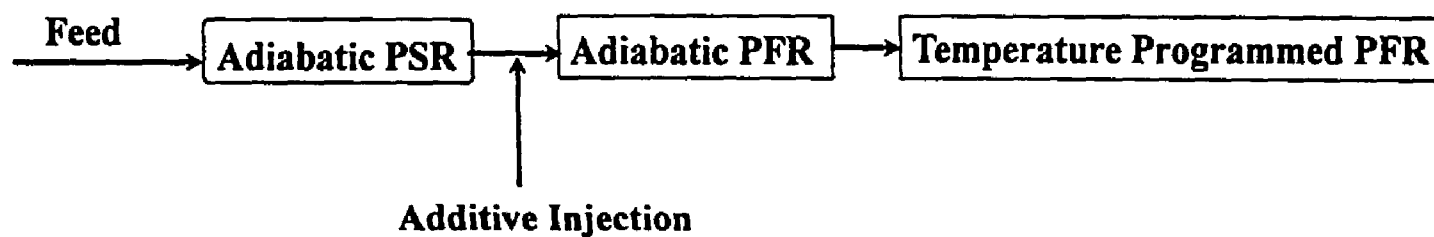


Fig 10.1 Turbulent Flow Incinerator Simulation

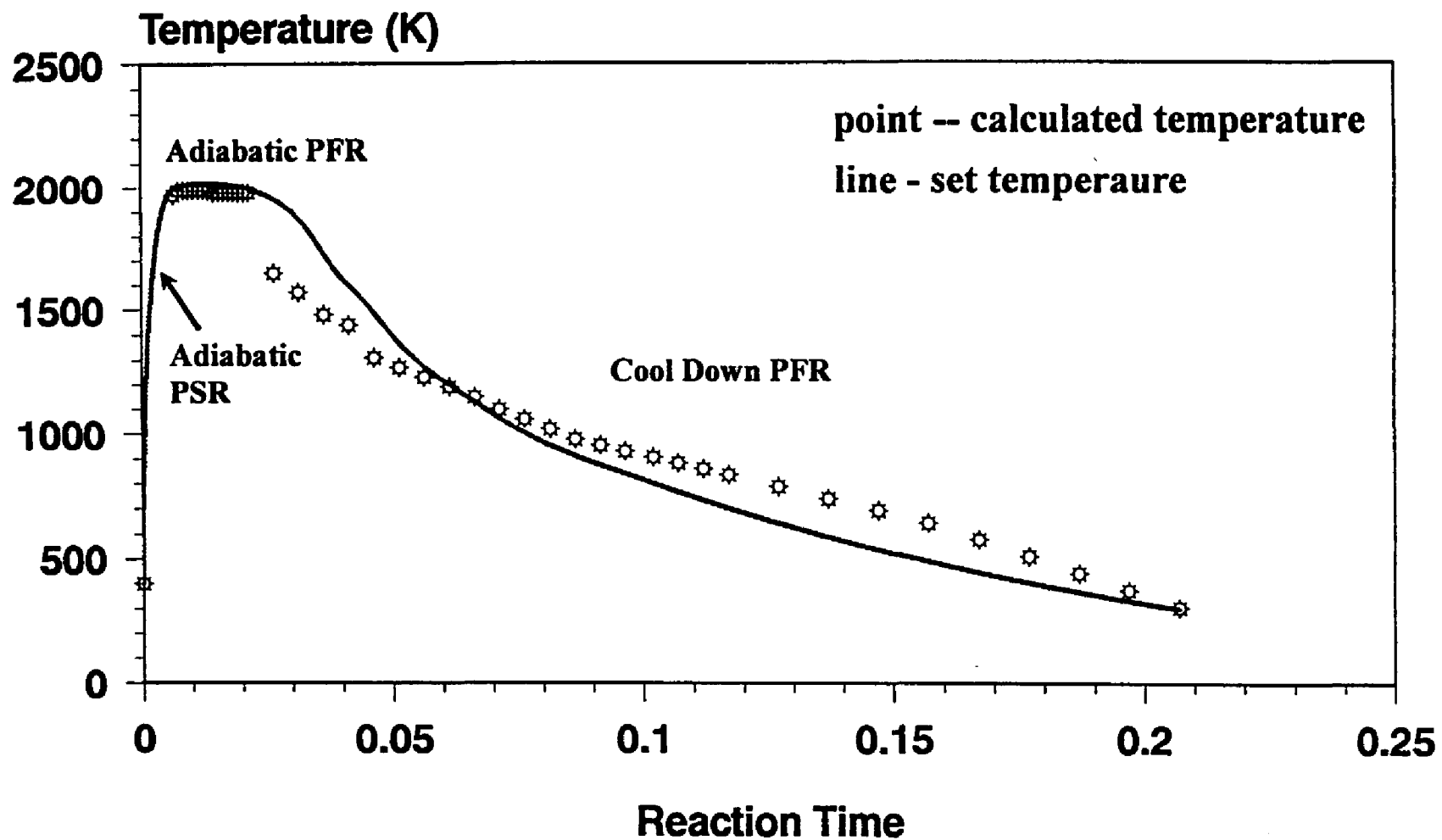


Fig 10.2 Incinerator simulation temperature profile

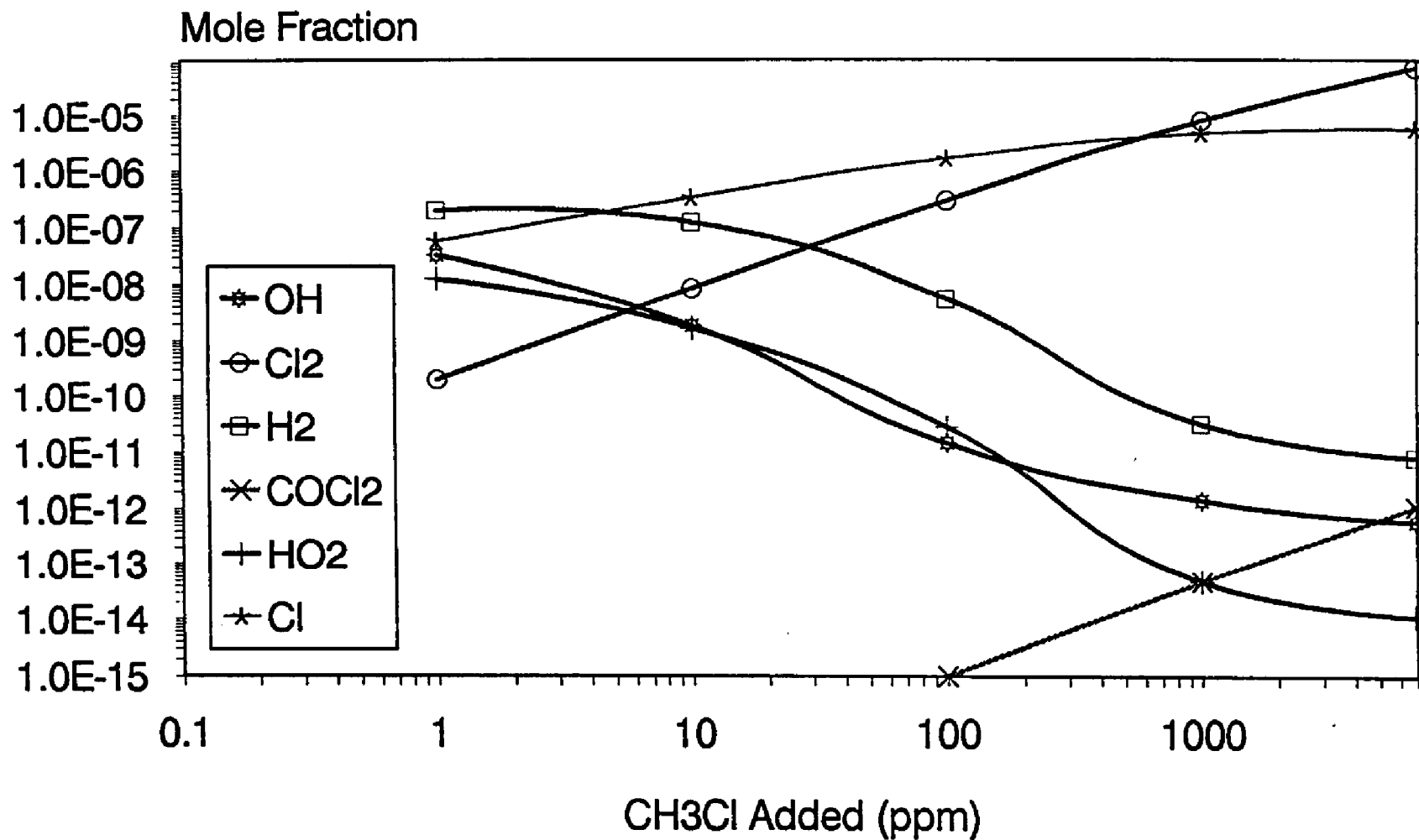


Fig 10.3 Effect of CH<sub>3</sub>Cl added in CH<sub>4</sub>/Air under fuel lean condition (equivalence ratio 0.8); calculated in burnout zone

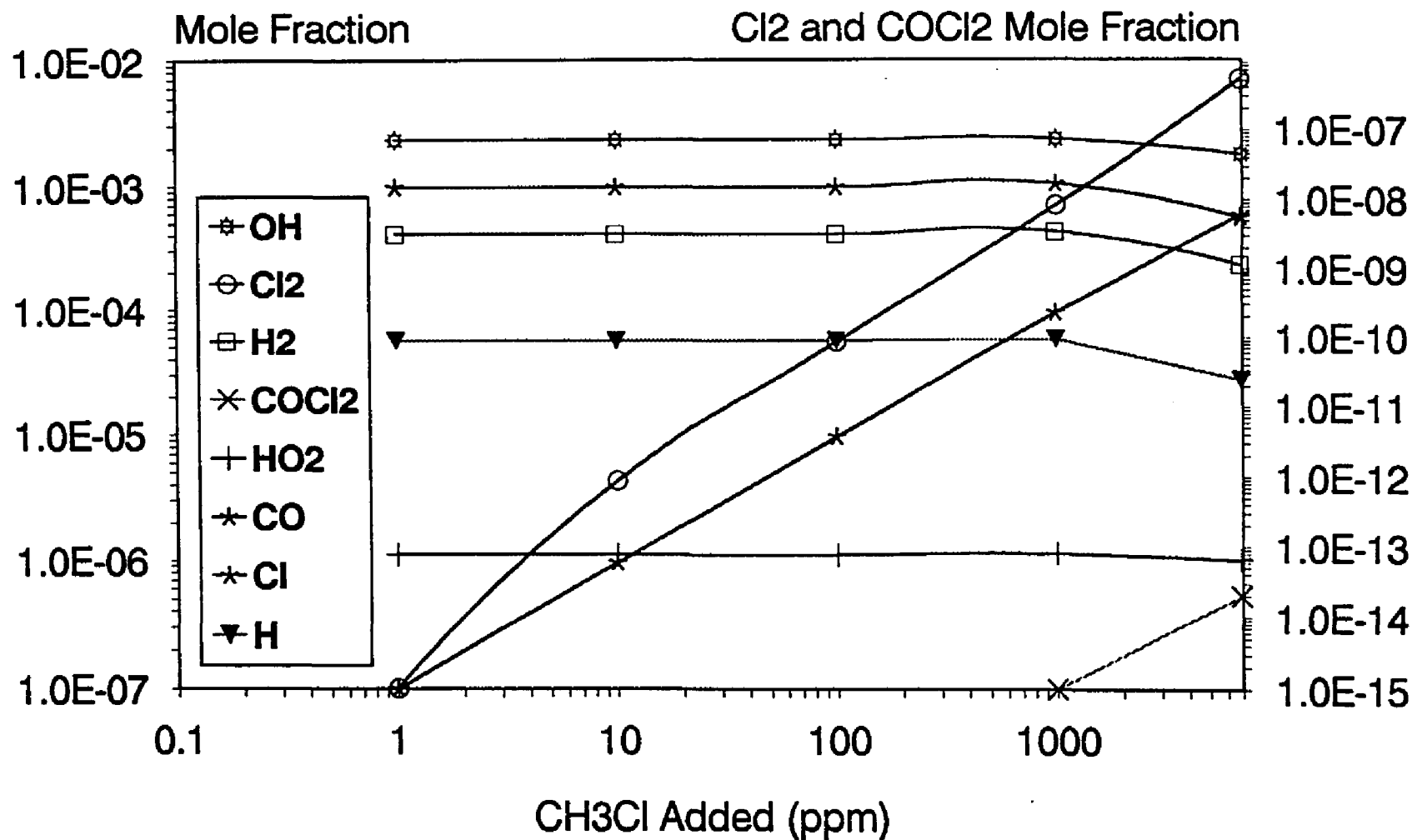


Fig 10.4 Effect of CH<sub>3</sub>Cl added in CH<sub>4</sub>/Air under fuel lean condition (equivalence ratio 0.8); calculated at exit 320K.

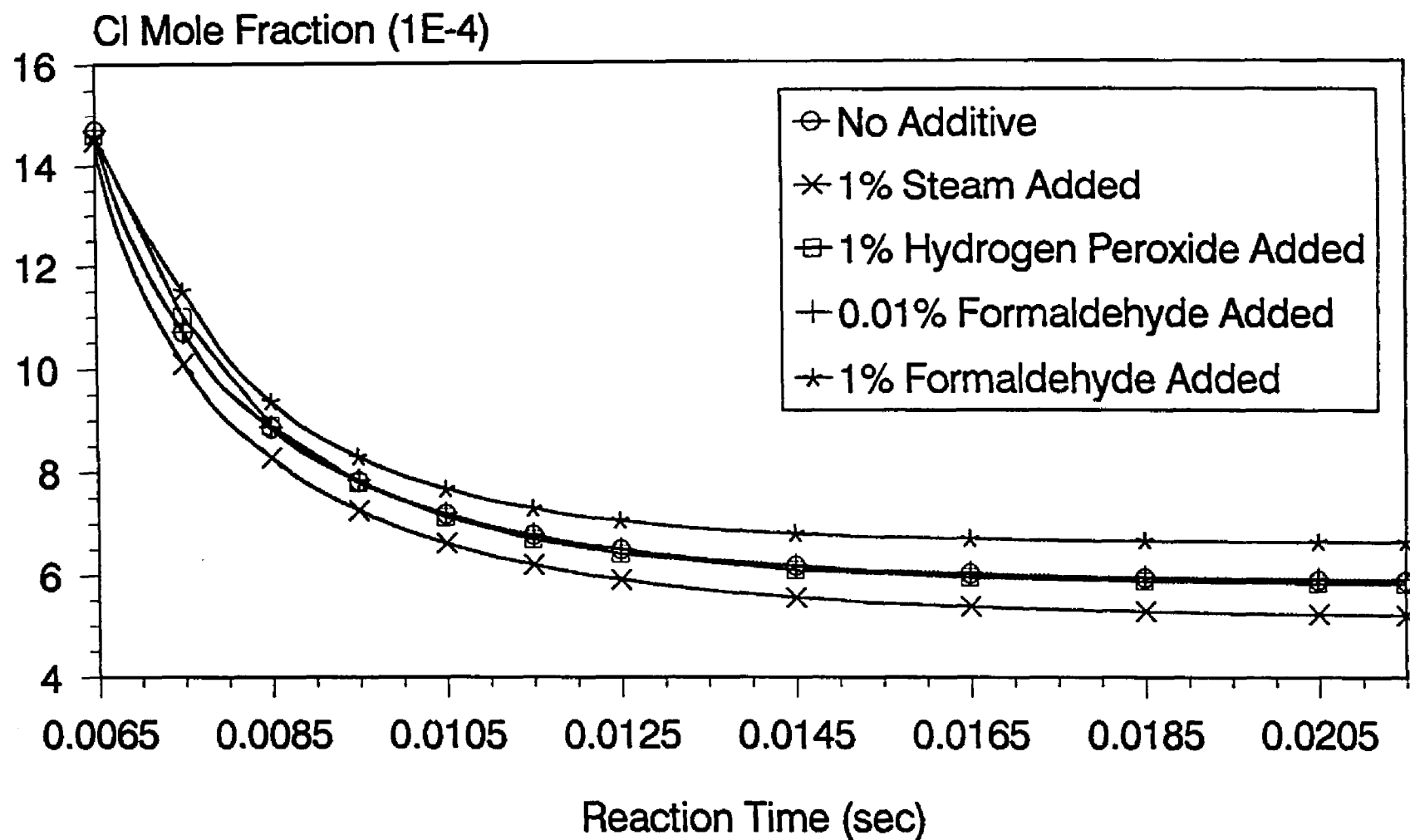


Fig 10.5 Cl atom mole fraction versus reaction time in the high temperature burnout zone

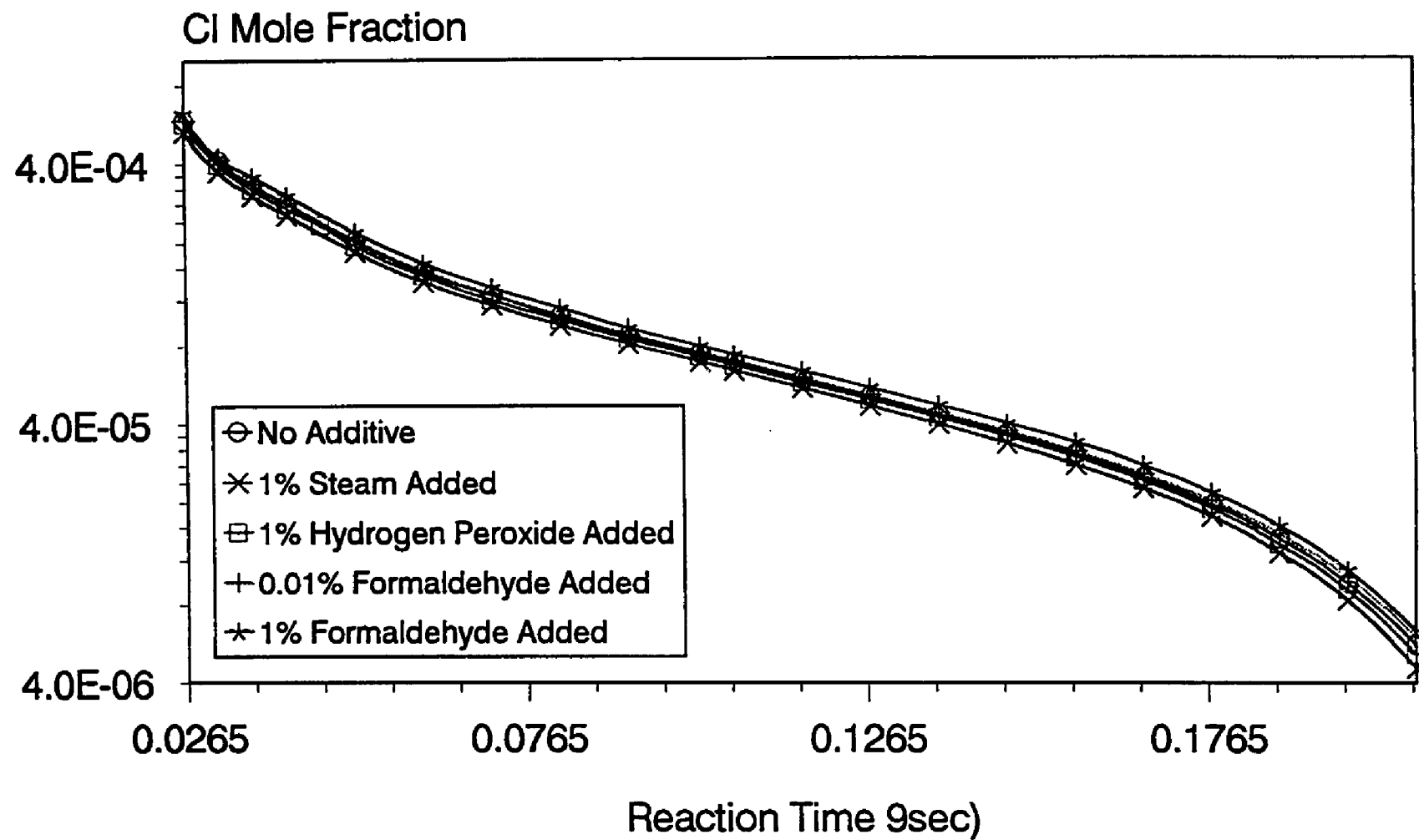


Fig 10.6 Cl atom mole fraction versus reaction time in the low temperature cool down zone

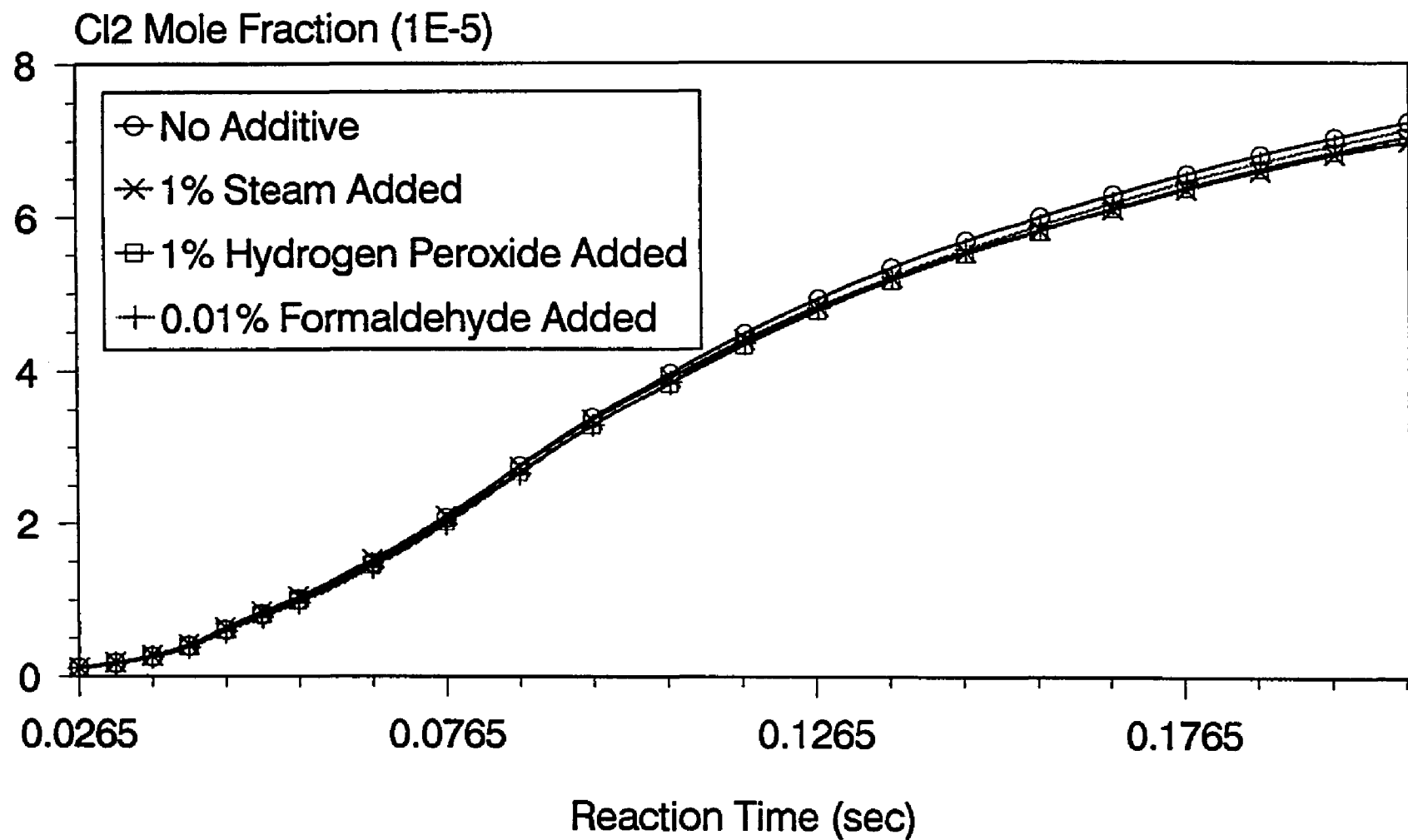


Fig 10.7 Cl<sub>2</sub> mole fraction versus reaction time in the low temperature cool down zone

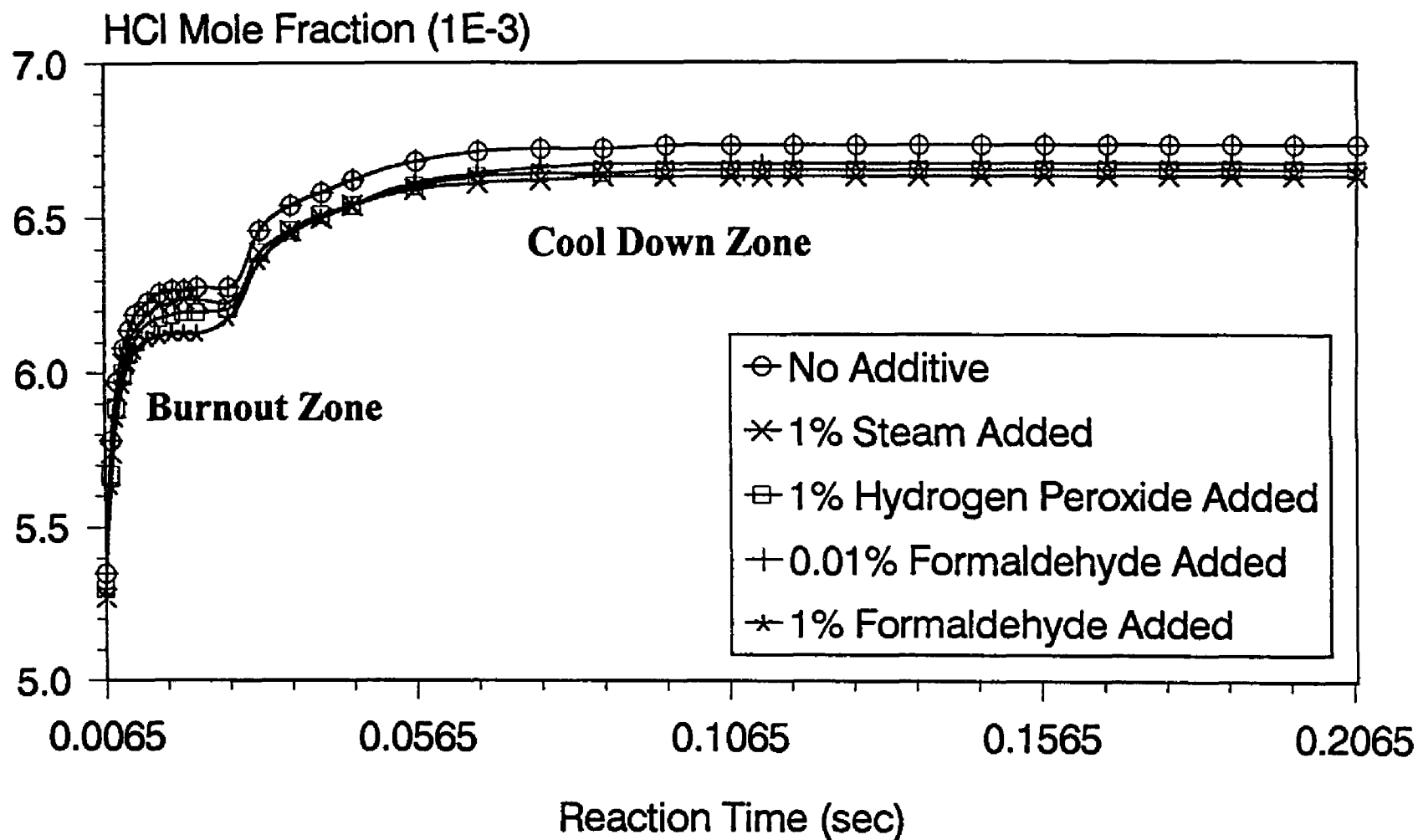
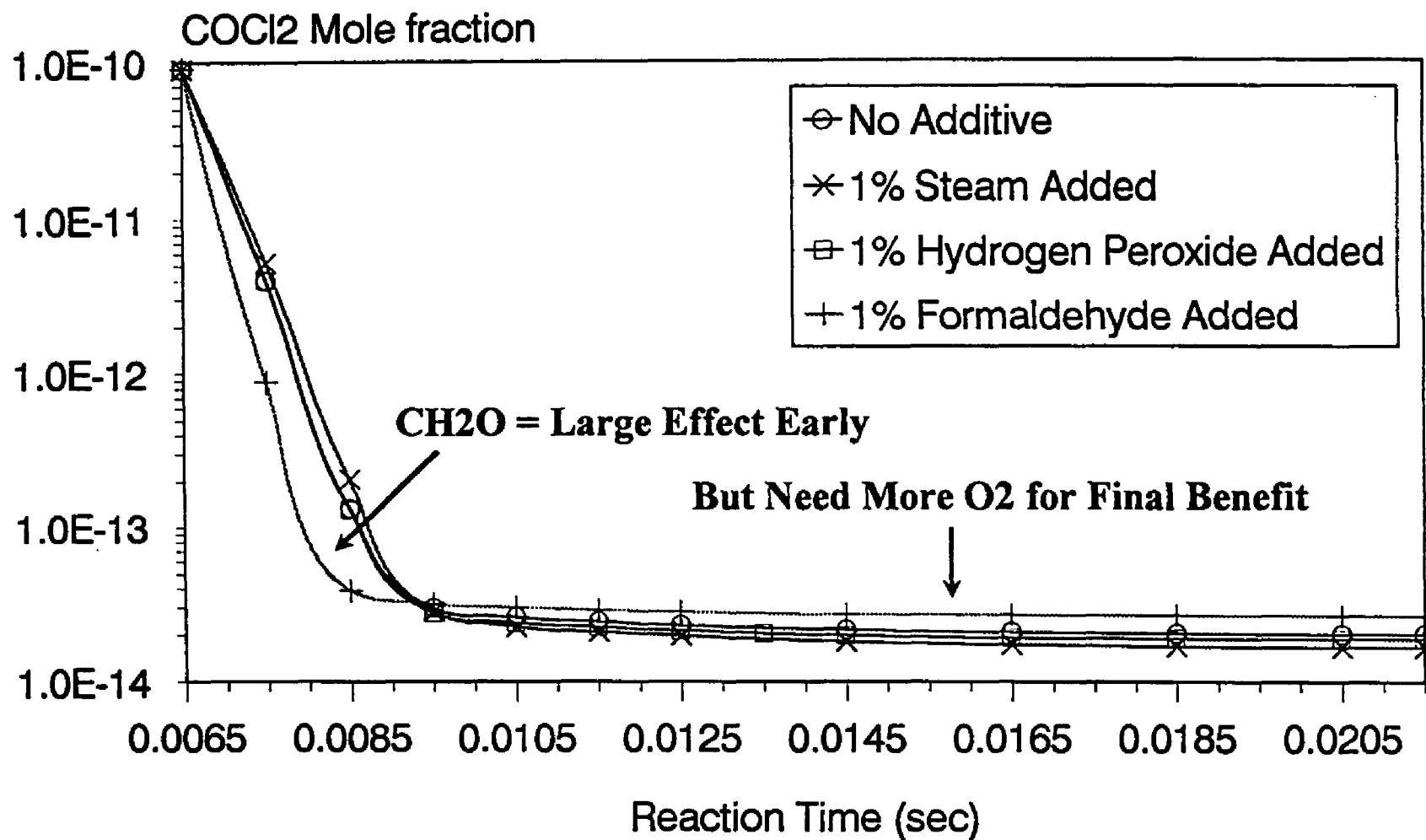


Fig 10.8 HCl mole fraction versus reaction time throughout the reactor





**Fig 10.9 COCl<sub>2</sub> mole fraction versus reaction time in the high temperature burnout zone**

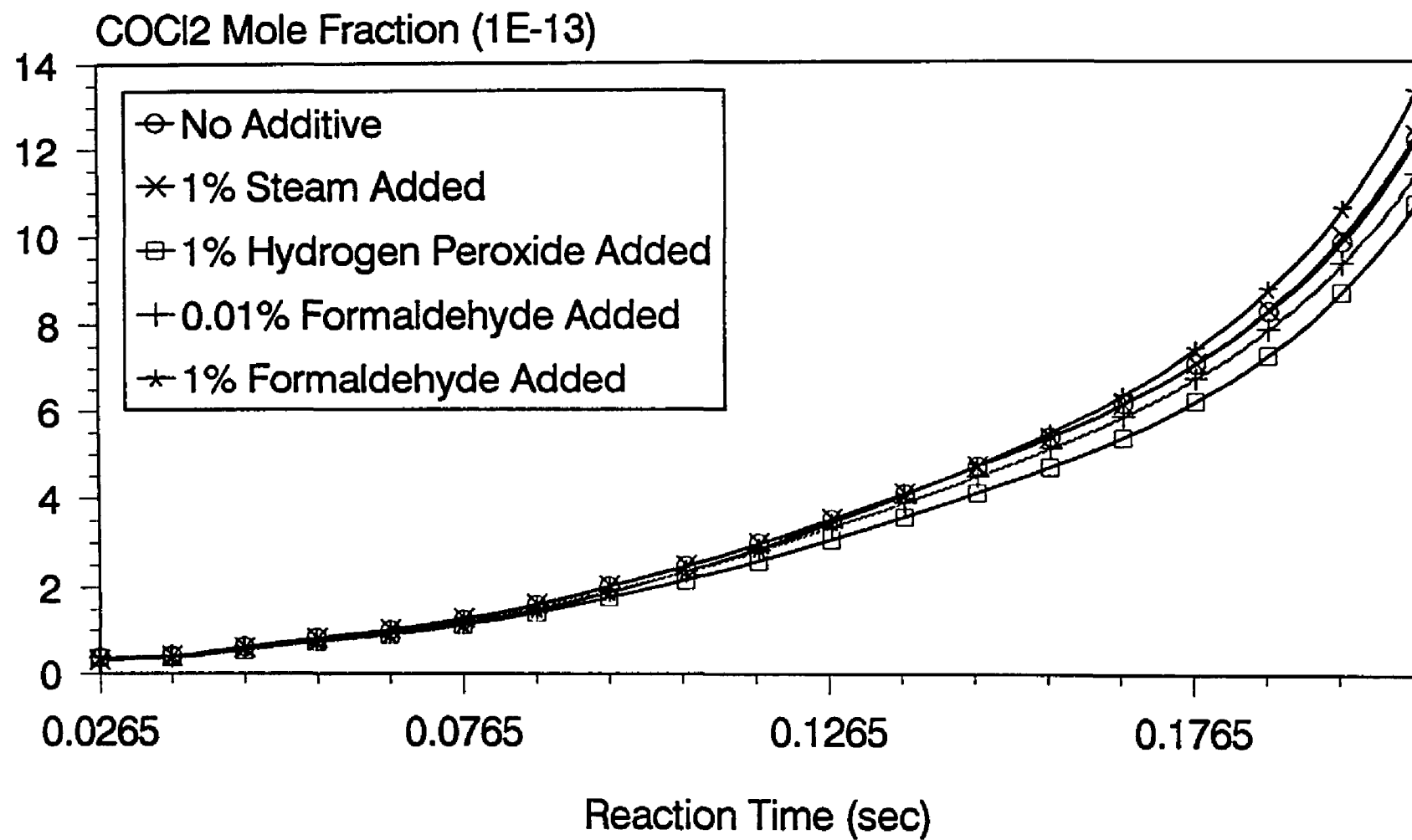
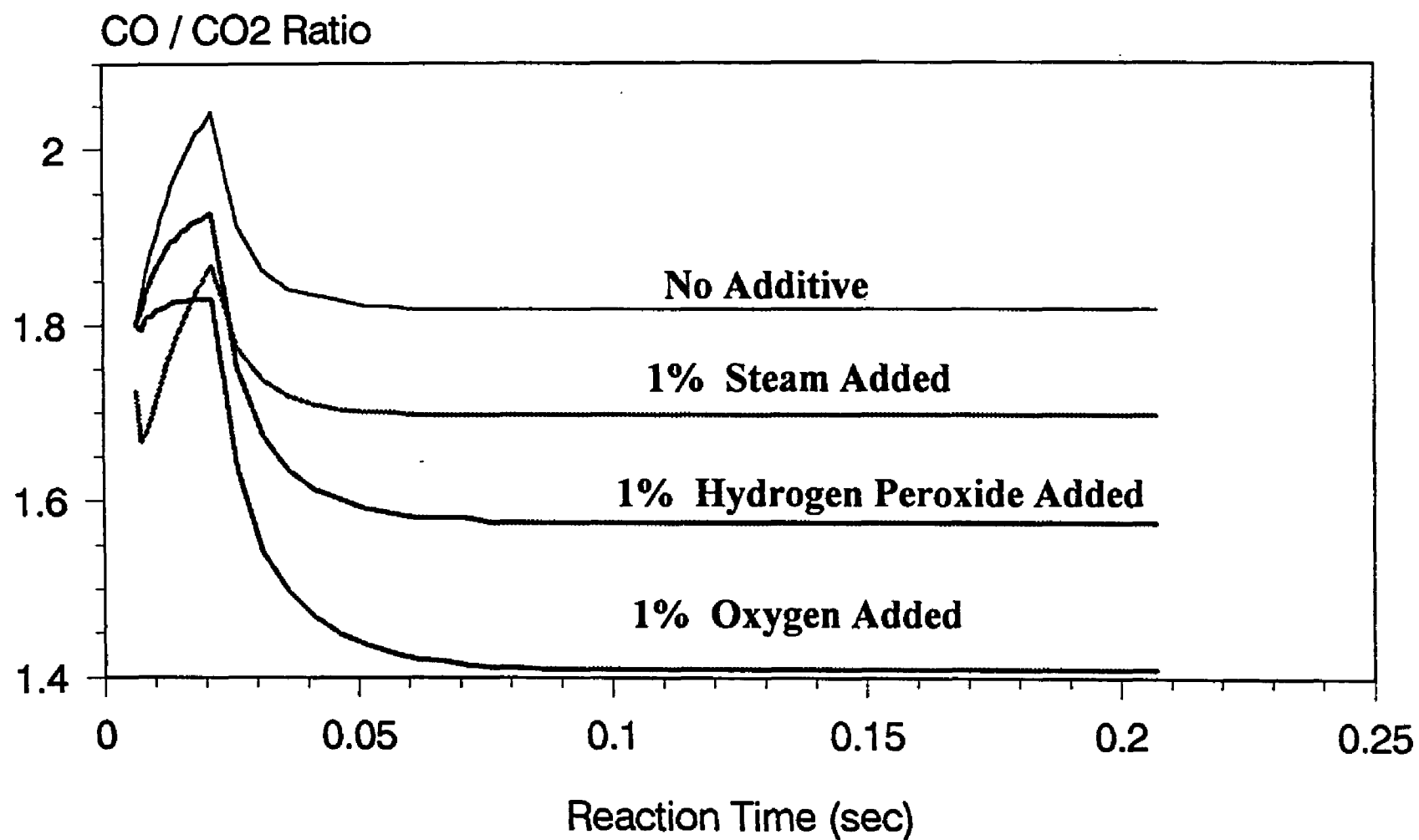


Fig 10.10 COCl<sub>2</sub> mole fraction versus reaction time in the low temperature cool down zone



**Fig 10.11 CO/CO<sub>2</sub> ratio versus reaction time under fuel rich condition (equivalence ratio 1.5)**

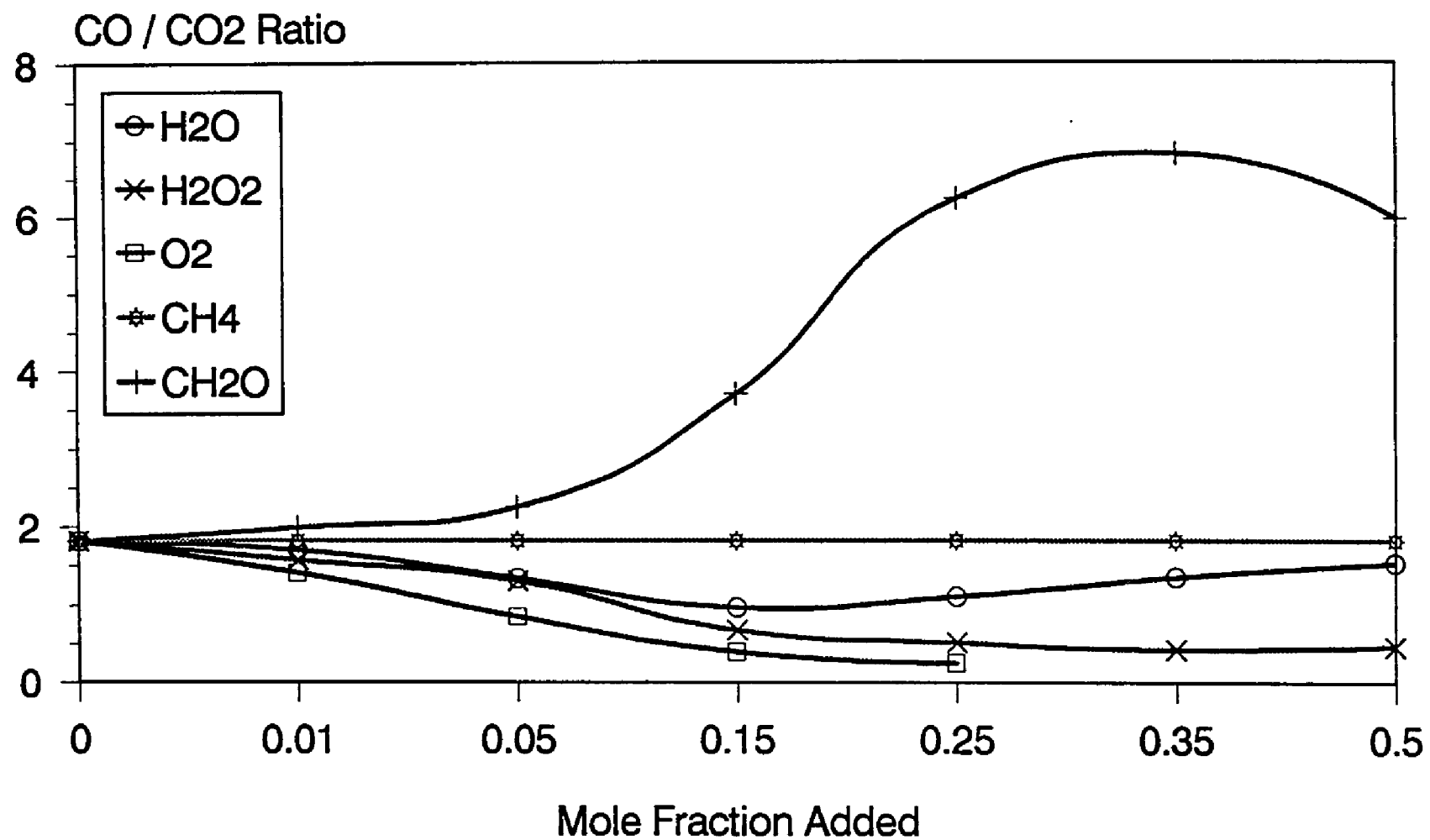


Fig 10.12 CO/CO<sub>2</sub> ratio calculated at exit 320K under fuel rich condition (equivalence ratio 1.5)

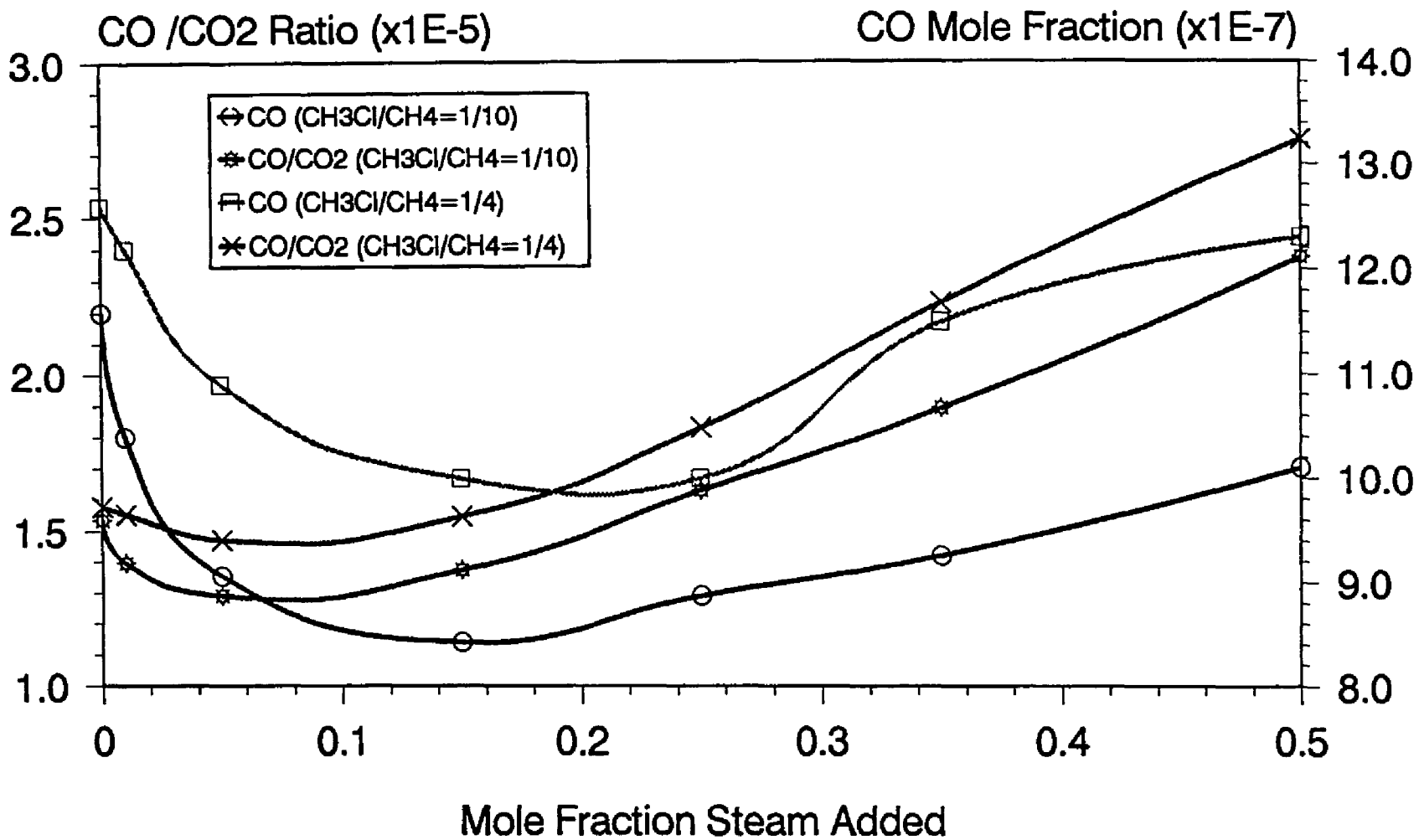


Fig 10.13 CO/CO<sub>2</sub> ratio versus addition of steam under fuel lean condition (equivalence ratio 0.8)

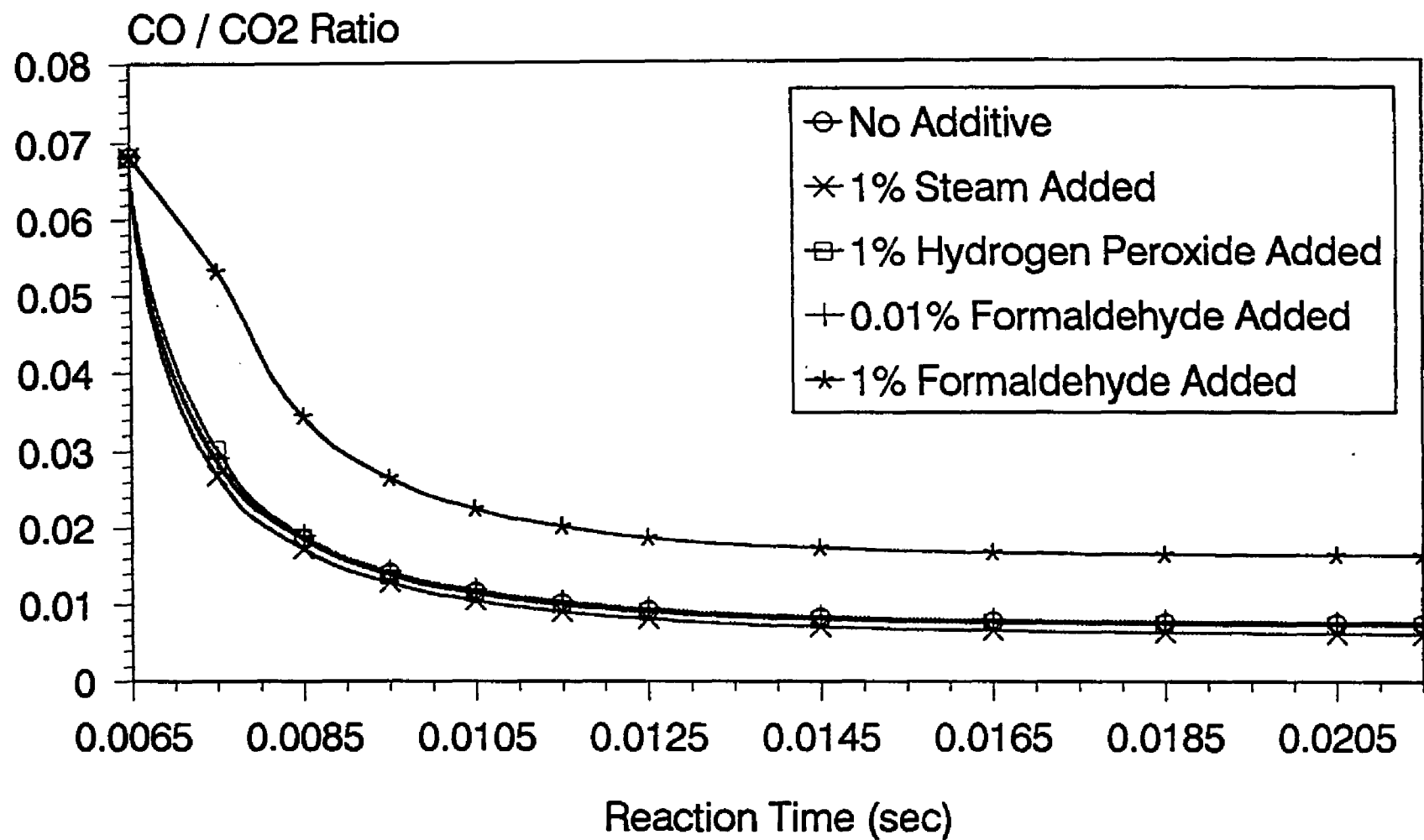


Fig 10.14 CO/CO<sub>2</sub> ratio versus reaction time in the high temperature burnout zone

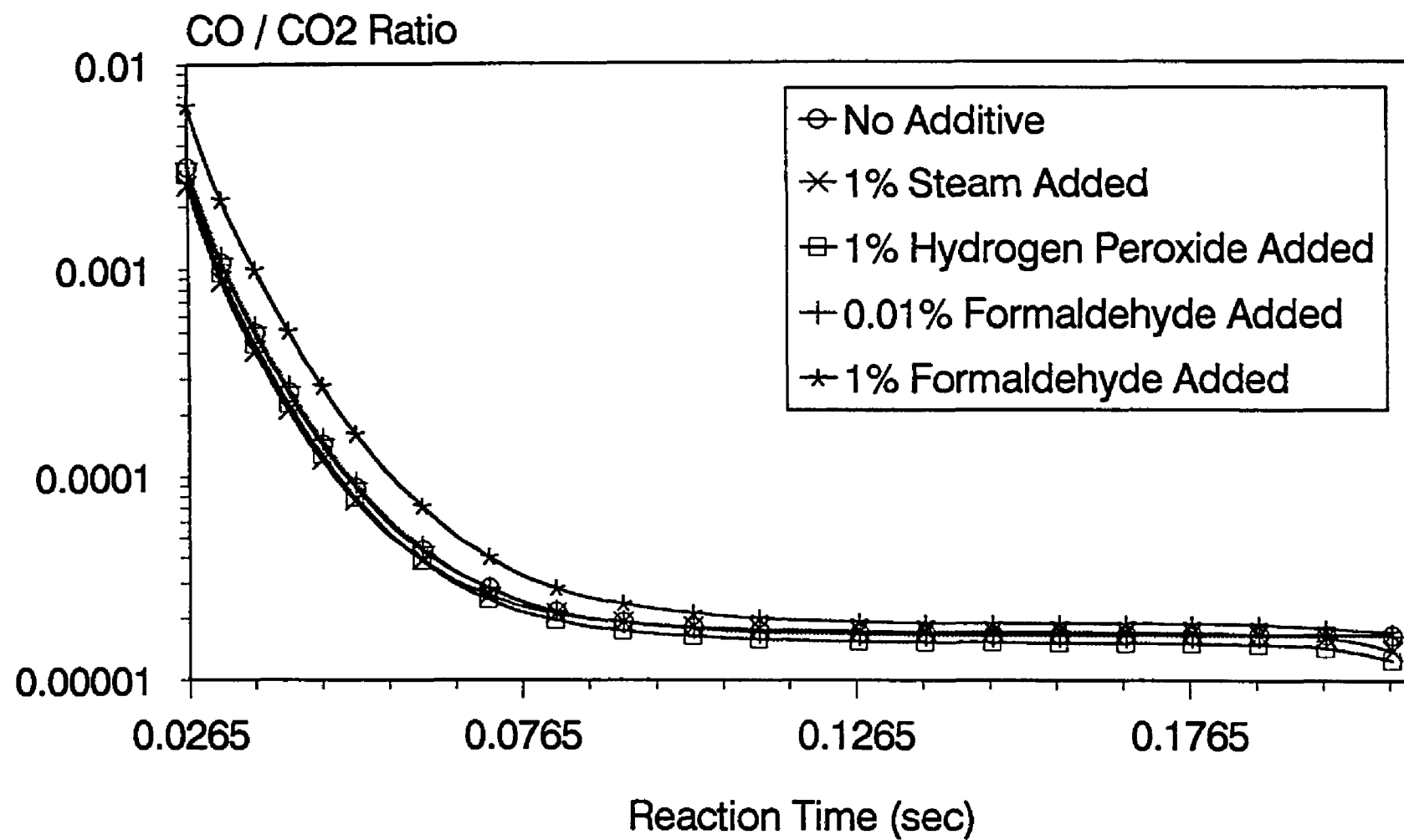


Fig 10.15 CO/CO<sub>2</sub> ratio versus reaction time in the low temperature cool down zone

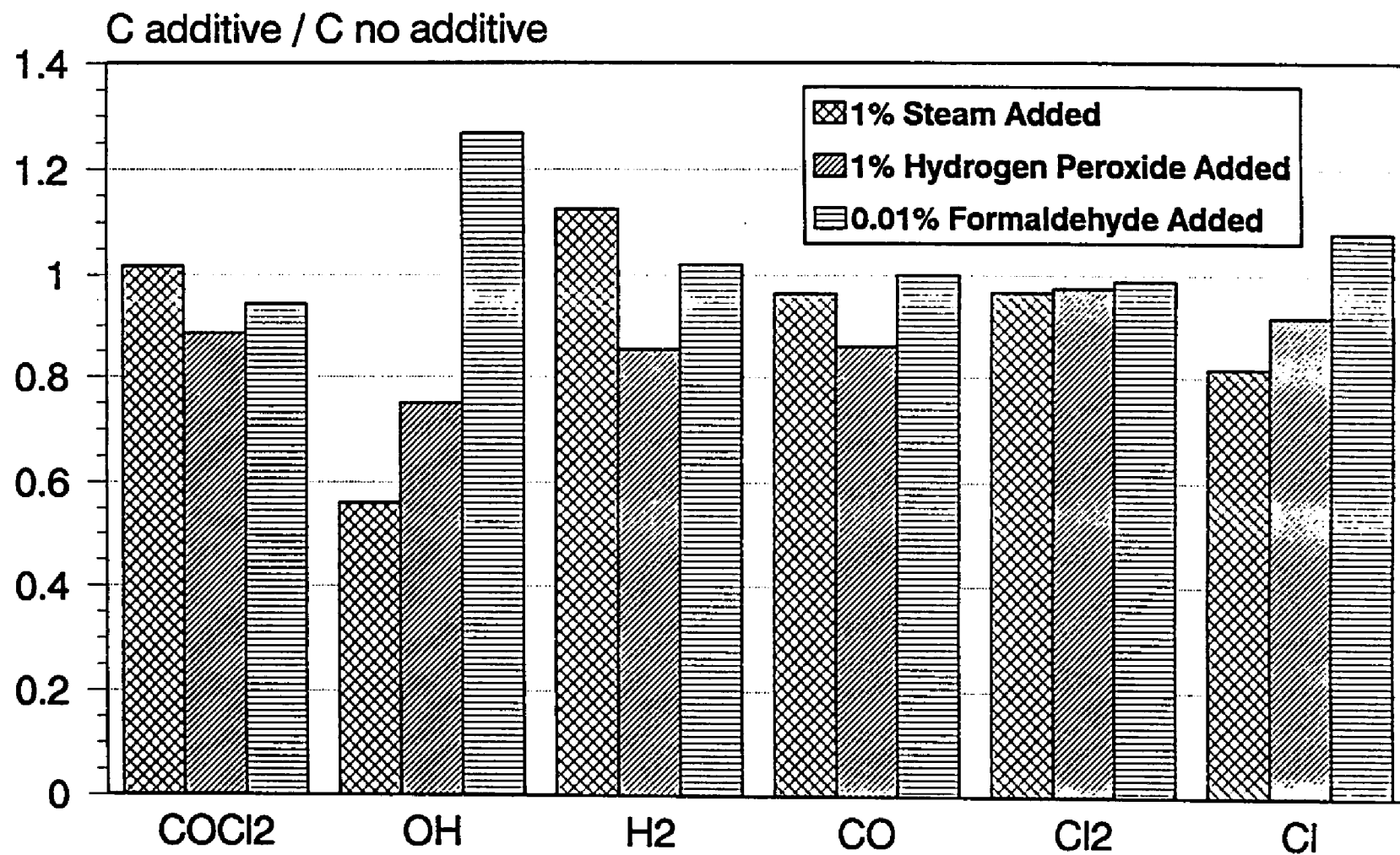


Fig 10.16 Fraction change in products versus additive.



## REFERENCES

1. Cherimisimoff, P.N.; Pollution Engineering, p42 - 49, Feb. 1987.
2. Westbrook, C.K.; 19th Symposium (International) on Combustion, p 126, The Combustion Inst., 1982.
3. Karma, D. and Senkan, S.M., Combust. Sci. Tech.; 54, 333, 1987.
4. Chang, W.D., Karra, S.D., and Senkan, S.M., Combust. Sci. Tech., 49, 107, 1986.
5. Benson S.W. and Weissman, M., Int'l J. Chem. Kin., Vol.16, 307, 1984.
6. Dean, A.M., J. Phys. Chem.; 89, 4600, 1985.
7. Dean, A.M. and Bozzelli, J.W., Comb. Sci. & Tech., 80, 63, 1991.
8. Tsao, H. M.Sc. thesis, New Jersey Inst. Tech. 1987.
9. Huang, S.H.; M. Sc. Thesis, New Jersey Inst. Tech. 1987.
10. Won, Y.S. and Bozzelli, J.W., American Society of Mechanical Engineering HTD-Vol. 104, p 131 1988.
11. Shilov, A. E., et al., J. Fiz. Kim., vol. 33, 6, 1959.
12. Holbrook, K. A.; Trans. Faraday Soc., 57, 2151, 1961.
13. Frost, W., et al., Can. J. Chem., 43, 3052, 1965.
14. Kondo, O., et al., Bull. Chem. Soc. Jpn., 53, 2133, 1980.
15. LeMoan, G., C. R. Aczd. Sci., Paris, 258, 1535, 1964.
16. Karra, S.B., Gutman, D., and Senkan, S.M.; Combust. Sci. Tech. vol. 60, 45, 1988.
17. Miller, D.L., Senser, D.W., Cundy, V.A., and Matula, R.A.; Hazardous Waste, vol. 1, no. 1, p 1, 1984.
18. Roesler, J.F., Yetter, R.A., and Dryer, F.L.; Combust. Sci. Tech., vol. 85, p 1, 1992.
19. Koshland, C.P., Lee, S., and Lucas, D.; Combust. Flame, vol. 92, 106, 1993.
20. Hung, S.L. and Pfefferle L.D.; Comb. Sci. & Tech., vol. 87, p91, 1993.

21. Skoog, D.A.; Principles of Instrumental Analysis, Saunders College Publishing, New York, 1985.
22. Benson, S.W., Thermochemical Kinetics, John Wiley, New York, 1976.
23. Ritter, E.R. and Bozzelli, J.W., *Int. J. Chem. Kinetics*, 23, 767, 1991.
24. Ritter, E.R., *J. Chem. Info. Sci.* 31, 400, 1991.
25. Allara, D.L. and Shaw, R.J.; *J. Phys. Chem. Ref. Data*, 9, 523, 1980.
26. Baulch, D.L., Duxbury, J., Grant, S.J., and Montague, D.C.; *J. Phys. Chem. Ref. Data*, Supplement 1, 10, 1981.
27. Atkinson, R.A. et al.; *J. Phys. Chem. Ref. Data*, 18, 881, 1989.
28. National Institute Standard and Technology Kinetics Data base, NIST Gaithersburg, MD 1989.
29. Bozzelli lecture handout
30. Zabel, F.; *Int. J. Chem. Kinetic*; 9, 655, 1977.
31. Kerr, J.A. and Moss, S.J.: *Handbook of Bimolecular and Termolecular Gas Reaction* Vol. I & II, CRC Press Inc., 1981.
32. Barat, R.B. and Bozzelli, J.W.; *J. Phys. Chem.*, 96, 2494, 1992.
33. Howard, C.J., *J. Chem. Phys.* 65, 4771, 1976.
34. Perry, R.A., Atkinson, R., and Pitts, J.N., *J. Chem. Phys.* 67, 458, 1977.
35. Liu, A., Mulac, W.A., and Jonah, C.D., *J. Phys. Chem.* 93, 4092, 1989.
36. Bozzelli, J.W., Magee, K., Karim, H.M.D., Dean, A.M., and Chang, A.Y.; paper submitted to *J. Phys. Chem.* August 1993.
37. Chen, Y. and Tschuikow-Roux, E., *J. Phys. Chem.* 96, 7266, 1992.
38. Lay, L.T., Ritter, E.R., and Bozzelli, J.W., *Chemical and Physical Processes in Combustion*, 1993, in press.
39. Benson, S.W.; *Can. J. Chem.*, 61, 881, 1983.

40. Reid, R.C., Prausnitz, J.M., and Polling, B.E., Properties of Gases and Liquids, 4th Ed., McGraw Hill, New York, 1989.
41. Ben Amotz, D. and Herschbach, D.R., J. Phys. Chem. 94, 3393, 1990.
42. Cohen, N., Int. J. Chem. Kinetics, 14, 1339, 1982; 15, 503, 1983.
43. Cohen, N. and Westberg, K.R.; Int. J. Chem. Kinetics, 18, 99, 1986.
44. Cohen, N. and Benson, S.W.; J. Phys. Chem. 91, 162, 1987.
45. Cohen, N.; Int. J. Chem. Kinetics, 21, 909, 1989.
46. Lewis, G.N., Randall, M.; Pitzer, K.S., and Brewer, L.; Thermodynamics, 2nd Ed.; McGraw-Hill, New York, 1961.
47. Gilbert, R.G. and Smith, S.C.; Theory of Unimolecular and Recombination Reactions; Blackwell Scientific Publications, 1990.
48. Troe, J.; J. Phys. Chem., 83, 114, 1979.
49. Chuang, S.C. and Bozzelli, J.W., Environ. Sci. Tech., 20, 568, 1986.
50. Chang, S.H. and Bozzelli, J.W. AIChE J., 33, 1207, 1987.
51. Y. S. Won and J. W. Bozzelli, Combustion Science and technology, 85, 347, 1992.
52. Abbatt and Anderson, J. Phys. Chem., 95, 2382, 1991.
53. J. F. Blake, S. G. Wierschke, and W. L. Jorgensen; J. America Chemical Society, 111, 1919, 1989.
54. E. Arunan, S.J. Wategaonkar and D.W. Setser, J. Phys. Chem. 95, 1539, 1991.
55. Lias, S.G.; Bartmess, J.E.; Liebman, J.F.; Holmes, J.L.; Levin, R.D.; Mallard, G.M. J. Am. Chem. Soc. 107, 6089, 1985.
56. Ibid, J. Phys. Chem. Ref. Data, 17, Suppl. 1, 1988.
57. NIST Structures and Properties Database Number 25; Gaithersburg, MD 20899.
58. Paulino, J. A., Squires, R. R, J. Am. Chem. Soc., 113, 5573, 1991.
59. CHEMKIN computer code SAND87-8007.UC-4 supplied by Sandia National Labs, Livermore, CA. R.J. Kee and J.A. Miller.

60. Ritter, E., Bozzelli, J.W., and Dean, A.M. J. Phys. Chem., 94, 2493, 1990.
61. Karra, S.B. and Senkan, S.M., I&EC RESEARCH, 27, 447, 1988.
62. Tavakoli, J. and Bozzelli, J.W., paper presented at the Central States Technology Meeting, The Combust. Inst. Argonne, IL May 1987.
63. Unpublished studies on reactions of chloroform in methane/oxygen and 1,1,1 trichloroethane in methane/oxygen atmosphere. This laboratory, where initial decay of the hydrocarbon is observed with chlorocarbon present is observed to be faster than when the chlorocarbon is not present.  
(M.S. Thesis Yo-pin Wu 1989)
64. SENS is modification by NJIT of an early version of the SENKIN computer code SAND87-8248.UC-4 supplied by Sandia National Labs, Livermore, CA. R.J. Kee and A.E. Lutz.
65. Barat, R.B., Sarafim, A.F., Longwell, J.P., and Bozzelli, J.W. ; Comb. Sci. Tech.; vol. 74, p. 361, 1990
66. Roessler, J.F., Yetter, R.A., and Dryer, F.L; Comb. Sci. Tech.; vol 82, p.87, 1992.
67. Miller, J.A. and Bowman, C.T.; Energy and Combustion Science, 1, 1989.
68. Westmoreland P.R., Howard, J.B., Longwell, J.P., and Dean, A.M.; AIChE Journal, 32, 12, 1971, 1986.
69. FLAME computer code SAND87-8240.UC-4 supplied by Sandia National Labs, Livermore, CA. Kee, R.J., Grcar, J.F., Smooke, M.D., and Miller, J.A. 20.
70. Myers, R.Thomas, J. Phys. Chem. Vol.83, No.2, 1979.
71. More, R. and Capparelli, A.L., J. Phys. Chem. 84, 1870-1871, 1980.
72. Hansen, P.J. and Jurs, P.C., Anal. Chem., 59, 2322-2327, 1987.
73. Lai, W.Y., Chen, D.H., and Maddox, R.N., Ind. Eng. Chem. Res., 26, 1072, 1987.
74. Reid, R.C., Prausnitz, J.M., and Sherwood, T.K., The Properties of Gases and Liquids, 3th ed. McGraw-Hill, New York, 1977.
75. Reid, R.C., Prausnitz, J.M., and Poling, B.E., The Properties of Gases and Liquids, 4th ed. McGraw-Hill, New York, 1988.

76. CRC Handbook of Chemistry and Physics, 71th ed.; Weast, R.C. Ed.; The Chemical Rubber Co.; Cleveland, OH, 1991.
77. McClellan, A.L., Tables of Experimental Dipole Moments, Freeman, San Francisco, 1963.
78. Minikin, V.L., Osipov, O.A., and Zhdanov, Y.A.; Dipole Moments in Organic Chemistry, trans. from the Russian by B.J. Hazard, Plenum, New York, 1970.
79. MOPAC computer code 6th Ed, supplied by Frank J. Seiler Research Laboratory, United State Air Force Academy; Stewart, J.J.; 1990.
80. Mason, E.A. and Monchick, S.C. ; Theory of Transport Properties of Gases, 9th Intern. Symp. Combust., Academic, New York, 1963.
81. Chung, T.H., Lee, L.L., and Starling, K.E.; Ind. Eng. Chem. Fundam., 23, 8, 1984.
82. TRANSCALC computer code; poster section in Twenty-fourth International Symposium on Combustion, Sydney, Australia, July 5-10 1992.
83. Ho, W., Yu, Q.R., and Bozzelli, J.W.; Comb. Sci. Tech., 85, 23, 1992.
84. Ho, W. Barat, R.B., and Bozzelli, J.W.; Combustion and Flame, 88, 265, 1992.
85. Chiang H.M. and Bozzelli J.W.; Proceeding of Central and Eastern States Joint Technical Meeting, The Combustion Institute, New Orleans, LA, March 15-17, 1993
86. Roesler, J.F., Yetter, R.A., and Dryer, F.L.; poster section, Third International Congress on Toxic Combustion By-Products, MIT, Cambridge, MA, June 14-16, 1993.
87. Karra, S.B. and Senkan, S.M., Ind. Eng. Chem. Res., 27, 1163, 1988.
88. Qun, M. and Senkan, S.M., Hazardous Waste & Hazardous Materials, Vol. 7, No. 1, 1990.
89. Tsang, W.; Combustion Science and Technology, vol. 74, 99, 1990.
90. Tsang, W.; Waste Management, vol. 10, 217, 1990.
91. Lyon, R.; Twenty-Third Symposium (International) on Combustion, The Combustion Institute, 903, 1990.
92. Cooper, C.D. and Clausen, C.A.; Journal of Hazardous Materials, 24, 288, 1990.

93. Cooper, C.D. and Clausen, C.A.; *Journal of Hazardous Materials*, 27, 273, 1991.
94. Cobos, C.J., Baulch, D.L., Cox, R.A., Esser, C., Frank, P., Just, Th., Kerr, J.A., Troe, J., Pilling, M.J., Walker, R.W., and Warnatz, J.; *J. Phys. Chem. Ref. Data* 1992
95. Ritter, E.R. and Barat, R.B.; *Third International Congress on Toxic Combustion By-Products*, poster section, MIT, Cambridge, MA, 1993.
96. Ho, W. and Bozzelli, J.W.; *Twenty-Fourth Symposium (International) on Combustion*, The Combustion Institute, p943, 1992.
97. Miller, G., Cundy, V.A. and Lester T.; paper Submitted to *Combust Sci. Tech*, April 1993.
98. Puri, I.K., M.H. Yang, and Lee, K.Y.; *Comb. Flame*, vol. 92, p. 419, 1993.
99. Puri, I.K. and Lee, K.Y.; *Comb. Flame*, vol. 92, p. 440, 1993.
100. Hammins, A.; paper presented at *NIST Fluorocarbon Flame Inhibition Workshop*, New Orleans La, Mar 15, 1993.
101. Brouwer, J., Longwell, J.P., Sarofim, A.F., Barat, R.B., and Bozzelli, J.W. ; *Comb. Sci. and Tech.* vol. 85, p. 87, 1992.
102. Barat, R.B. et al.; poster section, *Twenty-Fourth Symposium (International) on Combustion*, The Combustion Institute, 1992. (paper submitted to *Comb. and Flame* 1993)